

Extrinsic and intrinsic regulation of  
differentiation and selection events during  
lymphocyte development

Inauguraldissertation

zur

Erlangung der Würde eines Doktors der Philosophie

vorgelegt der

Philosophisch-Naturwissenschaftlichen Fakultät

der Universität Basel

von

Fabian Klein

aus Deutschland

2019

Genehmigt von der Philosophisch-Naturwissenschaftlichen Fakultät  
auf Antrag von

Prof. Dr. Gennaro De Libero

Prof. Dr. Patrick Matthias

Basel, den 11.12.2018

Prof. Dr. Martin Spiess  
Dekan

---

# Table of Contents

<b>1. Summary</b> .....	<b>5</b>
<b>2. Introduction</b> .....	<b>7</b>
2.1. The hematopoietic system .....	7
2.2. The hematopoietic stem cell .....	7
2.3. Early hematopoiesis.....	8
2.3.1. Heterogeneity within early progenitors .....	11
2.3.2. Steady-state hematopoiesis .....	13
2.4. B-cell development .....	14
2.4.1. Lymphoid specification .....	15
2.4.2. Commitment to the B-cell fate .....	16
2.4.3. Early developmental stages .....	17
2.4.4. Late developmental stages .....	20
2.5. T-cell development.....	22
2.5.1. Seeding of the thymus.....	23
2.5.2. Initiation of the T-cell program.....	24
2.5.3. $\beta$ -selection.....	27
2.5.4. Final maturation steps.....	30
2.6. Flt3-ligand and IL-7 in lymphoid development.....	30
2.6.1. Instructive versus permissive action of cytokines .....	30
2.6.2. Flt3-ligand in early hematopoiesis .....	32
2.6.3. IL-7 in lymphopoiesis.....	34
<b>3. Aims of the thesis</b> .....	<b>40</b>
<b>4. Results</b> .....	<b>41</b>
4.1. Part 1: Flt3-ligand and IL-7 in lymphopoiesis.....	41
4.1.1. Permissive roles of cytokines interleukin-7 and Flt3-ligand in mouse B-cell lineage commitment .....	41

---

4.1.2.	Accumulation of multipotent hematopoietic progenitors in peripheral lymphoid organs of mice over-expressing interleukin-7 and Flt3-ligand .....	61
4.2.	Part 2: Role of the transcription factor Duxbl in T-cell development .....	94
4.2.1.	The transcription factor Duxbl mediates elimination of pre-T cells that fail $\beta$ -selection .....	94
<b>5.</b>	<b>Discussion .....</b>	<b>140</b>
5.1.	The roles of Flt3-ligand and IL-7 in lymphopoiesis .....	140
5.2.	Regulation of $\beta$ -selection by Duxbl.....	144
<b>6.</b>	<b>Abbreviations .....</b>	<b>150</b>
<b>7.</b>	<b>Acknowledgements.....</b>	<b>152</b>
<b>8.</b>	<b>References.....</b>	<b>154</b>
<b>9.</b>	<b>Appendix.....</b>	<b>178</b>
9.1.	Further publications .....	178
9.1.1.	Two distinct pathways in mice generate antinuclear antigen-reactive B cell repertoires .....	178
9.2.	Curriculum vitae.....	199

## 1. Summary

The development of lymphocytes is a precise, stepwise process that is subject to multiple extrinsic as well as intrinsic molecular mechanisms that guide cell differentiation and selection. Two essential regulators of lymphopoiesis are environmental signal mediators in the form of cytokines and transcription factors. Both influence proliferation, survival, differentiation and cell fate decisions.

In the present thesis, we investigated the role of the cytokines Flt3-ligand and IL-7 in lymphocyte development by the use of various mutant mouse strains. Our results unraveled crucial functions for both cytokines during lymphocyte differentiation. Flt3-ligand drives the proliferation of uncommitted progenitor populations such as CLP and EPLM, whereas IL-7 has a pro-survival effect on these cells. High levels of Flt3-ligand rescued the B-cell defect in IL-7<sup>-/-</sup> mice due to the tremendous expansion of the CLP and EPLM populations, surpassing the need for IL-7 as a survival factor. Thus, these observations clearly demonstrate that both, Flt3-ligand as well as IL-7, function in a permissive mode in the commitment process towards the B-cell lineage. Flt3 expression is suppressed upon commitment to the B-cell fate, but IL-7 has furthermore a proliferative function for committed CD19<sup>+</sup> progenitor cells. Constitutive over-expression of both Flt3-ligand and IL-7 resulted in a lympho- and myelo-proliferative disease. The two cytokines had a synergistic effect on the development of B cells, resulting in the accumulation of progenitors also in peripheral lymphoid organs. Interestingly, even MPPs could be detected in lymph nodes of these mice and transplantation experiments confirmed the functionality of these progenitors, since they were capable of long-term multilineage reconstitution. Thus, Flt3-ligand and IL-7 act in concert during lymphocyte development. We further provided evidence that peripheral lymphoid organs have the capability to support extramedullary hematopoiesis in pathological situations.

In a second study we focused on the molecular and transcriptional regulation of the first essential checkpoint of the antigen-receptor rearrangement in T-cell development, called  $\beta$ -selection. Even though almost half of the cells are eliminated at this checkpoint, only little is known about the underlying molecular mechanisms. Improvement of the current staging of thymocyte development by the addition of CD27 downregulation as a marker for cells that failed productive  $\beta$ -chain rearrangement at the DN3 stage allowed us to investigate this process in more detail than previously possible. Transcriptional analysis revealed a specific expression of the transcription factor Duxbl in cells prior to  $\beta$ -selection. Transgenic expression of Duxbl blocked the development of pre-T cells *in vitro* and *in vivo* due to increased apoptosis and cell cycle arrest. Further studies revealed the involvement of the Oas/RNaseL apoptosis

pathway in this Duxbl-mediated developmental arrest. Additional expression of the pro-survival factor Bcl2 partially rescued the block and *in vitro* knockdown experiments of Duxbl reduced apoptosis induction within the DN3 compartment. Thus, the specific expression of Duxbl in conjunction with the gain- and loss-of-function phenotypes of increased and reduced apoptosis, respectively, provide clear evidence for a key role of Duxbl in the elimination of DN3 cells that are not able to recombine a functional  $\beta$ -chain.

Overall, the results presented in this thesis, provide important new insights on the cell-extrinsic and -intrinsic regulation of differentiation and selection events in the development of lymphocytes. Furthermore, they highlight the validity of *in vivo* models for the investigation of immune cell development and function.

## 2. Introduction

### 2.1. The hematopoietic system

All organs involved in blood cell production and function belong to the hematopoietic system, including primarily bone marrow, spleen, thymus, and lymph nodes. The composition of blood cells can be roughly divided into erythrocytes, leukocytes, and thrombocytes. The function of thrombocytes, or platelets, is to prevent massive blood loss in the case of injuries by the formation of a blood clot. The largest portion of the blood is built by erythrocytes, or red blood cells, that are responsible for the oxygen transport throughout the body's tissues via binding of oxygen to hemoglobin that gives the cells their red color. By contrast, leukocytes are named white blood cells. They are classified into two separate lineages: lymphoid, composing mainly the adaptive immune system, and myeloid cells, composing mainly the innate immune system, that together defend our body against invading pathogens and transformed cells.

### 2.2. The hematopoietic stem cell

Due to the short lifespan of most mature blood cells, around  $10^{11}$  to  $10^{12}$  cells have to be newly generated every day in humans, a process that is termed hematopoiesis (Vaziri et al., 1994). During ontogeny the site of ongoing hematopoiesis changes. The first wave of hematopoietic cell production originates from the yolk sac at embryonic day (E) 7.5 and subsequently moves to the aorta-gonad-mesonephros from where the fetal liver and the bone marrow are seeded (Johnson and Moore, 1975; Medvinsky and Dzierzak, 1996; Orkin and Zon, 2008). Fetal liver is the major place of hematopoiesis during embryogenesis whereas the bone marrow is taking over after birth where it continues during adulthood. The only other primary lymphoid organ, that is responsible for the production of T leukocytes, is the thymus, which starts to be seeded already from E12 onwards (Boehm, 2008; Ramond et al., 2014).

The hematopoietic stem cell (HSC) is responsible for this continuous production due to its two defining properties: self-renewal capacity and multipotentiality to differentiate into all blood cell subsets. The first evidence for stem cell function in the hematopoietic system was described in the beginning of the 1960 by James Till and Ernest McCulloch, and was based on rescue of lethally irradiated mice by bone marrow transplantation (Becker et al., 1963; McCulloch and Till, 1960; Till and Mc, 1961).

Technical improvements in the field of fluorescence-activated cell sorting (FACS) resulted in the first characterization and purification of mouse HSCs in 1988 (Spangrude et al.,

1988). Based on these experiments it is known that a  $\text{Thy}^{\text{low}}\text{Sca1}^+$  population that lacks the expression of lineage-specific markers ( $\text{Lin}^-$ ) within the bone marrow contained the stem cell activity resulting in long-term reconstitution of erythroid, myeloid, and lymphoid cell types after transplantations. Since only about 25% of clonal reconstitutions by these cells were shown to be long term (Morrison and Weissman, 1994; Spangrude et al., 1995) the phenotype of HSCs was continuously refined and improved over the years. One important addition was c-kit (CD117) surface expression as a positive marker for self-renewal and stem cell activity resulting in the term LSK cells ( $\text{L}=\text{Lin}^-$ ,  $\text{S}=\text{Sca1}^+$ ,  $\text{K}=\text{c-kit}^+$ ) (Okada et al., 1992; Osawa et al., 1996b). Moreover, stem cell purity was further improved with exclusion of CD34 and Flt3 (CD135) expression on these cells (Adolfsson et al., 2001; Christensen and Weissman, 2001; Kondo et al., 1997b; Osawa et al., 1996a). Based on ability to long-term reconstitute lethally irradiated mice, HSCs were subdivided into  $\text{Flt3}^-\text{CD34}^-$  long-term HSCs and  $\text{Flt3}^-\text{CD34}^+$  short-term HSCs (Brown et al., 2018; Yang et al., 2005). Additionally, also molecules belonging to the SLAM family receptors were used to enrich for HSCs, marking them as  $\text{CD150}^+$  and  $\text{CD48}^-$ , resulting in almost 50% long-term multilineage reconstitution of single  $\text{Lin}^-\text{Sca1}^+\text{c-kit}^+\text{CD150}^+\text{CD48}^-$  cells (Kiel et al., 2005). Combining all described markers, the true HSCs must reside within the  $\text{Lin}^-\text{Sca1}^+\text{c-kit}^+\text{Flt3}^-\text{CD34}^-\text{CD150}^+\text{CD48}^-$  compartment. Another approach to identify HSCs was developed by analyzing the exclusion of a fluorescent dye from cells. One example for this strategy was described in 1996 using the fluorescent dye Hoechst 33342 (Goodell et al., 1996). Cells that excluded the Hoechst dye were shown in transplantation experiments to be highly enriched for HSCs without the use of any other marker.

The isolation of pure HSCs raised the possibility to investigate their cellular and metabolic properties and differences to other cell types in detail. The work of several groups revealed that HSCs are slowly dividing, mostly quiescent cells (Cabezas-Wallscheid et al., 2017; Cheshier et al., 1999; Foudi et al., 2009; Wilson et al., 2008), with high glycolytic (Simsek et al., 2010) but low mitochondrial activity (Vannini et al., 2016), that are dependent on autophagy (Ho et al., 2017) and have a low protein synthesis rate (Laurenti and Gottgens, 2018; Signer et al., 2014).

### 2.3. Early hematopoiesis

The first population downstream of the HSC compartment has lost its self-renewal capacity, but has retained the multipotentiality. These cells are therefore termed multipotent progenitors (MPPs) and are still able to differentiate into all blood lineages. The description of the common lymphoid progenitor (CLP),  $\text{Lin}^-\text{Sca1}^{\text{int}}\text{c-kit}^{\text{int}}\text{IL-7R}\alpha^+$ , (Kondo et al., 1997b) and

the common myeloid progenitor (CMP),  $\text{Lin}^- \text{Sca1}^- \text{c-kit}^+ \text{IL-7R}\alpha^- \text{Fc}\gamma\text{R}^{\text{low}} \text{CD34}^-$  (Akashi et al., 2000) by the group of Irving Weissman established the classical model of the hematopoietic tree proposing a stepwise differentiation of the cells toward different lineages and the simultaneous loss of other lineage potentials. In this view hematopoiesis is a unidirectional program of a sequence of defined differentiation events with the HSC at the apex, developing via restricted routes into all committed mature blood cell types (Figure 1).

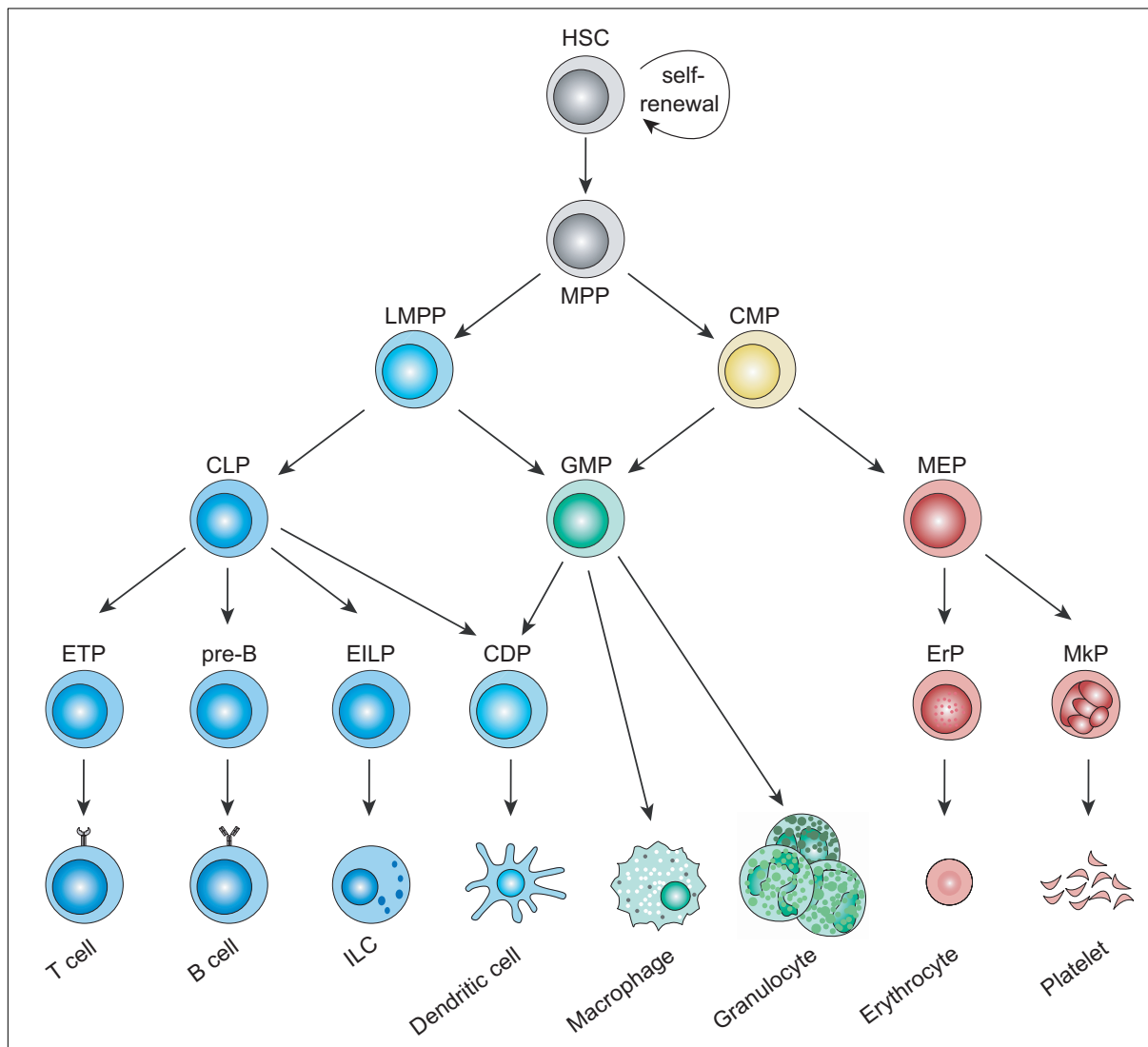


**Figure 1 | Classical hematopoietic tree.** Schematic representation of the classical hematopoietic tree with the HSC at the apex and the mature populations at the end of the differentiation process. Arrows indicate developmental progress and potential of the different progenitor populations. Colors indicate the affiliation of the populations to the erythroid/megakaryocyte (red), myeloid (green), or lymphoid (blue) lineage. Multipotent progenitors are colored grey. Progenitor populations with mixed lineage potentials have the corresponding mixed colors (erythroid/myeloid = yellow; lymphoid/myeloid = turquoise). HSC: hematopoietic stem cell, MPP: multipotent progenitor, LMPP: lymphoid-primed multipotent progenitor, CMP: common myeloid progenitor, CLP: common lymphoid progenitor, MEP: megakaryocytic-erythroid progenitor, GMP: granulocyte/macrophage progenitor, MkP: megakaryocyte committed progenitor, ErP: erythrocyte progenitor, EPLM: early progenitor with lymphoid and myeloid potential, EILP: early innate lymphoid progenitor, CDP: common dendritic cell progenitor, ILC: innate lymphoid cell, ETP: early thymic progenitor.

Based on these initial studies the first lineage decision subsequent of the MPP stage would result in the bifurcation to either the lymphoid lineage via the CLP or to the myeloid/erythroid lineage via the CMP. Thus, B, T, and innate lymphoid cells (ILCs), like natural killer cells (NK cells), are the progeny of the CLPs. Although the origin of dendritic cells (DCs) was controversial, a recent paper provided clear evidence for a lymphoid pathway for the generation of plasmacytoid DCs (pDCs) via an interleukin-7 receptor (IL-7R) positive progenitor (Rodrigues et al., 2018; Shortman and Naik, 2007). The CMP, on the other hand, gives rise to megakaryocytes and erythrocytes via the megakaryocytic-erythroid progenitor (MEP) and to monocytes/macrophages, granulocytes, and conventional DCs (cDCs) via the granulocytic-monocytic progenitor (GMP). The master transcription factors for the megakaryocytic-erythroid and granulocyte/monocyte lineages are Gata1 (Fujiwara et al., 1996; Pevny et al., 1991; Shivdasani et al., 1997) and Pu.1 (DeKoter et al., 1998), respectively. Over-expression of either one of these two factors was shown to result in a reprogramming of cells towards their corresponding lineage (Kulesa et al., 1995; Nerlov and Graf, 1998). Thus, hematopoietic development is not necessarily a unidirectional process, but contains the plasticity to overcome lineage restriction under certain circumstances. Whether this happens under normal undisturbed hematopoietic development is still unresolved.

The initial model of hematopoiesis was further challenged by the identification of several progenitor populations containing mixed lymphoid and myeloid potential. Adolfsson et al described the lymphoid-primed multipotent progenitor (LMPP), which is composed of the cells with highest Flt3 expression within the LSK compartment, that were capable to generate myeloid cells, like macrophages and granulocytes, but also lymphoid cells, like B and T cells (Adolfsson et al., 2005). However, these cells had lost the potential to differentiate to erythrocytes or megakaryocytes *in vitro* as well as *in vivo*. Based on these findings a revised road for the earliest hematopoietic developmental steps was proposed, in which the erythrocyte/megakaryocyte lineage restriction occurs before the lymphoid versus myeloid decision. Therefore, the LMPP was placed upstream of the CLP and GMP populations. Transcriptional analysis further confirmed the loss of an erythroid/megakaryocyte gene expression profile with concomitant myeloid signatures and upregulation of genes associated with lymphoid cells like *Rag1*, *Rag2*, *Dntt*, or *Ii7ra* (Mansson et al., 2007). Another population described to have mixed lineage potentials was the early progenitor with lymphoid and myeloid potential (EPLM) (Balciunaite et al., 2005b). As the name implicates these cells contain B, T, and myeloid potential and are defined as B220<sup>+</sup>CD117<sup>+</sup>CD19<sup>-</sup>NK1.1<sup>-</sup>.

Due to the identification of progenitors with diverse cell fates and mixed lymphoid and myeloid potentials, already in 2009 a new model for hematopoiesis was proposed. This “pairwise model” for hematopoiesis argues against the strict predefined pathways and branches of the classical hematopoietic tree and suggests instead that a specific cell fate can

be reached by more than one route and more than one intermediate progenitor (Figure 2) (Brown et al., 2018; Ceredig et al., 2009).

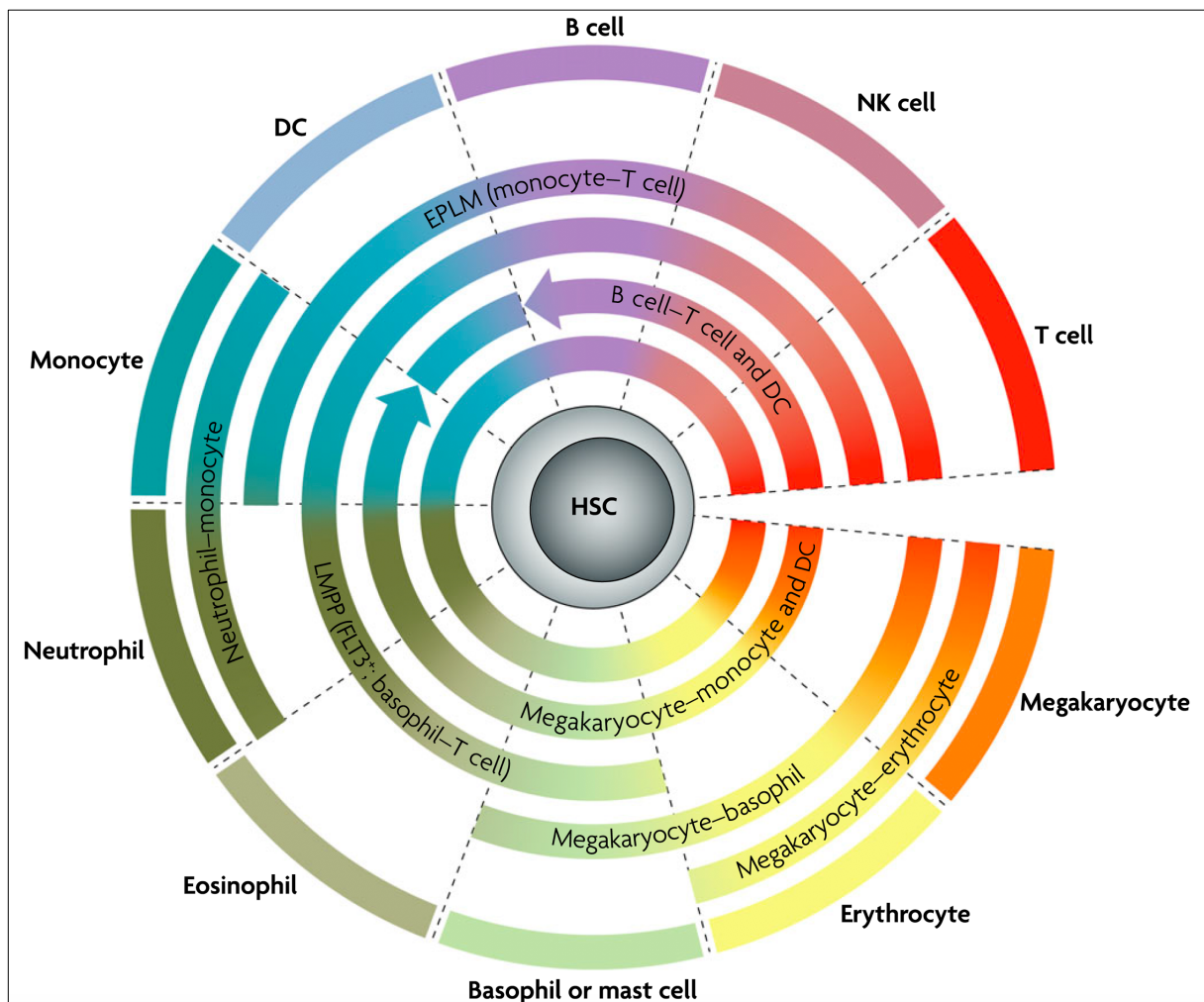


**Figure 2 | Pairwise model of hematopoiesis.** In this model hematopoiesis is depicted as a continuum of lineage relationships between HSCs and different cell fates. Partial arcs represent known progenitor populations having specific differentiation potentials and options. Overlapping arcs indicate that cell types can be reached by more than one route during hematopoiesis. HSC: hematopoietic stem cell, NK cell: natural killer cell, DC: dendritic cell, EPLM: early progenitor with lymphoid and myeloid potential, LMPP: lymphoid-primed multipotent progenitor. Taken from (Brown et al., 2018).

### 2.3.1. Heterogeneity within early progenitors

The identification of progenitor populations described in the previous section were all based on the expression of several surface markers. The mixed lineage potential that was observed for some of these progenitors could therefore result from heterogeneity within these defined populations. Technical progress in the field of single-cell analysis technologies and the usage of reporter and fate-mapping mice stimulated an important progression in the understanding of hematopoietic development and the composition of the progenitor populations. For instance, single-cell RNA sequencing of the EPLM population separated the

lymphoid-biased cells based on the overall gene expression profile, revealing that the Ly6D<sup>+</sup> fraction contains only lymphoid-biased cells, whereas the Ly6D<sup>-</sup> fraction was a mixture of different lineages (Alberti-Servera et al., 2017). A similar refinement was also implemented on the CLP, identifying Flt3 as an additional marker to define lymphoid multipotentiality (Karsunky et al., 2008). Furthermore, Ly6D was shown to mark the cells that were already biased to the B-cell lineage within the CLPs, whereas the Ly6D<sup>-</sup> fraction contained also T- and NK-cell potential (Inlay et al., 2009). Therefore, Ly6D<sup>+</sup> CLP were termed B-cell biased lymphoid progenitors (BLP) and the Ly6D<sup>-</sup> fraction was termed all lymphoid progenitors (ALP). Single-cell RNA sequencing of myeloid progenitors also revealed multiple progenitor subgroups, which could be separated into 18 different subpopulations based on their transcriptional profile (Paul et al., 2015). In particular the CMP was shown to be highly heterogeneous. Based on CD105 and CD150 expression the CMP could be sub-fractionated into four subpopulations with already defined lineage restrictions (Pronk et al., 2007). Using a Pu.1<sup>eYFP</sup> Gata1<sup>mCherry</sup> double reporter mouse Tim Schroeder's group was able to split the CMP population into cells expressing high Pu.1 levels and cells expressing Gata1 with low or no Pu.1 expression. These populations were shown to be already committed to the granulocyte/macrophage or megakaryocyte/erythrocyte lineage, respectively, concluding that the CMP is a mixture of GMPs and MEPs (Hoppe et al., 2016).

Even within the LSK compartment heterogeneity was described in several studies revealing differing relative outputs to the different lineages (Copley et al., 2012). For instance, labeling of LMPPs with lentiviral barcodes followed by subsequent transplantations into mice separated the LMPP population into three main groups containing lymphoid-biased, myeloid-biased, and DC-biased cells suggesting that the DC-fate should be considered as a distinct lineage based on their separate ancestry (Naik et al., 2013). Likewise, MPPs could be separated into three subpopulations based on the SLAM markers that were used to define HSCs and Flt3 expression. Therewith, megakaryocytic/erythroid-biased MPP2 (Flt3<sup>-</sup>CD150<sup>+</sup>CD48<sup>+</sup>), myeloid-biased MPP3 (Flt3<sup>-</sup>CD150<sup>-</sup>CD48<sup>+</sup>), and lymphoid-biased MPP4 (Flt3<sup>+</sup>CD150<sup>-</sup>CD48<sup>+</sup>) were identified (Pietras et al., 2015). In line with these results CD150 downregulation within the CD34<sup>-</sup> LSK compartment was already previously linked with reduced megakaryocyte/erythrocyte differentiation potential (Morita et al., 2010). Despite the detailed analysis and phenotypical definition of HSCs several studies also revealed that the HSC compartment itself contains some lineage bias already (Copley et al., 2012). The Müller-Sieburg and Eaves groups showed a diverse relative output to the myeloid and lymphoid lineages in limiting dilution analysis and single-cell transplantation experiments (Dykstra et al., 2007; Muller-Sieburg et al., 2004). The expression of CD41 and CD86 likewise revealed myeloid and lymphoid biased HSCs (Gekas and Graf, 2013; Shimazu et al., 2012). Furthermore, by using a mouse model reporting the expression of von Willebrand factor (vWF)

the HSC compartment was separated into vWF<sup>-</sup> and vWF<sup>+</sup> cells (Sanjuan-Pla et al., 2013). The results of this study identified vWF<sup>+</sup> platelet-primed HSCs to reside at the top of hematopoiesis, further confirming that heterogeneity exists already at the stem cell level during development.

Collectively, these data argue in favor of a revised model of hematopoiesis in which imprinting to a specific lineage is initiated already at the HSC level resulting in a progressive or graded commitment to the various differentiated cell types during hematopoiesis.

### **2.3.2. Steady-state hematopoiesis**

The architecture of the hematopoietic tree is mainly built up by results derived from cell potential measurements in colony or transplantation assays. However, this can be significantly different in the unperturbed bone marrow environment. This issue was addressed by several groups using barcoding and inducible labeling of HSCs. For instance, unique integration of the “sleeping beauty” transposon in a doxycycline inducible system in stem and progenitor cells was used to generate barcodes, which could be stably incorporated into the genome and detectable by subsequent sequencing (Sun et al., 2014). Surprisingly, this system indicated that HSCs contribute only partly to steady-state hematopoiesis in an unperturbed setting, which is instead mainly driven by the MPP compartment. This result was further supported by experiments using inducible fluorescent labeling of the HSC compartment (Busch et al., 2015). Contrary to that, another group reported that HSCs indeed contribute more during steady state hematopoiesis than proposed by the ones described above and that HSC contribution is multilineage (Sawai et al., 2016).

Most recently two groups investigated lineage fates of stem cells and progenitors in unperturbed hematopoiesis. The group of Hans-Reimer Rodewald generated a mouse model enabling barcoding based on the Cre-loxP recombination system (Pei et al., 2017). Tagging of single-cells was induced specifically in HSCs and analysis of different progenitor and mature populations for their barcode overlap revealed that HSCs mostly gave rise to multiple lineages. Furthermore, a major myelo-erythroid and a common lymphoid pathway was detected, supporting the classical tree-like model of hematopoiesis. However, they lacked analysis of megakaryocytic fate, which was addressed in detail by the group of Fernando D. Camargo. They made use again of the doxycycline inducible transposon system revealing that megakaryocyte lineage fate descends directly from long-term HSCs independently of other hematopoietic fates (Rodriguez-Fraticelli et al., 2018). Furthermore, they were able to show that progenitor subsets like CMP, GMP, and MEP consist largely of cells with unilineage outcome, suggesting that these populations are composed of a mix of already lineage-restricted cells. Multilineage outcome was only detected in the MPP populations with biases to

different lineages, as described before. Therefore, their model is still in line with a progressive developmental restriction to the different lineages, but it indicates that this is happening much earlier during native hematopoiesis and is more clonally heterogeneous than previously believed.

Taken together, the exact early developmental pathways from HSCs to the different mature blood lineages have been studied extensively, but are still under debate and need further analysis in the future in order to unravel the exact mechanisms and pathways underlying hematopoiesis.

## **2.4. B-cell development**

The development of B lymphocytes is an absolute requirement for the generation of a fully functional adaptive immune system, as they are responsible for the production of antibodies, that protect our body against all kind of harmful invading objects like pathogens and venoms. During embryogenesis B-cell development takes place in the fetal liver and postnatally in the bone marrow. The process involves several highly controlled successive stages and checkpoints ensuring the generation of the B-cell receptor (BCR) consisting of a heavy and light immunoglobulin chain, lacking self-reactivity. The capability of the BCR to recognize the tremendous amounts of different antigens is achieved by random recombination of gene segments facilitated by the recombination activated genes, *Rag1* and *Rag2* (Mombaerts et al., 1992; Shinkai et al., 1992). The initial diversity is encoded by the presence of multiple V-, D- (only heavy chain), and J-gene segments, which gets further increased by the introduction of deletions and insertions during the recombination process at the V-D and D-J junctions, resulting in a theoretical diversity of  $>10^{13}$  (Elhanati et al., 2015; Glanville et al., 2009; Nadel and Feeney, 1997). Surface and intracellular markers, cell cycle status, as well as the progress of rearrangement of the immunoglobulin heavy and light chain genes can be used in order to divide the developmental pathway of B cells into separate stages (Ehlich et al., 1994; Hardy and Hayakawa, 2001; Osmond et al., 1998; ten Boekel et al., 1995). Once B cells have accomplished to successfully produce a functional BCR they undergo final maturation processes in the spleen. During the course of an immune response, antigens are detected via the BCR, which results in the final differentiation of B cells to either memory B cells, which ensure a long-lasting protection against the pathogen, or plasma cells, which start to secrete antibodies, the soluble form of the BCR, to fight against the infection.

### 2.4.1. Lymphoid specification

Initial priming to the B-cell lineage takes place already within the LSK compartment. Several important transcriptional regulators are involved in the initiation of the B-cell program.

At the MPP stage Ikaros (encoded by *Ikzf1*), Pu.1 (encoded by *Spi1*), E2A (encoded by *Tcf3*), and Foxo1 have been associated with lymphoid priming of chromatin and enhancers (Nutt and Kee, 2007). Thus, Pu.1 acts in a dose dependent manner in the decision between the granulocyte/macrophage and the lymphoid fates. On the one hand, high Pu.1 levels will drive the cells into the myeloid direction whereas lower Pu.1 concentrations favor a lymphoid choice (DeKoter and Singh, 2000). Ikaros is regulating this process by direct repression of *Spi1* via binding to its promoter (Zarnegar and Rothenberg, 2012). Mice deficient for either Pu.1 or Ikaros displayed a severe defect in the formation of LMPPs and CLPs resulting in arrested lymphopoiesis (Nichogiannopoulou et al., 1999; Scott et al., 1994; Yoshida et al., 2006). Therefore, both factors are absolutely required for the first developmental stages of lymphoid specification. Later on, they were shown to regulate Flt3 and IL-7R expression as well as the earliest expression of lymphoid specific genes like *Rag1*, *Rag2* and *Dntt* (Carotta et al., 2010; DeKoter et al., 2002; Heizmann et al., 2013; Ng et al., 2009; Reynaud et al., 2008). Since Pu.1 and Ikaros regulate the expression of Flt3 and IL-7R, which are markers that are used to define LMPPs and CLPs, it was difficult to resolve the precise function and the exact developmental stage at which these factors are absolutely required. However, recently the group of Stephen Nutt reported, by the use of a Rag2 reporter mouse, that Pu.1 is indeed essential for the developmental progression of MPPs towards LMPPs as well as the subsequent formation of CLPs (Pang et al., 2018).

Moreover, the basic helix-loop-helix transcription factor E2A is involved at this early timepoints of B lymphopoiesis. Mice deficient for E2A display a developmental block in the development of B cells after the CLP stage (Bain et al., 1994; Zhuang et al., 1994). However, E2A plays also a role in the formation of LMPPs from HSCs as shown by reduced LMPP numbers in these mice and reduced transcription of lymphoid lineage genes (Dias et al., 2008). E2A is likewise involved in the induction of lymphoid-associated genes including *I17ra*, *Rag1*, and *Dntt* and interestingly, many of these genes share potential binding sites for Pu.1 and Ikaros indicating that these factors act in concert in the regulation of early lymphoid priming (Boller and Grosschedl, 2014). Furthermore, E2A promotes the expression of Foxo1, a factor that was shown to be important at different stages during B-cell development including the activation of Rag1 and IL-7R expression (Amin and Schlissel, 2008; Dengler et al., 2008).

### 2.4.2. Commitment to the B-cell fate

Final commitment to the B-cell lineage is achieved by the upregulation of the transcription factors Ebf1 (early B-cell factor 1) and Pax5 (paired box 5). These two factors are exclusively expressed in B-cells in the hematopoietic system and mice deficient for either of the two show a complete block of B lymphopoiesis, slightly earlier in development for Ebf1 than for Pax5 (Lin and Grosschedl, 1995; Urbanek et al., 1994).

Ebf1 was shown to become directly activated by E2A and since ectopic Ebf1 expression in E2A deficient mice is able to partially restore B-cell development, induction of Ebf1 expression seems to be one of the key functions of E2A (Seet et al., 2004; Smith et al., 2002). Ebf1 starts to be expressed at the BLP stage and its expression is mediated by two distinct promoters. The distal  $\alpha$ -promoter has potential binding sites for E2A, Ikaros, Ebf1 and shows responsiveness to Stat5 signaling, whereas the proximal  $\beta$ -promoter is driven by Ets1, Pu.1, Runx1, and Pax5 (Roessler et al., 2007; Smith et al., 2002). Ebf1 in turn activates several B-cell specific genes including *Cd79a*, *Cd79b*, *Blk*, *Igll1*, *Vpreb1* as well as *Foxo1* and *Pax5* (Akerblad et al., 1999; Akerblad and Sigvardsson, 1999; Hagman et al., 1991; Zandi et al., 2008). Ebf1 bound regions in the genome were shown to be highly enriched in binding sites for several other transcriptional regulators including E2A and Pax5, furthermore underpinning the complex cross-regulatory feedback loops that stabilize specification and commitment to the B-cell lineage (Gyory et al., 2012; Lin et al., 2010). In addition to its activating role Ebf1 is also repressing several genes important for other lineages, thereby directly antagonizing alternative cell fates. In particular, *Tcf7* and *Gata3*, which are essential for early T-cell development, are regulated by Ebf1 and were increased upon loss of Ebf1 (Banerjee et al., 2013; Nechanitzky et al., 2013). Moreover, *Id2*, which is a key player for the development of ILCs, and *Id3* are directly repressed by Ebf1 (Thal et al., 2009). This in turn leads to an increase of E2A activity, since Id proteins antagonize the DNA-binding ability of E proteins, thereby further strengthening B-cell specification. Likewise, Ebf1 inhibits myeloid differentiation, because of its repression of *Cebpa* (Pongubala et al., 2008). In summary, Ebf1 is repressing important key regulators of the T cell, ILC, and myeloid fates. This is further confirmed by the fact that inactivation of Ebf1 in already committed pro-B cells can result in a lineage conversion to T cells and ILCs (Nechanitzky et al., 2013). In addition to its role in the regulation of gene expression, Ebf1 acts furthermore on the epigenetic landscape, changing the chromatin accessibility, thereby paving the way for B-cell programming (Boller et al., 2016; Li et al., 2018).

Upregulation of Pax5 is required to fully establish B-cell commitment. Mice deficient for Pax5 exhibit an arrested B-cell development at the pro-B stage, which is characterized by the expression of many B-cell specific genes and D<sub>H</sub> to J<sub>H</sub> rearrangements of the heavy chain. (Nutt et al., 1999; Nutt et al., 1997). Normally pro-B cells are defined as

B220<sup>+</sup>CD19<sup>+</sup>CD117<sup>+</sup>CD127<sup>+</sup>, but since Pax5 is controlling the expression of CD19, these cells are negative for this marker in Pax5 deficient mice (Nutt et al., 1998). Analysis for a corresponding CD19<sup>-</sup> population in WT mice led to the discovery of the EPLM population (Balciunaite et al., 2005b). Similar to the EPLM population, Pax5 deficient pro-B cells were shown to retain the capability for *in vitro* and *in vivo* differentiation into myeloid and T-lymphoid cells (Rolink et al., 1999b; Rolink et al., 2002). However, the clear-cut difference between these cells is the high efficiency of EPLM to generate B-cells, which is completely missing in Pax5 deficient pro-B cells. Upon conditional inactivation of Pax5 already committed pro-B and even mature B cells regained the possibility to differentiate into other lineages, further strengthening the importance of this factor for the B-cell fate (Cobaleda et al., 2007; Mikkola et al., 2002). Therefore, Pax5 is not only important for the commitment to the B-cell fate, but is also an absolute requirement for all subsequent stages during the life of a B-cell. This is because it not only establishes, but also maintains the global-lineage-specific architecture of B cells until its downregulation upon plasma-cell differentiation (Horcher et al., 2001; Johanson et al., 2018; Nutt et al., 2001). Similarly to Ebf1, components of the pre-BCR and BCR including *CD19*, *Blnk*, *CD79a*, and *Igll1* are target genes of Pax5 (Cobaleda et al., 2007). Furthermore, Pax5 binds to the distal  $\alpha$ -promoter of *Ebf1* and therefore a main function of Pax5 is also to maintain and enhance Ebf1 levels resulting in a positive feedback loop between these two factors ensuring B-cell specification (Roessler et al., 2007). The importance of this feedback mechanism is further illustrated by the fact that cells with heterozygous loss of both Ebf1 and Pax5 displayed an increased T-cell potential *in vivo* and *in vitro*, demonstrating the collaborative activity of these two factors in preserving B-cell identity (Ungerback et al., 2015). However, Pax5 is not only acting as an activator but also as a repressor, promoting B-cell commitment by inactivation of non-B-cell genes. This includes the genes encoding the surface receptors Mcsf-R and Notch1, which are key players in myeloid and T-cell development, respectively (Souabni et al., 2002; Tagoh et al., 2006). This also explains the fact that pro-B cells deficient for Pax5 gain the capability to differentiate into myeloid and T-lymphoid cells. Therefore, Pax5 represses surface receptors and Ebf1 antagonizes transcription factor genes of alternative cell fates, resulting in a double-lock mechanism to establish B-cell specification.

### 2.4.3. Early developmental stages

After the BLP stage surface expression of B220 is one of the first markers associated with B-cell progenitors. Therefore, the Ly6D<sup>+</sup> EPLM population might developmentally arise from the BLP, which is also implied by the overlapping surface expression of c-kit (CD117), IL-7R (CD127), and Flt3 (CD135) between these two populations. A large fraction of the Ly6D<sup>+</sup> EPLM already expresses Ebf1, but is not yet fully committed to the B-cell lineage, since the

cells still retain T-cell potential in limiting dilution assays (Alberti-Servera et al., 2017). Thus, these Ebf1 positive cells most likely resemble the last stage before commitment to the B-cell fate. Recently, the group of Mikael Sigvardsson revealed another way to dissect successive developmental stages from the CLP until final commitment (Jensen et al., 2018). By the use of the surface markers Gfra2 and Bst1 they were able to split BLPs into the three distinct subpopulations BLP1, BLP2, and BLP3. Gfra2 upregulation in BLP2 cells coincided with Ebf1 induction and subsequently with the expression of B-cell specific genes. Thus, these cells most likely overlap with the Ebf1<sup>+</sup>Ly6D<sup>+</sup> fraction of the EPLM population described above. At the BLP3 stage, identified by additional Bst1 expression, cells are committed to the B-cell lineage and Pax5 expression is initiated. All successive populations after commitment are marked by the expression of CD19, which is induced by Pax5.

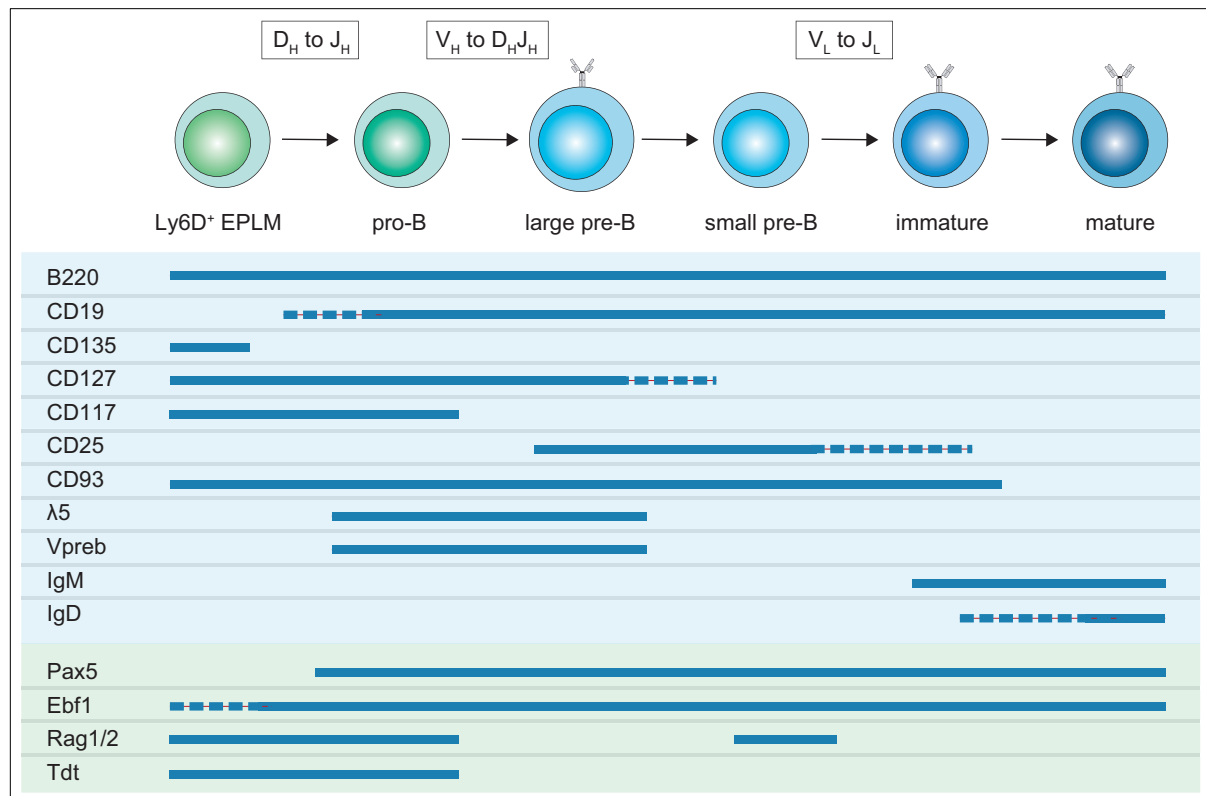


**Figure 3 | Early B-cell development.** Schematic representation of early B-cell developmental stages in the bone marrow. Sequential stages are connected by arrows indicating the developmental progression from Ly6D<sup>+</sup> EPLM up to mature B cells. Recombination process is indicated in boxes above the different populations. Table below the populations shows surface marker expression of the different populations (blue) as well as intracellular expression of transcription factors and genes involved in the recombination process (green). EPLM: early progenitor with lymphoid and myeloid potential

The different early developmental stages in the bone marrow can be further separated by the use of the surface markers c-kit, CD25, IL-7R, CD93, by the status of the rearrangements of the heavy and light chain loci, and by their cell cycle status (Figure 3) (Ceredig and Rolink, 2002; Rolink et al., 1994; ten Boekel et al., 1995).

The first committed cell, the pro-B cell, is marked by the expression of CD19 and c-kit and is characterized genotypically by  $D_H$ - $J_H$  rearrangements of the heavy chain loci (ten Boekel et al., 1995). After completion of the  $V_H$ - $D_H$ - $J_H$  recombination cells are tested for an effective rearrangement. Only if the recombination process resulted in the expression of a functional heavy chain cells are allowed to proceed in development. This selection is achieved by the formation of the pre-BCR, which is composed of the heavy chain and the surrogate light chain proteins VpreB and  $\lambda 5$ , together with the signaling molecules  $Ig\alpha$  and  $\beta$  (Karasuyama et al., 1990; Kitamura et al., 1992; Kudo and Melchers, 1987; Sakaguchi and Melchers, 1986). Cells that reach this status are termed large pre-B cells, defined as  $c\text{-kit}^-CD25^+CD127^+$  (Rolink et al., 1994). Signaling of the pre-BCR on the surface of these cells initiates a proliferative expansion and induces survival signals, thereby enriching for cells with a successful heavy chain rearrangement (Ohnishi and Melchers, 2003; Rolink et al., 2000; ten Boekel et al., 1995). Signaling via the pre-BCR furthermore ensures allelic exclusion by inducing a transient downmodulation of the recombination machinery (Grawunder et al., 1995; Mostoslavsky et al., 2004). The proliferation and survival signals during that step are further mediated by IL-7R signaling, which acts in concert with the pre-BCR for an effective expansion. Cells undergo five to six divisions in total after activation of the pre-BCR (Decker et al., 1991; Rolink et al., 2000). At the same time, the pre-BCR initiates a transcriptional program including the activation of E2A, Irf4, Irf8 and Aiolos, which will eventually induce cell-cycle arrest as well as opening of the light chain locus (Lazorchak et al., 2006; Lu et al., 2003; Ma et al., 2006; Mandal et al., 2009; Stadhouders et al., 2014). Aiolos in particular, through repression of the *Igll1* gene, is responsible for the termination of the pre-BCR complex (Thompson et al., 2007). Induction of cell-cycle arrest at that stage is essential for further differentiation, as demonstrated by an impaired development if growth supporting genes are not efficiently silenced (Lindner et al., 2017).

The transition from proliferation to quiescence marks the entrance to the small pre-B stage (Parker et al., 2005). These cells are defined by a downregulation of the IL-7R and their reduced size compared to the proliferating large pre-B cells. Furthermore, the recombination machinery becomes re-expressed initiating recombination at the  $\kappa$  or  $\lambda$  immunoglobulin light chain loci (ten Boekel et al., 1995). For the light chain, besides allelic exclusion, also isotype exclusion is applied, resulting in the expression of only one light chain that is either  $\kappa$  or  $\lambda$  (Mostoslavsky et al., 1998; Neuberger et al., 1989).

Once a light chain is generated the BCR is formed successfully, provided that pairing of the light chain with the heavy chain is possible. Surface IgM expression defines the cells as immature B cells, which can be distinguished from mature recirculating B cells by the expression of CD93 (Rolink et al., 1998). If pairing of the light chain with the heavy chain is not

successful or the resulting BCR has specificity against self-antigens, secondary rearrangements of the light chain can be initiated, a process known as receptor editing (Gay et al., 1993; Rolink et al., 1993; Tiegs et al., 1993). It is believed that the BCR signal strength of newly formed immature B cells determines whether cells continue in development or have to undergo receptor editing. In that scenario anti-nonsel BCRs with effective pairing of the heavy and light chains induce the right amount of BCR signaling (tonic BCR signaling) resulting in developmental progression of these cells. An autoreactive BCR, on the other hand, induces a much stronger signal, whereas inefficient pairing results in a signal that is too weak (Tussiwand et al., 2009). The importance of an appropriate BCR signal is further highlighted by the developmental perturbation in mice with deficiencies in regulators of the BCR signal strength (Khan et al., 1995; Liu et al., 1998; Sato et al., 1996). For their final maturation steps immature B cells leave the bone marrow and migrate to the spleen.

#### 2.4.4. Late developmental stages

Around  $2 \times 10^6$  immature B cells per day reach the periphery in a mouse (Rolink et al., 1998; Rolink et al., 1999a). Approximately 25% of these have undergone receptor editing (Casellas et al., 2001; Retter and Nemazee, 1998). Immature B cells that have migrated to the spleen from the bone marrow are called transitional B cells. They can be distinguished from their mature counterparts by surface receptor expression, their short half-life time and their susceptibility to anti-IgM induced apoptosis (Allman et al., 2001; Loder et al., 1999; Rolink et al., 1998). Based on the expression of several markers transitional B cells can be subdivided into  $CD93^+CD21^-CD23^-IgM^{high}IgD^{low}$  T1, and  $CD93^+CD21^+CD23^-IgM^{high}IgD^{int}$  T2 populations (Rolink et al., 2004). A third transitional B-cell population called T3 is nowadays believed to contain mainly anergic B cells (Merrell et al., 2006). In contrast to mature B-cell populations transitional B cells still undergo apoptosis upon BCR triggering, indicating that they are still subject to selection against autoreactive B cells (Carsetti et al., 1995). Transitional B cells become also sensitive to the action of the pro-survival factor Baff as demonstrated by the block at the T1 stage occurring in  $Baff^{-/-}$  or  $Baff-R^{-/-}$  mice (Gross et al., 2001; Schiemann et al., 2001; Thompson et al., 2000; Yan et al., 2001). This dependency on Baff for survival persists also in mature marginal zone and follicular B-cell (MZB and FoB) populations, whereas B1 B cells are Baff-independent (Rauch et al., 2009).

The conventional B2 B cells, consisting of MZB and FoB, together with B1 B cells represent the different mature B cell populations (Figure 4). B1 cells were first described in 1983 as a unique B-cell population (Hayakawa et al., 1983). They are defined as  $CD19^{high}CD11b^+CD23^-IgM^{high}IgD^{low}$  and can be further subdivided into  $CD5^+$  and  $CD5^-$  B1a and B1b cells, respectively. Their predominant locations are the peritoneum and pleural cavities.

Whether B1 B cells share a common progenitor with B2 B cells or represent a completely separate lineage has been under debate for a long time. Due to the absence of N-nucleotide additions in the VDJ junctions of the majority of B1 B cells they are thought to be mainly fetally derived, since the Tdt enzyme, which is responsible for these additions during recombination, is only expressed during adulthood (Desiderio et al., 1984; Feeney, 1992). The group of Kenneth Dorshkind identified a distinct B1 progenitor in the fetal bone marrow of mice, proposing a distinct developmental pathway for B1 B cells (Montecino-Rodriguez et al., 2006). However, others proposed that BCR signal strength as well as responsiveness to T-cell independent antigens determines B1 fate from a common progenitor with B2 cells (Lam and Rajewsky, 1999). Since the two models are not mutually exclusive both pathways might actually contribute. B1 B cells are responsible for the production of so called natural antibodies, which can bind to different conserved pathogen-associated antigens (Panda and Ding, 2015). Thus, the B1 BCRs exhibit a more restricted repertoire with the preferential usage of certain germline V(D)J gene segments, representing a rather innate response to pathogens (Kantor et al., 1997; Tornberg and Holmberg, 1995).

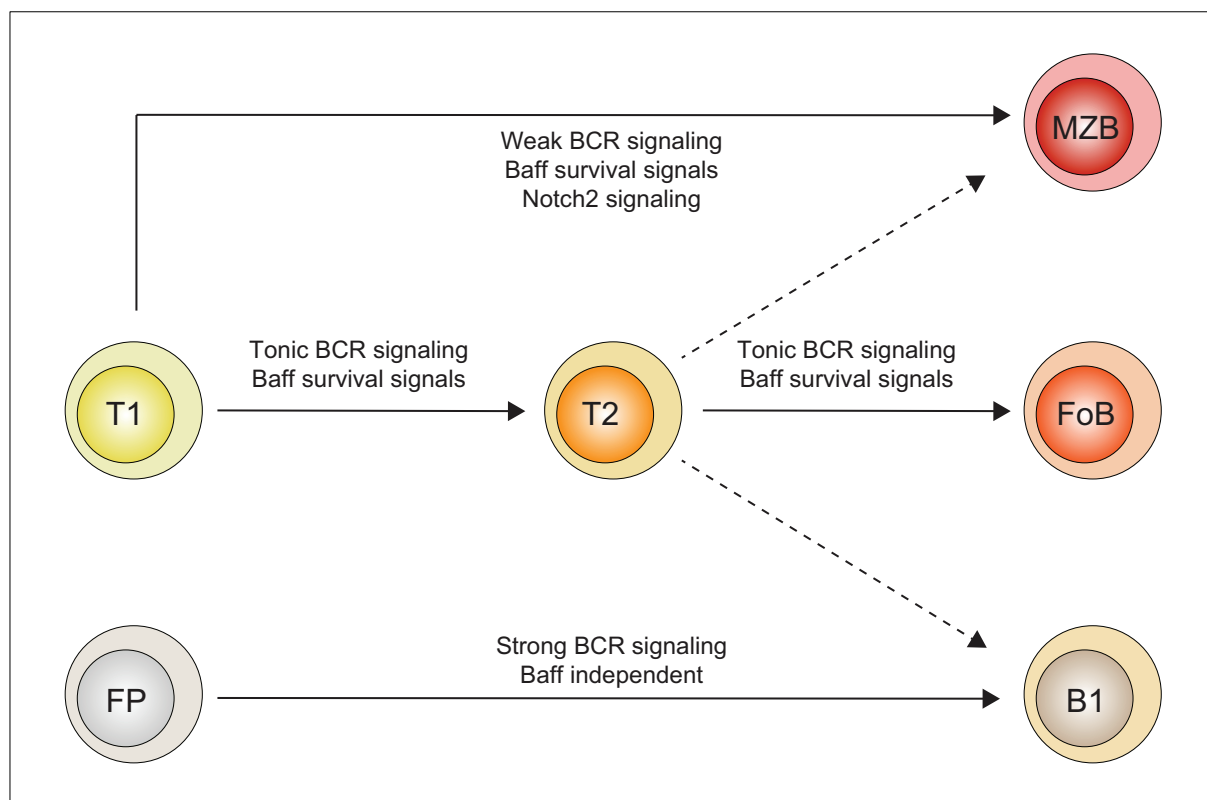


**Figure 4 | Late stages of B-cell development.** Schematic representation for the generation of mature B-cell subsets. MZB and FoB cells are derived from transitional B cells, which undergo their final maturation steps in the spleen. BCR signal strength and the induction of Notch2 signaling are responsible for the bifurcation to either the MZB or FoB fate. Origin of B1 B cells remains still controversial as some experiments indicate a separate origin from a distinct fetal B1 progenitor, whereas other data argue for a common origin with B2 cells, in which case BCR signal strength and BCR specificity direct differentiation to the B1 fate. B2 development is dependent on Baff survival signaling, whereas B1 cells are independent of that. T1: transitional 1; T2: transitional 2; MZB: marginal zone B cell; FoB: follicular B cell; FP: fetal progenitor. Adapted from (Pillai and Cariappa, 2009).

The B2 B-cell populations are the progeny of transitional B cells. The decision between the MZB and FoB-cell fate was proposed to rely on BCR-signaling strength (Pillai and Cariappa, 2009). Weak signaling promotes MZB, whereas stronger signals promote FoB-cell differentiation (Casola et al., 2004). An apparent difference between FoB and MZB cells is the dependency of the latter on Notch2 signaling, manifested by the strong reduction of this population in conditional Notch2-deficient mice (Saito et al., 2003). A recent study indeed postulated that BCR signals influence the MZB-lineage choice by regulating the surface expression of Adam10 (Hammad et al., 2017), which is important for the activation of Notch2 (Gibb et al., 2010). Furthermore, they showed that an Adam10 positive fraction within the T1 population is most likely the direct progenitor of MZB cells whereas T2 cells only marginally contribute to the MZB-cell pool. As suggested by their name MZB are located between the marginal sinus and the red pulp of the spleen and build a first line of defense against encapsulated blood-borne bacterial pathogens (Pillai et al., 2005). They are defined as  $CD19^+CD93^-CD21^{high}CD23^{low}IgM^{high}IgD^{low}$ . The large majority of mature B cells belong to the FoB population characterized as  $CD19^+CD93^-CD21^+CD23^+IgM^{low}IgD^{high}$ . They are located in the follicles of the spleen and lymph nodes adjacent to the T-cell zone, thereby mediating mainly T-cell dependent immune responses.

## 2.5. T-cell development

The second arm of the adaptive immune system is built by T lymphocytes. Development of T cells is restricted to the thymus. As it is for B cells, the development of T cells follows a highly controlled pathway including several important checkpoints, ultimately leading to the production of a functional T-cell receptor (TCR) that lacks reactivity to self-antigens. The successive stages can be distinguished by the use of surface markers as well as by the status of the rearrangement of the TCR  $\beta$ - and  $\alpha$ -chain (Ceredig and Rolink, 2002). In many instances this process shows similarities to the generation of B cells; however, it also involves many factors and regulations that are unique to T-cell development. Cells that have passed all stages and selection checkpoints mature either towards a CD4-positive or CD8-positive cell. T cells expressing CD4 are classified as helper cells, since their main function is to support other cells by the production of cytokines or by direct cell-cell interactions to fight against different kinds of infections. Moreover, a specific subset of CD4 T cells, termed regulatory T cells, was shown to have an important function in controlling immune responses and to specifically prevent reactions to self-antigens. CD8 T cells, or cytotoxic T cells, on the other hand, directly recognize and eliminate transformed cells that were either infected or display an abnormal phenotype like in the case of cancer cells. In addition to the conventional

$\alpha\beta$ -T cells several other T-cell subsets mature in the thymus, such as  $\gamma\delta$ -T cells, MAIT (mucosal associated invariant T) cells, and NK-T cells.

### 2.5.1. Seeding of the thymus

The production of T lymphocytes takes place exclusively in the thymus. Continuous production therefore requires migration of hematopoietic progenitors from the bone marrow via the blood to the thymus. In order to do so progenitors have to be mobilized from the bone marrow into circulation. HSCs can be found in the peripheral blood, where downstream progenitor populations like MPPs, LMPPs, and CLPs can also be detected at very low frequencies (Goodman and Hodgson, 1962; Lai and Kondo, 2007; Perry et al., 2006; Schwarz and Bhandoola, 2004; Wright et al., 2001). However, the physiological mechanism underlying the mobilization of bone marrow progenitors into the blood is still not completely resolved. Migration of cells is mainly driven by chemokines and their corresponding receptors. Homing and retention of cells to the bone marrow environment was shown to be regulated by the chemokine receptor Cxcr4, whose expression forces the cells to migrate towards its ligand Cxcl12, which is highly expressed by bone marrow endothelial cells (Ceradini et al., 2004; Pitchford et al., 2009). Sphingosine-1 phosphate receptor 1 (S1PR<sub>1</sub>) plays a role in the mobilization of immature B cells from the bone marrow and might therefore be also relevant for the egress of earlier progenitors (Allende et al., 2010).

The next step after mobilization from the bone marrow into circulation is the efficient homing to the thymus. Several groups independently postulated that settling of the thymus is a very rare event with around 10 cells entering per day (Kadish and Basch, 1976; Spangrude and Scollay, 1990; Wallis et al., 1975). Efficient homing requires the concerted action of several chemokine receptors, integrins and selectin ligands (Scimone et al., 2006). For instance, efficient thymic settling relies on the expression of Psgl-1 on the entering cells and the presence of P-selection on the thymic endothelium (Gossens et al., 2009). Progenitors lacking Psgl-1 were defective in the generation of thymocytes in competition with wild-type controls (Rossi et al., 2005). Moreover, the chemokine receptors Ccr7 and Ccr9 were demonstrated to function in thymus seeding. The ligands for these two receptors, Ccl21/Ccl19 and Ccl25 respectively, are produced by the stromal epithelial cells of the thymus (Misslitz et al., 2004; Tenno et al., 2018; Uehara et al., 2002). Both Ccr7- as well as Ccr9-deficient cells were defective in generating thymocytes after intravenous but not intrathymic injections (Krueger et al., 2010; Schwarz et al., 2007; Zlotoff et al., 2010).

The exact bone marrow progenitor population to settle the thymus has been a matter of debate for a long time, since many different progenitors harbor T-cell potential. The necessity of Ccr7, Ccr9, and Psgl-1 for efficient trafficking and entrance into the thymus

implicates that these receptors must be expressed by potential candidates, unless they get upregulated during their migration in the blood. HSCs are negative for both Ccr7 and Ccr9, and indeed HSCs were shown to rapidly generate T-cells only after intrathymic but not intravenous injections (Schwarz et al., 2007). Several independent approaches localized the major thymus seeding capacity to be within the Flt3 positive pool of progenitor cells, including the LMPP and CLP populations (Saran et al., 2010; Serwold et al., 2009). A part of LMPPs and most CLPs express Ccr7, whereas Ccr9 expression is more limited to only subsets of these Ccr7<sup>+</sup> LMPPs and CLPs (Krueger et al., 2010; Zlotoff and Bhandoola, 2011). Additionally, Psgl-1 expression is highest on Ccr9<sup>+</sup> LMPPs and Ly6D<sup>-</sup> CLPs (Sultana et al., 2012). Therefore, it is reasonable to predict that the most competent thymus settling progenitors reside within these subsets of LMPPs and CLPs.

### 2.5.2. Initiation of the T-cell program

The most immature populations in the thymus are generally characterized by the absence of expression of CD4 and CD8 and are therefore termed double negative (DN). By the use of several additional surface markers DN thymocytes can be further subdivided into consecutive stages as summarized in Figure 5. The earliest progenitors are defined by high expression of CD44 and c-kit and the absence of CD25 (DN1) (Godfrey et al., 1993; Godfrey et al., 1992; Massa et al., 2006). Cells that have just entered the thymus, named early thymic progenitors (ETPs), furthermore express Flt3 and are negative for IL-7R. These cells are not yet committed to the T-cell lineage, but instead contain the potential to differentiate into B cells, NK cells, as well as a variety of myeloid cells (Balciunaite et al., 2005c; Bell and Bhandoola, 2008; Ceredig et al., 2007; Luc et al., 2012; Luis et al., 2016; Wada et al., 2008).

The T-lineage program in ETPs is initiated by the activation of Notch1 signaling. This is specifically induced in the thymic environment due to the dense presentation of the Notch1 ligand Delta-like 4 (Dll4) on thymic epithelial cells, which triggers the release of intracellular Notch1 domain (Love and Bhandoola, 2011). Association with the DNA-bound recombining binding protein suppressor of hairless (Rbpj) results in the recruitment of a transcriptional co-activator complex to activate the expression of Notch1 target genes (Radtke et al., 2013). The absolute requirement of Notch1 for T-cell development is manifested by the complete absence of mature T cells and also T-cell precursors in the thymus in its absence (Radtke et al., 1999). Moreover, expression of constitutively active Notch1 in hematopoietic progenitors resulted in a severely altered lymphoid development in the bone marrow, namely a block in B-cell development and instead the ectopic generation of T cells (Pui et al., 1999). Due to the importance of Notch1 during these early stages, this first part of the development of T cells in the thymus is termed "Notch-dependent". Notch1 signaling drives proliferation of the cells and

becomes increasingly important also for their viability as they progress through early development.

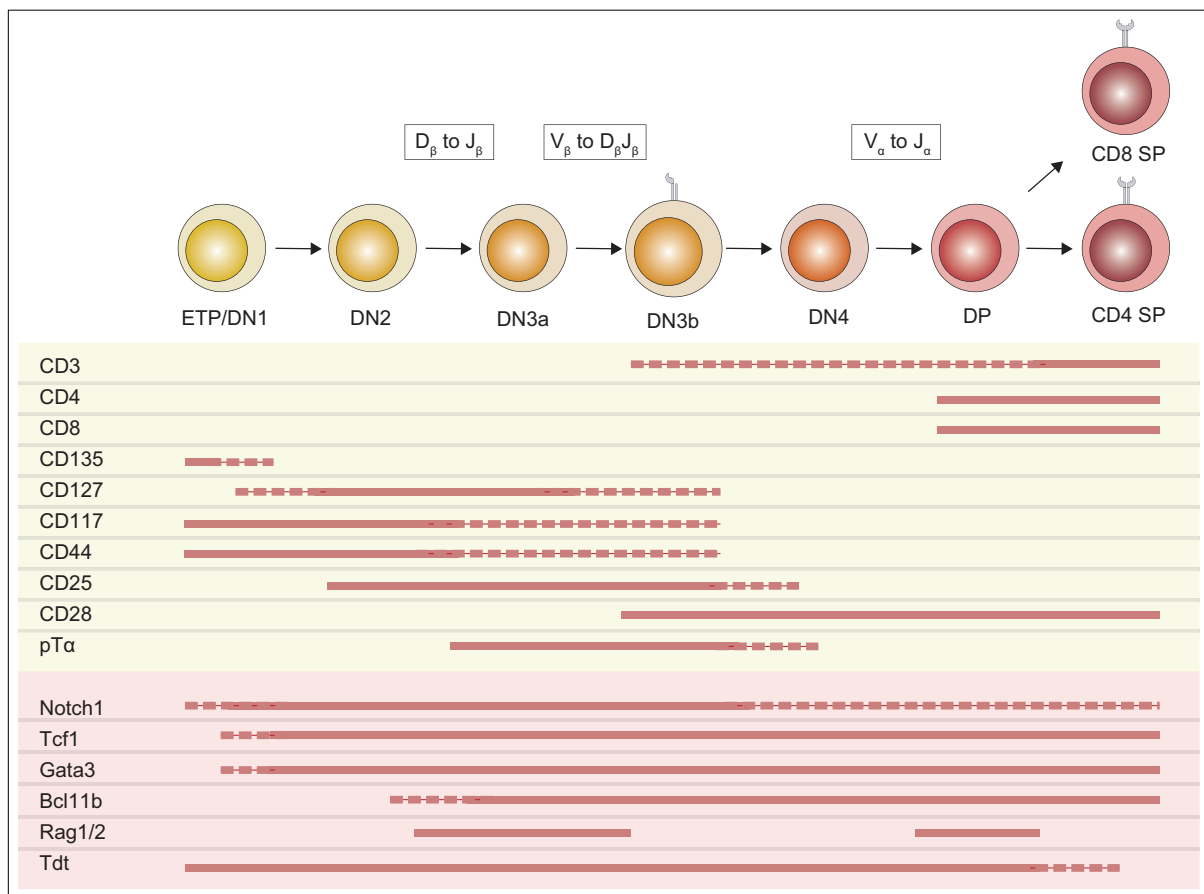


**Figure 5 | T-cell development.** Schematic representation of early T-cell development stages in the thymus. Sequential stages are connected by arrows indicating the developmental progression from ETPs up to mature SP T cells. Recombination processes are indicated in boxes above the different populations. Table below the populations shows surface marker expression of the different populations (yellow) as well as intracellular expression of transcription factors and genes involved in the recombination process (red). DN: double negative, DP: double positive, SP: single positive.

Transcriptionally, Notch1 signaling in ETPs is responsible for the initiation of the expression of several important regulators of early T-cell development, including the induction of the genes *Hes1*, *Gata3* and *Tcf7*. *Hes1* is a transcriptional repressor that is turned on in ETPs and stays highly expressed until final commitment to the T-cell lineage (Wendorff et al., 2010). It was shown to play a role in antagonizing myeloid differentiation and supporting proliferative expansion of ETPs (De Obaldia et al., 2013; Tomita et al., 1999). *Tcf7* and *Gata3* are two absolutely crucial genes for T-cell fate initiation and are activated in parallel by Notch1. Deficiency of either of the two was shown to impair survival and differentiation of ETPs as well as their progeny (Germar et al., 2011; Hosoya et al., 2009). *Tcf7* was proven to be activated by Notch1 directly, but its expression becomes independent of Notch1 in the later stages of T-cell development (Germar et al., 2011; Weber et al., 2011). Primarily it collaborates with

Notch1 in the positive regulation of T-cell specification. Over-expression of Tcf1 resulted in the activation of T-cell specific genes in multipotent progenitors including *Gata3*, *Bcl11b*, *Il2ra*, *CD3g*, *Lat*, *Lck*, and endogenous *Tcf7* even in the absence of Notch1 signaling (Weber et al., 2011). Most recently, the mechanism of this activation by Tcf1 was shown to rely on its ability to target silent chromatin and increases its accessibility, thereby controlling the epigenetic identity of T cells (Johnson et al., 2018). Similarly, Gata3 has important dose-dependent functions for survival, growth, specification and commitment during early T cell specification, and remains crucial also at later differentiation stages after TCR expression (Hosoya et al., 2010; Yui and Rothenberg, 2014). In addition, Gata3 expression in ETPs is responsible for the exclusion of the B-cell fate (Garcia-Ojeda et al., 2013). However, the expression level of Gata3 has to be tightly controlled, since enforced expression resulted in an impaired T-cell development as severe as in the absence of Gata3 (Xu et al., 2013).

Transition to the DN2 stage is marked by the up-regulation of the surface receptor CD25 (IL2 receptor  $\alpha$ , *Il2ra*), which is also directly induced by Notch1. At this stage the expression of several key transcriptional regulators like *Runx1*, *Gfi1*, *Ets1*, *Tcf12*, as well as *Gata3* and *Tcf7* is further increased. As a consequence, initial expression of the T cell specific genes *Thy1*, *Cd3g*, *Cd3d*, and *Cd3e* can be detected. Furthermore, *Rag1/2* gene expression is activated, initiating the process of rearrangement of the TCR $\beta$ , TCR $\gamma$ , and TCR $\delta$  chains (Rothenberg, 2014). Upregulation of the IL-7R on these cells becomes important for their expansion as well as for the decision between the  $\alpha\beta$  and  $\gamma\delta$  T-cell fate (Huang et al., 2001; Ye et al., 2001). Nevertheless, DN2 cells are still not fully committed to the T-cell lineage as they were shown to retain the capability to differentiate into NK cells, DCs, mast cells, a subset of ILCs, macrophages, and granulocytes (Rothenberg, 2011; Taghon et al., 2007; Wong et al., 2012).

Committed cells were initially discovered with the use of a Lck-GFP transgene reporter mouse (Masuda et al., 2007). Based on reporter expression the DN2 population could be subdivided into GFP<sup>-</sup>, which retained dendritic cell potential, and GFP<sup>+</sup> cells, which were fully committed to the T-cell lineage. Functionally this step is dependent on the up-regulation of the transcription factor Bcl11b, whose activation is absolutely required for T-lineage commitment (Ikawa et al., 2010; Li et al., 2010a; Li et al., 2010b). The enhancer and promoter regions that participate in *Bcl11b* activation contain binding sites for Rbpj, Tcf1, Gata3, and Runx1, which were all shown to positively regulate *Bcl11b* expression (Garcia-Ojeda et al., 2013; Li et al., 2013; Weber et al., 2011). Thus, it can be envisaged that a certain threshold expression of these regulators has to be reached for proper Bcl11b activation, since they are expressed already at earlier stages of T-cell development. Concurrent with Bcl11b activation, E-protein- and Notch1-dependent gene expression increases, resulting in the upregulation of genes

belonging to the VDJ recombination machinery including *Rag1*, *Rag2*, *Dnmt*, *CD3e* and the first expression of the *Ptcra* gene, encoding the surrogate chain for a rearranged *TCR $\beta$*  gene product (Georgescu et al., 2008; Takeuchi et al., 2001; Xu et al., 2013). At the same time many genes important in the early stages become silenced. Phenotypically this is determined by a reduction of c-kit expression on the surface of the cells, potentially directly regulated by *Bcl11b*. Furthermore, *Spi1* expression is terminated at this point, which is another contributor to lineage exclusion, since its termination antagonizes the myeloid and DC fate (Anderson et al., 2002). Additionally, genes involved in the progenitor-like phenotype before commitment get repressed such as *Tal1*, *Gfi1b*, *Hhex*, *Bcl11a*, *Lmo2*, *Mf2c*, and *Lyl1* (Mingueneau et al., 2013). Overall, proliferation of the cells slows down, while recombination activity intensifies by the time that the first crucial checkpoint of T-cell development is reached.

### 2.5.3. $\beta$ -selection

At the DN3a stage cells are characterized by lower c-kit and CD44 expression, but sustained high levels of CD25. Morphologically these cells are very small in size since they undergo TCR $\beta$  rearrangements, which requires exit from cell cycle (Hathcock et al., 2011; Lin and Desiderio, 1994). Accordingly, highest expression of the recombination machinery is detected in these cells. Moreover, CD3 components, Notch1, Tcf1, Gata3, and E proteins reach their expression maxima.

VDJ-recombination itself is a random and imprecise process, failing in two-thirds of the attempts to maintain the translational reading frame, thereby generating non-functional  $\beta$ -chains. On account of this, almost half of the cells are not able to productively rearrange their TCR $\beta$  loci on any allele (Mallick et al., 1993). Removal of cells with a non-functional rearrangement consists the first important checkpoint in T-cell development, termed  $\beta$ -selection. During this process it is ensured that only those cells with a productive  $\beta$ -chain will undergo further differentiation, whereas the others will die by apoptosis. This selection is achieved by assembling of the pre-TCR, which is composed of a productively rearranged  $\beta$ -chain, the CD3 signaling components, and the invariant pre-T cell receptor  $\alpha$  (pT $\alpha$ ) chain (Saint-Ruf et al., 1994) (Figure 6). Expression of the *Ptcra* gene, that encodes the pT $\alpha$ -chain, is jointly regulated by Notch1 and E proteins and reaches its highest expression in DN3a cells (Ikawa et al., 2006; Reizis and Leder, 2002). Subsequent signaling by the pre-TCR is dependent both on its extracellular domains, which are important for oligomerization, and its intracellular cytoplasmic tail, which facilitates signal transduction. This signaling results in survival and proliferative expansion of DN3 cells (Aifantis et al., 2002; Irving et al., 1998; Jacobs et al., 1996; Yamasaki et al., 2006). Moreover, signaling is constitutive and ligand independent, which is believed to lead to a rapid internalization and degradation of the pre-

TCR complex, since only very low expression can be detected on the surface of pre-T cells (Panigada et al., 2002; Yamasaki and Saito, 2007). The requirement of pre-TCR signaling for further differentiation is manifested by the arrest of T-cell development in mice deficient for the pT $\alpha$  chain, the CD3 signaling components, or the genes of the recombination machinery (Fehling et al., 1995; Malissen et al., 1995; Shinkai et al., 1992).

Pre-TCR signaling disrupts the state of quiescence and induces a phase of proliferation that is strictly required for further differentiation (Kreslavsky et al., 2012). Moreover, it induces key survival signals. Thus, increased cell size as well as upregulation of the co-stimulatory markers CD27, CD28, and CD71 can be used to define the DN3b stage in development, which is composed of cells that have passed the  $\beta$ -selection checkpoint and express a functional pre-TCR (Brekelmans et al., 1994; Gravestien et al., 1996; Taghon et al., 2006; Williams et al., 2005). Furthermore, *Rag1/2* gene expression is downregulated thereby terminating TCR $\beta$  rearrangements, ensuring allelic exclusion, as well as excluding the  $\gamma\delta$ -T-cell fate (Aifantis et al., 1998; Lopez-Rodriguez et al., 2015; Saint-Ruf et al., 2000).

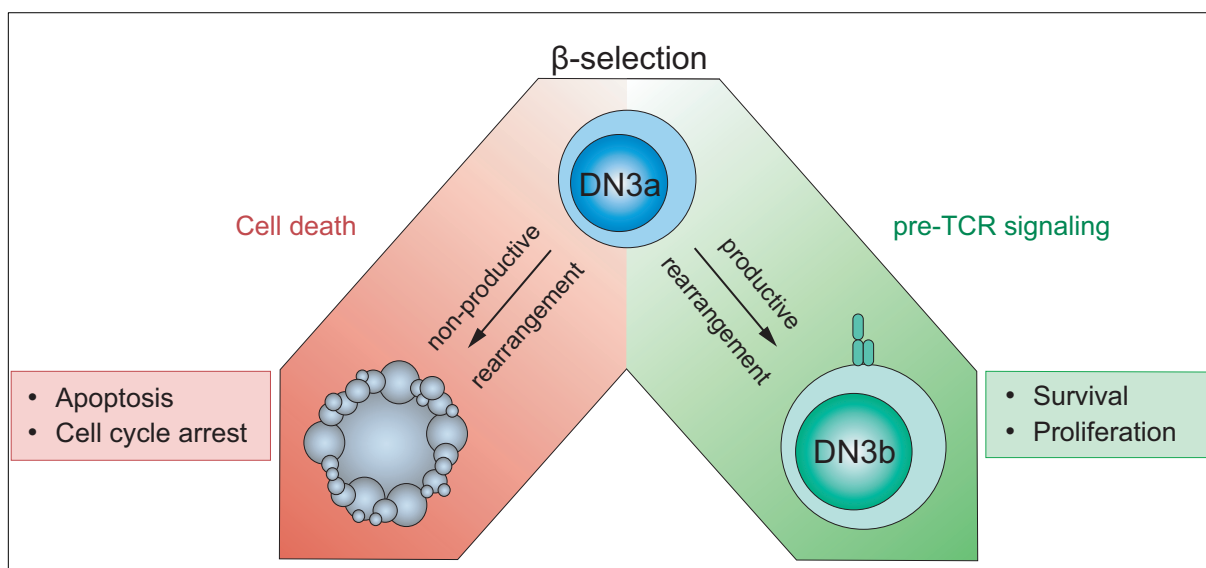


**Figure 6 |  $\beta$ -selection.** Schematic representation of the concept of  $\beta$ -selection. DN3a cells undergoing TCR $\beta$  recombination either produce a functional rearrangement on one allele or fail to rearrange on both. Productive rearrangement will lead to the formation of the pre-TCR and subsequent signaling results in survival, proliferation as well as differentiation of the cells. Cells with a non-productive rearrangement on the other hand will undergo apoptosis. Pre-TCR: pre-T cell receptor.

On a transcriptional level, pre-TCR signaling induces the activity of several important programs responsible for expansion and survival of the cells. For instance, NF $\kappa$ B as well as NFAT activity are turned on and are indispensable for the transition through  $\beta$ -chain selection (Aifantis et al., 2001; Mandal et al., 2005; Voll et al., 2000). Another important factor that becomes activated is c-myc. It regulates the cellular proliferation and growth of the cells (Dose

et al., 2006; Douglas et al., 2001). In addition, Notch1 signaling was shown to act cooperatively with the pre-TCR further promoting the survival, cellular expansion and differentiation of the cells (Ciofani et al., 2004; Ciofani and Zuniga-Pflucker, 2005; Tussiwand et al., 2011). However, soon after pre-TCR activation Notch1 gets downregulated due to the induction of Id3, which antagonizes E proteins that promote and sustain Notch1 expression (Yashiro-Ohtani et al., 2009). Thus, pre-T cells become independent of Notch1 soon after passage through the  $\beta$ -selection checkpoint, hereby switching from the “Notch-dependent” to the “TCR-dependent” part of T-cell development. Once cells have passed  $\beta$ -selection they also downregulate IL-7R and become sensitive to chemokine receptor Cxcr4 signaling as another co-stimulus controlling survival and proliferation via PI3K activation (Janas et al., 2010; Trampont et al., 2010).

Since a large fraction of the cells fail to rearrange an in frame  $\beta$ -chain or are incapable of pairing with the pT $\alpha$ -chain, programmed induction of apoptosis in these cells is a requirement to prevent accumulation of non-functional cells. Studies in the late nineties proposed a role of the p53 pathway in the regulation of apoptosis at this checkpoint. p53 gets activated during VDJ recombination as this process involves the generation of DNA double-strand breaks. In the case of a non-functional rearrangement cells lack survival signals from the pre-TCR and instead accumulate p53, which in turn induces pro-apoptotic proteins such as Noxa, Puma, and Bid (Mandal et al., 2008). By contrast, successful generation of the  $\beta$ -chain suppresses the p53 pathway via the pre-TCR (Costello et al., 2000). This is supported by the fact that pre-T cells defective in pre-TCR signaling are partially rescued from the differentiation block when p53 is deleted (Bogue et al., 1996; Haks et al., 1999; Mombaerts et al., 1995). More recently, activity of the transcription factor Miz-1 was associated with p53 regulation during  $\beta$ -selection by the induction of ribosomal protein L22 expression (Rpl22), which was previously described to be a negative regulator of p53 translation (Anderson et al., 2007; Rashkovan et al., 2014; Saba et al., 2011; Stadanlick et al., 2011). In addition to this intrinsic apoptosis pathway the extrinsic Fas system was also linked to the pre-TCR checkpoint. Fas is expressed on the surface of thymocytes and after binding to Fas-ligand apoptosis can be induced via interaction of the cytoplasmic death domain with adapter molecules inducing a downstream caspase activation cascade (Ashkenazi and Dixit, 1998). Similarly, to the p53 pathway, deficiency of Fas or downstream adapters led to pre-T cell differentiation even in the absence of pre-TCR signaling (Newton et al., 2000; Yasutomo et al., 1997).

However, the involvement of these factors still not fully resolves the underlying mechanisms of apoptosis induction in cells with a non-functional rearrangement. Especially since the described factors like p53, Miz-1, Rpl22, and Fas are not differentially expressed between DN3a and DN3b thymocytes (Immgen Database). Therefore, the exact factors,

mechanisms, and regulations responsible for the induction of apoptosis have to be further investigated in order to completely understand the  $\beta$ -selection process.

#### **2.5.4. Final maturation steps**

During the proliferative expansion after pre-TCR triggering, cells lose the expression of CD25, thereby entering the DN4 stage defined as CD44<sup>+</sup>CD117<sup>+</sup>CD25<sup>-</sup>. Subsequently, also as a result of pre-TCR signaling, CD4 and CD8 expression is induced, assigning the double positive (DP) stage. *Rag* genes become re-expressed and initiate the recombination of the TCR $\alpha$  locus (Koch and Radtke, 2011). Once a functional TCR is expressed by DP cells its functionality and specificity is tested for binding to peptide-major histocompatibility complex (MHC) complexes presented by cortical thymic epithelial cells (cTECs) and DCs (Klein et al., 2009). Interactions of intermediate affinity for self-peptide-MHC complexes positively select the cells and induce survival (Starr et al., 2003). The recombination machinery is again rapidly repressed in order to ensure allelic exclusion. Depending on whether the interaction was successful with MHCI or MHCII the cells will now develop in either CD8 or CD4 single positive (SP) T cells, respectively. At the same time, the chemokine receptor Ccr7 becomes upregulated and facilitates the migration into the medulla, where the cells undergo negative selection (Ueno et al., 2004). During this process, cells with a high affinity to self-antigens, which are presented by medullary thymic epithelial cells (mTECs), are eliminated, thereby ensuring tolerance and reducing the risk for the generation of autoreactive T cells (Palmer, 2003). Upregulation of S1PR<sub>1</sub> expression on mature SP thymocytes finally mediates the egress from the thymus into the circulation, where the concentration of its chemokine S1P is higher (Matloubian et al., 2004).

## **2.6. Flt3-ligand and IL-7 in lymphoid development**

### **2.6.1. Instructive versus permissive action of cytokines**

Cytokines play important roles in the regulation of hematopoiesis as they influence survival, proliferation, differentiation, and maturation of cells (Metcalf, 2008). In lineage specification cytokines can act either in an instructive or a permissive manner. The induction of a specific signaling cascade that results in a genetic programming that determines lineage fate specification describes an instructive cytokine (Figure 7, left panel). A permissive cytokine, on the other hand, influences the selection of cells with appropriate receptor expression by regulating the survival and/or proliferation capacity (Figure 7, right panel). In many cases investigations identifying the exact action of a cytokine led to conflicting results, thus, the

precise mode of action of many cytokines studied remains unresolved. For instance, deletion of either the cytokine or its receptor reduces the lineage output, a result which is compatible with both instructive and permissive function of the cytokine. It should be noted however, that deficiencies never resulted in a complete absence of a lineage, which could be taken as evidence for permissive roles of cytokines, but could also be explained by compensatory mechanisms and redundancy in the system (Brown et al., 2018).

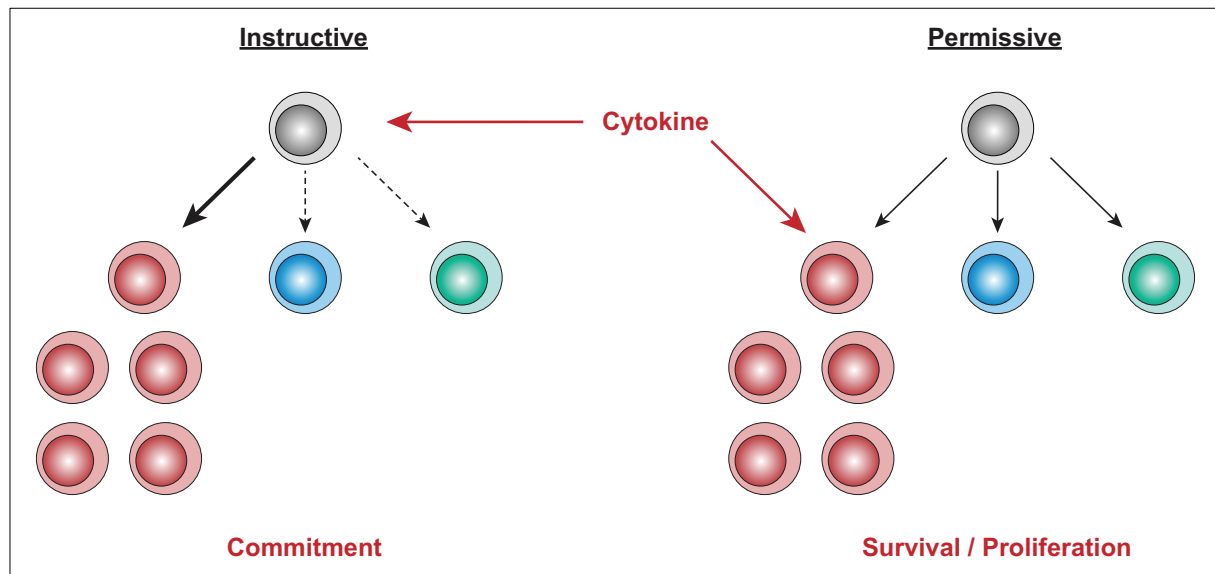


**Figure 7 | Instructive vs permissive action of cytokines.** Schematic representation for a permissive versus instructive action of a cytokine. If a cytokine has an instructive role it initiates a cell-type specific program in the target cell resulting in differentiation and commitment to a certain lineage. A Permissive action on the other hand influences the survival or proliferation of the target cells resulting in its expansion compared to other receptor negative cell types. Adapted from (Brown et al., 2018).

First experiments providing evidence for instructive roles of cytokines were performed in 1982 revealing the impact of macrophage colony-stimulating factor (M-CSF) and granulocyte-macrophage colony-stimulating factor (GM-CSF) in the cell fate decision of macrophages and granulocytes, respectively (Metcalf and Burgess, 1982). These findings were confirmed by technical improvements explicitly proving the instructive mode of action of M-CSF and GM-CSF on the GMP progenitor population (Rieger et al., 2009). Moreover, induction of the transcriptional regulators Pu.1 and Gata1 by M-CSF and Epo was shown to instruct myeloid and erythroid cell fate specification, respectively (Grover et al., 2014; Mossadegh-Keller et al., 2013). Nevertheless, most experimental evidence for instructive function of cytokines are derived from *in vitro* studies and might therefore not reflect the mechanisms of *in vivo* steady-state hematopoiesis.

Two essential cytokines for the development of lymphocytes are Fms-like tyrosine kinase 3 (Flt3) ligand and interleukin-7 (IL-7).

### 2.6.2. Flt3-ligand in early hematopoiesis

Flt3 (or Flk2/CD135) is so far the only receptor identified for the cytokine Flt3-ligand. As Flt3 belongs to the type III receptor tyrosine kinases it has an extracellular part with five immunoglobulin-like domains and a cytoplasmic part with two tyrosine kinase domains (Matthews et al., 1991; Rosnet et al., 1991). Binding of soluble as well as membrane-bound Flt3-ligand initiates receptor homo-dimerization that in turn induces a conformational change resulting in phosphorylation of the tyrosine kinase domains (Tsapogas et al., 2017). Stimulation of the receptor is followed by rapid internalization and degradation (Turner et al., 1996). The signaling cascade downstream of the receptor ultimately leads to Ras/Mek/Erk, PI3K, signal transducer and activator of transcription (Stat) 3, and on some occasions Stat5a activation in a cell-context dependent manner (Laouar et al., 2003; Marchetto et al., 1999; Zhang and Broxmeyer, 2000; Zhang et al., 2000).

Flt3 is mostly expressed on early hematopoietic progenitors, whereas more mature populations are Flt3 negative, with the exception of the dendritic cell compartment (Hagman et al., 1991; Karsunky et al., 2003; Liu et al., 2009; Onai et al., 2013; Rosnet et al., 1991) (Figure 8). Upregulation of Flt3 within the LSK population was associated with the loss of self-renewal capacity, which allowed the definition of true HSCs as Flt3 negative and MPPs as Flt3 positive (Adolfsson et al., 2001). Moreover, the LMPP population was defined as the 25% of cells with the highest Flt3 expression of the LSK population (Adolfsson et al., 2005). These studies also linked Flt3 expression with a loss of megakaryocyte and erythrocyte potential by MPPs. This is further strengthened by the absence of Flt3 on all megakaryocyte/erythrocyte progenitor populations. Surprisingly, lineage tracing of Flt3 expression resulted in labeling of all lineages, including megakaryocyte and erythrocyte progenitors and their progeny, suggesting that all hematopoietic cells develop through a Flt3 positive stage (Boyer et al., 2011; Buza-Vidas et al., 2011). Expression of Flt3 on HSCs remains controversial, as one group could not find labeled HSCs in the lineage-tracing model, whereas another group did find partial labeling. Analysis of *Flt3* mRNA expression at the single-cell level revealed that indeed small fractions of LT- as well as ST-HSCs express Flt3, in agreement with the rising concept of heterogeneity within the HSC compartment (Mead et al., 2017; Mooney et al., 2017). Even though Flt3<sup>+</sup> MPPs have robust myeloid potential, downstream progenitors such as the CMP or GMP switch off its expression (Boyer et al., 2011). Lymphoid progenitor populations on the other hand, such as the CLP, EPLM, and ETP populations, retain Flt3 expression until final commitment (Buza-Vidas et al., 2011; Karsunky et al., 2008; Luc et al., 2012). In the B-cell lineage, for instance, Pax5 downregulates Flt3 expression, resulting in its absence on all CD19 positive cells (Holmes et al., 2006).

Functionally, Flt3-ligand was originally identified as a proliferation promoting factor for early Flt3<sup>+</sup> progenitors. However, in *in vitro* culture systems Flt3-ligand alone had only a limited effect, whereas combination with other cytokines such as stem cell factor (SCF), GM-CSF, IL-3, IL-6, or IL-11 demonstrated its importance for the generation of myeloid cells (Broxmeyer et al., 1995; Jacobsen et al., 1995). Especially for DC cultures Flt3-ligand turned out to be very important (Brasel et al., 2000; Brawand et al., 2002). On the other hand, there was no positive effect on erythrocyte or megakaryocyte growth and differentiation (Banu et al., 1999). In combination with SCF and/or IL-7 Flt3-ligand also improved *in vitro* generation of B cells as it acts on its progenitor populations (Namikawa et al., 1996; von Muenchow et al., 2017).

Deficiency for either Flt3 or Flt3-ligand is causing defects in myeloid and lymphoid progenitors (Mackarechtschian et al., 1995; McKenna et al., 2000). Notably, the effect was more pronounced in the Flt3-ligand knockout mice, with decreased B-cell progenitors, NK cells, and DCs, indicating the possibility of the existence of another not yet identified receptor for Flt3-ligand. Additional analysis revealed that Flt3-ligand is furthermore important for normal production and/or maintenance of CLPs and MPPs, while HSCs seemed to be independent (Sitnicka et al., 2002). These knockout models ruled out an absolute requirement of Flt3-ligand for hematopoiesis, but clearly demonstrated its importance for the generation of lymphoid and myeloid cells, whereas it is dispensable for the megakaryocyte and erythroid lineages. These findings raised the question whether the role of the Flt3-Flt3-ligand system is just permissive with regards to proliferation and survival, or whether it has also an instructive function for the lymphoid/myeloid pathway. This was addressed by the generation of a Flt3-ligand transgenic mouse model, in which, additionally to its endogenous expression, Flt3-ligand expression is driven by the  $\beta$ -actin promoter, causing sustained high *in vivo* levels (Tsapogas et al., 2014). In these mice a massive expansion of all Flt3<sup>+</sup> cells and their progeny was detected including MPPs, CLPs, EPLMs, CMPs, GMPs, mature myeloid cells, pDCs, and cDCs. On the contrary, these mice suffered from severe anemia caused by the reduction of erythroid and megakaryocyte progenitors and consequently also their mature progeny. Detailed analysis provided clear evidence for an instructive role of Flt3-ligand in early hematopoiesis, initiating lymphoid/myeloid specification in MPPs and suppressing the megakaryocyte/erythrocyte fate (Tsapogas et al., 2014).

With regards to lymphoid development, Flt3-ligand has a positive effect on B-cell precursors as it increases their generation in the transgenic mouse (Tsapogas et al., 2014), whereas cell numbers are reduced in the absence of Flt3 signaling (McKenna et al., 2000). Whether this effect is based on a permissive or an instructive mode of action needs further investigation. Interestingly, Flt3-ligand over-expression resulted in a disturbed development from the pro-B cell stage onwards, with reduced numbers of pre-B and immature B cells (Tsapogas et al., 2014). Since Flt3 expression is turned off upon Pax5 induction, this must be

an indirect effect. One hypothesis is that due to the expansion of IL-7R<sup>+</sup> CLP/EPLM progenitors and pDCs, which are also IL-7R positive, in Flt3-ligand transgenic mice, IL-7 availability is decreased, thus affecting the proliferation of pre-B cells. The production of T lymphocytes is not affected in Flt3-ligand or Flt3 deficient mice (Mackarechtschian et al., 1995; McKenna et al., 2000). However, in combination with IL-7R deletion, the IL-7R mediated block in T-cell development is amplified (Sitnicka et al., 2007). This is most likely attributed to the Flt3<sup>+</sup> ETPs, which were shown to rely on Flt3-ligand production by thymic epithelial cells (Kenins et al., 2010). Moreover, Flt3-ligand is also involved in the regulation of ILC numbers, since it acts on their early progenitors (Baerenwaldt et al., 2016).

Due to its function in promoting the proliferation of hematopoietic progenitor cells it is not surprising that deregulated Flt3 signaling can cause hematopoietic malignancies. Specifically, activating mutations in the human *FLT3* gene are frequently found in leukemic cells. The most common one, termed *FLT3*-ITD, results in a constitutive activation of the cytoplasmic kinase domains and is found in 25% of the cases of acute myeloid leukemia. Moreover, it is associated with a poor clinical prognosis (Gilliland and Griffin, 2002; Nakao et al., 1996). This clinical significance further illustrates the importance of further investigations to unravel the exact mechanism and regulations involved in Flt3 signaling.

### 2.6.3. IL-7 in lymphopoiesis

Three decades ago IL-7 was discovered as a growth factor in *in vitro* cultures of progenitor B cells (Namen et al., 1988). These were soon followed by studies revealing that this effect holds true for T cells as well. Further investigations led to the conclusion that the receptor for IL-7 is mainly expressed by lymphoid cells (Ceredig and Rolink, 2012). The IL-7R is composed of two subunits: the  $\alpha$ -chain (IL-7R $\alpha$ , or CD127) and the common  $\gamma$ -chain (or CD132). Only if both chains dimerize on the cell membrane IL-7 can bind and trigger intracellular signaling. The common  $\gamma$ -chain is not unique to the IL-7R as it is furthermore part of the receptor complexes for the cytokines IL-2, IL-4, IL-9, IL-15, and IL-21 (Jiang et al., 2005). Likewise, specificity of the  $\alpha$ -chain is not limited to IL-7 alone. In complex with the thymic stromal lymphopoietin receptor (TSLPR) chain it additionally can bind the cytokine TSLP (Pandey et al., 2000; Park et al., 2000). Signaling via the IL-7R after binding of IL-7 is initiated by Janus kinases (Jak) 1 and 3. Jak1 is associated with the intracellular domain of the  $\alpha$ -chain, while Jak3 associates with the common  $\gamma$ -chain (Suzuki et al., 2000). Ligand binding facilitates cross-phosphorylation of Jak1 and Jak3, which allows for Jak mediated phosphorylation of a tyrosine residue within the  $\alpha$ -chain (Foxwell et al., 1995; Kasai et al., 2018). Recruitment of further signaling molecules ultimately results in the activation of Stat5 by phosphorylation-dependent dimerization and subsequent translocation into the nucleus. Stat5 then initiates

gene expression of factors important for survival, proliferation, as well as differentiation (Hennighausen and Robinson, 2008). For instance, activation of the anti-apoptotic genes *Bcl2* and *Mcl1* is mediated by Stat5, thereby promoting survival (Jiang et al., 2004; Opferman et al., 2003). Proliferation of cells, on the other hand, is induced by the expression of cyclin D3, a positive regulator of the cell cycle (Cooper et al., 2006). In addition to Stat5, IL-7R signaling further activates PI3K/Akt, Mapk/Erc, and Src kinase pathways, which are facilitators of survival and proliferation too (Clark et al., 2014; Fleming and Paige, 2001; Page et al., 1995; Venkitaraman and Cowling, 1994; Yasuda et al., 2008). The various pathways downstream of IL-7R activation indicate a cell-type and context-dependent induction of specific signaling events, leading to varying outcomes.

While the common  $\gamma$ -chain is expressed by nearly all hematopoietic cells, restricted expression of the IL-7R  $\alpha$ -chain provides the specificity for IL-7 signaling. Consequently, IL-7R expression in the hematopoietic system is almost limited to lymphoid cells such as B- and T-cell progenitors as well as mature T cells, innate lymphoid cells like ILC2s and ILC3s, but also certain DCs, such as migratory DCs and pDCs (Chappaz and Finke, 2010; Hoyler et al., 2012; Rodrigues et al., 2018; Vogt et al., 2009) (Figure 8). Initiation of IL-7R expression on early progenitors is associated with lymphoid specification, in particular since its surface expression is used to define the CLP stage. Transcriptional activation of the *Il7ra* gene was shown to be mediated by Pu.1 and also by Ikaros, resulting in *Il7ra* mRNA detection already at the LMPP stage (DeKoter et al., 2002; Yoshida et al., 2006). Moreover, the expression of the IL-7R is under the control of extracellular signals as it is upregulated by factors like Flt3-ligand, type-I interferons, and tumor necrosis factor (TNF), whereas IL-2, IL-4, IL-6, and IL-15 suppress its expression (Borge et al., 1999; Park et al., 2004; Pleiman et al., 1991; Tian et al., 2005). The latter can act as survival factors for different hematopoietic cell types. Therefore, one hypothesis is that cells, which do not require IL-7 signaling for their survival anymore downregulate IL-7R in order to stop the consumption of IL-7, which is only available at limited amounts under steady state conditions. Suppression of IL-7R by other survival factors and even by IL-7 signaling itself thus prevents needless consumption of IL-7 (Park et al., 2004).

The significance of IL-7R signaling for lymphoid differentiation is demonstrated by the dramatic defect for both B- and T-cell generation in mice defective for either the cytokine or its receptor (Peschon et al., 1994; von Freeden-Jeffry et al., 1995). During B-cell specification IL-7R is expressed by uncommitted progenitors such as the CLP and EPLM as well as on CD19<sup>+</sup> pro-B and large pre-B cells, but gets downregulated at the small pre-B stage. In *Il7<sup>-/-</sup>* or *Il7r<sup>-/-</sup>* mice B-cell development is perturbed, as indicated by the absence of pro-B cells and their progeny (Peschon et al., 1994; von Freeden-Jeffry et al., 1995). Additional over-expression of the pro-survival gene *Bcl2* in these mice did not rescue the defect in B-cell development indicating that the role of IL-7 for B-cell differentiation is not only permissive in the sense of

providing survival signals, but acts in an instructive manner in promoting B-cell specification (Kondo et al., 1997a; Maraskovsky et al., 1998). Subsequent studies on the effect of IL-7 absence on CLP strengthened this hypothesis due to a significant decrease of CLP numbers and especially a reduction of *Ebf1* transcript levels in this compartment (Dias et al., 2005). Thus, it was concluded that IL-7R signaling instructs B-cell commitment by the induction of *Ebf1* in the CLP population. This assumption was further based on the discovery of Stat5 binding sites within the *Ebf1* and *Pax5* promoters and by a partial rescue of B-cell potential in *Il7<sup>-/-</sup>* CLPs by *Ebf1* over-expression (Hirokawa et al., 2003; Kikuchi et al., 2005; Roessler et al., 2007). However, *in vivo* binding of Stat5 to the *Ebf1* and *Pax5* promoters could not be confirmed. More detailed analysis of the *Il7<sup>-/-</sup>* CLP compartment revealed that the reduction was specific to the Ly6D<sup>+</sup> fraction, in which *Ebf1* expression and further specification to the B-cell fate is initiated (Tsapogas et al., 2011). Thus, the observed reduction of *Ebf1* levels in *Il7<sup>-/-</sup>* CLPs might actually result from the elimination of the *Ebf1*<sup>+</sup>Ly6D<sup>+</sup> CLP compartment due to a potential role of IL-7 in survival. In accordance with that the group of Meinrad Busslinger showed that transgenic *Bcl2* expression in mice with B-cell specific deletion of Stat5 could restore pro-B cell differentiation (Malin et al., 2010). In addition, they also observed a partial restoration of committed pro-B cells in *Il7<sup>-/-</sup>* mice by *Bcl2* over-expression and neither Stat5 nor IL7-R signaling was absolutely critical for *Ebf1* and *Pax5* transcription in their experiments. These data support a rather permissive survival-mediated role of IL-7 in B-cell specification.

After commitment to the B-cell lineage IL-7 does not only promote survival, but also the proliferation of pre-B cells (Cooper et al., 2006; Mandal et al., 2009). After effective expansion of pre-B cells IL-7R $\alpha$  expression is suppressed via pre-BCR signaling (Ochiai et al., 2012). This is important for further development, since loss of IL-7R signaling is allowing  $\kappa$  light-chain transcription, which is normally silenced due to a repressed chromatin configuration on the  $\kappa$  locus by Stat5 (Malin et al., 2010; Mandal et al., 2011). In accordance with that, IL-7 removal from *in vitro* pro-B cell cultures initiates light chain rearrangements and further maturation to IgM<sup>+</sup> B cells (von Muenchow et al., 2017). However, sustained high *in vivo* levels of IL-7 did not block B-cell differentiation, but instead expanded all IL-7R positive precursor and also mature B-cell populations (Ceredig et al., 2003; Fisher et al., 1995). Interestingly, pro-B and pre-B cells were even detected in the periphery of these mice in large numbers, including the spleen and lymph nodes (Mertsching et al., 1996). Whether these resulted from *in situ* generation of B cells or whether this was just a result of emigration of the cells from the bone marrow is not clear.

Altogether, it is apparent that IL-7 is the most crucial cytokine for mouse B-cell development. However, not all mature B-cell populations are missing in the absence of IL-7. As these unaffected populations mainly present a MZB or B1 phenotype, it is believed that fetal B-cell development is not dependent on IL-7. Neonatal mice defective for IL-7 have almost

unchanged B-cell numbers (Carvalho et al., 2001). Similarly, also human B cells seem to be unaffected in the absence of IL-7 (Noguchi et al., 1993; Puel et al., 1998). However, it has to be considered that patients with IL-7 deficiency are always infants, as without treatment they don't reach adulthood. Therefore, the difference in IL-7 dependency between humans and mice might just reflect the difference in this dependency between fetal and adult B cells. This idea is supported by the observation that *ex vivo* cultured human pre-B cells exhibited an increased IL-7 dependency compared to cord blood derived pre-B cells (Parrish et al., 2009).

*Il7<sup>-/-</sup>* and *Il7r<sup>-/-</sup>* mice display a severe block in the generation of T lymphocytes, similar to B cells (Peschon et al., 1994; von Freeden-Jeffry et al., 1995). Even though expression of IL-7R on ETPs is not detectable by FACS, they were shown to be responsive to IL-7, suggesting that IL-7R expression might be just below the detection limit. IL-7R becomes strongly upregulated on DN2 cells and is crucial for their survival and proliferation. However, IL-7R signaling is not involved in the commitment to the  $\alpha/\beta$  T-cell lineage, since Bcl2 over-expression as well as deficiency for the pro-apoptotic genes *Bax* and *Bim* rescued  $\alpha/\beta$  T-cell development in *Il7r<sup>-/-</sup>* mice (Akashi et al., 1997; Khaled et al., 2002; Kondo et al., 1997a; Maraskovsky et al., 1997; Pellegrini et al., 2004). Thymocyte numbers are not fully restored in these mouse models, since IL-7 has not only a major function for the survival of DN2/3 cells, but is also responsible for their expansion. Thus, IL-7 is also essential for the *in vitro* propagation of pre-T cells (Balciunaite et al., 2005a; Gehre et al., 2015). In contrast to  $\alpha/\beta$  T cells, the development of  $\gamma/\delta$  T cells is not rescued by additional Bcl2 expression, indicating that IL-7 is more than just a survival and proliferation factor for these cells. Indeed, IL-7R signaling was proposed to influence the  $\alpha/\beta$  versus  $\gamma/\delta$  T-cell decision at the DN2 stage by regulating the chromatin accessibility of the TCR $\gamma$  locus (Huang et al., 2001; Ye et al., 2001).

At the  $\beta$ -selection checkpoint IL-7 acts cooperatively with pre-TCR and Notch1 signaling in the proliferation and differentiation of the cells and prevents *TCRa* rearrangements similarly to the light chains in pre-B cells (Boudil et al., 2015). Therefore, in analogy to B-cell development, IL-7R has to be suppressed at the DN3-DP transition for further maturation and initiation of *TCRa* recombination. This is reflected *in vitro* by the fact, that pre-T cells do not properly differentiate to the DP stage unless IL-7 is removed from the cultures (Balciunaite et al., 2005a; Tussiwand et al., 2011). Downregulation of IL-7R on DP cells might also be important for the regulation of IL-7 availability in the thymus. Since the DP stage is by far for the major population of thymocytes, consumption of IL-7 by this population might negatively influence other IL-7 dependent populations. This hypothesis is supported by reduced *Bcl2* expression and increased apoptosis of DN cells when IL-7R $\alpha$  expression was induced on all thymocytes (Munitic et al., 2004).

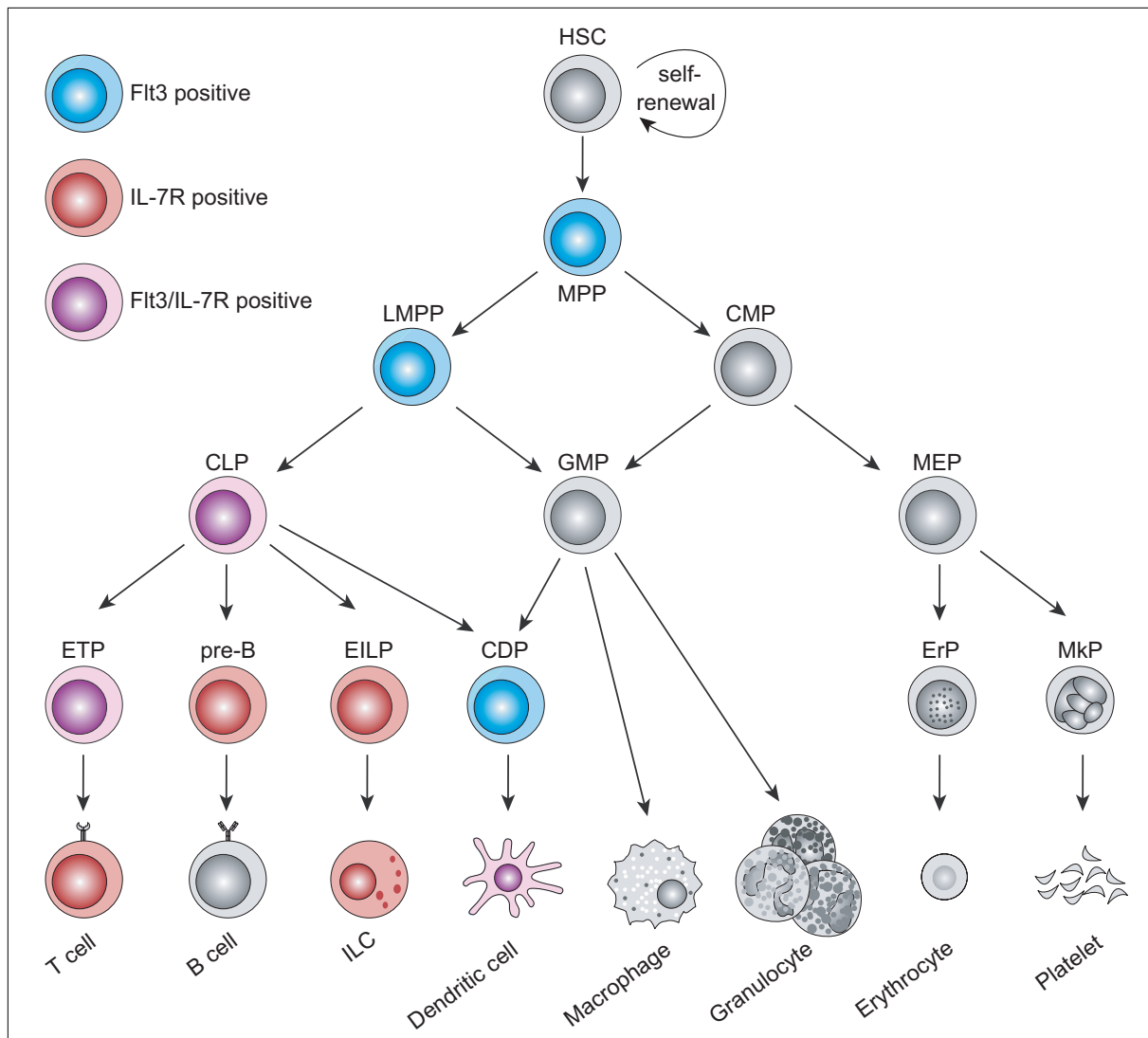


**Figure 8 | Flt3 and IL-7R expression in the hematopoietic system.** Schematic representation of the classical hematopoietic tree indicating expression of Flt3 and IL-7R in different colors of the cells. Blue marks expression of Flt3, red IL-7R expression, and violet cells that express both receptors. Arrows indicate developmental progress and potential of the different progenitor populations. HSC: hematopoietic stem cell, MPP: multipotent progenitor, LMPP: lymphoid-primed multipotent progenitor, CMP: common myeloid progenitor, CLP: common lymphoid progenitor, MEP: megakaryocytic-erythroid progenitor, GMP: granulocyte/macrophage progenitor, MkP: megakaryocyte committed progenitor, ErP: erythrocyte progenitor, EPLM: early progenitor with lymphoid and myeloid potential, EILP: early innate lymphoid progenitor, CDP: common dendritic cell progenitor, ILC: innate lymphoid cell, ETP: early thymic progenitor.

Unlike B cells, IL-7 signaling remains crucial for both survival and proliferation of mature naïve as well as memory T cells in the periphery (Chetoui et al., 2010; Lali et al., 2004; Li et al., 2010c; Swainson et al., 2007). Thus, induced deletion of *Il7ra* caused a rapid decrease of peripheral T cells before thymic output was affected (Jacobs et al., 2010). Moreover, treatment of mice with IL-7/anti-IL-7 complexes as well as transgenic expression of IL-7 promoted the expansion of peripheral T cells even though development in the thymus was not affected (Boyman et al., 2008; Mertsching et al., 1995). Interestingly, the CD4-to-CD8 ratio was altered

in IL-7 transgenic mice, indicating that mature CD8 T cells are more responsive to IL-7R signaling than CD4 T cells (Tan et al., 2002).

Mutations in the human *IL7RA* gene or other components of the IL-7R signaling pathway result in severe combined immunodeficiency (SCID), manifested by the absence of T-cells. These mutations have to be corrected by bone marrow transplantations or gene replacement therapy since the adaptive immune response is absolutely required for sufficient protection against pathogens (Buckley, 2004).

Apart from B and T lymphopoiesis, ILC development is also known to transit through IL-7R<sup>+</sup> stages, as they are most likely derived from the CLP as well (Gronke et al., 2016). In addition, most ILCs, with the exception of NK cells, retain IL-7R expression also upon maturation. While ILC1s and ILC2s do not absolutely require IL-7 for their survival, ILC3s and in particular lymphoid tissue inducer cells (LTi cell) are clearly dependent on functional IL-7R signaling (Daussy et al., 2014; Robinette et al., 2017). Since LTi cells are crucial for the generation of lymphoid structures such as lymph nodes and Peyer's patches, IL-7 or IL-7R deficiency results in the absence of Peyer's patches (Adachi et al., 1998; Yoshida et al., 1999). In addition, IL-7 mediated survival of ILC3s is important for correct lymph node function as they were shown to regulate homing of lymphocytes to adult lymph nodes (Yang et al., 2018).

As evident from the above, both Flt3-ligand as well as IL-7 have essential roles during lymphopoiesis. This is highlighted by the complete absence of progenitor and mature B cells and the exacerbated defect in T-cell development, when both cytokines are absent (Sitnicka et al., 2003; Sitnicka et al., 2007). The effect of the two cytokines is mostly restricted to separate stages in development, as Flt3-ligand acts on earlier progenitors, whereas IL-7R signaling has also essential roles for already committed B- and T-cell progenitors. However, some stages during differentiation, such as CLP, EPLM, and ETP, indeed are positive for both receptors, thereby enabling a potential synergistic action of the two cytokines on these populations (Figure 8).

### 3. Aims of the thesis

The regulation of lymphocyte development is of central interest, as the adaptive immunity is absolutely required for life. Disturbances in the differentiation process often result in immunodeficiency, autoimmunity or leukemia.

In the past years several conflicting results were obtained regarding the role of IL-7 in B-cell commitment. While some reports provided evidence for an instructive function of IL-7, others argued for an only permissive mode of action. The CLP and EPLM populations are of particular interest in that sense, since they contain the last uncommitted B-cell progenitors and are heavily affected by the absence of IL-7. Since the Flt3-ligand transgenic mouse, that was previously generated in our lab, leads to a dramatic expansion of the CLP and EPLM populations, we aimed to address the exact function of IL-7 in B-cell commitment *in vivo* by making use of these mice and other combinations of mutant mouse strains. We thus aimed at unravelling, in an *in vivo* setting, the functions of IL-7 and Flt3-ligand on commitment to the B-cell lineage and their potential synergistic role on lymphocyte development.

Another important aspect of lymphocyte development is the selection of cells with functional rearrangements of their antigen-receptor chains. Especially within the thymus the majority of cells are eliminated during the differentiation process due to failure of successful recombination. However, little is known about the mechanisms that regulate the first essential checkpoint, the  $\beta$ -selection, which induces the elimination of almost half of the cells. Therefore, investigation of the detailed mechanisms that initiate apoptosis and identification of key mediators in this process was one major aim of this work. Moreover, genetic modification of mice for detailed analysis of potential candidates was the major tool we planned to implement in order to validate the exact molecular pathways involved in the apoptosis induction during  $\beta$ -selection.

## **4. Results**

### **4.1. Part 1: Flt3-ligand and IL-7 in lymphopoiesis**

#### **4.1.1. Permissive roles of cytokines interleukin-7 and Flt3-ligand in mouse B-cell lineage commitment**

Lilly von Muenchow, Llucia Alberti-Servera, Fabian Klein, Giuseppina Capoferri, Daniela Finke, Rhodri Ceredig, Antonius Rolink, and Panagiotis Tsapogas

November 2016 – Proceedings of the National Academy of Sciences



# Permissive roles of cytokines interleukin-7 and Flt3 ligand in mouse B-cell lineage commitment

Lilly von Muenchow<sup>a</sup>, Lucia Alberti-Servera<sup>a</sup>, Fabian Klein<sup>a</sup>, Giuseppina Capoferri<sup>a</sup>, Daniela Finke<sup>b,c</sup>, Rhodri Ceredig<sup>d</sup>, Antonius Rolink<sup>a</sup>, and Panagiotis Tsapogas<sup>a,1</sup>

<sup>a</sup>Developmental and Molecular Immunology, Department of Biomedicine, University of Basel, 4058 Basel, Switzerland; <sup>b</sup>Research Department, University Children's Hospital Basel, 4056 Basel, Switzerland; <sup>c</sup>Developmental Immunology, Department of Biomedicine, University of Basel, 4058 Basel, Switzerland; and <sup>d</sup>Discipline of Physiology, National University of Ireland, H91 DK59 Galway, Ireland

Edited by Max D. Cooper, Emory University, Atlanta, GA, and approved November 4, 2016 (received for review August 10, 2016)

Hematopoietic cells are continuously generated throughout life from hematopoietic stem cells, thus making hematopoiesis a favorable system to study developmental cell lineage commitment. The main factors incorporating environmental signals to developing hematopoietic cells are cytokines, which regulate commitment of hematopoietic progenitors to the different blood lineages by acting either in an instructive or a permissive manner. *Fms*-like tyrosine kinase-3 (Flt3) ligand (FL) and Interleukin-7 (IL-7) are cytokines pivotal for B-cell development, as manifested by the severely compromised B-cell development in their absence. However, their precise role in regulating B-cell commitment has been the subject of debate. In the present study we assessed the rescue of B-cell commitment in mice lacking IL-7 but simultaneously overexpressing FL. Results obtained demonstrate that FL overexpression in IL-7-deficient mice rescues B-cell commitment, resulting in significant *Ebf1* and *Pax5* expression in Ly6D<sup>+</sup>CD135<sup>+</sup>CD127<sup>+</sup>CD19<sup>-</sup> precursors and subsequent generation of normal numbers of CD19<sup>+</sup> B-cell progenitors, therefore indicating that IL-7 can be dispensable for commitment to the B-cell lineage. Further analysis of Ly6D<sup>+</sup>CD135<sup>+</sup>CD127<sup>+</sup>CD19<sup>-</sup> progenitors in IL-7- or FL-deficient mice overexpressing *Bcl2*, as well as in IL-7 transgenic mice suggests that both FL and IL-7 regulate B-cell commitment in a permissive manner: FL by inducing proliferation of Ly6D<sup>+</sup>CD135<sup>+</sup>CD127<sup>+</sup>CD19<sup>-</sup> progenitors and IL-7 by providing survival signals to these progenitors.

hematopoiesis | cytokines | commitment | immunology

Hematopoiesis, the generation of all blood cells from hematopoietic stem cells (HSCs), takes place continuously in the adult bone marrow. Accumulating evidence suggests that HSCs generate the different hematopoietic lineages via oligopotent progenitors having limited self-renewal capacity and restricted developmental potentials. Activation of lineage-specific gene transcription in these progenitors eventually leads to their commitment to a particular lineage. Cytokines are the most prominent environmental factors regulating hematopoietic lineage commitment, doing so by acting either in an instructive or a permissive manner (1). In the instructive model, cytokines induce a signaling cascade in progenitors leading to the initiation of a lineage-specific gene program, typically through up-regulation and/or activation of transcription factors, eventually resulting in commitment to a particular lineage. In contrast, the permissive model advocates that commitment of progenitors to different lineages occurs in a cell-autonomous, stochastic manner, with cytokines acting as a selection rather than a commitment factor, promoting the survival and/or proliferation of a specific lineage at the expense of other lineages originating from the same progenitor. Elucidating the precise mode of action of cytokines is technically challenging and therefore the instructive versus permissive role of cytokines is hotly debated (2–4). Although the permissive model was favored in the past, recent data provide solid evidence for the instructive action of several cytokines including M-CSF, G-CSF, EPO, and *fms*-like tyrosine kinase-3 (Flt3) ligand (5–8). However, our understanding of how cytokines regulate hematopoiesis remains elusive, as different cytokines can act in various ways and their function might be

cell-context dependent (9). Moreover, most studies to date have addressed cytokine-regulated myeloid differentiation with relatively little information on lymphoid lineage commitment.

That Interleukin-7 (IL-7) is a crucial cytokine for B-cell development is demonstrated by the dramatic defect in B-cell generation in mice lacking either the cytokine (10) or its receptor (11). Interestingly, whereas human B-cell progenitors are also responsive to IL-7 (12), disruption of IL-7 signaling caused by mutations does not ablate B-cell development in man (13, 14). IL-7 was initially identified as a growth factor for B-cell progenitors (15) and early studies demonstrated that *in vivo* overexpression of the prosurvival gene *Bcl2* did not rescue B-cell development in the absence of IL-7 signaling, suggesting that IL-7 acts in an instructive manner in B-cell commitment (16, 17). The subsequent findings that uncommitted common lymphoid progenitors (CLPs) from *Il7*<sup>-/-</sup> mice lacked expression of the transcription factor early B-cell factor 1 (*Ebf1*) (18) and that *Ebf1* overexpression partially restored B-cell generation from these CLPs (19), led to the hypothesis that IL-7, through *Stat5* activation, instructs commitment to the B-cell lineage by initiating *Ebf1* expression in uncommitted progenitors. Supporting this hypothesis, a putative *Stat5* binding site was later identified in one of the *Ebf1* promoters (20). However, a more recent study has shown that *Bcl2* can rescue B-cell generation in a *Stat5* conditional knockout mouse (21). Furthermore, the *Ebf1*-expressing fraction of CLP (Ly6D<sup>+</sup> CLP) is dramatically reduced in *Il7*<sup>-/-</sup> mice (22), therefore providing an alternative possibility for the reduced *Ebf1* expression observed in *Il7*<sup>-/-</sup> CLPs. Interestingly, B-cell lineage commitment is initiated

## Significance

The generation of different blood lineages is regulated by hematopoietic cytokines, either in an instructive or in a permissive manner. The cytokines Interleukin-7 and *fms*-like tyrosine kinase-3 (Flt3) ligand are required for B-cell development but their precise mode of action remains controversial. Our study has addressed the role of these cytokines in B-cell commitment by analyzing the progenitor stage where B-cell commitment occurs in mice overexpressing one of the two cytokines in the absence of the other. Our results demonstrate a permissive role for both cytokines in B-cell commitment. Interleukin-7 promotes survival of progenitors instead of up-regulation of B-cell commitment factors early B-cell factor 1 (*Ebf1*) and paired box 5 (*Pax5*), as previously hypothesized, whereas Flt3 ligand facilitates progenitor expansion by inducing their proliferation.

Author contributions: A.R. and P.T. designed research; L.v.M., L.A.-S., F.K., G.C., and P.T. performed research; D.F. and R.C. contributed new reagents/analytic tools; L.v.M., L.A.-S., F.K., A.R., and P.T. analyzed data; D.F. and R.C. revised the manuscript; A.R. and P.T. supervised the project; and P.T. wrote the paper.

The authors declare no conflict of interest.

This article is a PNAS Direct Submission.

<sup>1</sup>To whom correspondence should be addressed. Email: panagiotis.tsapogas@unibas.ch.

This article contains supporting information online at [www.pnas.org/lookup/suppl/doi:10.1073/pnas.1613316113/-DCSupplemental](http://www.pnas.org/lookup/suppl/doi:10.1073/pnas.1613316113/-DCSupplemental).

at the molecular level in Ly6D<sup>+</sup>CD19<sup>-</sup> progenitors (23). Hence, whereas the importance of IL-7 as a growth factor for committed B-cell progenitors has been well established, it remains unclear whether it instructs oligopotent progenitors to commit to the B-cell lineage through *Ebf1* and *Pax5* up-regulation.

Ft3 ligand (FL), the only known ligand for the Ft3 receptor (CD135), is a cytokine important for the generation of many hematopoietic lineages and its function has gained much attention as mutations in FL signaling are commonly found in acute myeloid leukemias (AMLs) (24). Committed B-cell progenitors do not express CD135, because expression of the B-cell commitment factor Pax5 (paired box 5) leads to its down-regulation (25). However, upon transplantation, bone marrow progenitors from *Ft3l<sup>-/-</sup>* and *Ft3l<sup>+/+</sup>* mice reconstitute the B-cell compartment poorly (26, 27), and FL was found to be essential for maintaining normal numbers of uncommitted B-cell progenitors (28).

Recently, we described a FL-transgenic mouse model (hereafter *Ft3ltg*) expressing high levels of FL in vivo, which has enabled us to suggest an instructive role for FL in early stages of hematopoiesis (8). By breeding these mice with *Il7<sup>-/-</sup>* mice, we herein show that increased FL levels can rescue B-cell commitment in CD135<sup>+</sup>CD127<sup>+</sup>CD19<sup>-</sup> progenitors and restore early CD19<sup>+</sup> B-cell progenitor numbers in the absence of IL-7 signaling, suggesting a permissive role for IL-7 in B-cell commitment. Further analyses of a combination of mouse genotypes overexpressing or lacking FL and IL-7, as well as the prosurvival gene *Bcl2*, have enabled us to identify a permissive role for both IL-7 and FL in B-cell commitment.

## Results

**Increased in Vivo Levels of FL Rescue B-Cell Commitment in *Il7<sup>-/-</sup>* Ly6D<sup>+</sup> CD19<sup>-</sup> Progenitors.** We have previously characterized an uncommitted B-cell progenitor with combined lymphoid and myeloid potential [early progenitor with lymphoid and myeloid potential (EPLM)] (29). EPLM can be further subdivided by SiglecH, CD11c, CD115, and Ly6D expression enabling us to identify the Ly6D<sup>+</sup>SiglecH<sup>-</sup>CD11c<sup>-</sup>CD115<sup>-</sup> fraction of EPLM (hereafter Ly6D<sup>+</sup> EPLM) as the population containing most B-cell potential, while being devoid of myeloid potential (Fig. S1B). This EPLM subpopulation is identified as Lin<sup>-</sup>CD19<sup>-</sup>CD117<sup>int</sup>B220<sup>int</sup> Ly6D<sup>+</sup>CD135<sup>+</sup>CD127<sup>+</sup> (Fig. 1A), therefore partially overlapping phenotypically with Ly6D<sup>+</sup> CLPs (Fig. S1A) and pre/pro-B cells (30, 31). Ly6D<sup>+</sup> EPLM numbers in *Il7<sup>-/-</sup>* and *Ft3l<sup>-/-</sup>* mice are significantly decreased compared with WT: 7-fold for *Il7<sup>-/-</sup>* and 13-fold for *Ft3l<sup>-/-</sup>*, respectively, and a similar dramatic decrease was observed in Ly6D<sup>+</sup> CLPs from both mutant mice (Fig. 1B and C). FL deficiency also affected the numbers of Ly6D<sup>-</sup> EPLM and CLP, whereas IL-7 did not (Fig. S1C and D). Therefore, Ly6D<sup>+</sup> EPLM/CLP represent the earliest developmental stage of the B-cell pathway affected by the absence of IL-7.

We have recently generated a mouse model expressing high in vivo levels of FL (8). The progenitor compartment of these mice showed a dramatic increase in EPLM and CLP numbers, with their Ly6D<sup>+</sup> fractions increased 90-fold and 28-fold, respectively, relative to WT (Fig. 1D and E). We crossed *Ft3ltg* with *Il7<sup>-/-</sup>* mice to assess the extent to which increased FL levels could potentially rescue the loss of Ly6D<sup>+</sup>CD19<sup>-</sup> progenitors in *Il7<sup>-/-</sup>* mice. As shown in Fig. 2A and B, in vivo overexpression of FL leads to a

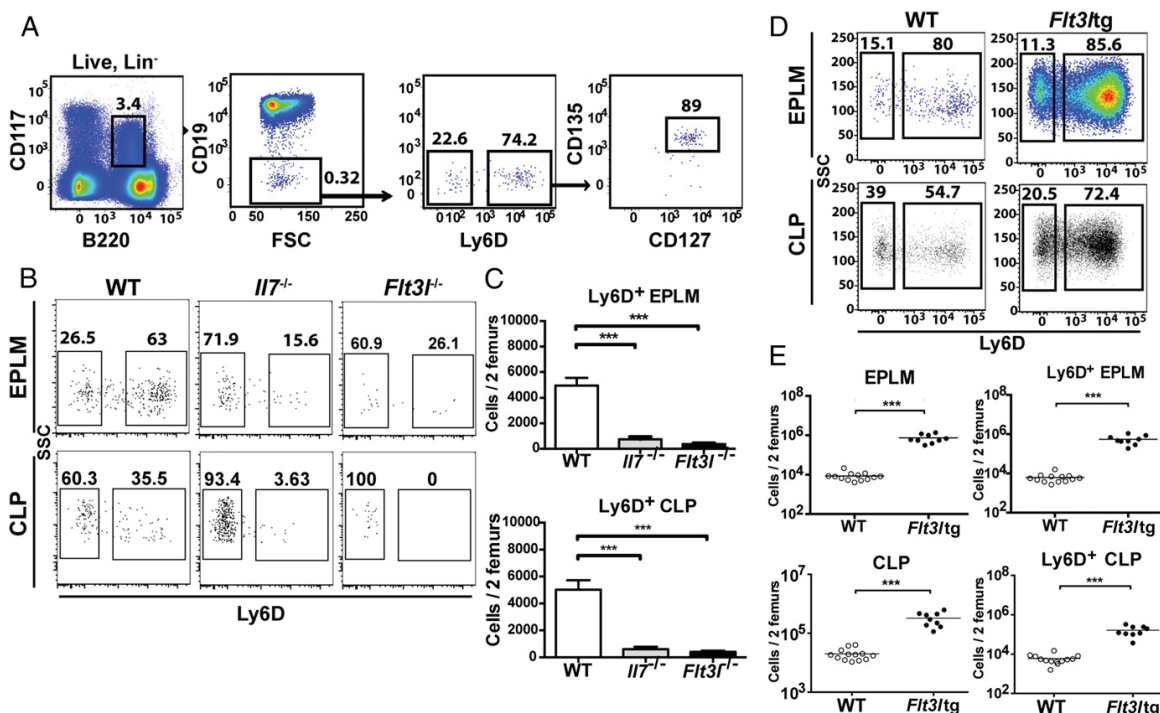


**Fig. 1.** IL-7 and FL are necessary for the generation of a normal Ly6D<sup>+</sup>CD135<sup>+</sup>CD127<sup>+</sup>CD19<sup>-</sup> compartment. (A) FACS plots showing the gating strategy used for identification of Ly6D<sup>+</sup> EPLM and their percentage of CD135 and CD127 expression. Lineage staining was as follows: SiglecH, CD115, CD11c, NK1.1, Gr-1. (B) Representative FACS plots of EPLM (Upper row) and CLP (Lower row) from the bone marrow of WT, *Il7<sup>-/-</sup>*, and *Ft3l<sup>-/-</sup>* mice. (C) Absolute numbers of Ly6D<sup>+</sup> EPLM (Upper graph) and CLP (Lower graph) from the bone marrow of WT ( $n = 13$ ), *Il7<sup>-/-</sup>* ( $n = 5$ ), and *Ft3l<sup>-/-</sup>* ( $n = 10$ ) mice. (D) Representative FACS plots of EPLM and CLP from WT and *Ft3ltg* mice. (E) Absolute numbers of total EPLM and CLP (Left graphs) and Ly6D<sup>+</sup> EPLM and CLP (Right graphs) from WT and *Ft3ltg* mice. \*\*\* $P \leq 0.001$ .

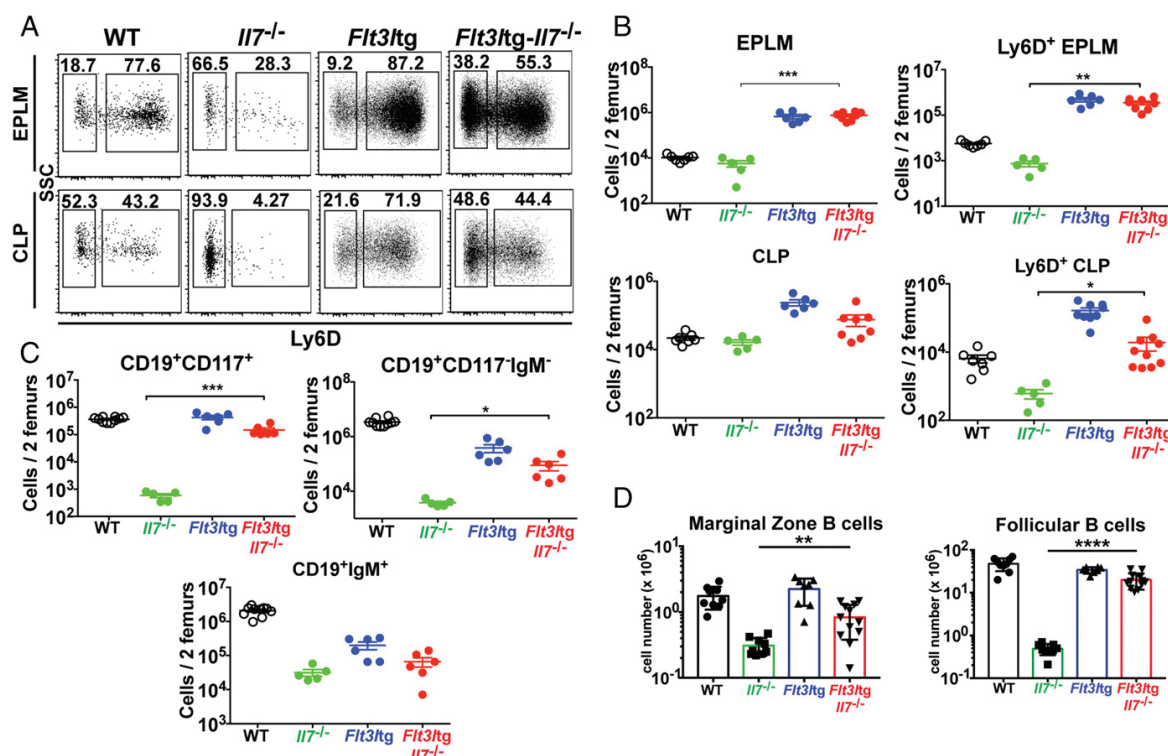


**Fig. 2.** Increased in vivo FL levels rescue B-cell generation in *Il7*<sup>-/-</sup> mice. (A) Representative FACS plots of EPLM (Upper) and CLP (Lower) from WT, *Il7*<sup>-/-</sup>, *Flt3ltg*, and *Flt3ltg-Il7*<sup>-/-</sup> mice. (B) Numbers of EPLM (Upper Left), CLP (Lower Left), Ly6D<sup>+</sup> EPLM (Upper Right), and Ly6D<sup>+</sup> CLP (Lower Right) from the mouse genotypes indicated on the x axes. For each mouse genotype, mean  $\pm$  SEM is shown. (C) Numbers of CD19<sup>+</sup>CD117<sup>+</sup> (Upper Left), CD19<sup>+</sup>CD117<sup>-</sup>IgM<sup>+</sup> (Upper Right), and CD19<sup>+</sup>IgM<sup>+</sup> (Lower) bone marrow cells from the mice indicated on the x axes. For each mouse genotype, mean  $\pm$  SEM is shown. (D) Numbers of CD19<sup>+</sup>CD21<sup>high</sup>CD23<sup>low</sup> marginal zone (Left) and CD19<sup>+</sup>CD21<sup>+</sup>CD23<sup>+</sup> follicular (Right) B cells in the spleens of WT or mutant mice, as indicated on the x axes. For each mouse genotype, mean  $\pm$  SD is shown. \* $P < 0.05$ , \*\* $P < 0.01$ , \*\*\* $P < 0.001$ , \*\*\*\* $P < 0.0001$ .

significant increase in *Flt3ltg-Il7*<sup>-/-</sup> EPLM and CLP numbers, reaching levels of those in *Flt3ltg* mice. Crucially, a full rescue of Ly6D<sup>+</sup> EPLM and CLP can be seen in these mice, with a striking 470-fold and 31-fold increase in numbers compared with their *Il7*<sup>-/-</sup> counterparts (Fig. 2A and B). Furthermore, the numbers of the earliest committed CD19<sup>+</sup>CD117<sup>+</sup> pro-B cells were fully restored in *Flt3ltg-Il7*<sup>-/-</sup> mice, showing a 251-fold increase compared with *Il7*<sup>-/-</sup> (Fig. 2C and Fig. S2). However, this rescue was less pronounced in downstream CD19<sup>+</sup>CD117<sup>-</sup>IgM<sup>+</sup> and CD19<sup>+</sup>IgM<sup>+</sup> B-cell stages, because these cells require IL-7 to expand. As a consequence of this rescue in bone marrow B-cell development, numbers of splenic marginal zone and follicular B cells were significantly increased in *Flt3ltg-Il7*<sup>-/-</sup> mice compared with *Il7*<sup>-/-</sup> (Fig. 2D). Whereas thymic T-cell development was not rescued in *Flt3ltg-Il7*<sup>-/-</sup> mice (Fig. S3), a significant increase in splenic T-cell numbers was observed (Fig. S4) as a result of their expansion upon FL overexpression (32).

To assess whether these rescued *Flt3ltg-Il7*<sup>-/-</sup> Ly6D<sup>+</sup>CD19<sup>-</sup> progenitors could give rise to B cells in vitro, we sorted *Flt3ltg-Il7*<sup>-/-</sup> Ly6D<sup>+</sup> EPLM and plated them at limiting dilution on OP9 stromal cells in the presence of IL-7. As shown in Fig. 3A, *Flt3ltg-Il7*<sup>-/-</sup> Ly6D<sup>+</sup> EPLM could generate B cells at similar frequencies to their WT and *Flt3ltg* counterparts, whereas the few *Il7*<sup>-/-</sup> Ly6D<sup>+</sup> EPLM isolated could not. A rescue in Ly6D<sup>+</sup> EPLM was also observed when *Il7*<sup>-/-</sup> mice were injected with FL (Fig. 3E) and when plated under the same conditions these rescued Ly6D<sup>+</sup> EPLM also showed a restored in vitro B-cell potential (Fig. S5A). Further,

when transplanted into irradiated *Rag2*<sup>-/-</sup> mice, they were able to generate IgM<sup>+</sup> B cells (Fig. S5B and C). Thus, increased FL levels restore the generation of Ly6D<sup>+</sup> progenitors, rather than merely expanding the few Ly6D<sup>+</sup> EPLM/CLPs found in *Il7*<sup>-/-</sup> mice. RT quantitative PCR (RT-qPCR) analysis of Ly6D<sup>+</sup> EPLM from *Flt3ltg-Il7*<sup>-/-</sup> mice revealed significant expression of *Ebf1*, *Pax5*, and *Foxo1* transcription factors' mRNA in the absence of IL-7 (Fig. 3B). *Ebf1* expression at the protein level was confirmed by intracellular FACS staining (Fig. 3C and D). Even though the percentage of *Flt3ltg-Il7*<sup>-/-</sup> Ebf1<sup>+</sup>Ly6D<sup>+</sup> EPLM did not reach WT levels, it was similar to the one found in *Flt3ltg* mice, which produce IL-7. Therefore, *Ebf1/Pax5* expression and subsequent commitment to the B-cell fate can occur in the absence of IL-7 signaling, arguing against an instructive role of this cytokine in B-cell commitment.

CD127 (IL7R $\alpha$ ) is a receptor shared between IL-7 and thymic stromal lymphopoietin (TSLP), a cytokine capable of rescuing B-cell development when overexpressed in the absence of IL-7 (33). Because TSLP is produced by dendritic cells (34), which are dramatically expanded in *Flt3ltg* mice (8), in vivo FL overexpression could lead to increased levels of TSLP, thereby rescuing B-cell development in *Flt3ltg-Il7*<sup>-/-</sup> mice. To investigate this possibility, we injected *Il7*<sup>-/-</sup> or *Il7ra*<sup>-/-</sup> mice with FL as described above and assessed the rescue of Ly6D<sup>+</sup> EPLM and downstream CD19<sup>+</sup> progenitors. FL injections into *Il7*<sup>-/-</sup> mice resulted in a significant increase in Ly6D<sup>+</sup> EPLM and CD19<sup>+</sup>CD117<sup>+</sup> B-cell progenitors, comparable to the rescue observed in *Flt3ltg-Il7*<sup>-/-</sup>

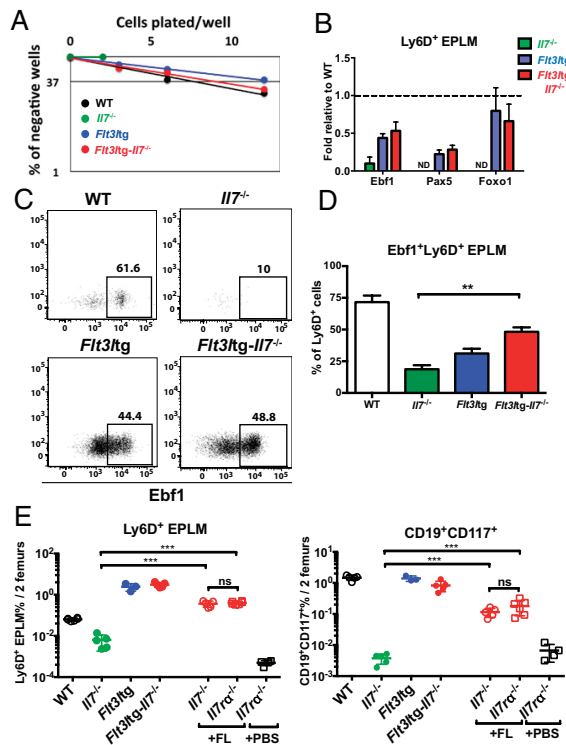


**Fig. 3.** Increased in vivo FL rescues B-cell commitment in the absence of IL-7 and/or TSLP. (A) In vitro limiting dilution analysis of Ly6D<sup>+</sup> EPLM B-cell potential. Ly6D<sup>+</sup> EPLM were sorted from WT, *Il7<sup>-/-</sup>*, *Flt3tg*, and *Flt3tg-Il7<sup>-/-</sup>* mice and plated at the indicated concentrations on OP9 stromal cells together with IL-7. One representative out of four independent experiments is shown. (B) RT-qPCR analysis showing expression of *Ebf1*, *Pax5*, and *Foxo1* mRNAs in Ly6D<sup>+</sup> EPLM sorted from the indicated mouse genotypes. Bars show fold expression relative to WT (set as 1). Error bars represent the SEM from three to six independent experiments. (C) Representative FACS plots showing expression of Ebf1 protein within the Ly6D<sup>+</sup> EPLM of the indicated WT or mutant mice. (D) Percentages of Ebf1-expressing Ly6D<sup>+</sup> EPLM from WT ( $n = 7$ ), *Il7<sup>-/-</sup>* ( $n = 3$ ), *Flt3tg* ( $n = 11$ ), and *Flt3tg-Il7<sup>-/-</sup>* ( $n = 6$ ) mice. Bars show mean  $\pm$  SEM. (E) Ly6D<sup>+</sup> EPLM (Left), and CD19<sup>+</sup>CD117<sup>+</sup> (Right) numbers from WT ( $n = 5$ ), *Il7<sup>-/-</sup>* ( $n = 5$ ), *Flt3tg* ( $n = 3$ ), and *Flt3tg-Il7<sup>-/-</sup>* ( $n = 5$ ) mice, as well as from *Il7<sup>-/-</sup>* ( $n = 5$ ) and *Il7<sup>-/-</sup>* ( $n = 6$ ) mice injected intraperitoneally with 10 daily doses of 10  $\mu$ g FL each (indicated as +FL) or PBS (+PBS,  $n = 4$ ). Shown is the mean  $\pm$  SEM. n.s., not significant, \*\* $P \leq 0.01$ , \*\*\* $P \leq 0.001$ .

mice (Fig. 3E). FL-injected *Il7<sup>-/-</sup>* mice also demonstrated a significant rescue of Ly6D<sup>+</sup> EPLM and CD19<sup>+</sup>CD117<sup>+</sup> pro-B cells, indicating that the observed rescue of B-cell commitment in *Flt3tg-Il7<sup>-/-</sup>* mice is not mediated through the action of TSLP.

**IL-7 Promotes Survival, but Not Proliferation, of Ly6D<sup>+</sup>CD135<sup>+</sup>CD127<sup>+</sup>CD19<sup>-</sup> Progenitors.** Even though our *Flt3tg-Il7<sup>-/-</sup>* mouse model suggests that IL-7 is dispensable for B-cell commitment, the dramatic decrease in *Il7<sup>-/-</sup>* Ly6D<sup>+</sup> EPLM/CLPs argues for a role of IL-7 in the maintenance of this population when FL levels are limiting, by promoting either their survival or their proliferation. To investigate the potential role of IL-7 as a survival factor for Ly6D<sup>+</sup>CD135<sup>+</sup>CD127<sup>+</sup>CD19<sup>-</sup> progenitors, we crossed *Il7<sup>-/-</sup>* mice with mice expressing the prosurvival gene *Bcl2* (35). *Bcl2tg-Il7<sup>-/-</sup>* mice demonstrated a minor but statistically significant 2.6-fold increase in Ly6D<sup>+</sup> EPLM and 2.2-fold increase in Ly6D<sup>+</sup> CLP numbers compared with *Il7<sup>-/-</sup>* mice (Fig. 4A and B). Cell cycle stage analysis of Ly6D<sup>+</sup> EPLM of these mice indicated that most of the cells rescued by *Bcl2* are in a quiescent

state (Fig. S6) and do not proliferate in response to cytokines, thereby compromising to some extent the rescue of these progenitors' numbers. Importantly, when plated on OP9 stromal cells plus IL-7, *Bcl2tg-Il7<sup>-/-</sup>* Ly6D<sup>+</sup> EPLM generated B cells at frequencies similar to WT mice (Fig. 4C), indicating that these rescued Ly6D<sup>+</sup> cells had B-cell potential. Indeed, when analyzing bone marrow CD19<sup>+</sup> committed progenitors, we could see a significant 68-fold increase in the earliest CD19<sup>+</sup>CD117<sup>+</sup> pro-B-cell compartment, compared with *Il7<sup>-/-</sup>* (Fig. 4D). Due to their quiescent state (Fig. S6) (36) and the IL-7 dependence of their proliferation, *Bcl2tg-Il7<sup>-/-</sup>* CD19<sup>+</sup>CD117<sup>+</sup> immature B cells showed a less pronounced, but significant rescue (Fig. 4D). In the spleens of these mice, marginal zone and follicular B-cell numbers were increased, whereas as previously reported (16), T-cell numbers were rescued (Fig. S7). Therefore, providing an extra *Bcl2*-mediated survival signal in vivo partially rescues *Il7<sup>-/-</sup>* Ly6D<sup>+</sup>CD19<sup>-</sup> progenitors with B-cell potential and restores significantly the generation of CD19<sup>+</sup> progenitors. This result suggests a role for IL-7 in facilitating the survival of Ly6D<sup>+</sup>CD135<sup>+</sup>CD127<sup>+</sup>CD19<sup>-</sup> progenitors.

To evaluate the potential proliferative effect of IL-7 on Ly6D<sup>+</sup>CD135<sup>+</sup>CD127<sup>+</sup>CD19<sup>-</sup> progenitors, we analyzed a transgenic mouse model, in which *Il7* expression is driven by an MHC class II promoter, resulting in increased in vivo levels of IL-7 (37). These mice exhibit a lymphoproliferative phenotype with increased numbers of CD19<sup>+</sup> B cells (38). In contrast to bone marrow CD19<sup>+</sup> cells, Ly6D<sup>+</sup> EPLM numbers did not increase in response to elevated IL-7 (Fig. 5A–C). In addition, the cell cycle profile of Ly6D<sup>+</sup> EPLM remained unaltered in *Il7tg* mice compared with WT (Fig. 5D), arguing against a proliferative action of IL-7 on these progenitors. To exclude the possibility that a proliferative signal by FL present in these mice compromised the effect of increased IL-7 on the cell cycle status of Ly6D<sup>+</sup> EPLM, we crossed *Il7tg* with *Flt3l<sup>-/-</sup>* mice. Overexpression of IL-7 in vivo did not result in a significant increase in Ly6D<sup>+</sup> EPLM or CLP numbers in the absence of FL (Fig. 5E and Fig. S8). In contrast, a threefold increase in CD19<sup>+</sup>CD117<sup>+</sup> numbers was observed (Fig. 5F), in agreement with the proliferative effect of IL-7 on CD19<sup>+</sup> B cells. This resulted in a small, but significant, increase in splenic follicular B cells (Fig. S9). Moreover, cell cycle analysis of *Il7tg-Flt3l<sup>-/-</sup>* Ly6D<sup>+</sup> EPLM showed no significant change in their cycling profile compared with their *Flt3l<sup>-/-</sup>* counterparts (Fig. 5G). Therefore, we conclude that, whereas IL-7 acts as a proliferative factor for CD19<sup>+</sup> committed B cells, it does not do so for their Ly6D<sup>+</sup>CD135<sup>+</sup>CD127<sup>+</sup>CD19<sup>-</sup> precursors.

#### FL Induces Proliferation of Ly6D<sup>+</sup>CD135<sup>+</sup>CD127<sup>+</sup>CD19<sup>-</sup> Progenitors.

As evident in Fig. 5G, loss of in vivo FL signaling affected the proliferative status of Ly6D<sup>+</sup> EPLM. Comparison of Ly6D<sup>+</sup> EPLM numbers in mice either lacking or overexpressing FL showed a 14-fold reduction in *Flt3l<sup>-/-</sup>* Ly6D<sup>+</sup> EPLM numbers compared with WT, whereas *Flt3tg* Ly6D<sup>+</sup> EPLM increased 105-fold (Fig. 6A). A similar response to FL levels was observed for Ly6D<sup>+</sup> CLPs (Fig. 6A). Cell cycle analysis of Ly6D<sup>+</sup> EPLM from these mice showed a significant increase in the percentage of Ki67<sup>+</sup>DAPI<sup>+</sup> cells and a decrease in the percentage of Ki67<sup>+</sup> cells when FL signaling was absent, whereas *Flt3tg* Ly6D<sup>+</sup> EPLM showed the reverse (Fig. 6B and Fig. S10). Thus, our data indicate that FL promotes the proliferation of Ly6D<sup>+</sup>CD135<sup>+</sup>CD127<sup>+</sup>CD19<sup>-</sup> progenitors.

To evaluate whether FL also regulates the survival of Ly6D<sup>+</sup>CD135<sup>+</sup>CD127<sup>+</sup>CD19<sup>-</sup> progenitors, we crossed *Flt3l<sup>-/-</sup>* mice with *Bcl2tg* mice. Thus, *Bcl2tg-Flt3l<sup>-/-</sup>* mice showed a minor twofold increase in Ly6D<sup>+</sup> EPLM numbers compared with their *Flt3l<sup>-/-</sup>* counterparts (1.8-fold for Ly6D<sup>+</sup> CLPs) (Fig. 6C). Nevertheless, the in vitro B-cell potential of *Flt3l<sup>-/-</sup>* Ly6D<sup>+</sup> EPLM progenitors was not improved by *Bcl2* overexpression (Fig. 6D). Downstream CD19<sup>+</sup> progenitors also demonstrated a partial, but

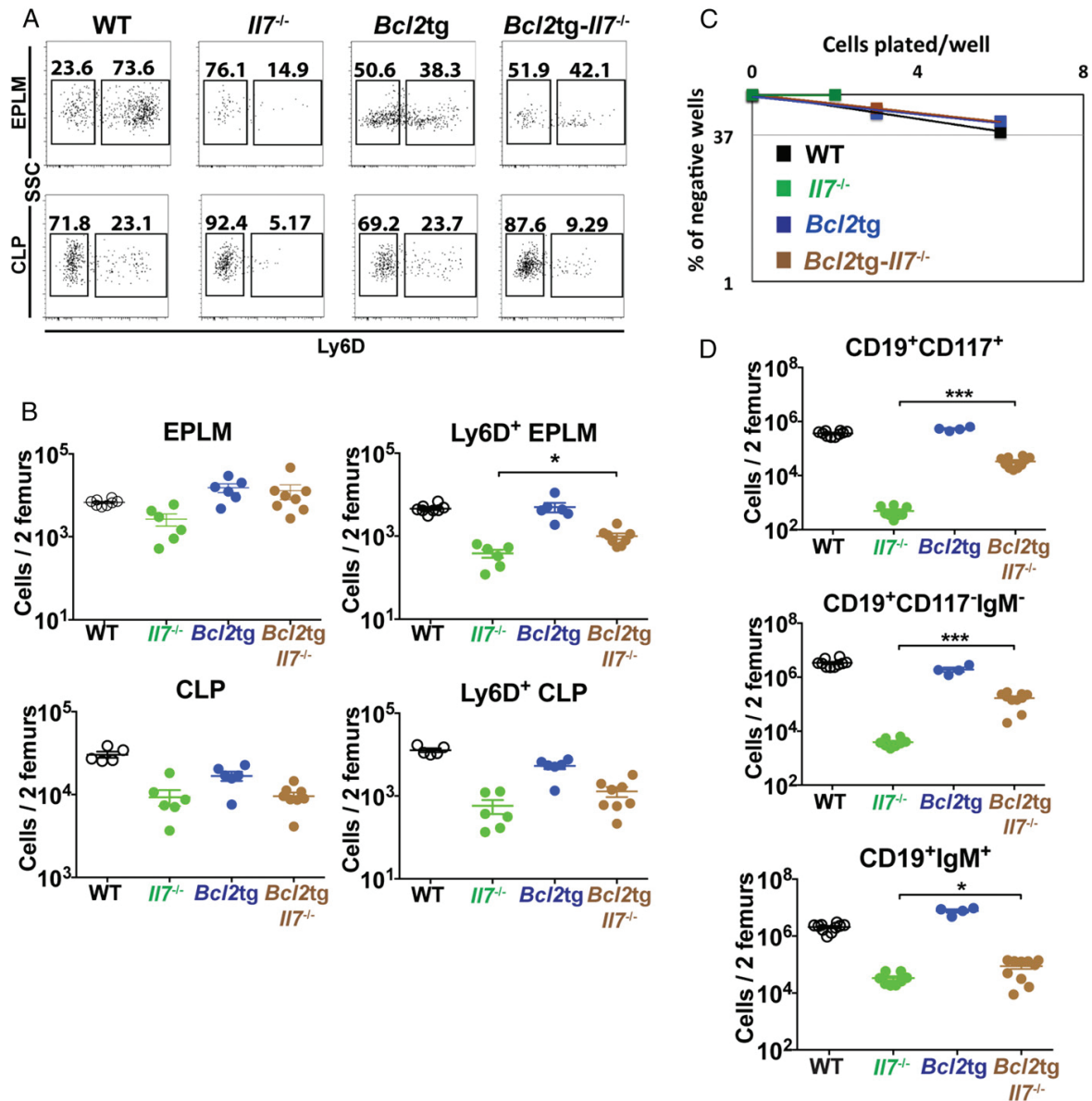


**Fig. 4.** *Bcl2* overexpression partially rescues B-cell commitment in *I17*<sup>-/-</sup> mice. (A) Representative FACS plots of EPLM (Upper) and CLP (Lower) from WT, *I17*<sup>-/-</sup>, *Bcl2*tg, and *Bcl2*tg-*I17*<sup>-/-</sup> mice. (B) Numbers of EPLM (Upper Left), CLP (Lower Left), Ly6D<sup>+</sup> EPLM (Upper Right), and Ly6D<sup>+</sup> CLP (Lower Right) from WT and mutant mice, as indicated on the x axes. For each mouse genotype, mean  $\pm$  SEM is shown. (C) In vitro limiting dilution analysis of Ly6D<sup>+</sup> EPLM B-cell potential. Ly6D<sup>+</sup> EPLM were sorted from WT, *I17*<sup>-/-</sup>, *Bcl2*tg, and *Bcl2*tg-*I17*<sup>-/-</sup> mice and plated at the indicated concentrations on OP9 stromal cells together with IL-7. One representative of three independent experiments is shown. (D) Numbers of CD19<sup>+</sup>CD117<sup>+</sup> (Top), CD19<sup>+</sup>CD117<sup>-</sup>IgM<sup>-</sup> (Middle), and CD19<sup>+</sup>IgM<sup>+</sup> (Bottom) bone marrow cells from WT and mutant mice, as indicated on the x axes. For each mouse genotype, mean  $\pm$  SEM is shown. \* $P \leq 0.05$ , \*\*\* $P \leq 0.001$ .

significant, rescue (Fig. 6E). Our analysis of *Bcl2*tg-*Flt3l*<sup>-/-</sup> mice suggests that the reduction in Ly6D<sup>+</sup>CD135<sup>+</sup>CD127<sup>+</sup>CD19<sup>-</sup> progenitors observed in *Flt3l*<sup>-/-</sup> mice can only be partially explained by a survival role of FL. In contrast, the clear change in the numbers and cycling profile of these progenitors in response to the absence or overabundance of FL in vivo, as well as the inability of *Bcl2* to rescue their in vitro B-cell potential, points toward proliferation as being the main effector function of FL at this developmental stage.

**FL Does Not Instruct Commitment to the B-Cell Lineage.** The striking rescue in B-cell commitment observed in our *Flt3l*tg-*I17*<sup>-/-</sup> mice could be explained by a potential instructive role of FL when present at high levels in vivo. However, increased FL did not result in *Ebf1* or *Pax5* up-regulation (Fig. 3 B–D). Moreover, analysis of *Flt3l*<sup>-/-</sup> Ly6D<sup>+</sup> EPLM showed that, whereas absence of FL in vivo leads to a reduction in the numbers of Ly6D<sup>+</sup> EPLM (Fig. 1C), it does not significantly reduce the percentage

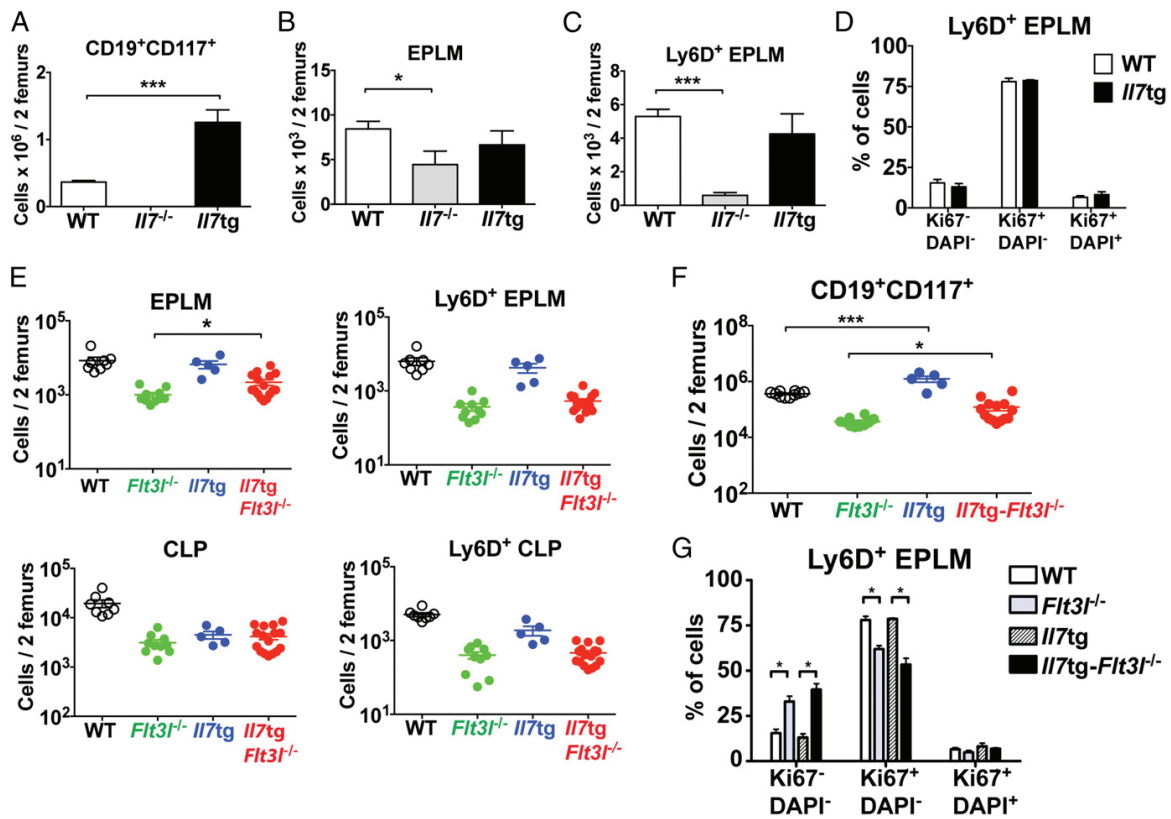


**Fig. 5.** IL-7 does not induce proliferation of Ly6D<sup>+</sup>CD135<sup>+</sup>CD127<sup>+</sup>CD19<sup>-</sup> progenitors. (A) CD19<sup>+</sup>CD117<sup>+</sup> numbers in bone marrow of WT ( $n = 10$ ), *Il7*<sup>-/-</sup> ( $n = 5$ ), and *Il7*tg ( $n = 8$ ) mice. (B) EPLM numbers in bone marrow of WT ( $n = 14$ ), *Il7*<sup>-/-</sup> ( $n = 7$ ), and *Il7*tg ( $n = 5$ ) mice. (C) Ly6D<sup>+</sup> EPLM numbers in bone marrow of WT ( $n = 14$ ), *Il7*<sup>-/-</sup> ( $n = 7$ ), and *Il7*tg ( $n = 5$ ) mice. (D) Cell cycle analysis of Ly6D<sup>+</sup> EPLM from WT ( $n = 5$ ) and *Il7*tg ( $n = 2$ ) mice. Graph shows percentages of Ki67<sup>-</sup>DAPI<sup>-</sup>, Ki67<sup>+</sup>DAPI<sup>-</sup>, and Ki67<sup>+</sup>DAPI<sup>+</sup> Ly6D<sup>+</sup> EPLM. Bars in A–D show mean  $\pm$  SEM. (E) Numbers of EPLM (Upper Left), CLP (Lower Left), Ly6D<sup>+</sup> EPLM (Upper Right), and Ly6D<sup>+</sup> CLP (Lower Right) from WT and mutant mice, as indicated on the x axis. For each mouse genotype, mean  $\pm$  SEM is shown. (F) Numbers of CD19<sup>+</sup>CD117<sup>+</sup> bone marrow cells from WT and mutant mice, as indicated on the x axis. For each mouse genotype, mean  $\pm$  SEM is shown. (G) Cell cycle analysis of Ly6D<sup>+</sup> EPLM from WT ( $n = 5$ ), *Flt3l*<sup>-/-</sup> ( $n = 3$ ), *Il7*tg ( $n = 2$ ), and *Il7*tg-*Flt3l*<sup>-/-</sup> ( $n = 3$ ) mice. Graph shows percentages of Ki67<sup>-</sup>DAPI<sup>-</sup>, Ki67<sup>+</sup>DAPI<sup>-</sup>, and Ki67<sup>+</sup>DAPI<sup>+</sup> Ly6D<sup>+</sup> EPLM. Bars show mean  $\pm$  SEM. \* $P \leq 0.05$ , \*\*\* $P \leq 0.001$ .

of Ebf1<sup>+</sup> cells within the population (Fig. 7 *A* and *B*), consistent with a permissive rather than instructive role of FL. Finally, the decrease in the Ebf1<sup>+</sup> fraction of Ly6D<sup>+</sup> EPLM upon exposure to high levels of FL was reflected in the increased ability of these progenitors to give rise to T cells in vitro, as manifested by the high frequency of T-cell clone generation when *Flt3l*tg Ly6D<sup>+</sup> EPLM were plated on OP9-DL1 stromal cells in the presence of IL-7 (Fig. 7*C*). The above data suggest that FL does not instruct commitment to the B-cell lineage through up-regulation of *Ebf1* and *Pax5* expression.

#### Discussion

Commitment to the B-cell lineage is mediated by the expression of Ebf1 and Pax5 transcription factors and it is initiated in Ly6D<sup>+</sup>CD135<sup>+</sup>CD127<sup>+</sup> progenitors before CD19 expression (30, 31). In *Il7*<sup>-/-</sup> mice, this Ly6D<sup>+</sup> CLP compartment is significantly reduced (22), a finding confirmed in the present study for both CLP and EPLM, a B220<sup>int/+</sup> population partly overlapping with CLP and pre/pro-B cells (Fig. 1 *B* and *C*). The proliferative effect of IL-7 on committed CD19<sup>+</sup> B-cell progenitors (38) makes the investigation of its role in B-cell commitment challenging when using CD19<sup>+</sup> cells as readout. Hence, we assessed the role of IL-7 in B-cell commitment by analyzing the Ly6D<sup>+</sup> CLP/EPLM compartment in

different mouse models. Our analysis of *Flt3l*tg-*Il7*<sup>-/-</sup> mice showed a complete rescue of Ly6D<sup>+</sup> CLP/EPLM numbers in vivo and their B-cell potential in vitro and in vivo, whereas Ebf1 and Pax5 were expressed at similar levels to *Flt3l*tg mice, thereby indicating that IL-7 signaling is not required for their up-regulation at the Ly6D<sup>+</sup>CD19<sup>-</sup> stage (Figs. 2 and 3). These results suggest that IL-7 is not acting as an instructive cytokine in B-cell commitment by initiating Ebf1 and Pax5 expression at the CD135<sup>+</sup>CD127<sup>+</sup>CD19<sup>-</sup> stage, as previously hypothesized (18–20), but rather as a permissive one.

Early investigations had shown that *Bcl2* overexpression in the absence of IL-7 signaling could rescue T-cell (39, 40) but not B-cell development (16, 17). However, a more recent study demonstrated a *Bcl2*-mediated rescue of CD19<sup>+</sup> progenitors in conditional *Stat5*<sup>-/-</sup> mice, as well as a strong activation of the prosurvival gene *Mcl1* expression by Stat5 (21), therefore suggesting a survival role for IL-7 in B-cell development. Our use of *Il7*<sup>-/-</sup> mice instead of *Il7ra*<sup>-/-</sup>, which allows the assessment of progenitor in vitro B-cell potential, and our focus on Ly6D<sup>+</sup>CD135<sup>+</sup>CD127<sup>+</sup>CD19<sup>-</sup> progenitors, has enabled us to confirm the latter findings and extend them to the CD19<sup>-</sup> stage where B-cell commitment events are initiated at the molecular level. Interestingly, *Il7*tg mice analysis showed that IL-7 indeed acts as a proliferative factor for committed CD19<sup>+</sup> cells, but not for their CD19<sup>-</sup> precursors. Even

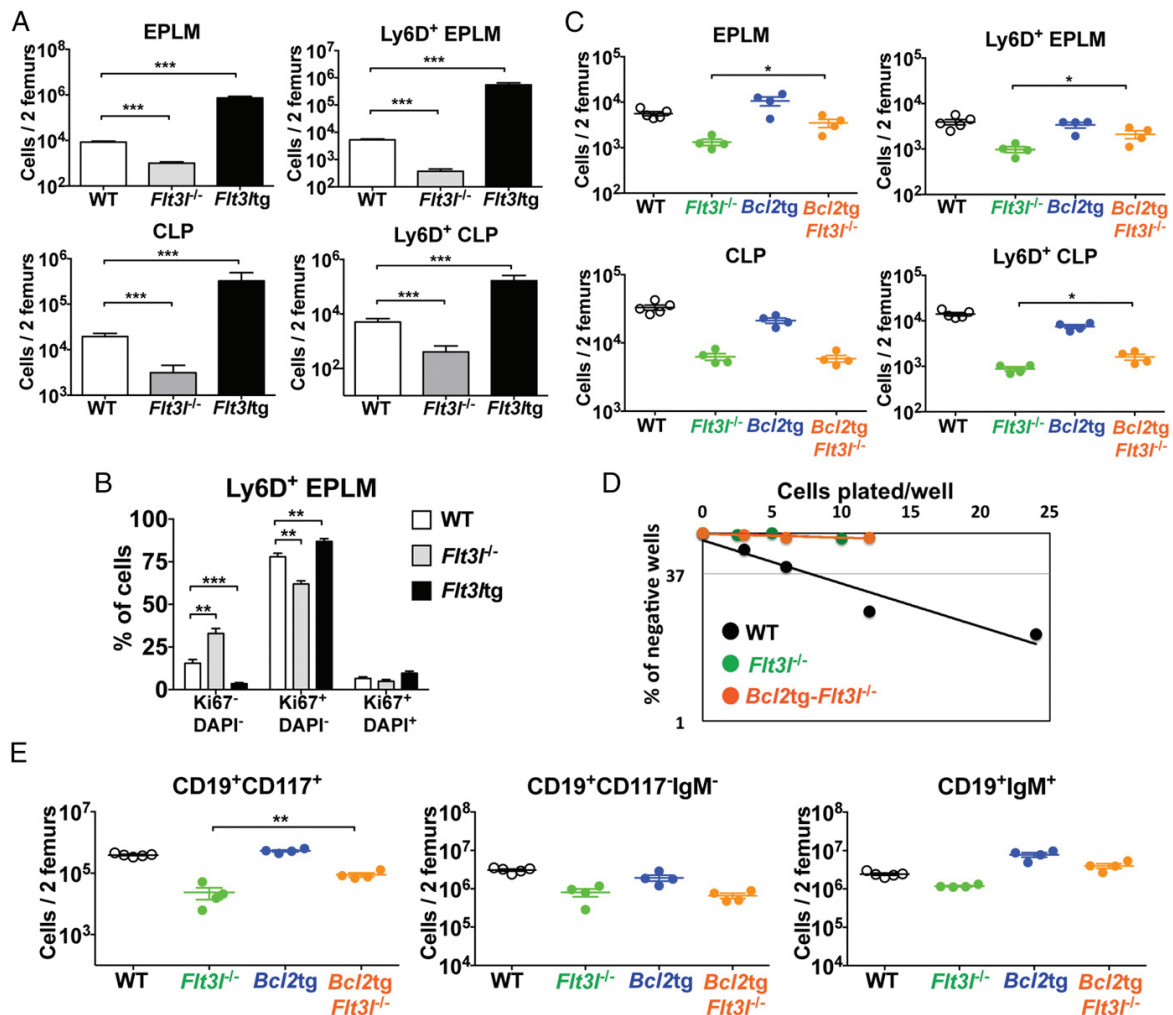


**Fig. 6.** FL promotes proliferation but not survival of  $\text{Ly6D}^+\text{CD135}^+\text{CD127}^+\text{CD19}^-$  progenitors. (A) Numbers of EPLM (Upper Left), CLP (Lower Left),  $\text{Ly6D}^+$  EPLM (Upper Right), and  $\text{Ly6D}^+$  CLP (Lower Right) from WT ( $n = 14$ ),  $\text{FIt3l}^{-/-}$  ( $n = 10$ ) and  $\text{FIt3l/tg}$  ( $n = 9$ ) mice. Bars show mean  $\pm$  SEM. (B) Cell cycle analysis of  $\text{Ly6D}^+$  EPLM from WT ( $n = 5$ ),  $\text{FIt3l}^{-/-}$  ( $n = 3$ ), and  $\text{FIt3l/tg}$  ( $n = 9$ ) mice. Graph shows percentages of  $\text{Ki67}^-\text{DAPI}^-$ ,  $\text{Ki67}^+\text{DAPI}^-$ , and  $\text{Ki67}^+\text{DAPI}^+$   $\text{Ly6D}^+$  EPLM. Bars show mean  $\pm$  SEM. (C) Numbers of EPLM (Upper Left), CLP (Lower Left),  $\text{Ly6D}^+$  EPLM (Upper Right), and  $\text{Ly6D}^+$  CLP (Lower Right) from WT and mutant mice, as indicated on the x axes. For each mouse genotype, mean  $\pm$  SEM is shown. (D) In vitro limiting dilution analysis of  $\text{Ly6D}^+$  EPLM B-cell potential.  $\text{Ly6D}^+$  EPLM were sorted from WT,  $\text{FIt3l}^{-/-}$ , and  $\text{Bcl2tg-FIt3l}^{-/-}$  mice and plated at the indicated concentrations on OP9 stromal cells together with IL-7. (E) Numbers of  $\text{CD19}^+\text{CD117}^+$  (Left),  $\text{CD19}^+\text{CD117}^-\text{IgM}^-$  (Middle), and  $\text{CD19}^+\text{IgM}^+$  (Right) bone marrow cells from WT and mutant mice, as indicated on the x axes. For each mouse genotype, mean  $\pm$  SEM is shown. \* $P \leq 0.05$ , \*\* $P \leq 0.01$ , \*\*\* $P \leq 0.001$ .

in the absence of FL, excess IL-7 was unable to significantly increase  $\text{Ly6D}^+$  CLP/EPLM numbers, whereas it did so for  $\text{CD19}^+$  B-cell progenitors (Fig. 5). Hence, we propose that the main role of IL-7 at the  $\text{CD135}^+\text{CD127}^+\text{CD19}^-$  stage is to provide survival signals to the progenitors until they commit to the B-cell lineage upon Pax5 and CD19 expression, after which it additionally induces their proliferation (Fig. 7D). This survival role becomes particularly critical when FL levels are limiting, thereby explaining the reduction in  $\text{Ly6D}^+$  CLP/EPLM seen in  $\text{Il7}^{-/-}$  mice. Our study, in agreement with previous data (21), identifies a common, permissive rather than instructive role for IL-7 in both B- and T-cell development (39, 40).

The rescue in B-cell commitment without active IL-7 signaling occurs when FL is expressed above physiological levels.

Even though a minor role for FL as a survival factor for  $\text{Ly6D}^+\text{CD135}^+\text{CD127}^+\text{CD19}^-$  progenitors cannot be excluded, the main effect of FL on these progenitors seems to be the induction of their proliferation, as suggested by their expansion and their increased cycling upon FL overexpression, with the reverse phenotype observed upon loss of FL signaling (Fig. 6). Moreover, increased FL leads to expansion of  $\text{Lin}^-\text{CD117}^+\text{Sca1}^+$  cells (LSK) (8), thereby increasing the developmental input into the  $\text{Ly6D}^+\text{CD135}^+\text{CD127}^+\text{CD19}^-$  progenitor stage. None of the mouse models analyzed in the present study gave any evidence for an instructive role of FL in B-cell commitment. In contrast, excess FL resulted in a proportional reduction of Ebf- and Pax5-expressing  $\text{Ly6D}^+\text{CD19}^-$  progenitors (Figs. 3 and 7). One explanation for this reduction could be the increased percentage of cycling  $\text{FIt3l/tg}$

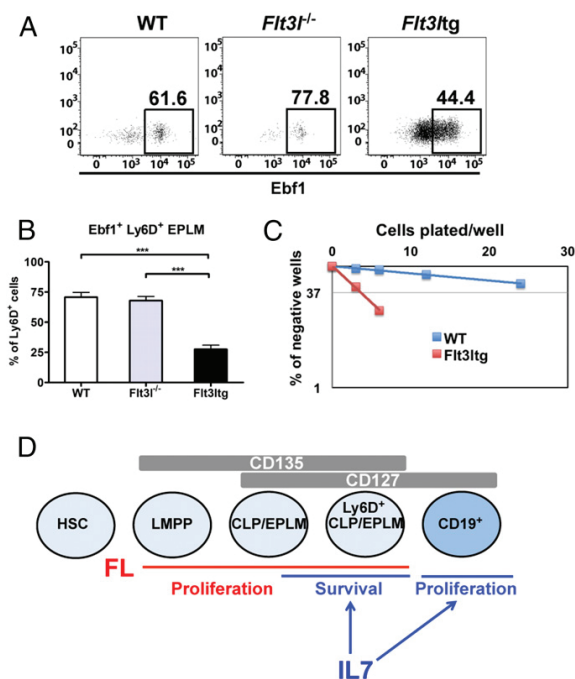


**Fig. 7.** FL does not instruct *Ebf1* expression and B-cell commitment. (A) Representative FACS plots showing expression of Ebf1 protein within the Ly6D<sup>+</sup> EPLM of WT, *FIt3l*<sup>-/-</sup>, and *FIt3ltg* mice. (B) Percentages of Ebf1-expressing Ly6D<sup>+</sup> EPLM from WT ( $n = 7$ ), *FIt3l*<sup>-/-</sup> ( $n = 5$ ), and *FIt3ltg* ( $n = 12$ ) mice. Bars show mean  $\pm$  SEM. (C) In vitro limiting dilution analysis of Ly6D<sup>+</sup> EPLM T-cell potential. Ly6D<sup>+</sup> EPLM were sorted from WT and *FIt3ltg* mice and plated at the indicated concentrations on OP9-DL1 stromal cells together with IL-7. One representative of four independent experiments is shown. (D) Schematic model for the permissive role of IL-7 and FL acting on hematopoietic progenitors and CD19<sup>+</sup> committed B-cell precursors. LMPP, lymphoid-primed multipotent progenitor. \*\*\* $P \leq 0.001$ .

Ly6D<sup>+</sup>CD19<sup>-</sup> progenitors, resulting in a decreased fraction initiating the B-cell developmental program. Alternatively, another environmental factor, responsible for initiation of *Ebf1/Pax5* expression and B-cell commitment, could be the limiting factor in *FIt3ltg* mice, thus leading to a smaller fraction of the expanded Ly6D<sup>+</sup>CD19<sup>-</sup> compartment entering the B-cell pathway. Our conclusion is that FL is mainly responsible for generating enough Ly6D<sup>+</sup>CD135<sup>+</sup>CD127<sup>+</sup>CD19<sup>-</sup> progenitors, both by inducing their proliferation and by increasing their developmental input from the LSK compartment (Fig. 7D) (41, 42). As a result, increased levels of FL in *FIt3ltg-Il7*<sup>-/-</sup> mice lead to a dramatic increase in Ly6D<sup>+</sup>CD135<sup>+</sup>CD127<sup>+</sup>CD19<sup>-</sup> progenitor numbers, therefore surpassing the need for the survival role of IL-7 at this stage and resulting in a sufficient fraction of them committing to the B-cell lineage.

The generation of B-cell progenitors in *FIt3ltg-Il7*<sup>-/-</sup> mice is reminiscent of the apparent IL-7 independency of human B lymphopoiesis, where relatively normal numbers of B cells are seen in patients with mutations in components of the IL-7 signaling pathway (13, 14). However, all patients with such mutations are neonates, and in neonatal *Il7*<sup>-/-</sup> mice, B-cell development also takes place (43). Therefore, the apparent difference in the IL-7 dependency of B-cell development between man and mouse could actually reflect the corresponding difference between fetal/neonatal and adult lymphopoiesis. Our data showing that increased FL signaling can rescue B-cell commitment in the absence of IL-7 could provide a potential explanation for this difference. Fetal/neonatal CD135<sup>+</sup>CD127<sup>+</sup>CD19<sup>-</sup> progenitors might

be exposed to higher levels of FL and/or show higher sensitivity to FL signaling than adult CD135<sup>+</sup>CD127<sup>+</sup>CD19<sup>-</sup> progenitors. Indeed, previous studies showed that despite a preferable response of fetal B-cell progenitors to TSLP, FL signaling remains an absolute requirement for fetal B lymphopoiesis (44, 45).

The instructive or permissive progenitor regulation of lineage commitment by cytokines is a complex process, in which cytokines can initiate developmental transcription programs in progenitors. However, the reverse is also true, because the particular epigenetic, transcriptional, and signaling landscape of a cell can affect its response to a cytokine (9). Indeed, whereas previous analysis of *FIt3ltg* mice indicated an instructive role for FL in promoting differentiation of multipotent progenitors toward lymphomyeloid and away from erythroid fate (8), our present data show that FL acts in a permissive manner for B-cell commitment of CD135<sup>+</sup>CD127<sup>+</sup>CD19<sup>-</sup> progenitors. In addition, whereas IL-7 induces proliferation of committed CD19<sup>+</sup> B-cell progenitors, it does not do so on CD127<sup>+</sup>CD19<sup>-</sup> progenitors, suggesting that upon commitment to the B-cell lineage, changes in the transcription factor and intracellular signaling landscape influence the effector function of IL-7. Therefore, our present data further support the notion of a cell context-dependent cytokine action.

The *Ebf1/Pax5* up-regulation and subsequent B-cell commitment in *FIt3ltg-Il7*<sup>-/-</sup> mice shown herein raises the issue of the potential extracellular regulation of B-cell commitment. One possibility could be that another environmental signal from the bone marrow microenvironment—other than IL-7, TSLP, and FL—initiates *Ebf1* expression in Ly6D<sup>+</sup>CD135<sup>+</sup>CD127<sup>+</sup>CD19<sup>-</sup> progenitors, resulting in Pax5/CD19 expression and B-cell commitment. Alternatively, as yet uncommitted Ly6D<sup>+</sup>CD135<sup>+</sup>CD127<sup>+</sup>CD19<sup>-</sup> progenitors could express Ebf1 in a cell-autonomous, stochastic manner with some obtaining sufficient Ebf1 to initiate the B-cell gene program and eventually commit to the B-cell lineage. The intricate transcription factor network sustaining B-cell commitment through a series of positive feedback regulatory loops (46) provides conceptual support for the latter hypothesis.

#### Materials and Methods

**Mice.** For breeding and analysis, age- and sex-matched C57BL/6 *FIt3l*<sup>-/-</sup> (27), *FIt3ltg* (8), *Il7*<sup>-/-</sup> (10), *Il7ra*<sup>-/-</sup> (11), *Il7tg* (38), and (C57BL/6  $\times$  C3H) *Bcl2tg* (35) mice backcrossed with C57BL/6 for at least five generations were used at 6–11 wk of age. All mice were bred and maintained in our animal facility under specific pathogen-free conditions. Animal experiments were carried out within institutional guidelines (authorization number 1888 from the cantonal veterinarian office, Basel).

**Antibodies, Flow Cytometry, and Sorting.** For analysis, cells were flushed from femurs of the two hind legs of mice. The procedure was performed in PBS containing 0.5% BSA and 5 mM EDTA. For detection of Ebf1 and cell cycle analysis, cells were fixed and permeabilized after cell-surface staining using the Foxp3 Fix/Perm buffer set (eBioscience), and subsequently stained with PE-conjugated anti-Ebf1 (T26-818) or FITC-conjugated anti-Ki67 (B56) and DAPI, according to the supplier's protocol. Flow cytometry was done using a BD LSRFortessa (BD Biosciences) and data were analyzed using FlowJo software (Treestar). For cell sorting, a FACSAria IIu (BD Biosciences) was used (>98% purity).

**In Vitro Limiting Dilution Assays.** Experiments have been performed as previously described (47). Briefly, OP9 or OP9-DL1 stromal cells were plated on flat-bottom 96-well plates 1 d before the initiation of cocultures, at a concentration of 3,000 cells per well. The following day, stromal cells were  $\gamma$ -irradiated (3,000 rad) and the sorted progenitor cells were added at different concentrations. Cultures were maintained in Iscove's modified Dulbecco's medium (IMDM) supplemented with  $5 \times 10^{-5}$  M  $\beta$ -mercaptoethanol, 1 mM glutamine, 0.03% (wt/vol) primatone, 100 units/mL penicillin, 100  $\mu$ g/mL streptomycin, 5% (vol/vol) FBS, and 10% (vol/vol) IL-7-conditioned medium. After 14 d in culture, all wells were inspected under an inverted microscope, and wells containing colonies of more than 50 cells were scored as positive.

**RT-qPCR.** RNA extraction was performed using TRI Reagent (Life Technologies) followed by cDNA synthesis using GoScript Reverse Transcriptase (Promega). RT-qPCR was performed using SYBR Green PCR Master Mix (Applied Biosystems).

**Statistical Analysis.** Statistical analysis was performed with Prism 6.0g software (GraphPad software). Two-tailed unpaired Student *t* tests were used for statistical comparisons. If not differently indicated, data are presented as mean values  $\pm$  SD or SEM. n.s., not significant or  $P > 0.05$ , \* $P \leq 0.05$ , \*\* $P \leq 0.01$ , \*\*\* $P \leq 0.001$ , \*\*\*\* $P \leq 0.0001$ .

1. Metcalf D (2008) Hematopoietic cytokines. *Blood* 111(2):485–491.
2. Ende M, Etzrodt M, Schroeder T (2014) Instruction of hematopoietic lineage choice by cytokine signaling. *Exp Cell Res* 329(2):207–213.
3. Enver T, Heyworth CM, Dexter TM (1998) Do stem cells play dice? *Blood* 92(2):348–351, discussion 352.
4. Metcalf D (1998) Lineage commitment and maturation in hematopoietic cells: The case for extrinsic regulation. *Blood* 92(2):345–347, discussion 352.
5. Grover A, et al. (2014) Erythropoietin guides multipotent hematopoietic progenitor cells toward an erythroid fate. *J Exp Med* 211(2):181–188.
6. Mossadegh-Keller N, et al. (2013) M-CSF instructs myeloid lineage fate in single haematopoietic stem cells. *Nature* 497(7448):239–243.
7. Rieger MA, Hoppe PS, Smejkal BM, Eitelhuber AC, Schroeder T (2009) Hematopoietic cytokines can instruct lineage choice. *Science* 325(5937):217–218.
8. Tsapogas P, et al. (2014) In vivo evidence for an instructive role of fms-like tyrosine kinase-3 (FLT3) ligand in hematopoietic development. *Haematologica* 99(4):638–646.
9. Sarrazin S, Sieweke M (2011) Integration of cytokine and transcription factor signals in hematopoietic stem cell commitment. *Semin Immunol* 23(5):326–334.
10. von Freeden-Jeffry U, et al. (1995) Lymphopenia in interleukin (IL)-7 gene-deleted mice identifies IL-7 as a nonredundant cytokine. *J Exp Med* 181(4):1519–1526.
11. Peschon JJ, et al. (1994) Early lymphocyte expansion is severely impaired in interleukin 7 receptor-deficient mice. *J Exp Med* 180(5):1955–1960.
12. Parrish YK, et al. (2009) IL-7 Dependence in human B lymphopoiesis increases during progression of ontogeny from cord blood to bone marrow. *J Immunol* 182(7):4255–4266.
13. Noguchi M, et al. (1993) Interleukin-2 receptor gamma chain mutation results in X-linked severe combined immunodeficiency in humans. *Cell* 73(1):147–157.
14. Puel A, Ziegler SF, Buckley RH, Leonard WJ (1998) Defective IL7R expression in T(-)B(+) NK(+) severe combined immunodeficiency. *Nat Genet* 20(4):394–397.
15. Namen AE, et al. (1988) Stimulation of B-cell progenitors by cloned murine interleukin-7. *Nature* 333(6173):571–573.
16. Kondo M, Akashi K, Domen J, Sugamura K, Weissman IL (1997) Bcl-2 rescues T lymphopoiesis, but not B or NK cell development, in common gamma chain-deficient mice. *Immunity* 7(1):155–162.
17. Maraskovsky E, Peschon JJ, McKenna H, Teepe M, Strasser A (1998) Overexpression of Bcl-2 does not rescue impaired B lymphopoiesis in IL-7 receptor-deficient mice but can enhance survival of mature B cells. *Int Immunol* 10(9):1367–1375.
18. Dias S, Silva H, Jr, Cumano A, Vieira P (2005) Interleukin-7 is necessary to maintain the B cell potential in common lymphoid progenitors. *J Exp Med* 201(6):971–979.
19. Kikuchi K, Lai AY, Hsu CL, Kondo M (2005) IL-7 receptor signaling is necessary for stage transition in adult B cell development through up-regulation of EBF. *J Exp Med* 201(8):1197–1203.
20. Roessler S, et al. (2007) Distinct promoters mediate the regulation of Ebf1 gene expression by interleukin-7 and Pax5. *Mol Cell Biol* 27(2):579–594.
21. Malin S, et al. (2010) Role of STAT5 in controlling cell survival and immunoglobulin gene recombination during pro-B cell development. *Nat Immunol* 11(2):171–179.
22. Tsapogas P, et al. (2011) IL-7 mediates Ebf-1-dependent lineage restriction in early lymphoid progenitors. *Blood* 118(5):1283–1290.
23. Mansson R, et al. (2008) B-lineage commitment prior to surface expression of B220 and CD19 on hematopoietic progenitor cells. *Blood* 112(4):1048–1055.
24. Gilliland DG, Griffin JD (2002) The roles of FLT3 in hematopoiesis and leukemia. *Blood* 100(5):1532–1542.
25. Holmes ML, Carotta S, Corcoran LM, Nutt SL (2006) Repression of Flt3 by Pax5 is crucial for B-cell lineage commitment. *Genes Dev* 20(8):933–938.
26. Mackarehtschian K, et al. (1995) Targeted disruption of the flk2/flt3 gene leads to deficiencies in primitive hematopoietic progenitors. *Immunity* 3(1):147–161.
27. McKenna HJ, et al. (2000) Mice lacking flt3 ligand have deficient hematopoiesis affecting hematopoietic progenitor cells, dendritic cells, and natural killer cells. *Blood* 95(11):3489–3497.
28. Sitnicka E, et al. (2002) Key role of flt3 ligand in regulation of the common lymphoid progenitor but not in maintenance of the hematopoietic stem cell pool. *Immunity* 17(4):463–472.
29. Balciunaite G, Ceredig R, Massa S, Rolink AG (2005) A B220+ CD117+ CD19– hematopoietic progenitor with potent lymphoid and myeloid developmental potential. *Eur J Immunol* 35(7):2019–2030.
30. Inlay MA, et al. (2009) Ly6d marks the earliest stage of B-cell specification and identifies the branchpoint between B-cell and T-cell development. *Genes Dev* 23(20):2376–2381.
31. Mansson R, et al. (2010) Single-cell analysis of the common lymphoid progenitor compartment reveals functional and molecular heterogeneity. *Blood* 115(13):2601–2609.
32. Sweet LK, Bosco N, Malissen B, Ceredig R, Rolink A (2009) Expansion of peripheral naturally occurring T regulatory cells by Fms-like tyrosine kinase 3 ligand treatment. *Blood* 113(25):6277–6287.
33. Chappaz S, Flueck L, Farr AG, Rolink AG, Finke D (2007) Increased TSLP availability restores T- and B-cell compartments in adult IL-7 deficient mice. *Blood* 110(12):3862–3870.
34. Kashyap M, Rochman Y, Spolski R, Samsel L, Leonard WJ (2011) Thymic stromal lymphopoietin is produced by dendritic cells. *J Immunol* 187(3):1207–1211.
35. Domen J, Gandy KL, Weissman IL (1998) Systemic overexpression of BCL-2 in the hematopoietic system protects transgenic mice from the consequences of lethal irradiation. *Blood* 91(7):2272–2282.
36. O'Reilly LA, Huang DC, Strasser A (1996) The cell death inhibitor Bcl-2 and its homologues influence control of cell cycle entry. *EMBO J* 15(24):6979–6990.
37. Fisher AG, et al. (1993) Lymphoproliferative disorders in an IL-7 transgenic mouse line. *Leukemia* 7(Suppl 2):S66–S68.
38. Mertsching E, Grawunder U, Meyer V, Rolink T, Ceredig R (1996) Phenotypic and functional analysis of B lymphopoiesis in interleukin-7-transgenic mice: expansion of pro/pre-B cell number and persistence of B lymphocyte development in lymph nodes and spleen. *Eur J Immunol* 26(1):28–33.
39. Akashi K, Kondo M, von Freeden-Jeffry U, Murray R, Weissman IL (1997) Bcl-2 rescues T lymphopoiesis in interleukin-7 receptor-deficient mice. *Cell* 89(7):1033–1041.
40. Maraskovsky E, et al. (1997) Bcl-2 can rescue T lymphocyte development in interleukin-7 receptor-deficient mice but not in mutant rag-1<sup>-/-</sup> mice. *Cell* 89(7):1011–1019.
41. Beaudin AE, Boyer SW, Forsberg EC (2014) Flk2/Flt3 promotes both myeloid and lymphoid development by expanding non-self-renewing multipotent hematopoietic progenitor cells. *Exp Hematol* 42(3):218–229.e4.
42. Dolence JJ, Gwin KA, Shapiro MB, Medina KL (2014) Flt3 signaling regulates the proliferation, survival, and maintenance of multipotent hematopoietic progenitors that generate B cell precursors. *Exp Hematol* 42(5):380–393.e3.
43. Carvalho TL, Mota-Santos T, Cumano A, Demengeot J, Vieira P (2001) Arrested B lymphopoiesis and persistence of activated B cells in adult interleukin 7(-/-) mice. *J Exp Med* 194(8):1141–1150.
44. Jensen CT, et al. (2008) FLT3 ligand and not TSLP is the key regulator of IL-7-independent B-1 and B-2 B lymphopoiesis. *Blood* 112(6):2297–2304.
45. Vossenrich CA, Cumano A, Müller W, Di Santo JP, Vieira P (2003) Thymic stromal-derived lymphopoietin distinguishes fetal from adult B cell development. *Nat Immunol* 4(8):773–779.
46. Rothenberg EV (2014) Transcriptional control of early T and B cell developmental choices. *Annu Rev Immunol* 32:283–321.
47. Ceredig R, Rauch M, Balciunaite G, Rolink AG (2006) Increasing Flt3L availability alters composition of a novel bone marrow lymphoid progenitor compartment. *Blood* 108(4):1216–1222.

## Supporting Information

von Muenchow et al. 10.1073/pnas.1613316113

## SI Materials and Methods

**Antibodies.** The following antibodies were used for flow cytometry (from BD Pharmingen, eBioscience, BioLegend, or produced in house): anti-B220 (RA3-6B2), anti-CD117 (2B8), anti-CD19 (1D3), anti-NK1.1 (PK136), anti-SiglecH (551), anti-CD11c (HL3), anti-CD115 (AFS98), anti-Ly6D (49-H4), anti-CD127 (SB/199), anti-CD135 (A2F10), anti-Sca1 (D7), anti-IgM (M41), anti-CD21 (7G6), anti-CD23 (B3B4), anti-CD4 (GK1.5), anti-CD8 (53.6.7), and anti-TCR $\beta$  (H57).

**RT-qPCR.** The primers used were as follows: *Ebfl1*, *Ebfl1*-F: 5'-CAGGAAACCCACGTGACAT-3' and *Ebfl1*-R: 5'-CCACGTGACTGTGGTAGACA-3'; *Pax5*, *Pax5*-F: 5'-ACGCTGACAGGGATGGTG-3' and *Pax5*-R: 5'-GGGGAACCTCCAAGAAATCAT-3'; *Foxo1*, *Foxo1*-F: 5'-AGTGGATGGTGAAGAGCGT-3' and *Foxo1*-R: 5'-GAAGGGACAGATTGTGGCG-3'; *Actin*, *Actin*-F: 5'-CTGTCGAGTCGCGTCCACC-3' and *Actin*-R: 5'-CGCAGCGATATCGTCATCCA-3'.

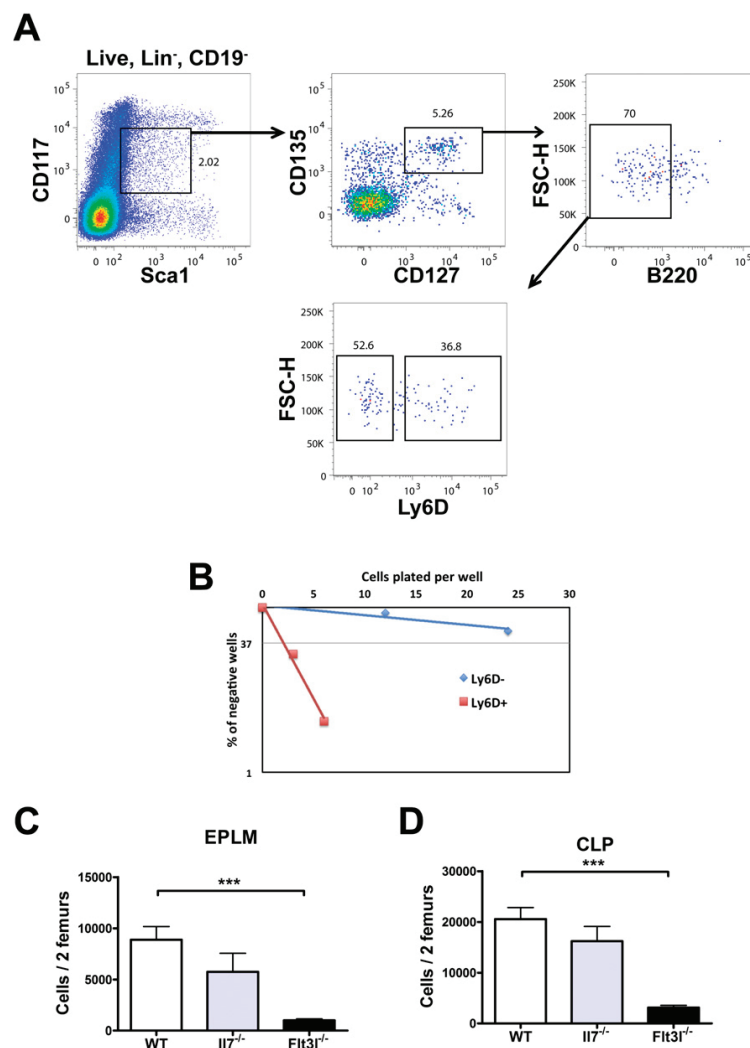


**Fig. S1.** (A) CLP FACS staining in WT mice. FACS plots showing the gating strategy used for the identification of Ly6D<sup>+</sup> CLP. Lineage staining was as follows: SiglecH, CD115, CD11c, NK1.1, Gr-1. (B) In vitro limiting dilution analysis of Ly6D<sup>+</sup> and Ly6D<sup>-</sup> EPLM B-cell potential. Cells were sorted as shown in Fig. 1A and plated at the indicated concentrations on OP9 stromal cells together with IL-7. A representative of three independent experiments is shown. (C and D) Numbers of EPLM (C) and CLP (D) progenitors in WT ( $n = 13$ ), *Il7*<sup>-/-</sup> ( $n = 5$ ), and *Flt3l*<sup>-/-</sup> ( $n = 10$ ) mice. EPLM were stained as shown in Fig. 1A and CLP as shown in A. Student's  $t$  test. \*\*\* $P \leq 0.001$ . Bars show mean  $\pm$  SEM.

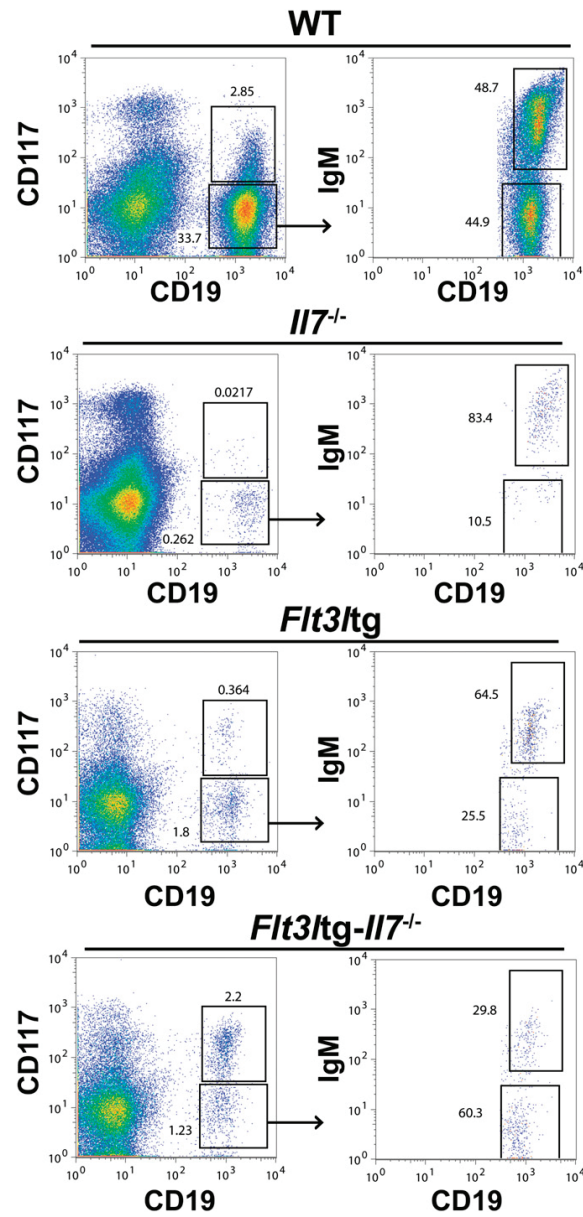


**Fig. S2.** Rescue of CD19<sup>+</sup> bone marrow B-cell progenitors in *Flt3ltg-I17*<sup>-/-</sup> mice. Representative FACS plots for the identification of CD19<sup>+</sup>CD117<sup>+</sup>, CD19<sup>+</sup>CD117<sup>-</sup>IgM<sup>-</sup>, and CD19<sup>+</sup>IgM<sup>+</sup> bone marrow cells are shown.

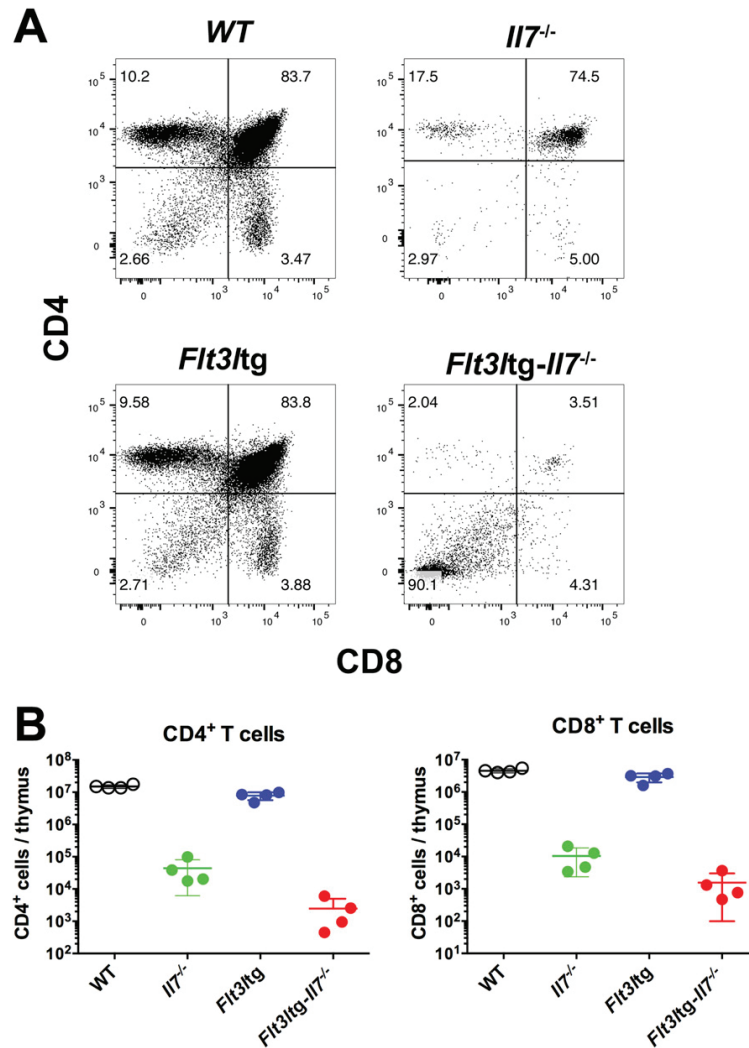


**Fig. S3.** Thymic T-cell development in *Flt3ltg-I17<sup>-/-</sup>* mice. (A) Representative FACS plots showing CD4/CD8 thymocyte staining from 6- to 8-wk-old WT, *I17<sup>-/-</sup>*, *Flt3ltg*, and *Flt3ltg-I17<sup>-/-</sup>* mice ( $n = 4$  per group). (B) Total numbers of CD4<sup>+</sup> (Left) and CD8<sup>+</sup> (Right) single-positive thymocytes from the mouse genotypes indicated on the x axes.

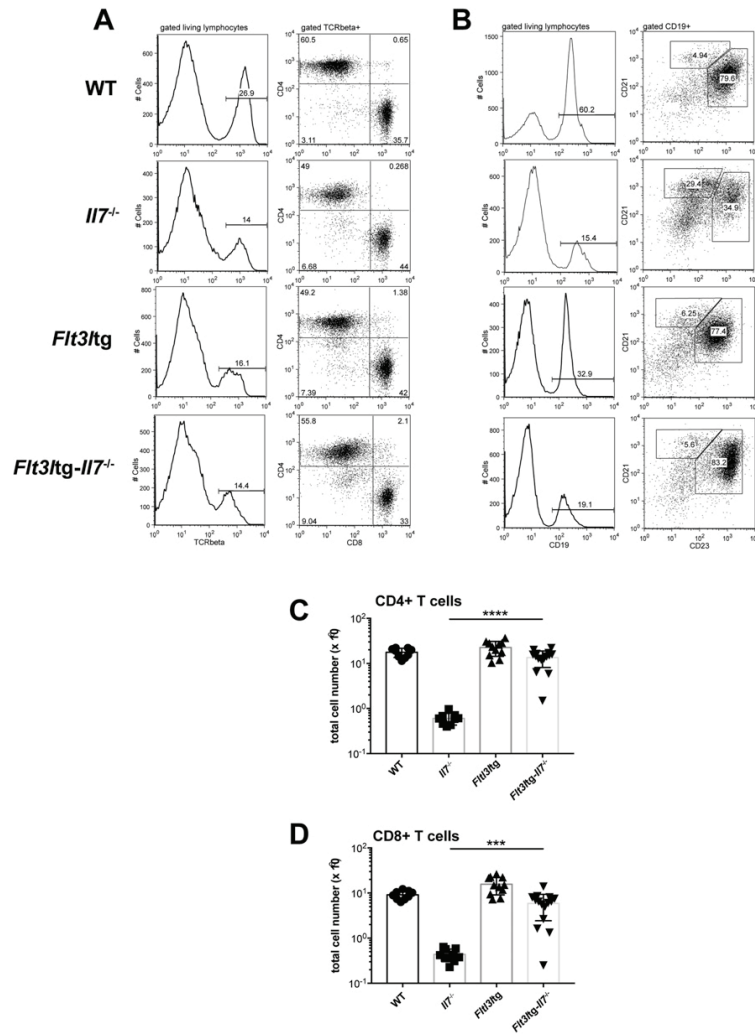


**Fig. 54.** (A) Representative FACS plots illustrating T cells in the spleens of WT (first row), *I17*<sup>-/-</sup> (second row), *Flt3ltg* (third row), and *Flt3ltg-I17*<sup>-/-</sup> (fourth row) mice. After gating on living lymphocytes, TCRβ<sup>+</sup> cells are further subgrouped in CD4<sup>+</sup> and CD8<sup>+</sup> T cells. (B) Representative FACS plots illustrating B cells in the spleens of WT (first row), *I17*<sup>-/-</sup> (second row), *Flt3ltg* (third row), and *Flt3ltg-I17*<sup>-/-</sup> (fourth row) mice. After gating on living lymphocytes, CD19<sup>+</sup> cells are further subgrouped in CD21<sup>high</sup>CD23<sup>low</sup> marginal zone B cells and CD21<sup>+</sup>CD23<sup>+</sup> follicular B cells. (C and D) Numbers of splenic CD4<sup>+</sup> (C) and CD8<sup>+</sup> (D) T cells, stained as shown in A, from WT and mutant mice as indicated on the x axes. \*\*\**P* < 0.001, \*\*\*\**P* < 0.0001. Student's *t* test; *n* = 9–15. Data shown above are mean ± SD.

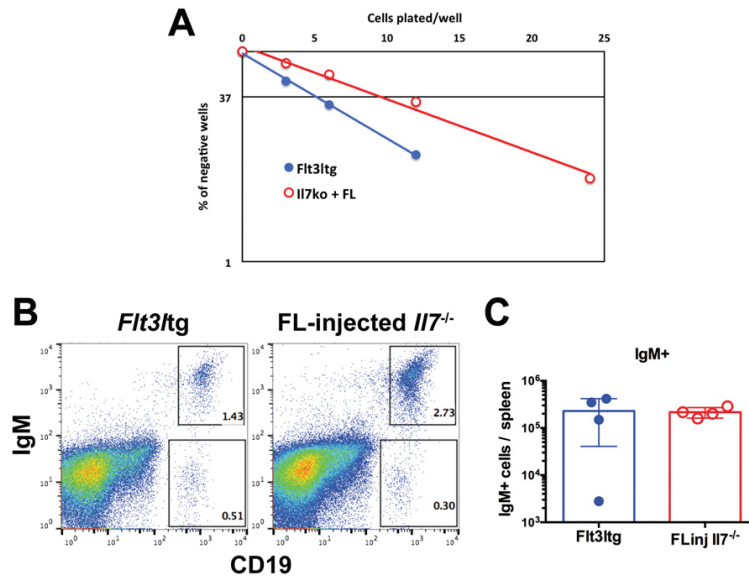


**Fig. S5.** B-cell potential of Ly6D<sup>+</sup> EPLM cells from *I17<sup>-/-</sup>* mice injected with FL. *I17<sup>-/-</sup>* mice were injected with FL (10 daily doses of 10  $\mu$ g per mouse) and Ly6D<sup>+</sup> EPLM were sorted from their bone marrows 1 d after the last injection. (A) In vitro limiting dilution analysis of the B-cell potential of FL-injected *I17<sup>-/-</sup>* Ly6D<sup>+</sup> EPLM. Cells were plated at the indicated concentrations on OP9 stromal cells plus IL-7. *Fit3Itg* Ly6D<sup>+</sup> EPLM were used as positive controls. (B and C) In vivo B-cell potential of FL-injected *I17<sup>-/-</sup>* Ly6D<sup>+</sup> EPLM. Five thousand Ly6D<sup>+</sup> EPLM from FL-injected *I17<sup>-/-</sup>* or *Fit3Itg* mice were i.v. injected into sublethally irradiated *Rag2<sup>-/-</sup>* mice. Four weeks after cell transfer, spleens were analyzed for expression of CD19 and IgM. (B) Representative FACS plots of recipient spleens. (C) Numbers of CD19<sup>+</sup>IgM<sup>+</sup> B cells harvested from the analyzed spleens ( $n = 4$  mice per group).

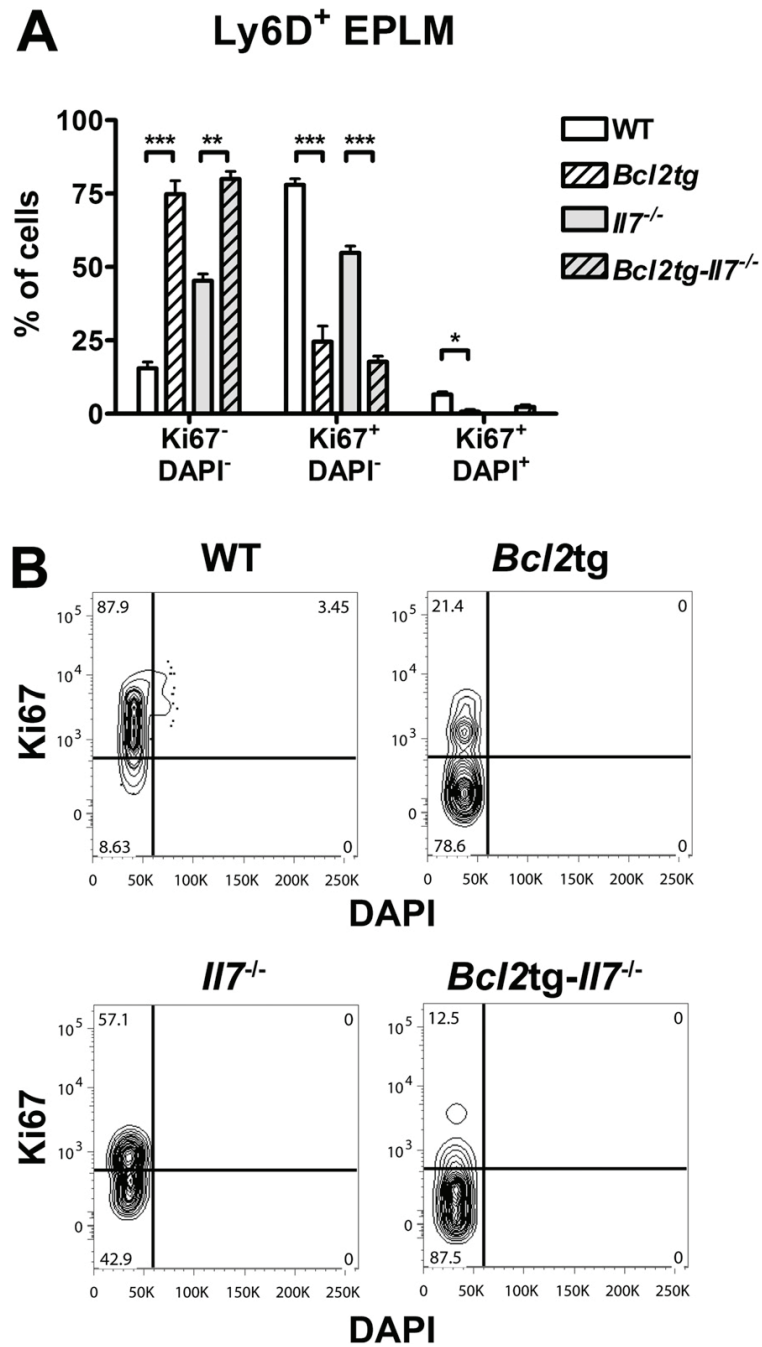


**Fig. 56.** Quiescent state of *Bcl2*-rescued cells in vivo. (A) Cell cycle analysis of Ly6D<sup>+</sup> EPLM from WT ( $n = 5$ ), *Bcl2tg* ( $n = 2$ ), *Il7<sup>-/-</sup>* ( $n = 2$ ), and *Bcl2tg-Il7<sup>-/-</sup>* ( $n = 4$ ) mice. Graph shows percentages of Ki67<sup>-</sup>DAPI<sup>-</sup>, Ki67<sup>+</sup>DAPI<sup>-</sup>, and Ki67<sup>+</sup>DAPI<sup>+</sup> Ly6D<sup>+</sup> EPLM. \* $P \leq 0.05$ , \*\* $P \leq 0.01$ , \*\*\* $P \leq 0.001$ . Student's  $t$  test. Bars show mean  $\pm$  SEM. (B) Representative Ki67/DAPI FACS plots of the Ly6D<sup>+</sup> EPLM cell cycle analysis collectively presented in A.

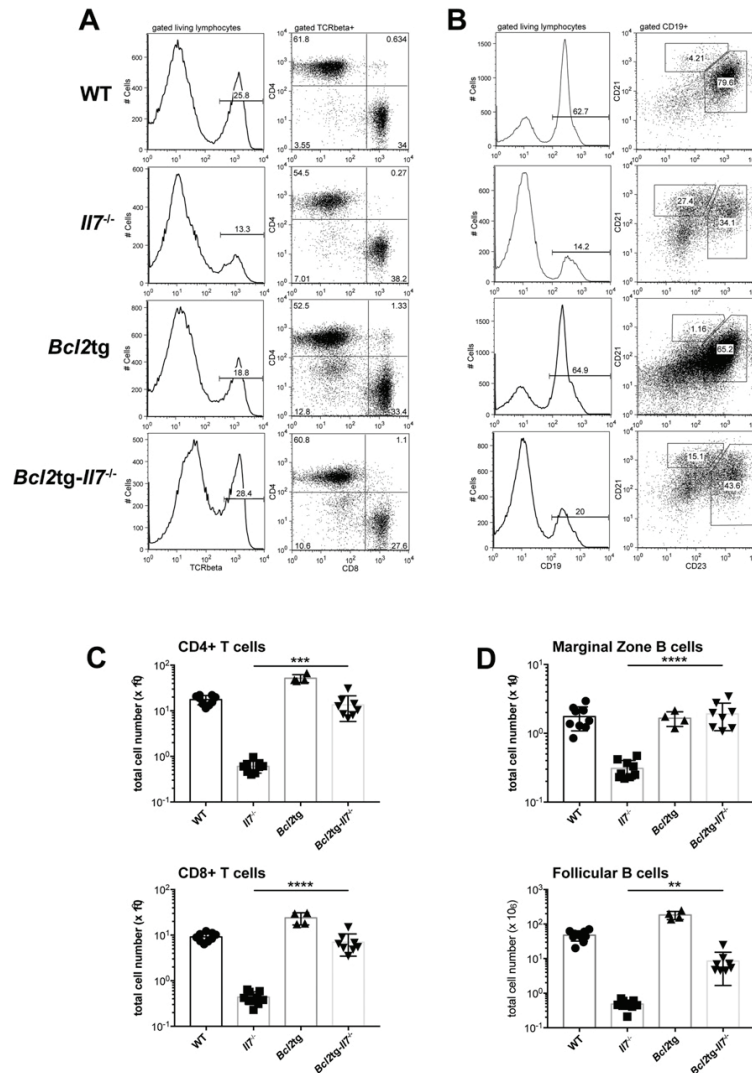


**Fig. S7.** Bcl2-mediated rescue of splenic T and B cells in the absence of IL-7. (A) Representative FACS plots illustrating T cells in the spleens of WT (first row), *Il7*<sup>-/-</sup> (second row), *Bcl2*<sup>tg</sup> (third row), and *Bcl2*<sup>tg</sup>-*Il7*<sup>-/-</sup> (fourth row) mice. After gating on living lymphocytes, TCRβ<sup>+</sup> cells are further subgrouped in CD4<sup>+</sup> and CD8<sup>+</sup> T cells. (B) Representative FACS plots illustrating B cells in the spleens of WT (first row), *Il7*<sup>-/-</sup> (second row), *Bcl2*<sup>tg</sup> (third row), and *Bcl2*<sup>tg</sup>-*Il7*<sup>-/-</sup> (fourth row) mice. After gating on living lymphocytes CD19<sup>+</sup> cells are further subgrouped in CD21<sup>high</sup>CD23<sup>low</sup> marginal zone B cells and CD21<sup>+</sup>CD23<sup>+</sup> follicular B cells. (C) Numbers of splenic CD4<sup>+</sup> (Upper) and CD8<sup>+</sup> (Lower) T cells, stained as shown in A, from WT and mutant mice as indicated on the x axes. (D) Numbers of splenic marginal zone (Upper) and follicular (Lower) B cells, stained as shown in B, from WT and mutant mice as indicated on the x axes. \*\**P* ≤ 0.01, \*\*\**P* ≤ 0.001, \*\*\*\**P* ≤ 0.0001. Student's *t* test; *n* = 4–9. Data shown above are mean ± SD.

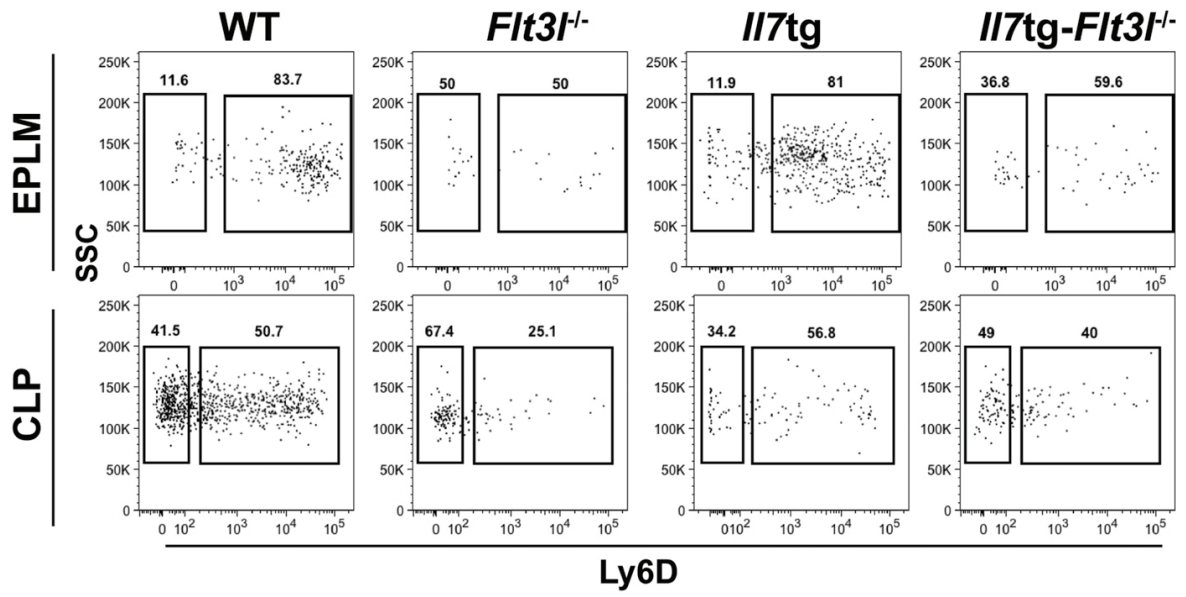
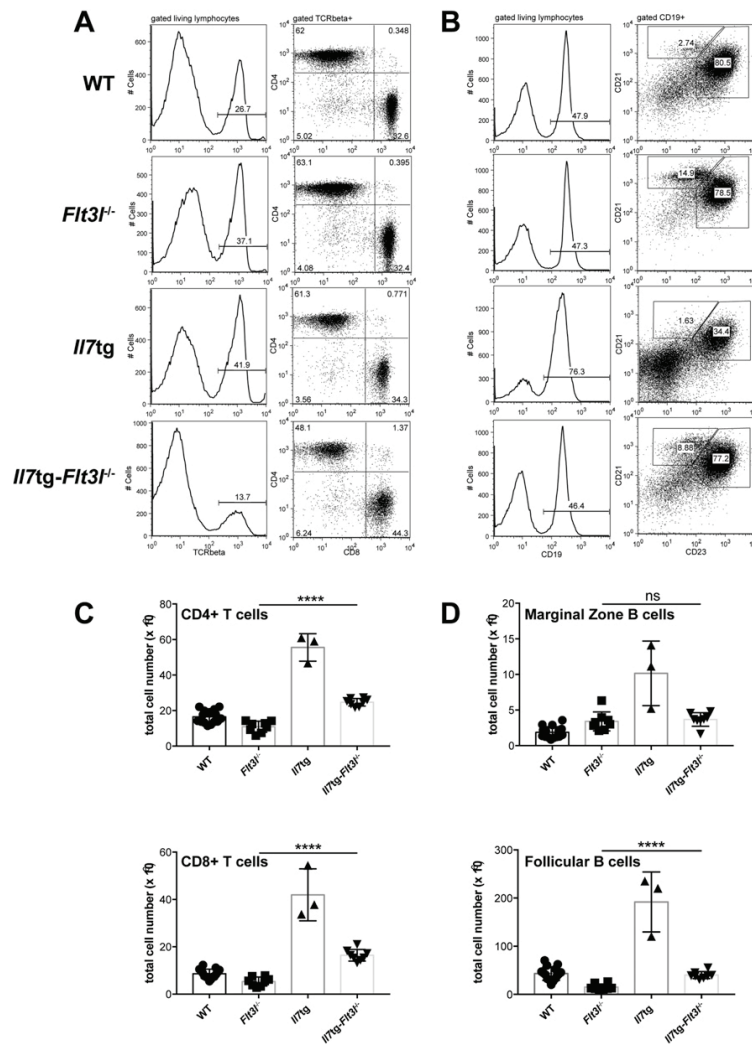
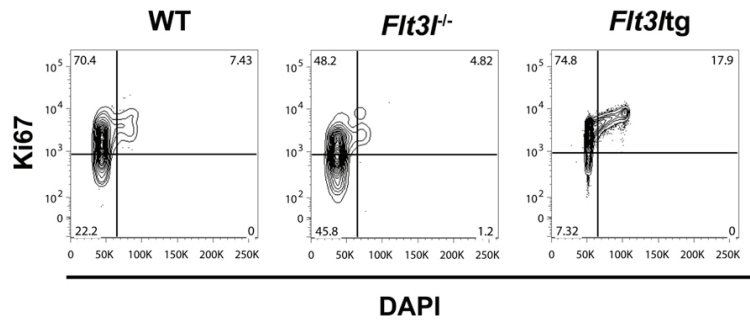


Fig. 58. Representative FACS plots of EPLM (Upper) and CLP (Lower) from WT, *Flt3l*<sup>-/-</sup>, *Il7tg*, and *Il7tg-Flt3l*<sup>-/-</sup> mice.



**Fig. 59.** Effect of IL-7 overexpression on WT and *Flt3l*<sup>-/-</sup> splenic T and B cells. (A) Representative FACS plots illustrating T cells in the spleens of WT (first row), *Flt3l*<sup>-/-</sup> (second row), *Il7tg* (third row), and *Il7tg-Flt3l*<sup>-/-</sup> (fourth row) mice. After gating on living lymphocytes, TCRβ<sup>+</sup> cells are further subgrouped in CD4<sup>+</sup> and CD8<sup>+</sup> T cells. (B) Representative FACS plots illustrating B cells in the spleens of WT (first row), *Flt3l*<sup>-/-</sup> (second row), *Il7tg* (third row), and *Il7tg-Flt3l*<sup>-/-</sup> (fourth row) mice. After gating on living lymphocytes, CD19<sup>+</sup> cells are further subgrouped in CD21<sup>high</sup>CD23<sup>low</sup> marginal zone B cells and CD21<sup>high</sup>CD23<sup>high</sup> follicular B cells. (C) Numbers of splenic CD4<sup>+</sup> (Upper) and CD8<sup>+</sup> (Lower) T cells, stained as shown in A, from WT and mutant mice as indicated on the x axes. (D) Numbers of splenic marginal zone (Upper) and follicular (Lower) B cells, stained as shown in B, from WT and mutant mice as indicated on the x axes. ns, not significant or  $P > 0.05$ , \*\*\*\* $P \leq 0.0001$ . Student's *t* test;  $n = 3-15$ . Data shown above are mean  $\pm$  SD.



**Fig. S10.** Effect of in vivo FL levels on Ly6D<sup>+</sup> EPLM cell cycle. Representative Ki67/DAPI FACS plots of the Ly6D<sup>+</sup> EPLM cell cycle analysis collectively presented in Fig. 6B.

#### **4.1.2. Accumulation of multipotent hematopoietic progenitors in peripheral lymphoid organs of mice over-expressing interleukin-7 and Flt3-ligand**

Fabian Klein, Lilly von Muenchow, Giuseppina Capoferri, Stefan Heiler, Llucia Alberti-Servera, Hannie Rolink, Corinne Engdahl, Michael Rolink, Mladen Mitrovic, Grozdan Cvijetic, Jan Andersson, Rhodri Ceredig, Panagiotis Tsapogas, Antonius Rolink

October 2018 – Frontiers in Immunology



# Accumulation of Multipotent Hematopoietic Progenitors in Peripheral Lymphoid Organs of Mice Over-expressing Interleukin-7 and Flt3-Ligand

Fabian Klein<sup>1</sup>, Lilly von Muenchow<sup>1</sup>, Giuseppina Capoferri<sup>1</sup>, Stefan Heiler<sup>1</sup>, Lucia Alberti-Servera<sup>1</sup>, Hannie Rolink<sup>1</sup>, Corinne Engdahl<sup>1</sup>, Michael Rolink<sup>1</sup>, Mladen Mitrovic<sup>1</sup>, Grozdan Cvijetic<sup>1</sup>, Jan Andersson<sup>1</sup>, Rhodri Ceredig<sup>2</sup>, Panagiotis Tsapogas<sup>1\*†</sup> and Antonius Rolink<sup>1†</sup>

## OPEN ACCESS

<sup>1</sup> Department of Biomedicine, Developmental and Molecular Immunology, University of Basel, Basel, Switzerland, <sup>2</sup> Discipline of Physiology, College of Medicine & Nursing Health Science, National University of Ireland, Galway, Ireland

### Edited by:

Barbara L. Kee,  
University of Chicago, United States

### Reviewed by:

Rodney P. DeKoter,  
University of Western Ontario, Canada  
John D. Colgan,  
University of Iowa, United States

### \*Correspondence:

Panagiotis Tsapogas  
panagiotis.tsapogas@unibas.ch

<sup>†</sup>These authors have contributed  
equally to this work

### Specialty section:

This article was submitted to  
B Cell Biology,  
a section of the journal  
Frontiers in Immunology

**Received:** 22 June 2018

**Accepted:** 11 September 2018

**Published:** 10 October 2018

### Citation:

Klein F, von Muenchow L, Capoferri G, Heiler S, Alberti-Servera L, Rolink H, Engdahl C, Rolink M, Mitrovic M, Cvijetic G, Andersson J, Ceredig R, Tsapogas P and Rolink A (2018) Accumulation of Multipotent Hematopoietic Progenitors in Peripheral Lymphoid Organs of Mice Over-expressing Interleukin-7 and Flt3-Ligand. *Front. Immunol.* 9:2258. doi: 10.3389/fimmu.2018.02258

Interleukin-7 (IL-7) and Flt3-ligand (FL) are two cytokines important for the generation of B cells, as manifested by the impaired B cell development in mice deficient for either cytokine or their respective receptors and by the complete block in B cell differentiation in the absence of both cytokines. IL-7 is an important survival and proliferation factor for B cell progenitors, whereas FL acts on several early developmental stages, prior to B cell commitment. We have generated mice constitutively over-expressing both IL-7 and FL. These double transgenic mice develop splenomegaly and lymphadenopathy characterized by tremendously enlarged lymph nodes even in young animals. Lymphoid, myeloid and dendritic cell numbers are increased compared to mice over-expressing either of the two cytokines alone and the effect on their expansion is synergistic, rather than additive. B cell progenitors, early progenitors with myeloid and lymphoid potential (EPLM), common lymphoid progenitors (CLP) and lineage<sup>-</sup>, Sca1<sup>+</sup>, kit<sup>+</sup> (LSK) cells are all increased not only in the bone marrow but also in peripheral blood, spleen and even lymph nodes. When transplanted into irradiated wild-type mice, lymph node cells show long-term multilineage reconstitution, further confirming the presence of functional hematopoietic progenitors therein. Our double transgenic mouse model shows that sustained and combined over-expression of IL-7 and FL leads to a massive expansion of most bone marrow hematopoietic progenitors and to their associated presence in peripheral lymphoid organs where they reside and potentially differentiate further, thus leading to the synergistic increase in mature lymphoid and myeloid cell numbers. The present study provides further *in vivo* evidence for the concerted action of IL-7 and FL on lymphopoiesis and suggests that extramedullary niches, including those in lymph nodes, can support the survival and maintenance of hematopoietic progenitors that under physiological conditions develop exclusively in the bone marrow.

**Keywords:** IL-7, Flt3-ligand, hematopoiesis, cytokines, B cell development

## INTRODUCTION

Cytokines are important regulators for the development and function of immune cells. Apart from influencing the survival, expansion and effector function of mature immune cells in peripheral lymphoid organs, cytokines also have a crucial role in the continuous generation of all blood cell lineages (hematopoiesis), which occurs in the bone marrow and thymus. During hematopoiesis cytokines can influence the lineage output of hematopoietic progenitors by selectively promoting their survival, proliferation or developmental potential (1–3). Two of the most important cytokines for the generation of lymphoid cells are Flt3-ligand (FL) and Interleukin-7 (IL-7).

FL is produced by many cell types, but within the hematopoietic system it acts mainly on early, multipotent progenitors, which are the ones expressing its receptor, CD135 (Flt3) (4–6). CD135 is the only known receptor for FL and belongs to the type-III tyrosine kinase receptor family, which also includes CD117 (kit) and platelet-derived growth factor receptor (PDGF-R). CD135 expression within the lineage<sup>-</sup>, Sca1<sup>+</sup>, kit<sup>+</sup> (LSK) compartment of hematopoietic progenitors is associated with loss of self-renewal capacity and preservation of multilineage developmental potential (7). Oligopotent myeloid and lymphoid progenitors retain CD135 expression until they become committed to their respective lineages. From that point on, they down-regulate expression of the receptor, with the exception of dendritic cells (DC), which remain CD135<sup>+</sup> after maturation. The importance of FL in B cell development is manifested by the reduced capacity of *Flt3l*<sup>-/-</sup> and *Flt3*<sup>-/-</sup> hematopoietic progenitors to reconstitute the B cell compartment of lymphopenic mice (8, 9). In addition, B cell regeneration after irradiation or chemically induced myeloablation is dependent on FL (10). Since CD135 is down-regulated in committed B cell progenitors after Pax5 expression (11), the effect of FL signaling on B cell development is attributed to its role in maintaining normal numbers of oligopotent CD135<sup>+</sup> common lymphoid progenitors (CLP) and early progenitors with lymphoid and myeloid potential (EPLM) (12, 13).

CLP are phenotypically defined by the expression of CD127, the  $\alpha$ -subunit of the receptor for IL-7 (14). CD127 expression is initiated at the CLP stage and remains expressed throughout the early stages of B cell development until the progenitors start to rearrange their light chain immunoglobulin genes (small pre-B stage). IL-7 was initially identified as a growth factor for B cells (15) and its essential role in lymphoid development has been proven both by its ability to maintain and expand lymphoid cells *in vitro* (16) and by the severe defect in B and T cell development observed in *Il7*<sup>-/-</sup> and *Il7ra*<sup>-/-</sup> mice (17, 18). Early T cell progenitors require IL-7 mainly for their survival, since over-expression of the anti-apoptotic protein Bcl2 can significantly rescue T cell development in *Il7ra*<sup>-/-</sup> mice (19, 20). IL-7 is also important for the survival and homeostatic expansion of mature T cells in the periphery (21). The fact that B cell development in *Il7ra*<sup>-/-</sup> mice cannot be rescued by Bcl2 over-expression (22, 23), together with the absence of early B-cell factor 1 (Ebf1) expression in *Il7ra*<sup>-/-</sup> CLP (24) has led to the hypothesis that

by initiating Ebf1 expression, IL-7 might act as an instructive cytokine for B cell commitment. However, this could also be explained by a survival role of IL-7 on CLP, since the Ebf1-expressing Ly6D<sup>+</sup> compartment of CLP is severely reduced in *Il7*<sup>-/-</sup> mice (25). Furthermore, B cell commitment in the absence of IL-7 signaling can be restored by over-expressing Bcl2 in mice lacking the IL-7 signaling mediator STAT5 (26) and by over-expressing FL in *Il7*<sup>-/-</sup> mice (13), therefore indicating that the role of this cytokine in commitment of progenitors to the B cell lineage is permissive, rather than instructive. Following Pax5 expression and lineage commitment, B cell progenitors require IL-7 for their survival and expansion. This has been clearly manifested in mice expressing high, sustained levels of IL-7, which resulted in expansion of pre-B cell progenitors in the bone marrow and in some cases in the development of B cell tumors (27–29). This increase in pro-B and pre-B cell numbers resulted in their accumulation in secondary lymphoid organs, such as spleen and lymph nodes.

As evident from the above, both FL and IL-7 are pivotal for the generation of normal B cell numbers, a fact highlighted by the complete absence of B cells in mice lacking both cytokines (30). Their combined effect is mostly exerted at different stages of B cell development, with FL being crucial for the generation of early multipotent progenitors and IL-7 for their survival and expansion after B cell commitment (13). However, they also act synergistically at the CLP/EPLM stage, where the receptors for both cytokines are simultaneously expressed, possibly through activation of separate signaling pathways (31). We have previously generated mice expressing high, sustained levels of human FL (hereafter FLtg) (32), which, when crossed to *Il7*<sup>-/-</sup> mice, showed a complete rescue of Ly6D<sup>+</sup> CLP/EPLM numbers (13). Interestingly, however, we have observed that mice over-expressing FL have reduced pre-B cell numbers compared to their wild-type (WT) counterparts (32). This could not be a direct effect of FL on pre-B cells, as they do not express CD135. Since pre-B cells are highly dependent on IL-7 for their expansion, we hypothesized that IL-7 availability might be reduced in FLtg bone marrow, due to the high number of CD127<sup>+</sup> CLP and EPLM progenitors, which might consume a large part of the available IL-7. Binding of IL-7 to its receptor on CD127<sup>+</sup> target cells has been proposed as a mechanism that regulates the abundance of the cytokine in different tissues (33).

In order to test this hypothesis, and to further study the synergy between FL and IL-7 in promoting lymphoid development *in vivo*, we bred FLtg mice with transgenic mice expressing high amounts of IL-7 (hereafter IL7tg) and analyzed the F<sub>1</sub> generation. Double transgenic mice (hereafter FLtgxIL7tg) had a phenotype that combined features of the single transgenic phenotypes and in terms of expansion of lymphoid cells, revealed synergy between the two cytokines. Thus, double transgenic mice exhibited splenomegaly and abnormally enlarged lymph nodes (LN), in which B and T cell numbers were increased more than in the single transgenic mice. Moreover, large numbers of B cell progenitors as well as CD19<sup>-</sup> multipotent progenitors were found in the LN of FLtgxIL7tg mice. Transplantation of LN FLtgxIL7tg cells into myelo-ablated recipients showed that they contained

hematopoietic progenitors with long-term multilineage developmental potential, suggesting that the LN niche can support the survival and maintenance of early hematopoietic progenitors.

## MATERIALS AND METHODS

### Mice

C57BL/6 (CD45.1<sup>+</sup> and CD45.2<sup>+</sup>), FLtg, IL7tg, FLtgxIL7tg and NOD/SCID/*Il2r $\gamma$* <sup>-/-</sup> mice were bred and maintained in our animal facility unit under specific pathogen-free conditions. All mice used were 5–9 weeks old. All animal experiments were carried out within institutional guidelines (authorization numbers 1886 and 1888 from cantonal veterinarian office, Canton Basel-Stadt).

### Antibodies, Flow Cytometry and Sorting

For analysis, cells were flushed from femurs and tibias of the two hind legs of mice or single-cell suspensions of spleen and lymph node (inguinal and axillary) cells were made. For blood analysis, blood was taken from the heart of euthanized animals or from the tail vein of live ones and white blood cells were isolated after separation with Ficoll. Stainings were performed in PBS containing 0.5% BSA and 5 mM EDTA. For intra-cellular Foxp3 staining, cells were fixed and permeabilized after cell-surface staining using the Foxp3 Fix/Perm buffer set (eBioscience), and subsequently stained with PE-conjugated anti-Foxp3. The following antibodies were used for flow cytometry (from BD Pharmingen, eBioscience, BioLegend, or produced in house): anti-B220 (RA3-6B2), anti-CD117 (2B8), anti-CD19 (ID3), anti-NK1.1 (PK136), anti-SiglecH (551), anti-CD11c (HL3), anti-Ly6D (49-H4), anti-CD127 (SB/199), anti-Sca1 (D7), anti-IgM (M41), anti-Foxp3 (FJK-16s), anti-CD4 (GK1.5), anti-CD8 (53.6.7), anti-Gr1 (RB6-8C5), anti-CD11b (M1.7015), anti-MHC-II (M5/114.15.2), anti-XCR1 (ZET), anti-CD93 (PB493), anti-CD48 (HM48-1), anti-CD150 (TC15-12F12.2), anti-Ter119 (TER-119), anti-CD3 (145-2C11), anti-CD41 (MWReg30), anti-CD105 (MJ7/18), anti-CD16/32 (2.4G2), anti-S1PR1 (713412), anti-CD44 (IM7), anti-CXCR4 (L276F12), anti-CD5 (53-7.3), and anti-Ki67 (B56). Lineage cocktail included antibodies against: CD4, CD8, CD11b, CD11c, Gr1, B220, CD19, Ter119, and NK1.1. Flow cytometry was done using a BD LSRFortessa (BD Biosciences) and data were analyzed using FlowJo Software (Treestar). For cell sorting, a FACSAria IIu (BD Biosciences) was used (>98% purity).

### Flt3-Ligand And IL-7 Quantification

Sera were collected from mice of all genotypes and ELISA was performed using the Invitrogen human Flt3-ligand and mouse IL-7 ELISA kits, following the provider's instructions.

### Quantitative PCR

Spleens were homogenized using the FastPrep<sup>®</sup> homogenizer (MP Biomedicals) and RNA was extracted with Trizol (Invitrogen) following the provider's protocol. Five hundred micrograms of total RNA was used to synthesize cDNA using the GoScript reverse transcriptase (Promega). Quantitative

PCR for the detection of *Il7* transcripts was performed using SYBR<sup>™</sup> Green (Promega). Primers used: *Hprt*-Forw: atcagtaacgggggacataaa; *Hprt*-Rev: tggggctgtactgcttaacca; *Il7*-Forw: GATAGTAATTGCCCGAATAATGAACCA; *Il7*-Rev: GTTTGTGTGCCTTGTGATACTGTTAG.

### *In vitro* Limiting Dilution B Cell Generation Assay

Experiments were performed as previously described (34). Briefly, OP9 stromal cells were plated on flat-bottom 96-well plates 1 day before the initiation of co-cultures, at a concentration of 3,000 cells per well. The following day stromal cells were  $\gamma$ -irradiated (3000 rad) and the sorted EPLM cells were added at different concentrations. Cultures were maintained in IMDM medium supplemented with  $5 \times 10^{-5}$  M  $\beta$ -mercaptoethanol, 1 mM glutamine, 0.03% (wt/vol) primatone, 100 U/mL penicillin, 100  $\mu$ g/mL streptomycin, 5% FBS and 10% IL-7-conditioned medium. After 10 days in culture all wells were inspected under an inverted microscope and wells containing colonies of more than 50 cells were scored as positive.

### *In vivo* Hematopoietic Reconstitution Assays

Ten million BM or LN cells from FLtgxIL7tg mice were injected intravenously into CD45.1<sup>+</sup> recipient mice, which had been sub-lethally irradiated (400 rad) ~2 h before injection. Mice were euthanized 12–16 weeks after cell transfer and their spleen, thymus and bone marrow was analyzed for the presence of donor cells. For secondary transplantations,  $6 \times 10^6$  BM cells from recipient mice were injected intravenously into sub-lethally irradiated CD45.1<sup>+</sup> recipients, in the same way. Secondary recipient spleens were analyzed after 9 weeks. For assessment of the *in vivo* B cell potential of EPLM,  $6 \times 10^4$  Ly6D<sup>+</sup> EPLM sorted from the BM or LN of FLtgxIL7tg mice were intravenously injected into NOD/SCID/*Il2r $\gamma$* <sup>-/-</sup> lymphopenic mice. Recipient spleens were analyzed for the presence of CD19<sup>+</sup>IgM<sup>+</sup> cells 3 weeks after cell transfer.

### Statistical Analysis

One-way ANOVA followed by a Tukey-test to correct for multiple comparisons between mouse genotypes was used. Statistical significance is indicated with asterisks in graphs. Non-significant differences are not indicated in the figures.

## RESULTS

### Expansion of Hematopoietic Cells in Secondary Lymphoid Organs of FLtgxIL7tg Mice

FLtg and IL7tg mice heterozygous for the corresponding transgenes were crossed, resulting in mice carrying both transgenes (FLtgxIL7tg), as well as wild-type (WT) and single-transgenic littermates, which were used as controls (Figure 1A). FLtgxIL7tg mice were viable but at around 5–6 weeks after birth, they developed large, clearly visible inguinal lymph nodes (LN), which continued to grow and therefore mice had to be

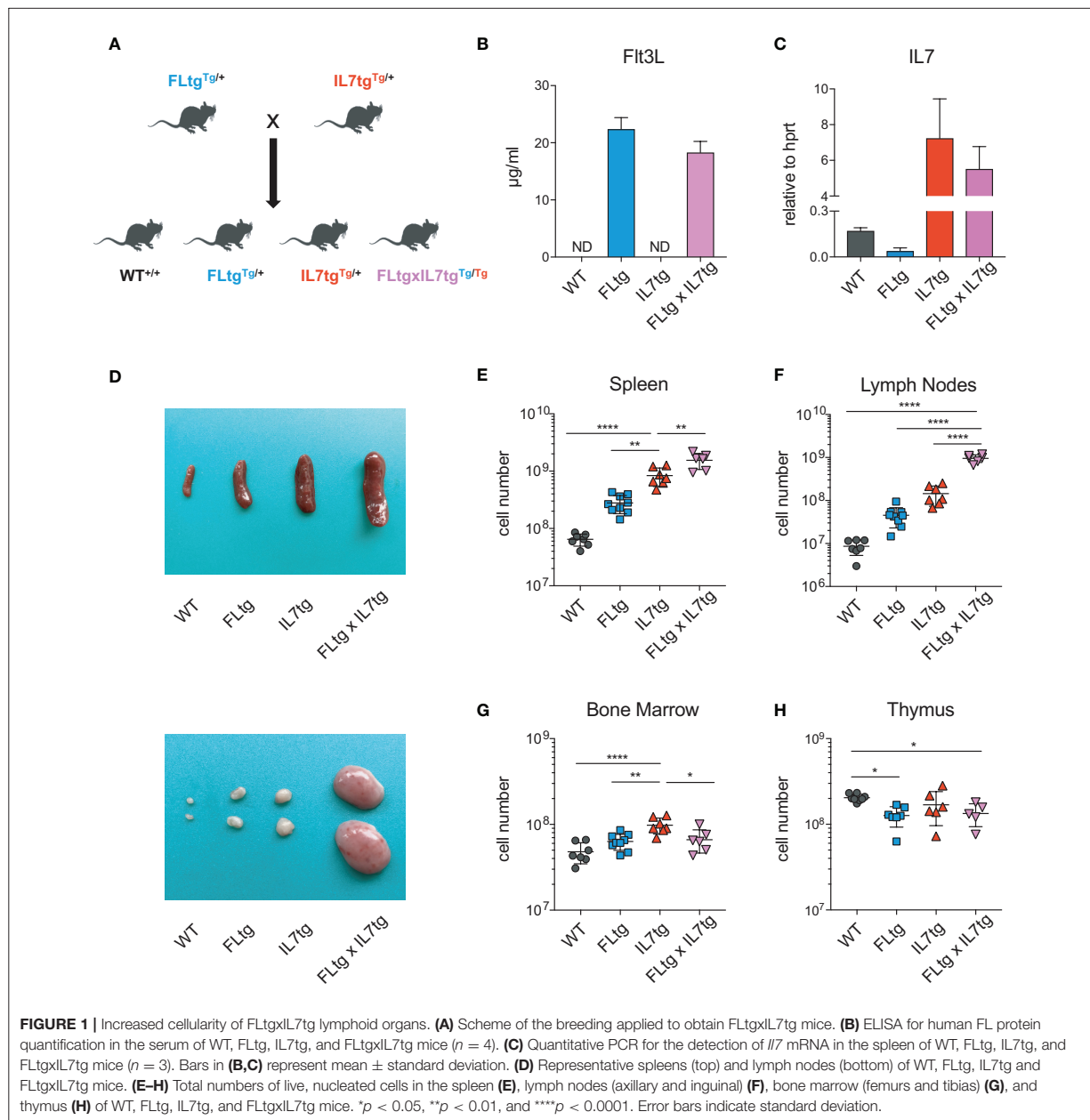
ethanized at the age of 9–10 weeks. None of the littermate controls exhibited this phenotype. All analyses of FLtgxIL7tg mice and their WT and single transgenic counterparts presented herein were done in 6–9 week old mice. We detected a massive increase in the amount of FL in the serum of FLtg and FLtgxIL7tg mice, which reached 22 and 18 ug/ml, respectively (**Figure 1B**). Even though IL-7 could not be detected in the serum of FLtgxIL7tg mice, as shown previously by *in situ* hybridization in IL7tg mice (35), a significant increase in *Il7* mRNA transcripts was observed in spleens of both IL7tg and FLtgxIL7tg mice (**Figure 1C**). Macroscopically, double transgenic mice exhibited a profound splenomegaly, with spleen size and average cellularity significantly larger than in single transgenic mice, in which the spleen was already increased compared to WT (**Figures 1D,E**). LN enlargement was even more striking, as shown in **Figure 1D**, with the average number of nucleated cells in all four inguinal and axillary LN reaching almost  $10^9$  cells, compared to  $3.4 \times 10^6$  for WT,  $45.4 \times 10^6$  for FLtg and  $145 \times 10^6$  for IL7tg mice (**Figure 1F**). All other LN examined macroscopically (brachial, mediastinal) showed similar enlargement compared to WT and single transgenic mice. FLtgxIL7tg BM cellularity was somewhat increased compared to WT (less than 2-fold and not statistically significant) and similar to the single transgenic controls (**Figure 1G**). On the contrary, thymus cellularity was slightly decreased in single and double transgenic mice compared to their WT littermates (**Figure 1H**).

Analysis of the enlarged spleens and LN of FLtgxIL7tg mice showed that several mature hematopoietic cells, which normally reside in these secondary lymphoid tissues, were remarkably increased. Thus, spleen and LN Gr1<sup>+</sup>CD11b<sup>+</sup> cells, including neutrophils and macrophages, were clearly increased in response to elevated FL levels (**Supplementary Figure 1A**). Also, and in agreement with what has been described previously in single FLtg mice (32), DC populations, including conventional DC of both types (CD11c<sup>+</sup>MHC-II<sup>+</sup>XCR1<sup>+</sup>cDC1 and CD11c<sup>+</sup>MHC-II<sup>+</sup>XCR1<sup>-</sup>cDC2), as well as B220<sup>+</sup>SiglecH<sup>+</sup> plasmacytoid DC (pDC), were all dramatically increased in response to FL over-expression (**Supplementary Figures 1B–E**), although the statistical analysis did not show a significant effect on LN cDC1 and cDC2. A clear effect of over-expressing both cytokines was also observed on splenic and LN T cells. FLtgxIL7tg mice had increased numbers of both CD4<sup>+</sup> and CD8<sup>+</sup> T cells in spleen (4.4- and 13-fold increase compared to WT, respectively) and LN (11- and 30-fold increase compared to WT, respectively) (**Supplementary Figures 2A,B**). This effect was also seen in the numbers of the CD4<sup>+</sup>Foxp3<sup>+</sup> regulatory T cell (Treg) fraction of CD4<sup>+</sup> T cells, particularly in the LN (**Supplementary Figures 2A,B**), as shown before under conditions of high FL availability (36). This increase in peripheral T cell numbers was probably not due to increased thymic output, since analysis of T cell developmental stages in the thymi of FLtgxIL7tg mice showed that over-expression of both cytokines did not significantly affect the numbers of T cell progenitors, including CD4<sup>+</sup> and CD8<sup>+</sup> single positive and CD4/CD8 double positive pro-T cells. Interestingly, FL over-expression resulted in a reduction in the numbers of the earliest double negative T cell progenitors (**Supplementary Figures 2C–E**).

We next examined B cell populations in the peripheral lymphoid organs of FLtgxIL7tg and single transgenic mice. Analysis of peritoneal B cells showed that IL-7 over-expression significantly increased the percent of B2 cells, whereas the frequency of the IL-7-independent (37) CD19<sup>+</sup>CD5<sup>+</sup>CD11b<sup>low</sup> B1a population was decreased by over-expression of both cytokines (**Supplementary Figures 3A,B**). Even though FL has been shown to be critical for the generation of B1a cells (30, 38), their relative frequency was not significantly increased upon FL over-expression, but rather slightly decreased, possibly due to the large expansion of myeloid cells in the peritoneal cavity (**Supplementary Figure 3B**). Mature, recirculating IgM<sup>+</sup>CD93<sup>-</sup> B cells were significantly increased in the LN of FLtgxIL7tg mice compared to WT (21-fold), whereas over-expressing either cytokine alone resulted in increased mature B cell numbers compared to WT, but to a smaller extent (**Figure 2A**). Mature IgM<sup>+</sup> B cells do not express CD135 and, unlike peripheral T cells, they are also CD127<sup>-</sup> and hence do not respond to either FL or IL-7. We therefore reasoned that the observed increase in their numbers in the periphery was the result of increased B cell progenitor numbers in the BM, as shown previously in IL7tg mice (29). Analysis of BM B cell progenitor populations showed a moderate 1.6-fold increase in the numbers of IgM<sup>+</sup>CD93<sup>+</sup> immature B cells, the population that exits the BM to recirculate in the periphery (**Figures 2B,C**). IgM<sup>-</sup> B cell progenitors showed a more pronounced increase compared to WT controls: 7.4-fold for CD19<sup>+</sup>CD117<sup>+</sup>IgM<sup>-</sup> pro-B cells, 3.7-fold for CD19<sup>+</sup>CD117<sup>-</sup>IgM<sup>-</sup>CD127<sup>+</sup>FSC<sup>large</sup> large pre-B and 2.3-fold for CD19<sup>+</sup>CD117<sup>-</sup>IgM<sup>-</sup>CD127<sup>-</sup>FSC<sup>small</sup> small pre-B cells (**Figures 2B,C**). This increase in BM CD19<sup>+</sup> B cell progenitors was mainly an effect of elevated IL-7 levels, since FL over-expression seemed to have a negative outcome on the numbers of pre-B and immature B cells (~2-fold decreased in FLtgxIL7tg mice compared to IL7tg). Thus, the reduction in pre-B and immature B cell numbers observed in FLtg mice (32) is also present when IL-7 is abundantly available (in FLtgxIL7tg mice) and is therefore unlikely to be caused by decreased IL-7 availability, as previously hypothesized.

### Accumulation of Lymphoid Progenitors in Peripheral Lymphoid Organs of FLtgxIL7tg Mice

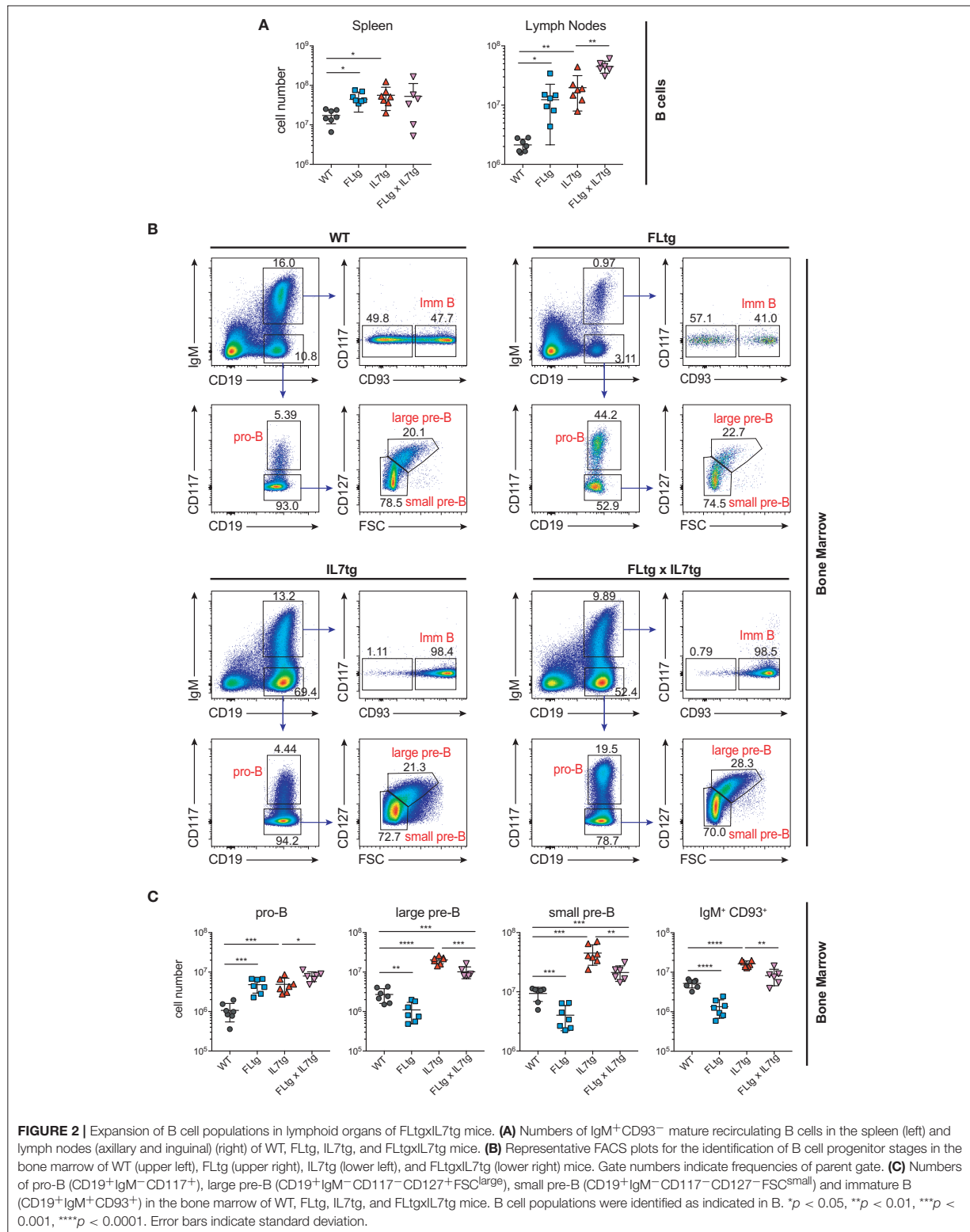
Previous analysis of IL7tg mice has shown an abundance of immature B cell progenitors in the spleen and LN, where these populations are normally not found in significant numbers (29). We therefore analyzed spleen and LN of FLtgxIL7tg mice for the presence of early B cell progenitors. Indeed, in both spleen and LN of IL7tg mice, all stages of CD19<sup>+</sup> committed B cell progenitors were detected (**Figures 3A,B**). Contrary to what was observed in the BM, however, additional FL over-expression, in FLtgxIL7tg mice, further increased the numbers of pro-B (4.6-fold in spleen and 16-fold in LN), large pre-B (1.8-fold in spleen and 11-fold in LN), small pre-B (2-fold in spleen and 12-fold in LN) and immature B (1.9-fold in spleen and 9.8-fold in LN) cells. Thus, FL and IL-7 seem to act synergistically in promoting the accumulation of immature B cell progenitors in

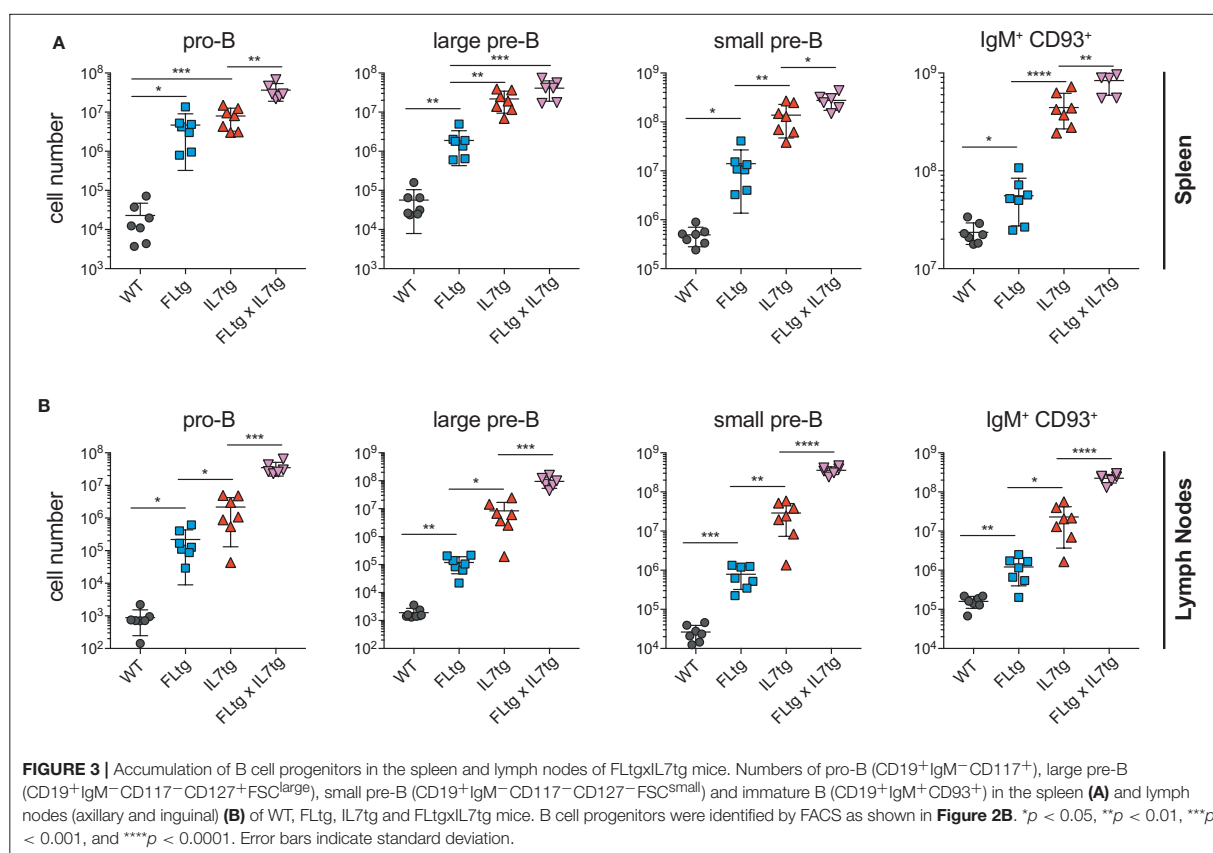


the peripheral lymphoid organs of mice over-expressing both cytokines.

Since CD135 is not detectable on CD19<sup>+</sup> B cell progenitors, this additional rise in their numbers in spleen and LN upon simultaneous FL and IL-7 over-expression is unlikely to be a direct effect of FL on their survival and/or proliferation. However, their immediate precursors, Ly6D<sup>+</sup> EPLM, are CD135<sup>+</sup> and have been shown to increase dramatically in response to elevated FL levels (13, 34, 39).

Therefore, we assessed their numbers in the BM and periphery of FLtgxIL7tg mice. As shown in **Figures 4A,B**, CD11c<sup>-</sup>NK1.1<sup>-</sup>SiglecH<sup>-</sup>CD19<sup>-</sup>B220<sup>int</sup>CD117<sup>int</sup>Ly6D<sup>+</sup> EPLM were indeed dramatically increased upon FL over-expression in the BM, whereas IL-7 over-expression did not increase their numbers and even reduced them when in combination with high FL expression (**Figure 4B**, FLtg compared to FLtgxIL7tg). Ly6D<sup>+</sup> EPLM were clearly detected in spleens of FLtg and FLtgxIL7tg mice, whereas in LN they were strikingly expanded



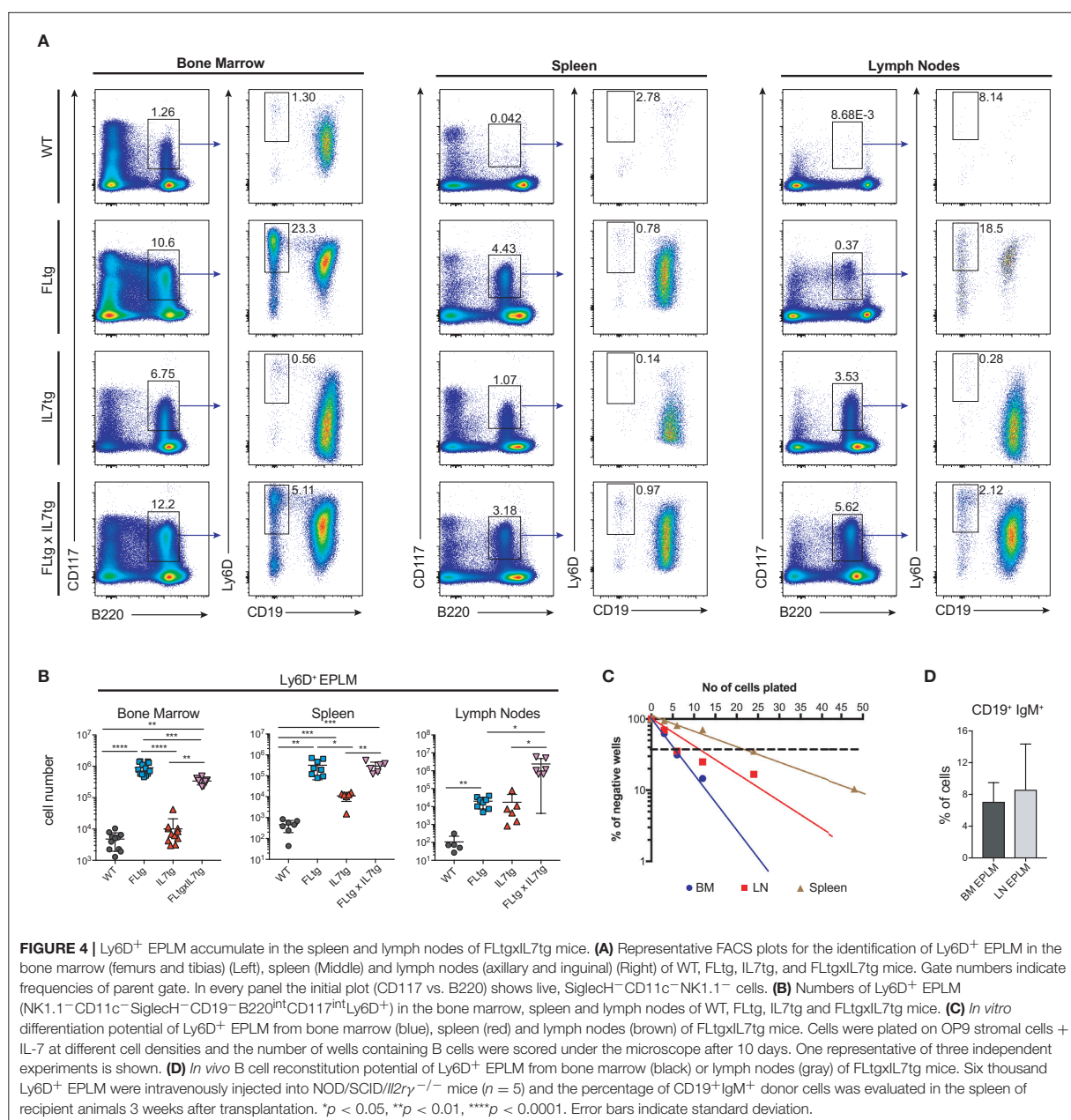


mainly upon over-expression of both cytokines. FLtg and IL7tg LN also had higher numbers of Ly6D<sup>+</sup> EPLM compared to WT, in which they were barely detectable. However, this increase was not statistically significant and was proportional to the corresponding overall increase in LN total cellularity (**Figure 1F**), whereas FLtgxIL7tg LN Ly6D<sup>+</sup> EPLM were 120- and 137-fold increased compared to their FLtg and IL7tg counterparts, respectively. This expansion is ~10 times higher than the corresponding LN cellularity difference between these mouse genotypes, indicating that FL and IL-7 synergistically promote the accumulation and/or expansion of Ly6D<sup>+</sup> EPLM in the LN of FLtgxIL7tg mice. Since Ly6D<sup>+</sup> EPLM are not yet committed to the B cell lineage (39, 40), we assessed the ability of these spleen- and LN-residing FLtgxIL7tg progenitors to generate B cells *in vitro* and *in vivo*. Sorting and plating FLtgxIL7tg Ly6D<sup>+</sup> EPLM on OP9 stromal cells together with IL-7 under limiting dilution conditions showed that these cells were able to give rise to CD19<sup>+</sup> B cells *in vitro* (**Figure 4C**). We noticed that the frequency of LN-derived Ly6D<sup>+</sup> EPLM that could generate B cells under these conditions was slightly reduced compared to their BM counterparts, which showed a frequency similar to WT BM-derived Ly6D<sup>+</sup> EPLM (13, 39). However, after transplantation into NOD/SCID/Il2ry<sup>-/-</sup>

lymphopenic mice, LN-derived FLtgxIL7tg Ly6D<sup>+</sup> EPLM were as capable as their BM-derived counterparts at generating IgM<sup>+</sup> B cells *in vivo* (**Figure 4D**). Thus, under conditions of simultaneous increase in FL and IL-7 availability, functional CD19<sup>-</sup>Ly6D<sup>+</sup> EPLM progenitors can reside and accumulate in the spleens and LN of mice.

### Hematopoietic Progenitors With Long-Term, Multilineage Reconstitution Capacity Reside in the LN of FLtgxIL7tg Mice

Apart from Ly6D<sup>+</sup> EPLM, CLP and LSK cells are greatly expanded in FLtg mice (32). We therefore investigated their potential expansion in the BM and presence in the spleen and LN of FLtgxIL7tg mice. Under conditions of high *in vivo* FL availability, CD135 becomes undetectable by flow cytometry (32), possibly due to the continuous binding of the ligand to its receptor. Thus, we identified CLP using the original Lin<sup>-</sup>CD117<sup>int</sup>Sca1<sup>int</sup>CD127<sup>+</sup> phenotype (14) (**Figure 5B**). We found CLP numbers to be significantly increased in the BM of mice over-expressing FL, whereas IL-7 over-expression did not have any effect (**Figure 5A**). This was also the case in the spleen,



where splenic FLtgxIL7tg CLP were increased compared to WT (Figure 5C). Similarly to EPLM, we observed a greater than 10-fold increase in LN FLtgxIL7tg CLP numbers compared to their single transgenic counterparts, which were already increased compared to WT (Figures 5E,F). CD127<sup>-</sup> LSK cell analysis showed a similar picture, with LSK being greatly increased in the BM and found in significant numbers in the spleen and LN of FLtgxIL7tg mice. Within the LSK compartment, the CD48<sup>-</sup>CD150<sup>+</sup> phenotype can be used to enrich for hematopoietic stem cells (HSC) with multilineage developmental

potential and self-renewal capacity (41). As shown in Figure 5A (bottom), CD48<sup>-</sup>CD150<sup>+</sup> LSK cells were significantly reduced in the BM of FLtg mice and this was also the case in FLtgxIL7tg BM (6-fold decreased compared to WT). These cells were detected at very low frequency in the spleen of FLtgxIL7tg mice (Figure 5C), and we could not detect them in the LN of any of the mouse genotypes analyzed (data not shown).

Taken together, our analysis shows that over-expression of both FL and IL-7 leads to a dramatic increase in all BM CD135<sup>+</sup> and CD127<sup>+</sup> progenitors and to their migration to

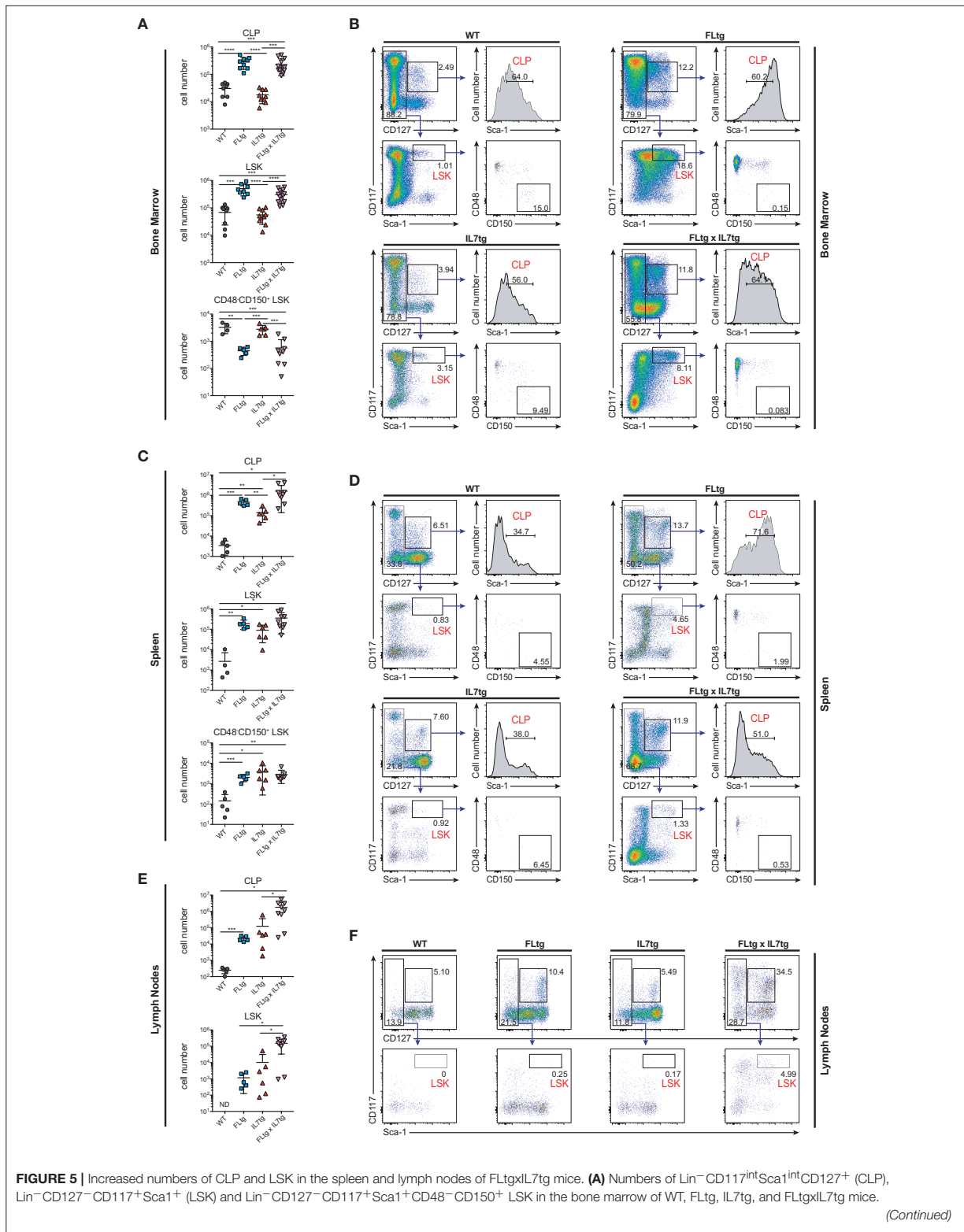


**FIGURE 5 |** Increased numbers of CLP and LSK in the spleen and lymph nodes of FLtgxIL7tg mice. **(A)** Numbers of Lin<sup>-</sup>CD117<sup>int</sup>Sca1<sup>int</sup>CD127<sup>+</sup> (CLP), Lin<sup>-</sup>CD127<sup>-</sup>CD117<sup>+</sup>Sca1<sup>+</sup> (LSK) and Lin<sup>-</sup>CD127<sup>-</sup>CD117<sup>+</sup>Sca1<sup>+</sup>CD48<sup>-</sup>CD150<sup>+</sup> LSK in the bone marrow of WT, FLtg, IL7tg, and FLtgxIL7tg mice.

(Continued)

**FIGURE 5 | (B)** Representative FACS plots for the identification of CLP, LSK, and CD48<sup>-</sup>CD150<sup>+</sup> LSK in the bone marrow (femurs and tibias) of WT, FLtg, IL7tg, and FLtgxIL7tg mice. Gate numbers indicate frequencies of parent gate. In every panel the upper left plot (CD117 vs. CD127) shows live, Lineage<sup>-</sup> cells. **(C)** Numbers of CLP, LSK and CD48<sup>-</sup>CD150<sup>+</sup> LSK in the spleens of WT, FLtg, IL7tg, and FLtgxIL7tg mice. **(D)** Representative FACS plots for the identification of CLP, LSK, and CD48<sup>-</sup>CD150<sup>+</sup> LSK in the spleens of WT, FLtg, IL7tg, and FLtgxIL7tg mice. Gate numbers indicate frequencies of parent gate. In every panel the upper plot (CD117 vs. CD127) shows live, Lin<sup>-</sup> cells. **(E)** Numbers of CLP and LSK in the LN of WT, FLtg, IL7tg, and FLtgxIL7tg mice. **(F)** Representative FACS plots for the identification of LSK in the LN of WT, FLtg, IL7tg, and FLtgxIL7tg mice. Gate numbers indicate frequencies of parent gate. In every panel the upper plot (CD117 vs. CD127) shows live, Lin<sup>-</sup> cells. \**p* < 0.05, \*\**p* < 0.01, \*\*\**p* < 0.001, and \*\*\*\**p* < 0.0001. Error bars indicate standard deviation.

the periphery, presumably due to space constraints in the BM. In support of this hypothesis, all CD19<sup>+</sup> B cell progenitor stages were found significantly increased in the peripheral blood of FLtgxIL7tg mice (Figures 6A,D). Strikingly, the same was true for CD135<sup>+</sup> Ly6D<sup>+</sup> EPLM, CLP and LSK progenitors, which were increased in the blood mainly in response to FL over-expression (Figures 6B,C,E). This effect of FL and IL-7 simultaneous over-expression in promoting the migration of cells from the BM to the periphery was seen mainly on progenitors, since mature B and T cell frequencies in the blood of FLtgxIL7tg mice were not dramatically changed, whereas the relative frequencies of cDC and NK cells were significantly increased in the blood of FLtg animals (Supplementary Figure 4). Thus, the synergistic effect of FL and IL-7 over-expression in expanding BM hematopoietic progenitors leads to their exit from the BM and accumulation not only in the spleen but also in LN, where some of these progenitors are undetectable in WT mice.

We next sought to evaluate whether these multipotent hematopoietic progenitors identified by flow cytometry in the LN of FLtgxIL7tg mice were functional, i.e., if they had the ability to generate multiple hematopoietic lineages upon transplantation. To this end, we infused  $10 \times 10^6$  unfractionated LN cells from CD45.2<sup>+</sup> FLtgxIL7tg, into sublethally irradiated congenic CD45.1<sup>+</sup> WT mice. FLtgxIL7tg BM cells were used as a positive control for the long-term reconstitution of hematopoietic lineages, since they contain functional hematopoietic progenitors. Recipient mice were analyzed 12–16 weeks after transplantation for the contribution of CD45.2<sup>+</sup> donor cells to the different hematopoietic lineages. As expected, overall engraftment of donor cells in the BM, spleen and thymus of recipient mice was significantly lower in LN-transplanted recipients compared to BM transplanted ones (Supplementary Figures 5A,B). Thus, in the FLtgxIL7tg LN transplanted hosts, 20% splenic, 5.4% BM and 6.8% thymic cells were of donor origin. Analysis of the spleen of FLtgxIL7tg LN-reconstituted mice showed that 21.8% CD19<sup>+</sup> B cells, 13.8% CD3<sup>+</sup> T cells, 16.3% NK1.1<sup>+</sup> NK cells, 14.7% SiglecH<sup>-</sup>CD11b<sup>-</sup>CD11c<sup>+</sup> DC, 4.5% CD11b<sup>+</sup>CD11c<sup>-</sup> myeloid cells and 15% Ter119<sup>+</sup> erythroid cells were of donor origin, with more than 80% of the transplanted mice showing donor-derived reconstitution in all the above lineages (Figures 7A–D). Donor contribution was also evaluated in the thymus of recipient mice, where we found small but clearly detectable populations of FLtgxIL7tg LN-derived CD4<sup>+</sup>, CD8<sup>+</sup>, and CD4/CD8 double positive T cell progenitors (Figures 7E–G). Furthermore, BM analysis showed that a significant fraction of CD19<sup>+</sup> B cell progenitors were of FLtgxIL7tg LN donor origin, with the average percent ranging from 5.6% for large pre-B to 13% for

immature IgM<sup>+</sup>CD93<sup>+</sup> B cells (Supplementary Figures 5C,D). Remarkably, we also found small but clearly detectable populations of donor-derived CLP (5%) and LSK (3.5%) 12 weeks after transplantation. Thus, FLtgxIL7tg LN contain progenitors with the long-term capacity to generate multiple hematopoietic lineages.

The presence of early hematopoietic progenitors in the host BM 12 weeks after transfer of FLtgxIL7tg LN cells, prompted us to assess their self-renewal capacity by re-transplanting them into secondary recipients. Six million unfractionated BM cells from FLtgxIL7tg LN-reconstituted mice and FLtgxIL7tg BM-reconstituted controls were intravenously injected into congenic CD45.1<sup>+</sup> irradiated WT hosts 12 weeks after the first transplantation. Nine weeks after secondary transfer, we could detect FLtgxIL7tg-derived donor cells in the secondary recipients' spleen. Importantly, CD45.2<sup>+</sup> cells were found in multiple hematopoietic lineages. Thus, FLtgxIL7tg LN donor-derived cells were found in: 0.1% CD19<sup>+</sup> B cells, 0.25% CD3<sup>+</sup> T cells, 0.6% CD11c<sup>+</sup> DC and 0.07% Ter119<sup>+</sup> erythroid cells (Figures 8A–D). These results indicate that there are FLtgxIL7tg LN-residing multipotent hematopoietic progenitors with self-renewal capacity. Overall, considering the significant multilineage contribution of FLtgxIL7tg LN-derived donor cells in host hematopoietic reconstitution more than 12 weeks after transfer, as well as their presence in secondary transplanted hosts after another 9 weeks, we conclude that the LN of FLtgxIL7tg mice contain hematopoietic progenitors with *in vivo* long-term multi-lineage reconstitution ability, some of which have self-renewal capacity.

## DISCUSSION

We have previously generated and analyzed mice with increased, sustained *in vivo* levels of either IL-7 (28, 29) or FL (13, 32, 39), which provided important insights to the roles of the two cytokines at different stages of the various lineages of hematopoiesis. In the present study we over-expressed both cytokines in order to evaluate the concerted action of both FL and IL-7 on the regulation of hematopoiesis in an *in vivo* setting. We find a synergistic effect of the two cytokines in promoting the generation and expansion of lymphoid cells, resulting in a profound enlargement of secondary lymphoid organs, such as spleen and LN, significantly more than what can be seen in single transgenic mice (Figure 1). Both spleen and LN of FLtgxIL7tg mice were populated by significant numbers of multipotent hematopoietic progenitors, which in WT mice are generally confined to the BM.

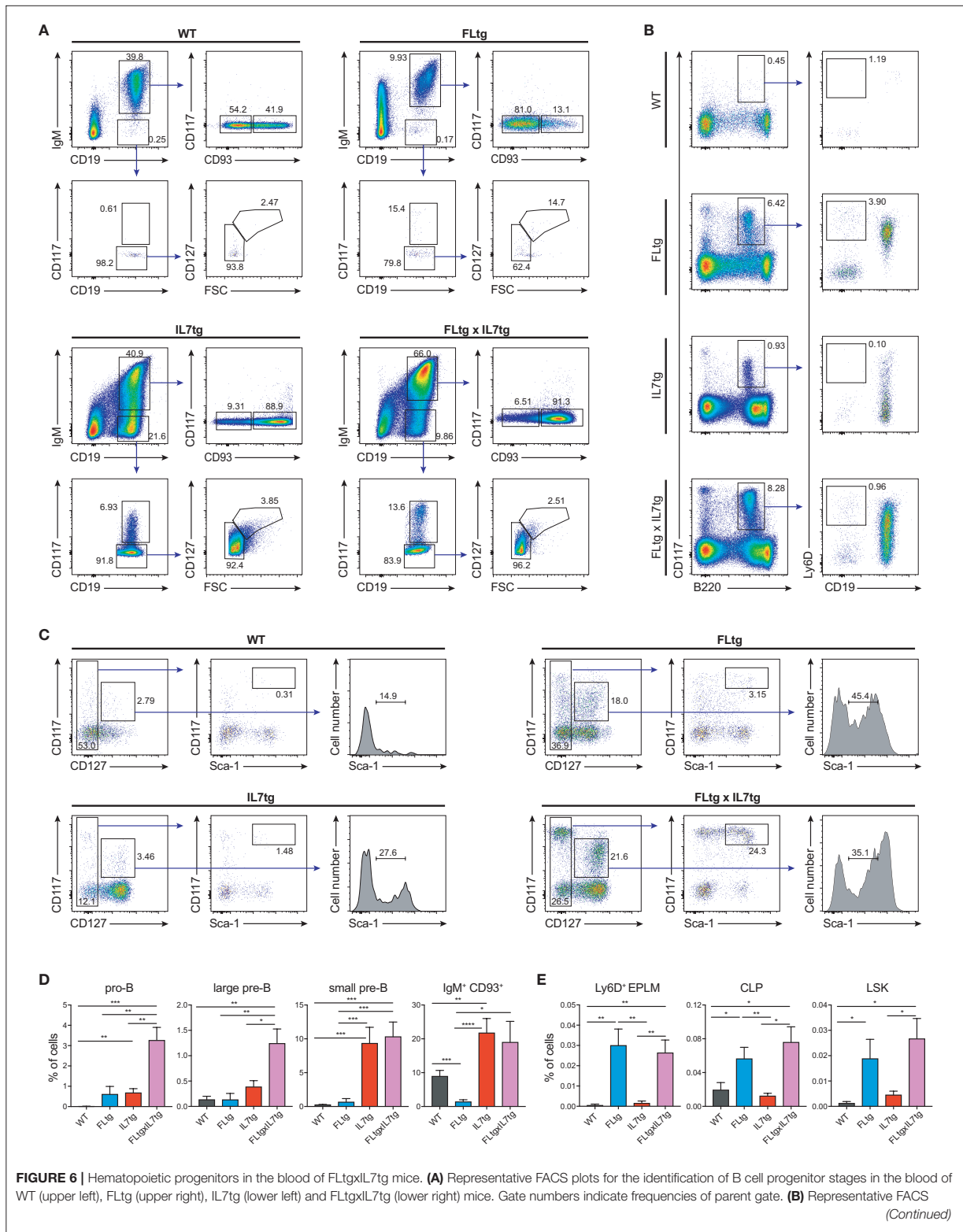


**FIGURE 6** | plots for the identification of Ly6D<sup>+</sup> EPLM in the blood of WT (upper left), FLtg (upper right), IL7tg (lower left), and FLTg $\times$ IL7tg (lower right) mice. Gate numbers indicate frequencies of parent gate. In every panel the left plot (CD117 vs. B220) shows live, NK1.1<sup>-</sup>CD11c<sup>-</sup>SiglecH<sup>-</sup> cells. **(C)** Representative FACS plots for the identification of LSK and CLP in the blood of WT (upper left), FLtg (upper right), IL7tg (lower left), and FLTg $\times$ IL7tg (lower right) mice. Gate numbers indicate frequencies of parent gate. In every panel the left plot (CD117 vs. CD127) shows live, Lin<sup>-</sup> cells. **(D)** Percentages of pro-B (CD19<sup>+</sup>IgM<sup>-</sup>CD117<sup>+</sup>), large pre-B (CD19<sup>+</sup>IgM<sup>-</sup>CD117<sup>-</sup>CD127<sup>+</sup>FSC<sup>large</sup>), small pre-B (CD19<sup>+</sup>IgM<sup>-</sup>CD117<sup>-</sup>CD127<sup>-</sup>FSC<sup>small</sup>) and immature B cell (CD19<sup>+</sup>IgM<sup>+</sup>CD93<sup>+</sup>) progenitors in the blood of WT ( $n = 9$ ), FLtg ( $n = 11$ ), IL7tg ( $n = 8$ ), and FLTg $\times$ IL7tg ( $n = 11$ ) mice. B cell progenitors were identified by FACS as shown in **(A)**. **(E)** Percentages of Ly6D<sup>+</sup> EPLM (CD11c<sup>-</sup>NK1.1<sup>-</sup>SiglecH<sup>-</sup>B220<sup>int</sup>CD117<sup>int</sup>Ly6D<sup>+</sup>CD19<sup>-</sup>), CLP (Lin<sup>-</sup>CD117<sup>int</sup>Sca1<sup>int</sup>CD127<sup>+</sup>) and LSK (Lin<sup>-</sup>CD117<sup>+</sup>Sca1<sup>+</sup>CD127<sup>-</sup>) progenitors in the blood of WT ( $n = 6$ ), FLtg ( $n = 6$ ), IL7tg ( $n = 7$ ), and FLTg $\times$ IL7tg ( $n = 10$ ) mice. The y-axis on all plots indicates % of live, nucleated blood cells. \* $p < 0.05$ , \*\* $p < 0.01$ , \*\*\* $p < 0.001$ , and \*\*\*\* $p < 0.0001$ . Error bars indicate standard deviation.

The enlarged spleens and LN of FLTg $\times$ IL7tg mice contained significantly increased populations of myeloid cells (**Supplementary Figure 1A**). This probably reflected the expansion in BM myeloid progenitors that FL over-expression induces (32). Indeed, when assessing early myelo-erythroid progenitor stages in FLTg $\times$ IL7tg BM, we observed a significant increase in the earliest identified myeloid progenitors, pre-GM and GMP (42), whereas early erythroid/megakaryocyte progenitors were decreased (**Supplementary Figure 6**), in accordance with the anemia and thrombocytopenia caused by elevated FL (32). Generation of DC is known to depend on FL and we indeed found all splenic and some LN DC populations significantly increased (**Supplementary Figure 1**). This could be the result of DC expansion in peripheral lymphoid organs, since these cells are CD135<sup>+</sup>, or could be due to FL-mediated expansion of their progenitors. Due to the inability to stain for CD135<sup>+</sup> in mice over-expressing FL (32) we were not able to assess the numbers of cDC and pDC progenitors (43–45).

Peripheral T cells were also increased dramatically in spleens and LN of FLTg $\times$ IL7tg mice, even though thymic size and T cell output was not increased. Thus, this seems to be mainly an effect of IL-7, which is known to regulate homeostasis of peripheral T cells, particularly of CD8<sup>+</sup> (46) which was the T cell population with the biggest expansion in FLTg $\times$ IL7tg mice (**Supplementary Figures 2A,B**). Interestingly, FL over-expression alone also resulted in some increase in mature T cell numbers. Since these cells are CD135<sup>-</sup>, we postulate that this is an indirect effect of high FL levels. Previous experiments, showing expansion of regulatory T cells upon increased FL availability, suggested that this is mediated by IL-2 produced by the expanded DC (36), thus providing a potential explanation for the observed increase in peripheral T cells when FL is over-expressed. The somewhat reduced thymopoiesis observed in FLTg $\times$ IL7tg mice might be a direct or secondary result of high FL expression by thymic stromal cells, since IL-7 over-expression alone in the IL7tg mouse model used herein did not affect T cell development (35). Since thymus seeding progenitors that migrate from the BM are multipotent and express CD135 (47, 48), it is conceivable that under the influence of increased FL levels a larger fraction of them differentiates toward myeloid or DC fates, thus resulting in somewhat reduced CD4/CD8 double-negative numbers.

The synergistic effect of FL and IL-7 is clearly manifested in the generation of B cells. Expression of the receptors for the two cytokines on B cell generating progenitors occurs at

slightly different developmental stages: CD135 is expressed on early progenitors (LSK, CLP, EPLM) and is down-regulated upon Pax5/CD19 expression and commitment to the B cell lineage, whereas CD127 is expressed from the CLP up to the small pre-B stage. Accordingly, both receptors are co-expressed during the CLP/EPLM developmental stage, in which a potential synergy between the two cytokines in promoting B cell development can occur. FL is mainly acting as a proliferative factor for CLP/EPLM progenitors, whereas IL-7 supports their survival, rather than expanding them (13). Thus, we find the number of these progenitors greatly expanded in the BM of FLtg and FLTg $\times$ IL7tg mice, while IL-7 over-expression does not further increase their numbers but rather decreases them slightly (**Figures 4B, 5A**). IL-7 acts as a proliferative factor for CD19<sup>+</sup> B cell progenitors in the BM, leading to a 5- to 9-fold increase in their numbers upon over-expression (when comparing IL7tg to WT or FLTg $\times$ IL7tg to FLtg). This effect of the two cytokines on the proliferation of hematopoietic progenitors was confirmed in the present study, since we found a significant increase in the percentage of cycling LSK in the BM of mice over-expressing FL, whereas IL-7 had a proliferative effect mainly on CD19<sup>+</sup> B cell progenitors (**Supplementary Figure 7**). This vast expansion of CD19<sup>+</sup> cells upon IL-7 over-expression could explain the slight reduction in FLTg $\times$ IL7tg Ly6D<sup>+</sup> EPLM numbers compared to FLtg mice, since the expanded progenitor populations have to compete for limited space in the BM. By contrast, in peripheral lymphoid tissues, such as the spleen and LN, which can enlarge to accommodate more cells, the synergistic effect of FL and IL-7 can be clearly seen, as FLTg $\times$ IL7tg spleen and LN contain significantly more CLP/EPLM and CD19<sup>+</sup> B cell progenitors of all stages compared to their single transgenic counterparts. Interestingly, the proliferative effect of the two cytokines observed in the BM was also seen in the LN (**Supplementary Figure 7**), indicating that progenitors continue to expand in response to the two cytokines after their migration to the periphery. The space restrictions imposed on cells in the BM might also be the reason for the observed reduction in the number of BM pre-B and immature cells when FL is over-expressed. We have previously hypothesized that this might be the result of reduced IL-7 availability in the BM of FLtg mice, but as the same effect seems to occur in FLTg $\times$ IL7tg mice, this is unlikely to be the reason. It is still possible that other trophic signals required for the expansion and/or survival of pre-B cells become limiting in the BM when CD135<sup>+</sup> progenitors expand massively, as is the case in FLtg and FLTg $\times$ IL7tg mice. However, this does not happen in the periphery, where the FL-mediated expansion of CLP/EPLM results in a corresponding

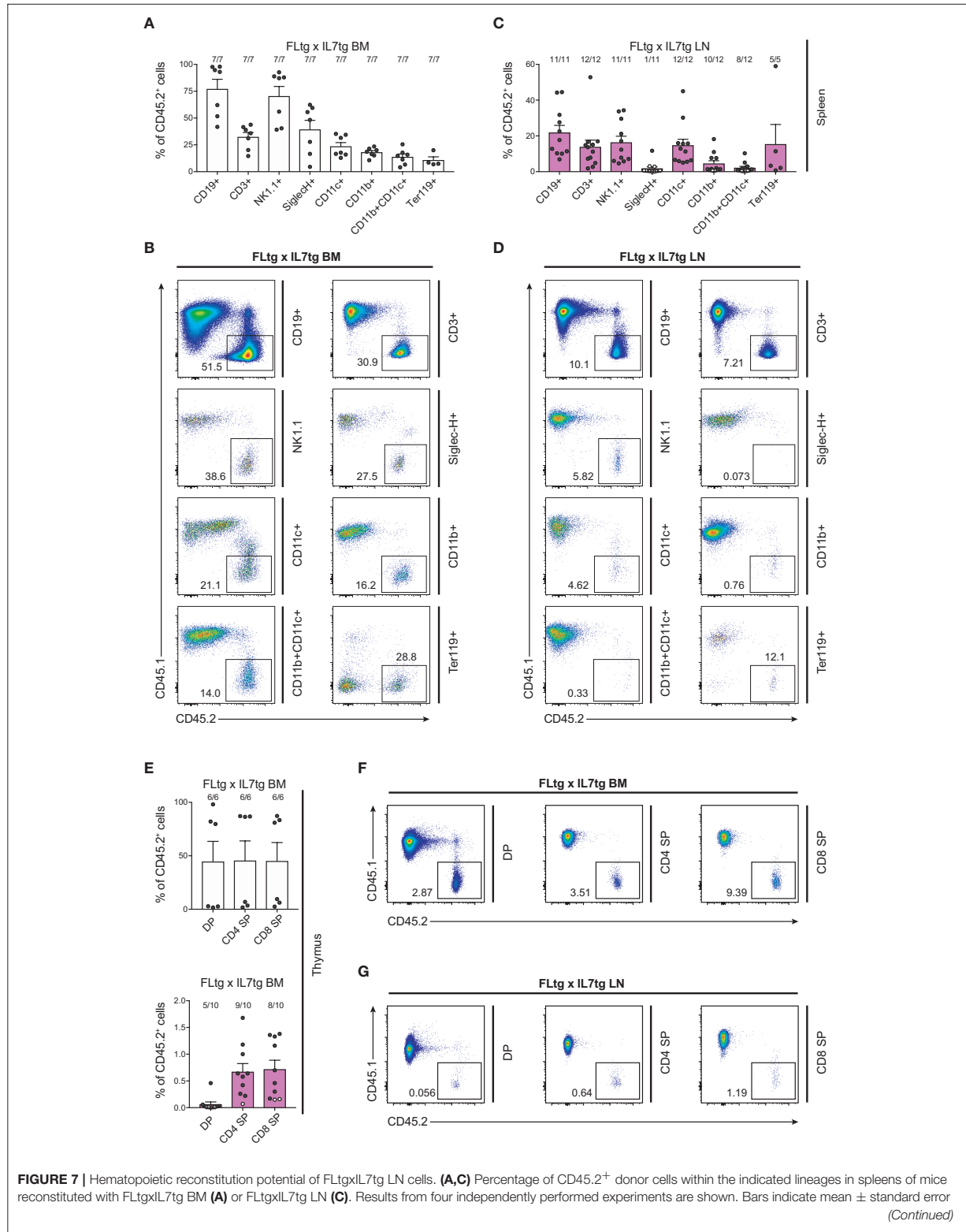


**FIGURE 7** | of the mean. Black circles represent mice where the corresponding lineage was scored as positive for the presence of donor-derived cells (>50 cells in the CD45.2<sup>+</sup> gate) and white circles mice with no reconstitution (<50 cells in the CD45.2<sup>+</sup> gate). The fraction of positive-to-total mice analyzed for each lineage is indicated above the corresponding bar. Lineages were defined as follows: CD19<sup>+</sup>: CD11b<sup>-</sup>CD11c<sup>-</sup>CD3<sup>-</sup>CD19<sup>+</sup>; CD3<sup>+</sup>: CD11b<sup>-</sup>CD11c<sup>-</sup>CD19<sup>-</sup>CD3<sup>+</sup>; NK1.1<sup>+</sup>: CD3<sup>-</sup>CD11c<sup>-</sup>B220<sup>-</sup>SiglecH<sup>-</sup>NK1.1<sup>+</sup>; SiglecH<sup>+</sup>: CD11b<sup>-</sup>NK1.1<sup>-</sup>B220<sup>+</sup>SiglecH<sup>+</sup>; CD11c<sup>+</sup>: NK1.1<sup>-</sup>SiglecH<sup>-</sup>B220<sup>-</sup>CD11b<sup>-</sup>CD11c<sup>+</sup>; CD11b<sup>+</sup>: NK1.1<sup>-</sup>SiglecH<sup>-</sup>B220<sup>-</sup>CD11c<sup>-</sup>CD11b<sup>+</sup>; CD11b<sup>+</sup>CD11c<sup>+</sup>: NK1.1<sup>-</sup>SiglecH<sup>-</sup>B220<sup>-</sup>CD11b<sup>+</sup>CD11c<sup>+</sup>; Ter119<sup>+</sup>: Ter119<sup>+</sup>. **(B,D)** Representative FACS plots showing the CD45.2<sup>+</sup> donor population identified within the lineages shown in **(A,C)**. Left: recipients transplanted with FLtgxIL7tg BM; Right: recipients transplanted with FLtgxIL7tg LN. **(E)** Percentage of CD45.2<sup>+</sup> donor cells within the indicated T cell populations in thymi of mice reconstituted with FLtgxIL7tg BM (upper) and FLtgxIL7tg LN (lower). Results from three independently performed experiments are shown. For FLtgxIL7tg BM: *n* = 6; for FLtgxIL7tg LN: *n* = 10. Bars indicate mean ± standard error of the mean. Black circles represent mice where the corresponding lineage was scored as positive for the presence of donor-derived cells (>50 cells in the CD45.2<sup>+</sup> gate) and white circles mice with no reconstitution (<50 cells in the CD45.2<sup>+</sup> gate). The ratio of positive-to-total mice analyzed for each lineage is indicated above the corresponding bar. Cells were identified as follows: DP: CD3<sup>+</sup>CD4<sup>+</sup>CD8<sup>+</sup>; CD4 SP: CD3<sup>+</sup>CD8<sup>-</sup>CD4<sup>+</sup>; CD8 SP: CD3<sup>+</sup>CD4<sup>-</sup>CD8<sup>+</sup>. **(F,G)** Representative FACS plots showing the CD45.2<sup>+</sup> donor population identified within the indicated thymic T cell populations. Upper: recipients transplanted with FLtgxIL7tg BM; lower: recipients transplanted with FLtgxIL7tg LN.

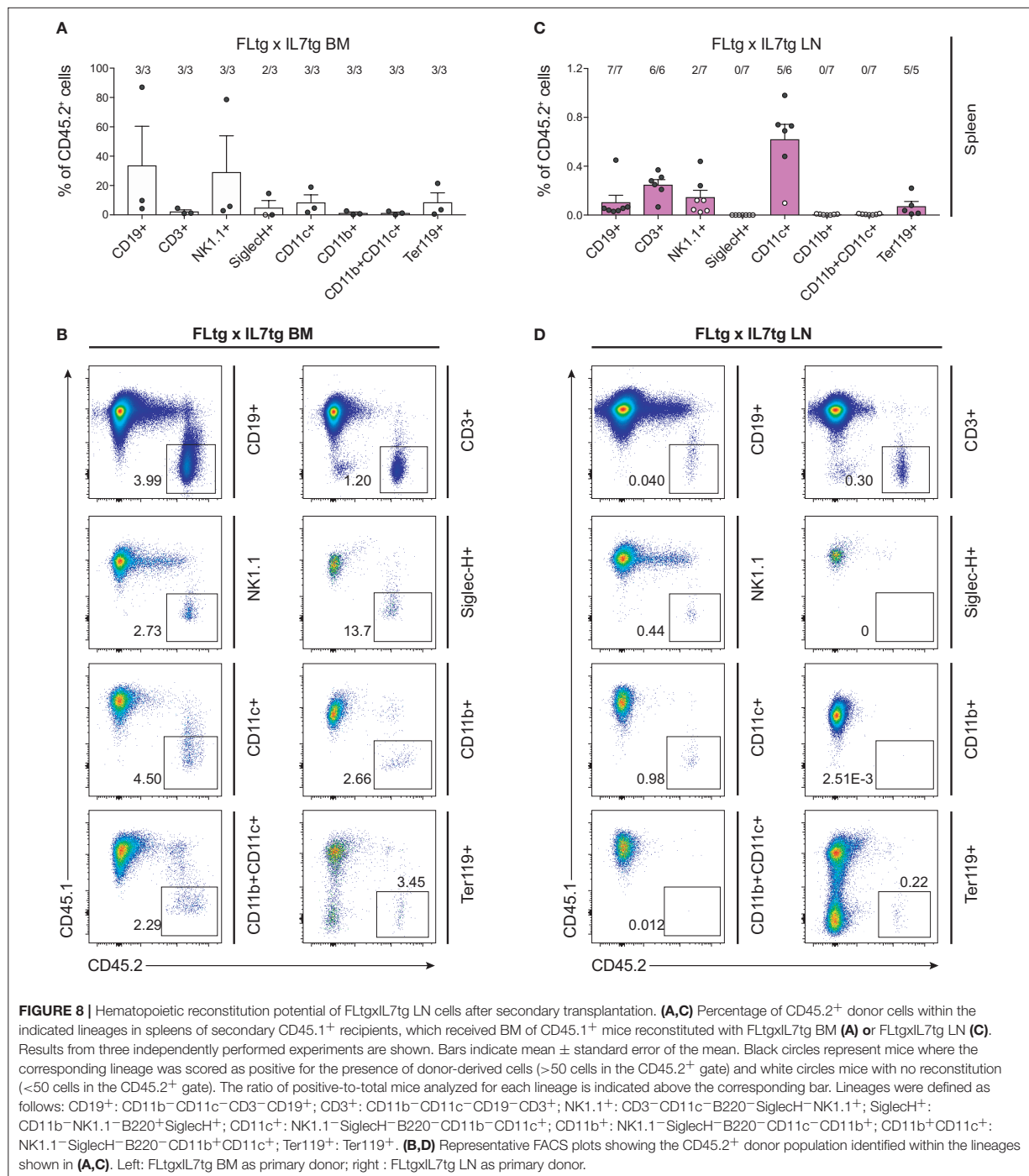
increase in pro-B and pre-B cell numbers. Taken together, FL and IL-7 act in concert to promote B cell development, FL by providing sufficient numbers of CLP/EPLM progenitors and IL-7 by promoting their survival and further expansion after commitment to the B cell fate.

FL over-expression resulted in a major expansion of LSK cells, which are largely CD135<sup>+</sup>. When IL-7 was additionally over-expressed, this resulted in the detection of significant LSK numbers in the spleen and LN of FLtgxIL7tg mice. Since LSK are CD127<sup>-</sup>, we hypothesize that the reason for their increase mainly in FLtgxIL7tg LN is again related to confined space and/or resources in the FLtgxIL7tg BM, thus leading to their migration to peripheral lymphoid organs when expanded by FL over-expression. In support of this hypothesis, LSK can also be detected in the blood of FLtgxIL7tg mice (**Figures 6C,E**). Expression of molecules associated with progenitor migration from the BM, such as S1PR<sub>1</sub>, CD44, and CXCR4 was not dramatically different between genotypes, with the exception of an FL-mediated increase in the CXCR4<sup>+</sup> fraction of B cell progenitors, which might be an indirect effect of FL, as these cells are CD135<sup>-</sup> (**Supplementary Figure 8**). This indicates that it is mainly competition for BM space/resources that leads to their accumulation in peripheral lymphoid organs. LSK are mostly comprised of multipotent progenitors with mixed lineage potentials and biases, but which are not considered to possess self-renewal capacity (7). Self-renewing HSC within the LSK compartment can be enriched for by staining with the SLAM markers CD48 and CD150, and are contained within the CD48<sup>-</sup>CD150<sup>+</sup> LSK fraction (41). We were not able to detect CD48<sup>-</sup>CD150<sup>+</sup> LSK cells in the LN of FLtgxIL7tg mice. However, as reported previously (32), and seen in **Figure 5A**, the CD48<sup>-</sup>CD150<sup>+</sup> fraction of LSK in the BM is severely reduced in numbers upon FL over-expression. These cells are CD135<sup>-</sup> when identified by flow cytometry, although some of them express mRNA for the receptor (49). Therefore we do not know if this reduction is a direct effect of FL-signaling. In addition, we cannot exclude that high FL availability might affect the expression of SLAM markers, thus resulting in some HSC losing the CD48<sup>-</sup>CD150<sup>+</sup> phenotype in FLtg and FLtgxIL7tg mice. The expression level of other important markers for the identification of progenitor stages, such as CD117 and Sca1, might also be changed upon FL over-expression. As shown in **Figures 5B,D**, Sca1 expression in the majority of FLtg and FLtgxIL7tg CLP is

relatively higher than the one of their WT and IL7tg counterparts. The same is true for CD117 expression in pro-B (**Figure 2B**). This might be the result of altered marker expression or a selective expansion of the (few in WT mice) cells expressing high levels of the corresponding proteins.

In order to functionally assess the precursor activity of hematopoietic progenitors found in the LN of FLtgxIL7tg mice, we transplanted LN cells from these mice into myeloablated WT recipients and assessed their long-term multilineage reconstitution capacity. We found a significant contribution of FLtgxIL7tg donor cells in lymphoid, myeloid, dendritic and erythroid lineages 12–16 weeks after transplantation. This is indicative of the presence of multipotent progenitors in the double transgenic LN, since myeloid and dendritic cells are not long-lived and therefore these donor cells could not be mature myeloid/dendritic cells transferred from the FLtgxIL7tg LN. In addition, we found donor contribution in all stages of recipient T cell development, suggesting that the FLtgxIL7tg LN contain progenitors with thymus-seeding potential. The exact nature of these precursors is not known, but they are known to have multilineage developmental capacity (47, 48). Furthermore, we detected donor progenitor cells in the BM of recipient animals, which upon transplantation into secondary recipients showed a small but clearly detectable contribution in the regeneration of different lineages. We conclude from this data that the LN of FLtgxIL7tg mice contain hematopoietic progenitors with long-term multilineage hematopoietic regeneration capacity. These could be HSC, which do not display the CD48<sup>-</sup>CD150<sup>+</sup> phenotype due to alterations in SLAM marker expression, or downstream multipotent progenitors that have acquired self-renewal capacity under conditions of high FL availability – possibly by an autocrine FL effect.

Irrespective of the precise nature of the multipotent hematopoietic progenitor that resides in FLtgxIL7tg LN, it is clear from our data that not only the spleen but also the LN of these double transgenic mice can support the survival of immature precursors, such as LSK, CLP, EPLM, and pre-B cells, which are normally only found in the BM. Extra-medullary hematopoiesis has been described in patients and has been mostly associated either with bone marrow failure or with myeloproliferative disease (50, 51). Similarly, disruption of hematopoiesis in mice caused by drug treatment (52), mutations



(53–55) or cytokine over-expression (56, 57) can lead to extra-medullary hematopoiesis. However, the main extra-medullary site where hematopoietic progenitors are detected in both patients and mice is the spleen, whereas no such precursors have

been reported in LN in these cases. Hematopoietic progenitors have been shown to circulate to the periphery through blood and lymph, but only very small numbers have been detected in lymph under normal conditions and they were practically undetected

in LN (58). A human NK precursor has been detected in LN (59), while it has been shown that at early time points after BM transplantation T cell lymphopoiesis can occur in extra-thymic sites, including LN (60). Interestingly, repeated administration of FL in mice has led to pronounced presence of immature hematopoietic progenitors in the spleen, as seen in our FLtg and FLtgxIL7tg mice, but not in LN (61). It appears that in FLtgxIL7tg mice, the expansion of both lymphoid and myeloid progenitors due to the combined action of both cytokines is sufficient to cause the accumulation of hematopoietic progenitors not only in the spleen but also in LN. This indicates that the environment in secondary lymphoid organs is able to support hematopoiesis in “emergency” situations, such as the one in FLtgxIL7tg mice, which manifest a pronounced myelo- and lympho-proliferative disease. However, it remains unknown whether this ability of the FLtgxIL7tg LN to support the accumulation of progenitors is due to alterations in the LN niche caused by high FL and IL-7 expression, e.g., up-regulated expression of other cytokines or adhesion molecules by LN stromal cells. Moreover, an interesting question is whether the FLtgxIL7tg LN is a site of on-going hematopoiesis, or if the progenitors only migrate there and accumulate without differentiating further. In support of the former hypothesis, FLtgxIL7tg LN-residing progenitors are functional in reconstituting hematopoietic cells after transfer to irradiated recipients (Figures 7, 8) and all hematopoietic developmental stages are represented in the LN in ratios similar to the ones found in WT BM. Further experiments would be needed to address this issue.

Collectively, our present analysis of FLtgxIL7tg mice demonstrates the *in vivo* synergistic action of FL and IL-7 in promoting lymphoid development and expansion. This is summarized in **Supplementary Figure 9**. Our data provide evidence that secondary lymphoid organs can support the maintenance of hematopoietic progenitors in conditions of abnormal hematopoiesis. Further studies of these mice might

elucidate the requirements for extra-medullary residence and hematopoietic activity of HSC; an issue of clinical importance for the treatment of lympho-proliferative disorders and blood malignancies.

## AUTHOR CONTRIBUTIONS

FK, LvM, GC, SH, LA-S, HR, CE, MR, MM, GCv, and PT performed experiments. FK, PT, and AR analyzed data. PT wrote the manuscript. JA and RC contributed experimental ideas and revised the manuscript. PT and AR designed the study.

## FUNDING

AR was holder of the chair in immunology endowed by L. Hoffmann – La Roche Ltd., Basel. This study was supported by the Swiss National Science Foundation (310030B\_160330/1) and by the People Program (Marie Curie Actions) of the European Union’s Seventh Framework Program FP7/2007-2013 under Research Executive Agency grant agreement number 315902. RC was supported by Science Foundation Ireland under grant numbers SFI09/SRC/B1794 and SFI07/SK/B1233b.

## ACKNOWLEDGMENTS

We thank Dr Geoffrey Brown for critical reading of the manuscript and helpful comments. We dedicate this paper to the memory of our colleague, friend, group leader and mentor AR.

## SUPPLEMENTARY MATERIAL

The Supplementary Material for this article can be found online at: <https://www.frontiersin.org/articles/10.3389/fimmu.2018.02258/full#supplementary-material>

## REFERENCES

1. Metcalf D. Hematopoietic cytokines. *Blood* (2008) 111:485–91. doi: 10.1182/blood-2007-03-079681
2. Brown G, Mooney CJ, Alberti-Servera L, Muenchow L, Toellner KM, Ceredig R, et al. Versatility of stem and progenitor cells and the instructive actions of cytokines on hematopoiesis. *Crit Rev Clin Lab Sci.* (2015) 52:168–79. doi: 10.3109/10408363.2015.1021412
3. Brown G, Tsapogas P, Ceredig R. The changing face of hematopoiesis: a spectrum of options is available to stem cells. *Immunol Cell Biol.* (2018). doi: 10.1111/imcb.12055. [Epub ahead of print].
4. Gilliland DG, Griffin JD. The roles of FLT3 in hematopoiesis and leukemia. *Blood* (2002) 100:1532–42. doi: 10.1182/blood-2002-02-0492
5. Stirewalt DL, Radich JP. The role of FLT3 in haematopoietic malignancies. *Nat Rev Cancer* (2003) 3:650–65. doi: 10.1038/nrc1169
6. Tsapogas P, Mooney CJ, Brown G, Rolink A. The Cytokine Flt3-Ligand in Normal and Malignant Hematopoiesis. *Int J Mol Sci.* (2017) 18:E1115. doi: 10.3390/ijms18061115
7. Adolfsen J, Borge OJ, Bryder D, Theilgaard-Monch K, Astrand-Grundstrom I, Sitnicka E, et al. Upregulation of Flt3 expression within the bone marrow Lin(-)Sca1(+)-c-kit(+) stem cell compartment is accompanied by loss of self-renewal capacity. *Immunity* (2001) 15:659–69. doi: 10.1016/S1074-7613(01)00220-5
8. Mackarehstschian K, Hardin JD, Moore KA, Boast S, Goff SP, Lemischka IR. Targeted disruption of the flk2/flt3 gene leads to deficiencies in primitive hematopoietic progenitors. *Immunity* (1995) 3:147–61.
9. McKenna HJ, Stocking KL, Miller RE, Brasel K, De Smedt T, Maraskovsky E, et al. Mice lacking flt3 ligand have deficient hematopoiesis affecting hematopoietic progenitor cells, dendritic cells, and natural killer cells. *Blood* (2000) 95:3489–97.
10. Buza-Vidas N, Cheng M, Duarte S, Nozad H, Jacobsen SE, Sitnicka E. Crucial role of FLT3 ligand in immune reconstitution after bone marrow transplantation and high-dose chemotherapy. *Blood* (2007) 110:424–32. doi: 10.1182/blood-2006-09-047480
11. Holmes ML, Carotta S, Corcoran LM, Nutt SL. Repression of Flt3 by Pax5 is crucial for B-cell lineage commitment. *Genes Dev.* (2006) 20:933–8. doi: 10.1101/gad.1396206
12. Sitnicka E, Bryder D, Theilgaard-Monch K, Buza-Vidas N, Adolfsen J, Jacobsen SE. Key role of flt3 ligand in regulation of the common lymphoid progenitor but not in maintenance of the hematopoietic stem cell pool. *Immunity* (2002) 17:463–72. doi: 10.1016/S1074-7613(02)00419-3
13. von Muenchow L, Alberti-Servera L, Klein F, Capoferri G, Finke D, Ceredig R, et al. Permissive roles of cytokines interleukin-7 and Flt3 ligand in mouse

- B-cell lineage commitment. *Proc Natl Acad Sci USA*. (2016) 113:E8122–30. doi: 10.1073/pnas.1613316113
14. Kondo M, Weissman IL, Akashi K. (1997). Identification of clonogenic common lymphoid progenitors in mouse bone marrow. *Cell* 91:661–72.
  15. Namen AE, Schmierer AE, March CJ, Overell RW, Park LS, Urdal DL, et al. B cell precursor growth-promoting activity. Purification and characterization of a growth factor active on lymphocyte precursors. *J Exp Med*. (1988) 167:988–1002.
  16. Rolink A, Kudo A, Karasuyama H, Kikuchi Y, Melchers F. Long-term proliferating early pre B cell lines and clones with the potential to develop to surface Ig-positive, mitogen reactive B cells *in vitro* and *in vivo*. *EMBO J*. (1991) 10:327–36.
  17. Peschon JJ, Morrissey PJ, Grabstein KH, Ramsdell FJ, Maraskovsky E, Gliniak BC, et al. Early lymphocyte expansion is severely impaired in interleukin 7 receptor-deficient mice. *J Exp Med* (1994) 180:1955–60.
  18. von Freeden-Jeffry U, Vieira P, Lucian LA, McNeil T, Burdach SE, Murray R. Lymphopenia in interleukin (IL)-7 gene-deleted mice identifies IL-7 as a nonredundant cytokine. *J Exp Med* (1995) 181:1519–26.
  19. Akashi K, Kondo M, von Freeden-Jeffry U, Murray R, Weissman IL. Bcl-2 rescues T lymphopoiesis in interleukin-7 receptor-deficient mice. *Cell* (1997) 89:1033–41.
  20. Maraskovsky E, O'Reilly LA, Teepe M, Corcoran LM, Peschon JJ, Strasser A. Bcl-2 can rescue T lymphocyte development in interleukin-7 receptor-deficient mice but not in mutant rag-1 $^{-/-}$  mice. *Cell* (1997) 89:1011–9.
  21. Carrette F, Surh CD. IL-7 signaling and CD127 receptor regulation in the control of T cell homeostasis. *Semin Immunol*. (2012) 24:209–17. doi: 10.1016/j.smim.2012.04.010
  22. Kondo M, Akashi K, Domen J, Sugamura K, Weissman IL. (1997). Bcl-2 rescues T lymphopoiesis, but not B or NK cell development, in common gamma chain-deficient mice. *Immunity* 7:155–62.
  23. Maraskovsky E, Peschon JJ, McKenna H, Teepe M, Strasser A. Overexpression of Bcl-2 does not rescue impaired B lymphopoiesis in IL-7 receptor-deficient mice but can enhance survival of mature B cells. *Int Immunol*. (1998) 10:1367–75.
  24. Dias S, Silva H Jr, Cumano A, Vieira P. Interleukin-7 is necessary to maintain the B cell potential in common lymphoid progenitors. *J Exp Med*. (2005) 201:971–9. doi: 10.1084/jem.20042393
  25. Tsapogas P, Zandi S, Ahsberg J, Zetterblad J, Welinder E, Jonsson JL, et al. IL-7 mediates Ebf-1-dependent lineage restriction in early lymphoid progenitors. *Blood* (2011) 118:1283–90. doi: 10.1182/blood-2011-01-332189
  26. Malin S, McManus S, Cobaleda C, Novatchkova M, Delogu A, Bouillet P, et al. Role of STAT5 in controlling cell survival and immunoglobulin gene recombination during pro-B cell development. *Nat Immunol*. (2010) 11:171–9. doi: 10.1038/ni.1827
  27. Fisher AG, Burdet C, LeMeur M, Haasner D, Gerber P, Ceredig R. Lymphoproliferative disorders in an IL-7 transgenic mouse line. *Leukemia* (1993) 7(Suppl. 2):S66–8.
  28. Fisher AG, Burdet C, Bunce C, Merckenschlager M, Ceredig R. Lymphoproliferative disorders in IL-7 transgenic mice: expansion of immature B cells which retain macrophage potential. *Int Immunol*. (1995) 7:415–23.
  29. Mertsching E, Grawunder U, Meyer V, Rolink T, Ceredig R. Phenotypic and functional analysis of B lymphopoiesis in interleukin-7-transgenic mice: expansion of pro/pre-B cell number and persistence of B lymphocyte development in lymph nodes and spleen. *Eur J Immunol*. (1996) 26:28–33. doi: 10.1002/eji.1830260105
  30. Sitnicka E, Brakebusch C, Martensson IL, Svensson M, Agace WW, Sigvardsson M, et al. Complementary signaling through flt3 and interleukin-7 receptor alpha is indispensable for fetal and adult B cell genesis. *J Exp Med*. (2003) 198:1495–506. doi: 10.1084/jem.20031152
  31. Ahsberg J, Tsapogas P, Qian H, Zetterblad J, Zandi S, Mansson R, et al. Interleukin-7-induced Stat-5 acts in synergy with Flt-3 signaling to stimulate expansion of hematopoietic progenitor cells. *J Biol Chem*. (2010) 285:36275–84. doi: 10.1074/jbc.M110.155531
  32. Tsapogas P, Swee LK, Nusser A, Nuber N, Kreuzaler M, Capoferri G, et al. *In vivo* evidence for an instructive role of fms-like tyrosine kinase-3 (FLT3) ligand in hematopoietic development. *Haematologica* (2014) 99:638–46. doi: 10.3324/haematol.2013.089482
  33. Mazzucchelli R, Durum SK. Interleukin-7 receptor expression: intelligent design. *Nat Rev Immunol*. (2007) 7:144–54. doi: 10.1038/nri2023
  34. Ceredig R, Rauch M, Balciunaite G, Rolink AG. Increasing Flt3L availability alters composition of a novel bone marrow lymphoid progenitor compartment. *Blood* (2006) 108:1216–22. doi: 10.1182/blood-2005-10-06643
  35. Mertsching E, Burdet C, Ceredig R. IL-7 transgenic mice: analysis of the role of IL-7 in the differentiation of thymocytes *in vivo* and *in vitro*. *Int Immunol*. (1995) 7:401–14.
  36. Swee LK, Bosco N, Malissen B, Ceredig R, Rolink A. Expansion of peripheral naturally occurring T regulatory cells by Fms-like tyrosine kinase 3 ligand treatment. *Blood* (2009) 113:6277–87. doi: 10.1182/blood-2008-06-161026
  37. Carvalho TL, Mota-Santos T, Cumano A, Demengeot J, Vieira P. Arrested B lymphopoiesis and persistence of activated B cells in adult interleukin 7 $^{-/-}$  mice. *J Exp Med* (2001) 194:1141–50. doi: 10.1084/jem.194.8.1141
  38. Jensen CT, Kharazi S, Boiers C, Cheng M, Lubking A, Sitnicka E, et al. FLT3 ligand and not TSLP is the key regulator of IL-7-independent B-1 and B-2 B lymphopoiesis. *Blood* (2008) 112:2297–304. doi: 10.1182/blood-2008-04-150508
  39. Alberti-Servera L, von Muenchow L, Tsapogas P, Capoferri G, Eschbach K, Beisel C, et al. Single-cell RNA sequencing reveals developmental heterogeneity among early lymphoid progenitors. *EMBO J* (2017) 36:3619–33. doi: 10.15252/embj.201797105
  40. Balciunaite G, Ceredig R, Massa S, Rolink AG. A B220 $^{+}$  CD117 $^{+}$  CD19 $^{-}$  hematopoietic progenitor with potent lymphoid and myeloid developmental potential. *Eur J Immunol*. (2005) 35:2019–30. doi: 10.1002/eji.200526318
  41. Kiel MJ, Yilmaz OH, Iwashita T, Yilmaz OH, Terhorst C, Morrison SJ. SLAM family receptors distinguish hematopoietic stem and progenitor cells and reveal endothelial niches for stem cells. *Cell* (2005) 121:1109–21. doi: 10.1016/j.cell.2005.05.026
  42. Pronk CJ, Rossi DJ, Mansson R, Attema JL, Norddahl GL, Chan CK, et al. Elucidation of the phenotypic, functional, and molecular topography of a myeloerythroid progenitor cell hierarchy. *Cell Stem Cell* (2007) 1:428–42. doi: 10.1016/j.stem.2007.07.005
  43. Onai N, Obata-Onai A, Schmid MA, Ohteki T, Jarrossay D, Manz MG. Identification of clonogenic common Flt3 $^{+}$ M-CSFR $^{+}$  plasmacytoid and conventional dendritic cell progenitors in mouse bone marrow. *Nat Immunol*. (2007) 8:1207–16. doi: 10.1038/ni1518
  44. Liu K, Vitorica GD, Schwickert TA, Guermonprez P, Meredith MM, Yao K, et al. *In vivo* analysis of dendritic cell development and homeostasis. *Science* (2009) 324:392–7. doi: 10.1126/science.1170540
  45. Rodrigues PF, Alberti-Servera L, Eremin A, Grajales-Reyes GE, Ivanek R, Tussiwand R. Distinct progenitor lineages contribute to the heterogeneity of plasmacytoid dendritic cells. *Nat Immunol*. (2018) 19:711–22. doi: 10.1038/s41590-018-0136-9
  46. Tan JT, Dudl E, LeRoy E, Murray R, Sprent J, Weinberg KI, et al. IL-7 is critical for homeostatic proliferation and survival of naive T cells. *Proc Natl Acad Sci USA*. (2001) 98:8732–7. doi: 10.1073/pnas.161126098
  47. Balciunaite G, Ceredig R, Rolink AG. The earliest subpopulation of mouse thymocytes contains potent T, significant macrophage, and natural killer cell but no B-lymphocyte potential. *Blood* (2005) 105:1930–6. doi: 10.1182/blood-2004-08-3087
  48. Luc S, Luis TC, Boukarabila H, Macaulay IC, Buza-Vidas N, Bourriez-Jones T, et al. The earliest thymic T cell progenitors sustain B cell and myeloid lineage potential. *Nat Immunol*. (2012) 13:412–9. doi: 10.1038/ni.2255
  49. Mooney CJ, Cunningham A, Tsapogas P, Toellner KM, Brown G. Selective expression of Flt3 within the mouse hematopoietic stem cell compartment. *Int J Mol Sci*. (2017) 18:E1037. doi: 10.3390/ijms18051037
  50. Johns JL, Christopher MM. Extramedullary hematopoiesis: a new look at the underlying stem cell niche, theories of development, and occurrence in animals. *Vet Pathol*. (2012) 49:508–23. doi: 10.1177/0300985811432344
  51. Chiu SC, Liu HH, Chen CL, Chen PR, Liu MC, Lin SZ, et al. Extramedullary hematopoiesis (EMH) in laboratory animals: offering an insight into stem cell research. *Cell Transplant* (2015) 24:349–66. doi: 10.3727/096368915X686850

52. Sefc L, Psenak O, Sykora V, Sulc K, Necas E. Response of hematopoiesis to cyclophosphamide follows highly specific patterns in bone marrow and spleen. *J Hematother Stem Cell Res.* (2003) 12:47–61. doi: 10.1089/152581603321210136
53. Hsieh PP, Olsen RJ, O'Malley DP, Konoplev SN, Hussong JW, Dunphy CH, et al. The role of Janus Kinase 2 V617F mutation in extramedullary hematopoiesis of the spleen in neoplastic myeloid disorders. *Mod Pathol.* (2007) 20:929–35. doi: 10.1038/modpathol.3800826
54. Sasaki M, Knobbe CB, Munger JC, Lind EF, Brenner D, Brustle A, et al. IDH1(R132H) mutation increases murine haematopoietic progenitors and alters epigenetics. *Nature* (2012) 488:656–9. doi: 10.1038/nature11323
55. Chang T, Krisman K, Theobald EH, Xu J, Akutagawa J, Lauchle JO, et al. Sustained MEK inhibition abrogates myeloproliferative disease in Nf1 mutant mice. *J Clin Invest* (2013) 123:335–9. doi: 10.1172/JCI63193
56. Peters M, Schirmacher P, Goldschmitt J, Odenthal M, Peschel C, Fattori E, et al. Extramedullary expansion of hematopoietic progenitor cells in interleukin (IL)-6-sIL-6R double transgenic mice. *J Exp Med.* (1997) 185:755–66.
57. Khaldoyanidi S, Sikora L, Broide DH, Rothenberg ME, Sriramarao P. Constitutive overexpression of IL-5 induces extramedullary hematopoiesis in the spleen. *Blood* (2003) 101:863–8. doi: 10.1182/blood-2002-03-0735
58. Massberg S, Schaerli P, Knezevic-Maramica I, Kollnberger M, Tubo N, Moseman EA, et al. Immunosurveillance by hematopoietic progenitor cells trafficking through blood, lymph, and peripheral tissues. *Cell* (2007) 131:994–1008. doi: 10.1016/j.cell.2007.09.047
59. Freud AG, Becknell B, Roychowdhury S, Mao HC, Ferketic AK, Nuovo GJ, et al. A human CD34(+) subset resides in lymph nodes and differentiates into CD56bright natural killer cells. *Immunity* (2005) 22:295–304. doi: 10.1016/j.immuni.2005.01.013
60. Maillard I, Schwarz BA, Sambandam A, Fang T, Shestova O, Xu L, et al. Notch-dependent T-lineage commitment occurs at extrathymic sites following bone marrow transplantation. *Blood* (2006) 107:3511–19. doi: 10.1182/blood-2005-08-3454
61. Shurin MR, Pandharipande PP, Zorina TD, Haluszczak C, Subbotin VM, Hunter O, et al. FLT3 ligand induces the generation of functionally active dendritic cells in mice. *Cell Immunol.* (1997) 179:174–84. doi: 10.1006/cimm.1997.1152

**Conflict of Interest Statement:** The authors declare that the research was conducted in the absence of any commercial or financial relationships that could be construed as a potential conflict of interest.

Copyright © 2018 Klein, von Muenchow, Capoferri, Heiler, Alberti-Servera, Rolink, Engdahl, Rolink, Mitrovic, Cvijetic, Andersson, Ceredig, Tsapogas and Rolink. This is an open-access article distributed under the terms of the Creative Commons Attribution License (CC BY). The use, distribution or reproduction in other forums is permitted, provided the original author(s) and the copyright owner(s) are credited and that the original publication in this journal is cited, in accordance with accepted academic practice. No use, distribution or reproduction is permitted which does not comply with these terms.



*Supplementary Material*

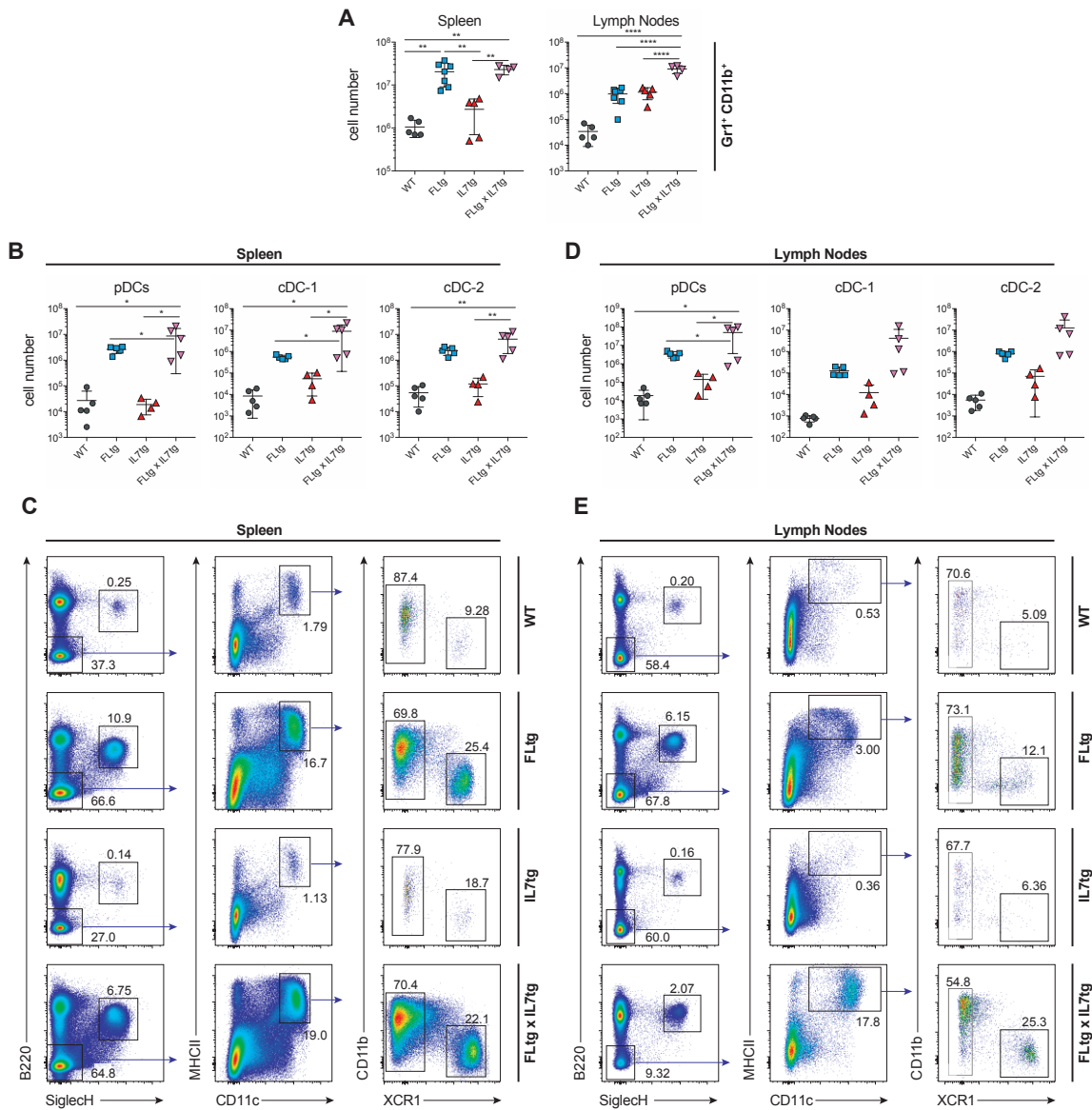
**Accumulation of multipotent hematopoietic progenitors in peripheral lymphoid organs of mice over-expressing interleukin-7 and Flt3-ligand**

**Fabian Klein<sup>1</sup>, Lilly von Muenchow<sup>1</sup>, Giuseppina Capoferri<sup>1</sup>, Stefan Heiler<sup>1</sup>, Lluvia Alberti-Servera<sup>1</sup>, Hannie Rolink<sup>1</sup>, Corinne Engdahl<sup>1</sup>, Michael Rolink<sup>1</sup>, Mladen Mitrovic<sup>1</sup>, Grozdan Cvijetic<sup>1</sup>, Jan Andersson<sup>1</sup>, Rhodri Ceredig<sup>2</sup>, Panagiotis Tsapogas<sup>1\*</sup>, Antonius Rolink<sup>1</sup>**

\* **Correspondence:** Panagiotis Tsapogas: [panagiotis.tsapogas@unibas.ch](mailto:panagiotis.tsapogas@unibas.ch)



## Supplementary Material

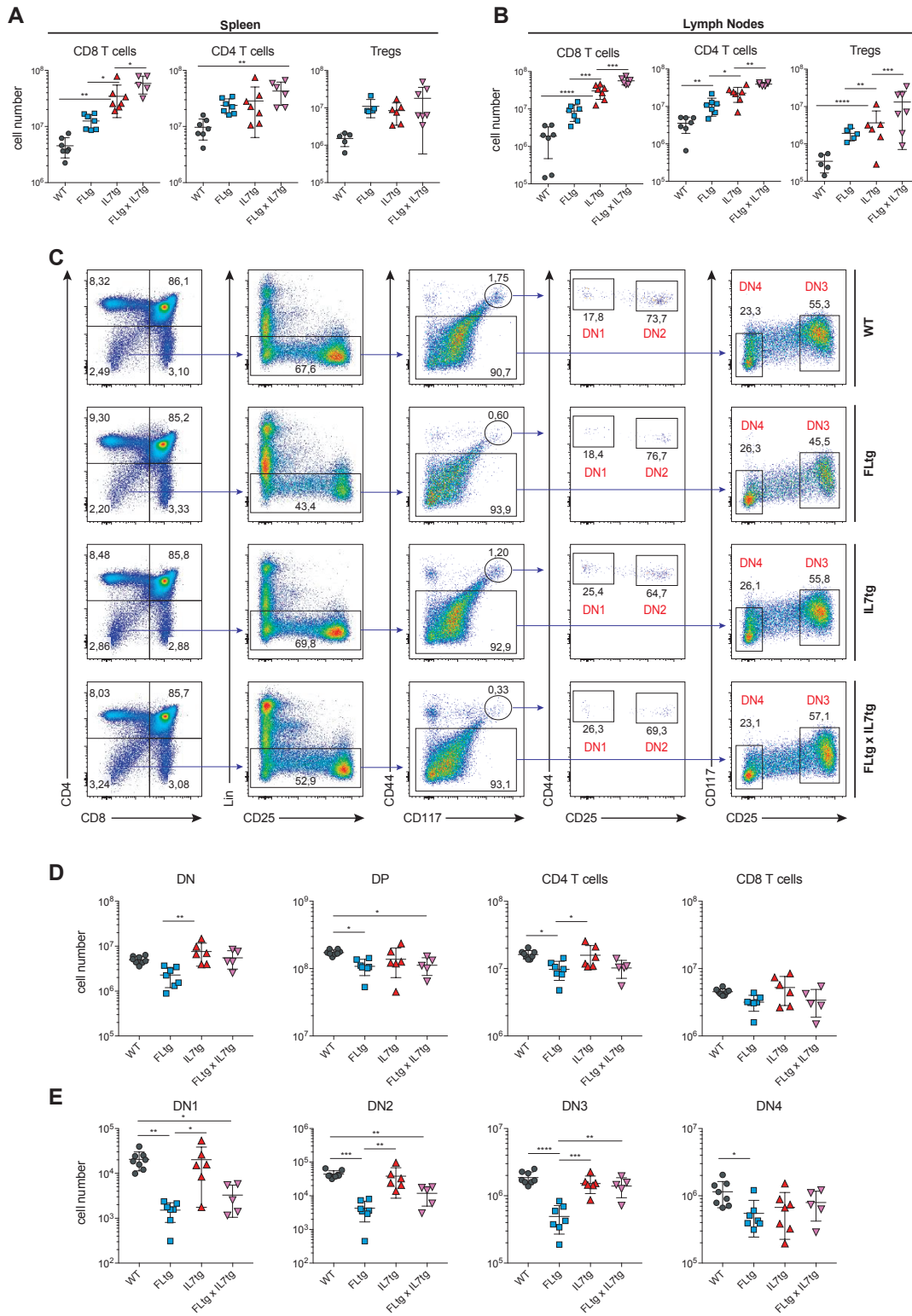


Supplementary Figure 1

## Myeloid and dendritic cells are increased in spleens and LN of FLtgIL7tg mice.

A) Numbers of myeloid cells in the spleen and lymph nodes (axillary and inguinal) of WT, FLtg, IL7tg and FLtg $\times$ IL7tg mice. Myeloid cells were identified as Gr1 $^{+}$ CD11b $^{+}$ . B, D) Dendritic cell numbers in the spleen and lymph nodes of WT, FLtg, IL7tg and FLtg $\times$ IL7tg mice. C, E) Representative FACS plots for the identification of cDC1 (B220 $^{-}$ SiglecH $^{-}$ MHC-II $^{+}$ CD11c $^{+}$ XCR1 $^{+}$ ), cDC2 (B220 $^{-}$ SiglecH $^{-}$ MHC-II $^{+}$ CD11c $^{-}$ XCR1 $^{-}$ ) and pDC (B220 $^{+}$ SiglecH $^{+}$ ) in the spleen (C) and lymph nodes (E) of WT, FLtg, IL7tg and FLtg $\times$ IL7tg mice. Numbers on gates indicate percentage of parent gate. \*:  $p < 0.05$ , \*\*:  $p < 0.01$ , \*\*\*\*:  $p < 0.0001$ . Error bars indicate standard deviation.

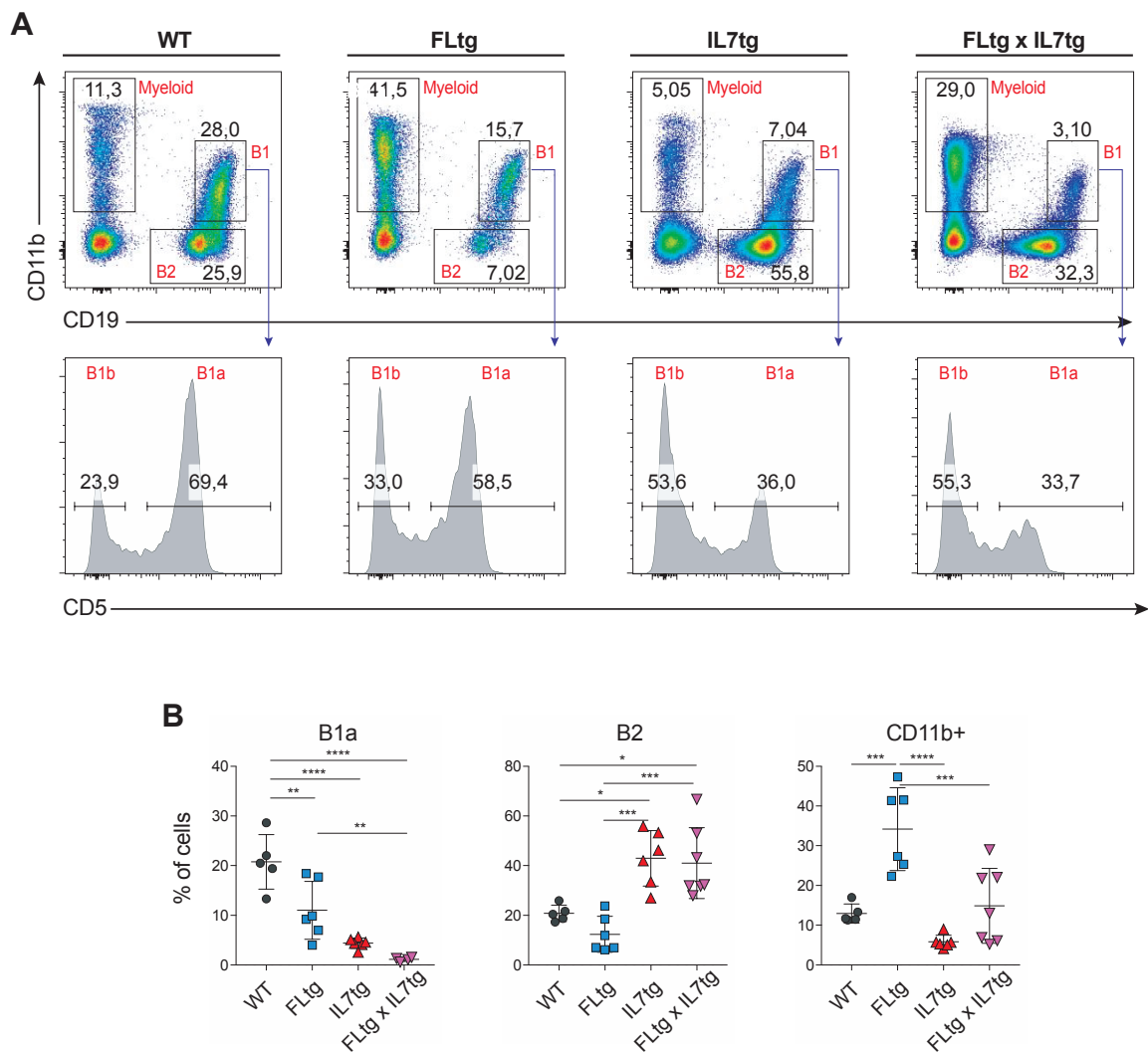
Supplementary Material



## Supplementary Material

**Supplementary Figure 2****T cell populations in FLtgxIL7tg mice**

A, B) Numbers of TCR $\beta^+$ CD8 $^+$  (left panel), TCR $\beta^+$ CD4 $^+$  (middle panel) and CD4 $^+$ Foxp3 $^+$  (right panel) T cells in the spleens (A) and lymph nodes (axillary and inguinal) (B) of WT, FLtg, IL7tg and FLtgxIL7tg mice. C) Representative FACS plots for the identification of double negative (DN) CD4 $^-$ CD8 $^-$  populations (DN1-4), double positive (DP; CD4 $^+$ CD8 $^+$ ), CD4 $^+$  and CD8 $^+$  thymocytes in the thymi of WT, FLtg, IL7tg and FLtgxIL7tg mice. Lineage cocktail contained antibodies against: CD3, B220, CD11c and Gr1. Numbers on gates indicate percentage of parent gate. D) Numbers of DN, DP, CD4 $^+$  and CD8 $^+$  thymocytes in the thymi of WT, FLtg, IL7tg and FLtgxIL7tg mice. E) Numbers of DN1 (Lin $^-$ CD4 $^-$ CD8 $^-$ CD117 $^+$ CD44 $^+$ CD25 $^-$ ), DN2 (Lin $^-$ CD4 $^-$ CD8 $^-$ CD117 $^+$ CD44 $^+$ CD25 $^+$ ), DN3 (Lin $^-$ CD4 $^-$ CD8 $^-$ CD117 $^-$ CD44 $^-$ CD25 $^+$ ) and DN4 (Lin $^-$ CD4 $^-$ CD8 $^-$ CD117 $^-$ CD44 $^-$ CD25 $^-$ ) T cell progenitors in the thymi of WT, FLtg, IL7tg and FLtgxIL7tg mice. \*: p<0.05, \*\*:p<0.01, \*\*\*:p<0.001, \*\*\*\*:p<0.0001. Error bars indicate standard deviation.

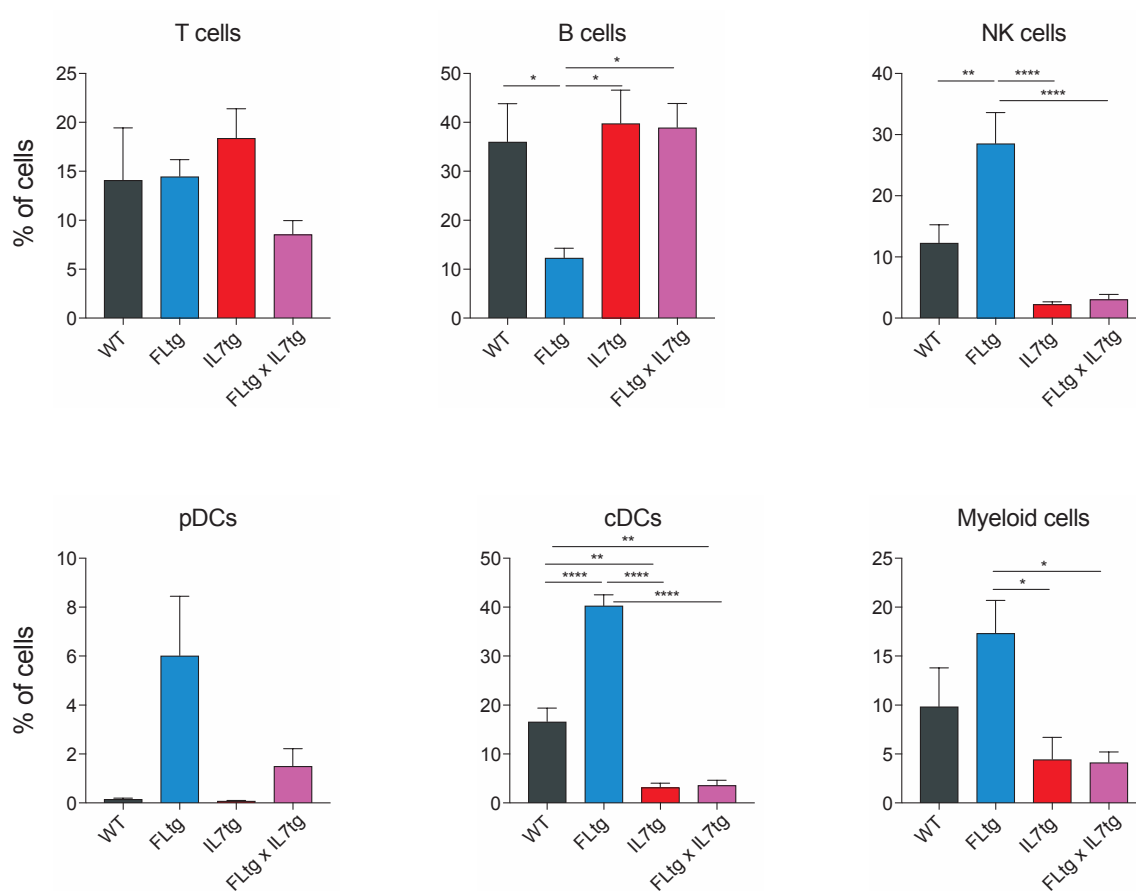


Supplementary Figure 3

**B1 cells in the peritoneal cavity of FLtgIL7tg mice.**

A) Representative FACS plots for the identification of B1a (CD19<sup>+</sup>CD11b<sup>+</sup>CD5<sup>+</sup>), B1b (CD19<sup>+</sup>CD11b<sup>+</sup>CD5<sup>-</sup>), B2 (CD19<sup>+</sup>CD11b<sup>-</sup>) and CD11b<sup>+</sup> (CD19<sup>-</sup>CD11b<sup>+</sup>) myeloid cells in the peritoneal cavity of WT, FLtg, IL7tg and FLtgxIL7tg mice. Gate numbers indicate frequencies of parent gate. B) Percentages of B1a (left panel), B2 (middle panel) and myeloid cells (right panel) in the peritoneal cavity of WT, FLtg, IL7tg and FLtgxIL7tg mice. \*: p<0.05, \*\*:p<0.01, \*\*\*:p<0.001, \*\*\*\*:p<0.0001. Error bars indicate standard deviation.

## Supplementary Material

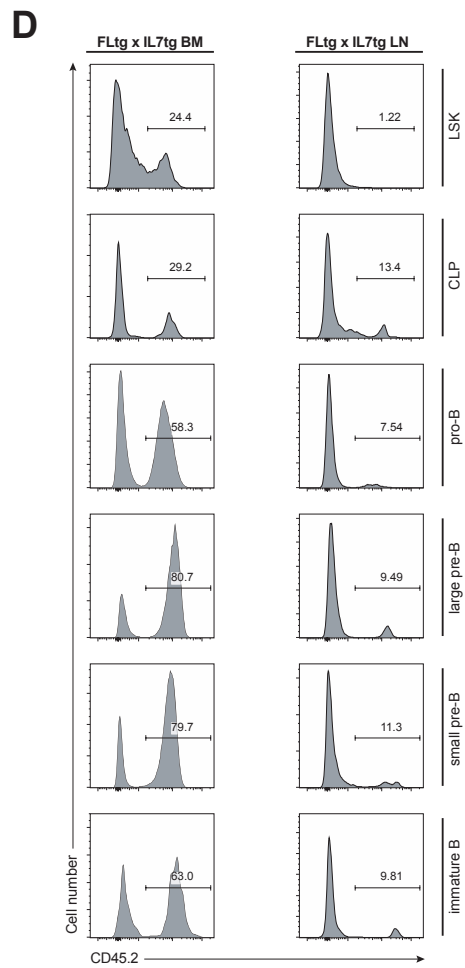
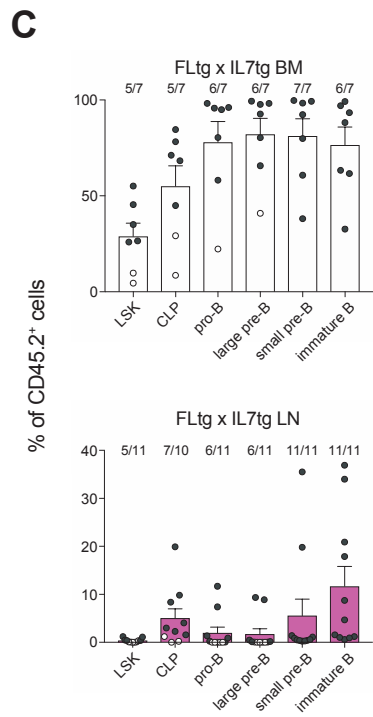
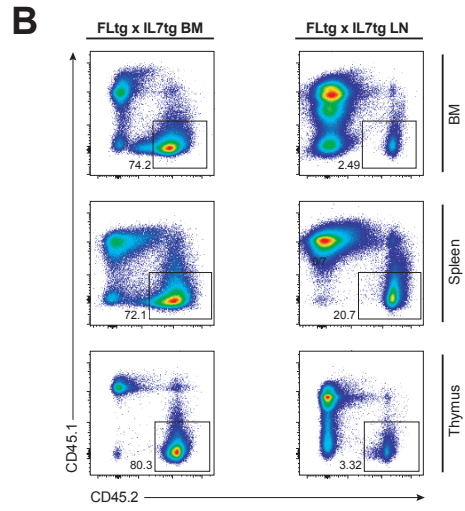
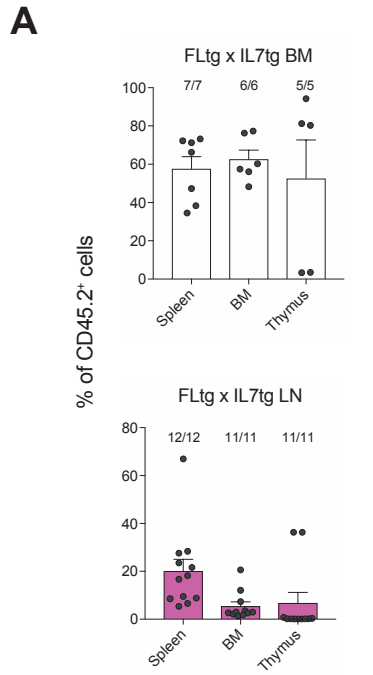


## Supplementary Figure 4

## Mature hematopoietic cell frequencies in peripheral blood of FLtgIL7tg mice.

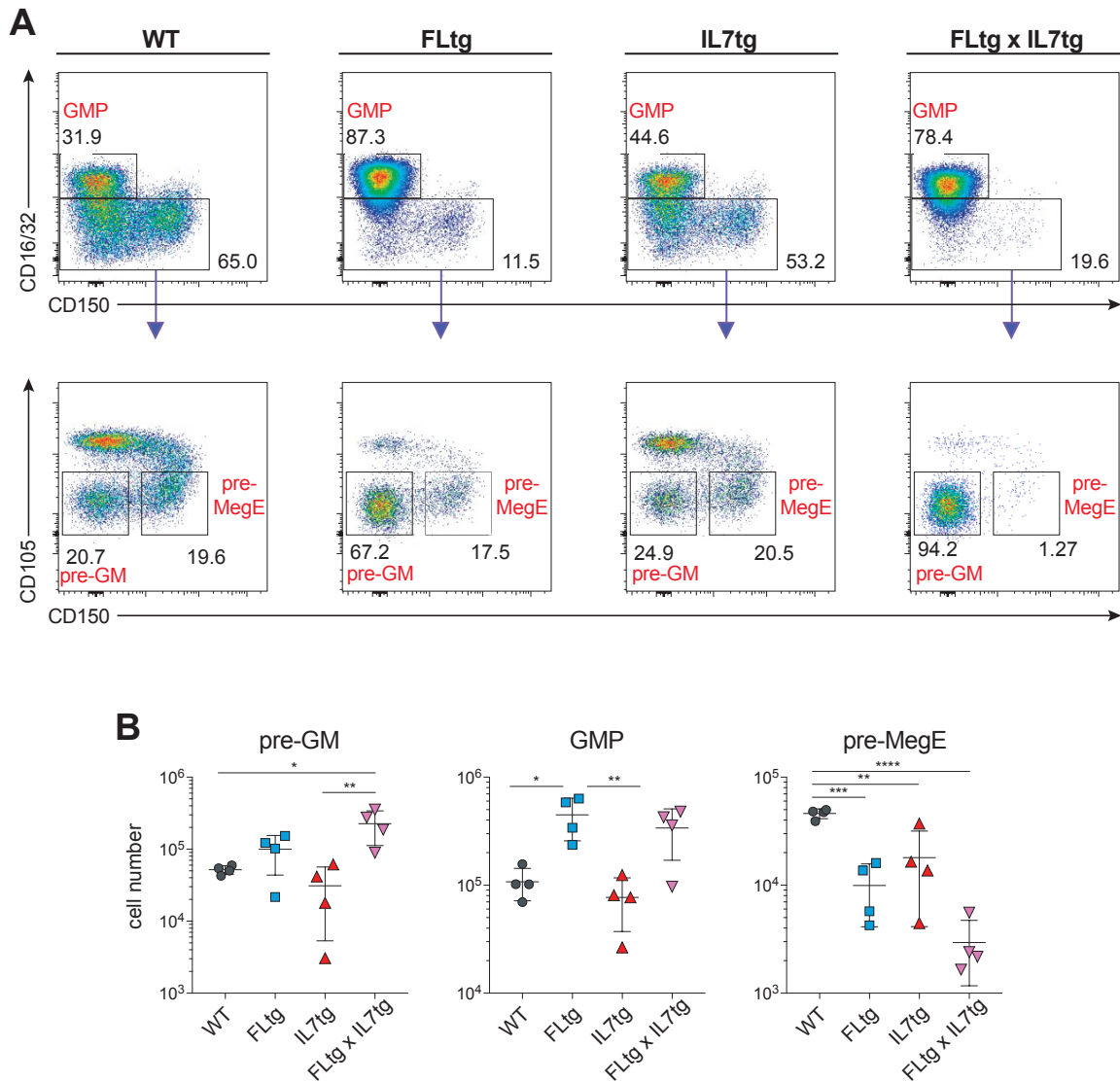
Percentages of T cells (CD3<sup>+</sup>), B cells (CD19<sup>+</sup>), NK cells (CD3-NK1.1<sup>+</sup>), plasmacytoid DC (pDC; B220<sup>+</sup>SiglecH<sup>+</sup>), conventional DC (cDC; CD3<sup>-</sup>NK1.1<sup>-</sup>B220<sup>-</sup>CD11b<sup>-</sup>CD11c<sup>+</sup>) and myeloid cells (CD3<sup>-</sup>NK1.1<sup>-</sup>B220<sup>-</sup>CD11c<sup>-</sup>CD11b<sup>+</sup>) in the peripheral blood of WT, FLtg, IL7tg and FLtgIL7tg mice (n=4 for all genotypes). \*: p<0.05, \*\*:p<0.01, \*\*\*\*:p<0.0001. Error bars indicate standard deviation.

Supplementary Material



**Supplementary Figure 5****Hematopoietic reconstitution potential of FLtgxIL7tg LN cells.**

A) Percentage of total CD45.2<sup>+</sup> donor cells in spleen, bone marrow and thymus of mice reconstituted with FLtgxIL7tg BM (upper graph) or FLtgxIL7tg LN (lower graph). Black circles represent mice where the total donor contribution was scored as positive (>50 cells in the CD45.2<sup>+</sup> gate). The fraction of positive-to-total mice analyzed for each organ is indicated above the corresponding bar. Results from four independently performed experiments are shown. Bars indicate mean ± standard error of the mean. B) Representative FACS plots indicating the total chimerism in the BM (upper plots), spleen (middle plots) and thymus (lower plots) of mice reconstituted with FLtgxIL7tg BM (left plots) and LN (right plots). C) Percentage of CD45.2<sup>+</sup> donor cells within the indicated progenitor populations (LSK: Lin<sup>-</sup>CD127<sup>-</sup>CD117<sup>+</sup>Sca1<sup>+</sup>; CLP: Lin<sup>-</sup>CD117<sup>int</sup>Sca1<sup>int</sup>CD127<sup>+</sup>; pro-B: CD19<sup>+</sup>IgM<sup>-</sup>CD117<sup>+</sup>; large pre-B: CD19<sup>+</sup>IgM<sup>-</sup>CD117<sup>-</sup>CD127<sup>+</sup>FSC<sup>large</sup>; small pre-B: CD19<sup>+</sup>IgM<sup>-</sup>CD117<sup>-</sup>CD127<sup>-</sup>FSC<sup>small</sup>; and immature B: CD19<sup>+</sup>IgM<sup>+</sup>CD93<sup>+</sup>) in the bone marrow of mice reconstituted with FLtgxIL7tg BM (up) or FLtgxIL7tg LN (down). Black circles represent mice where the corresponding cells were scored as positive for the presence of donor-derived cells (>50 cells in the CD45.2<sup>+</sup> gate) and white circles mice with no reconstitution (<50 cells in the CD45.2<sup>+</sup> gate). The ratio of positive-to-total mice analyzed for each progenitor population is indicated above the corresponding bar. Results from four independently performed experiments are shown. Bars indicate mean ± standard error of the mean. D) Representative FACS histograms showing the percentage of CD45.2<sup>+</sup> FLtgxIL7tg BM- (left) and LN-derived (right) donor cells within the indicated progenitor populations of reconstituted mice.

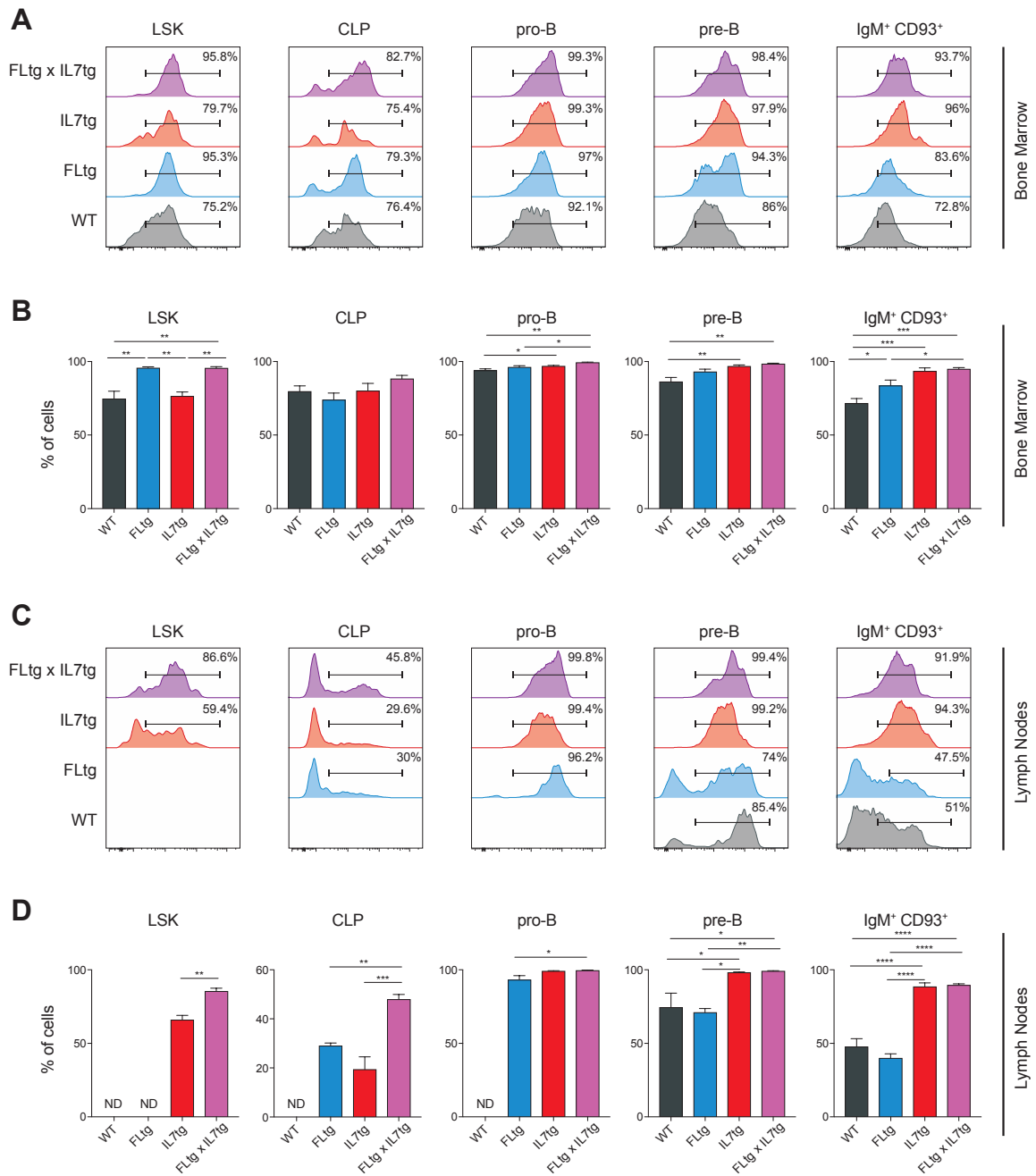


Supplementary Figure 6

## Myelo-erythroid progenitors in the BM of FLtgIL7tg mice.

A) Representative FACS plots for the identification of pre-GM, GMP and pre-MegE progenitors in the BM of WT, FLtg, IL7tg and FLtgIL7tg mice. Top FACS plots show cells that have been pre-gated as: live, CD117<sup>+</sup>Sca1<sup>-</sup>CD127<sup>-</sup>CD41<sup>-</sup> cells. B) Numbers of pre-GM (left), GMP (middle) and pre-MegE (right) progenitors in the bone marrow of WT, FLtg, IL7tg and FLtgIL7tg mice. Pre-GM: pre-granulocyte-macrophage progenitor (Lin<sup>-</sup>kit<sup>+</sup>Sca1<sup>-</sup>CD127<sup>-</sup>CD41<sup>-</sup>FcγR2/3<sup>-</sup>CD105<sup>+</sup>CD150<sup>-</sup>); GMP: granulocyte-macrophage progenitor (Lin<sup>-</sup>kit<sup>+</sup>Sca1<sup>-</sup>CD127<sup>-</sup>CD41<sup>-</sup>FcγR2/3<sup>+</sup>); pre-MegE: pre-megakaryocyte-erythroid progenitor (Lin<sup>-</sup>kit<sup>+</sup>Sca1<sup>-</sup>CD127<sup>-</sup>CD41<sup>-</sup>FcγR2/3<sup>-</sup>CD105<sup>+</sup>CD150<sup>+</sup>). \*: p<0.05, \*\*:p<0.01, \*\*\*:p<0.001, \*\*\*\*:p<0.0001. Bars indicate mean ± standard deviation.

## Supplementary Material



Supplementary Figure 7

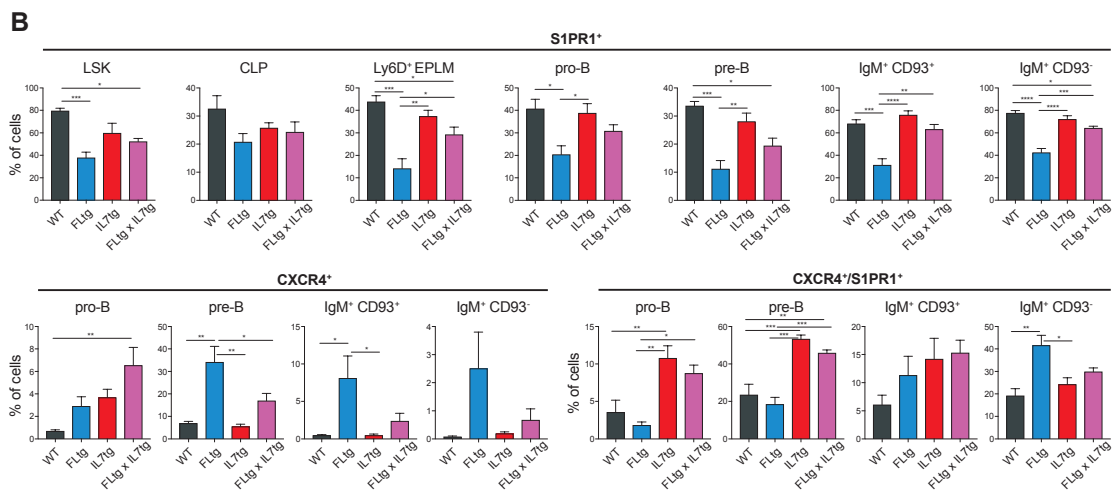
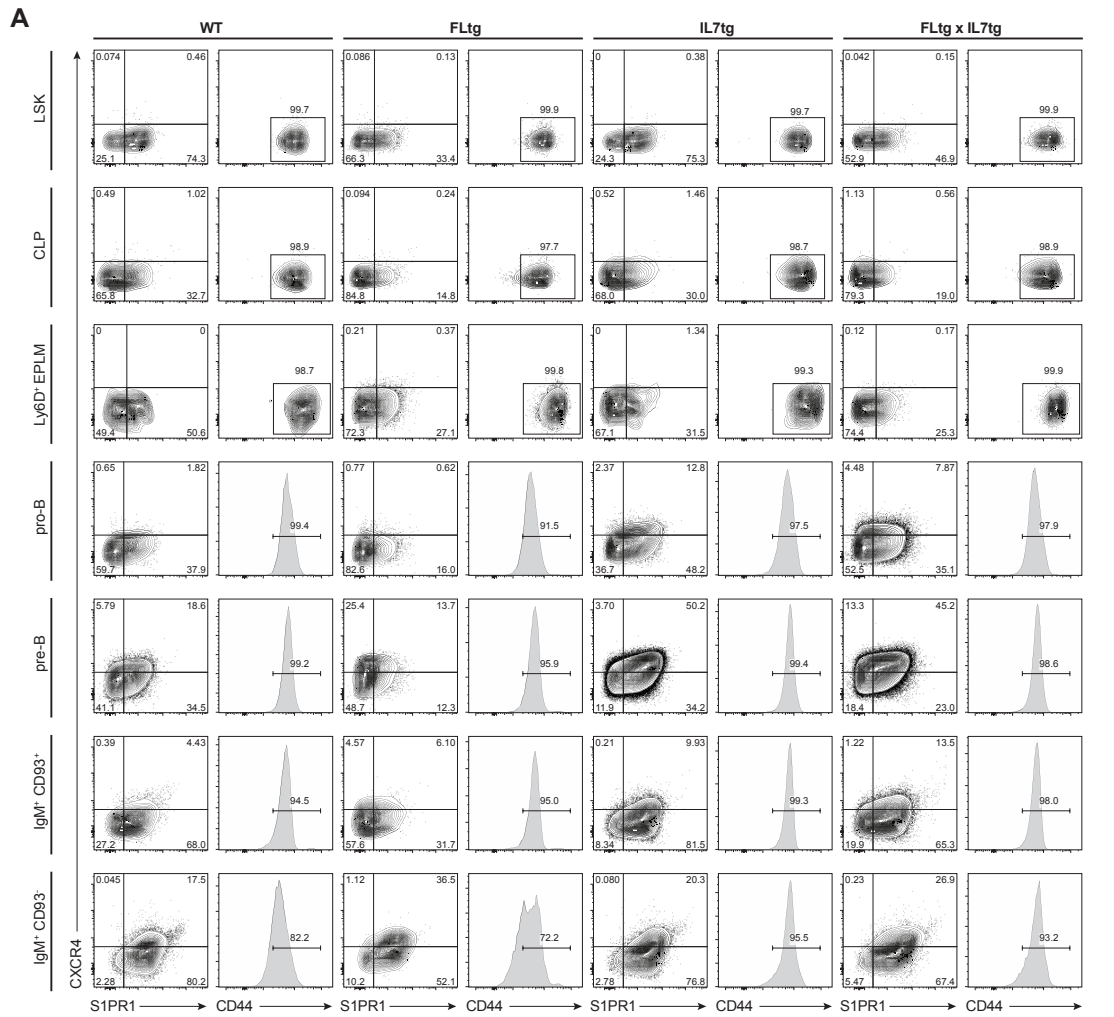
## Effect of FL and/or IL-7 over-expression on the cell-cycle status of BM and LN progenitors.

A) Representative FACS histograms showing the percentage of Ki67<sup>+</sup> cells within the indicated BM progenitor populations ((LSK: Lin-CD127-CD117<sup>+</sup>Sca1<sup>+</sup>; CLP: Lin-CD117<sup>int</sup>Sca1<sup>int</sup>CD127<sup>+</sup>; pro-B:

## Supplementary Material

CD19<sup>+</sup>IgM<sup>-</sup>CD117<sup>+</sup>; pre-B: CD19<sup>+</sup>IgM<sup>-</sup>CD117<sup>-</sup> and IgM<sup>+</sup>CD93<sup>+</sup>) of WT, FLtg, IL7tg and FLtgxIL7tg mice. B) Frequencies of Ki67<sup>+</sup> cells within the indicated BM progenitor populations of WT, FLtg, IL7tg and FLtgxIL7tg mice (n=4 for all genotypes). \*: p<0.05, \*\*:p<0.01, \*\*\*:p<0.001. Error bars indicate standard deviation. C) Representative FACS histograms showing the percentage of Ki67<sup>+</sup> cells within the indicated LN progenitor populations of WT, FLtg, IL7tg and FLtgxIL7tg mice. D) Frequencies of Ki67<sup>+</sup> cells within the indicated LN progenitor populations of WT, FLtg, IL7tg and FLtgxIL7tg mice (n=4 for all genotypes). \*: p<0.05, \*\*:p<0.01, \*\*\*:p<0.001, \*\*\*\*:p<0.0001. Error bars indicate standard deviation.

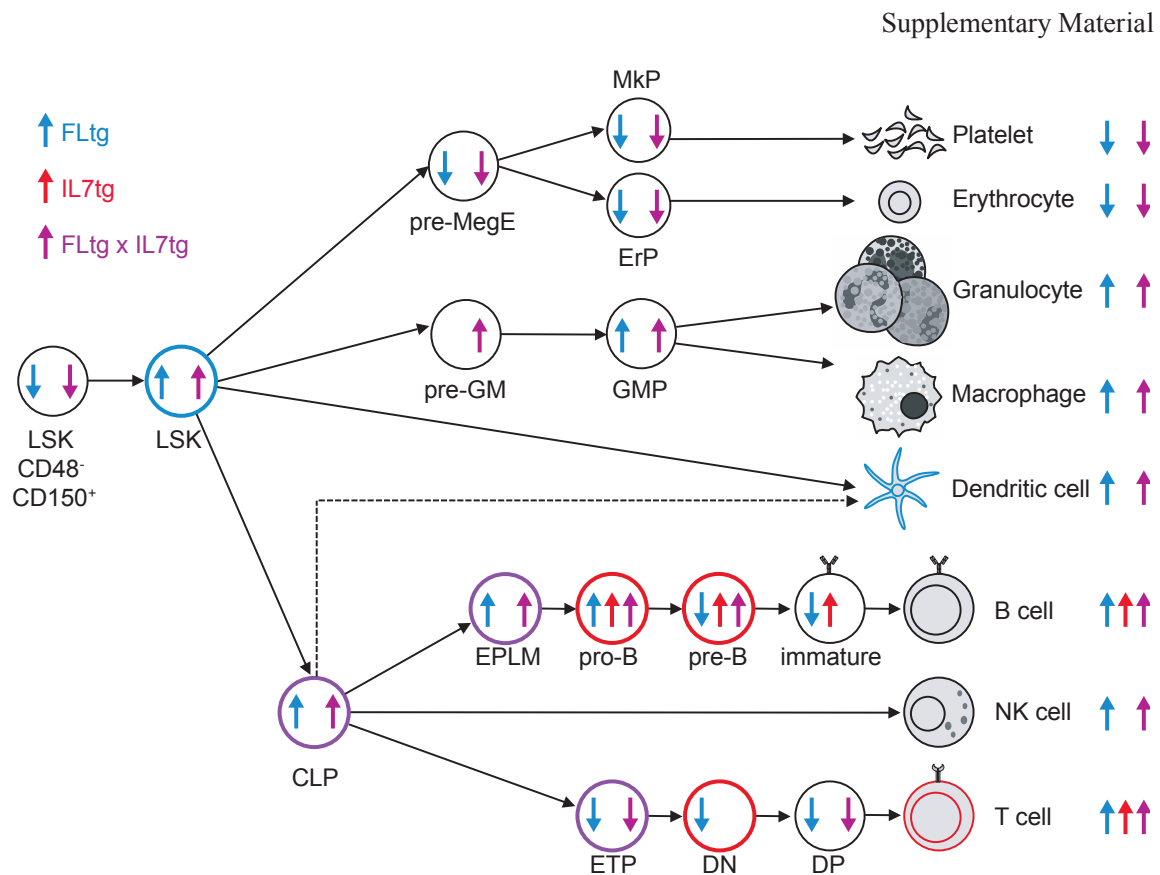
## Supplementary Material



## Supplementary Material

**Supplementary Figure 8****Expression of migratory-related proteins S1PR1, CD44 and CXCR4 on BM hematopoietic progenitors of FLtgxIL7tg mice.**

A) Representative FACS plots and histograms showing the percentages of S1PR1<sup>+</sup>, CXCR4<sup>+</sup>, S1PR1<sup>+</sup>CXCR4<sup>+</sup> and CD44<sup>+</sup> cells within the indicated BM progenitor populations (LSK: Lin<sup>-</sup>CD127<sup>-</sup>CD117<sup>+</sup>Sca1<sup>+</sup>; CLP: Lin<sup>-</sup>CD117<sup>int</sup>Sca1<sup>int</sup>CD127<sup>+</sup>; Ly6D<sup>+</sup> EPLM: NK1.1<sup>-</sup>CD11c<sup>-</sup>SiglecH<sup>-</sup>CD19<sup>-</sup>B220<sup>+</sup>CD117<sup>+</sup>Ly6D<sup>+</sup>; pro-B: CD19<sup>+</sup>IgM<sup>-</sup>CD117<sup>+</sup>; pre-B: CD19<sup>+</sup>IgM<sup>-</sup>CD117<sup>-</sup>; and ImmB: CD19<sup>+</sup>IgM<sup>+</sup>CD93<sup>+</sup>) of WT, FLtg, IL7tg and FLtgxIL7tg mice. B) Percentages of S1PR1<sup>+</sup>, CXCR4<sup>+</sup>, S1PR1<sup>+</sup>CXCR4<sup>+</sup> and CD44<sup>+</sup> cells within the indicated BM progenitor populations of WT, FLtg, IL7tg and FLtgxIL7tg mice (n=4 for all genotypes). \*: p<0.05, \*\*:p<0.01, \*\*\*:p<0.001, \*\*\*\*:p<0.0001. Error bars indicate standard deviation.



Supplementary Figure 9

**Summary of the effect of increased FL and/or IL-7 levels in the numbers of hematopoietic progenitor and mature cells.**

Schematic representation of BM hematopoietic progenitors (open circles) and peripheral mature blood cells (grey cells). Arrows indicate developmental relationships. Blue circles indicate progenitors that express CD135 (Flt3) on their surface, red circles progenitors that express CD127 (IL7R $\alpha$ ) and purple circles progenitors that express both. Colored vertical arrows indicate an increase or decrease in the numbers of the corresponding cells in FLtg (blue arrows), IL7tg (red arrows) and FLtgxIL7tg mice (purple arrows). For progenitor cells the picture summarizes data from the BM and for mature cells from peripheral lymphoid organs. LSK: Lineage-Kit<sup>+</sup>Sca1<sup>+</sup>; GMP: Granulocyte-Macrophage Progenitor; MkP: Megakaryocyte Progenitor; ErP: Erythrocyte Progenitor; CLP: Common Lymphoid Progenitor; EPLM: Early Progenitor with Lymphoid and Myeloid potential; ETP: Early Thymic Progenitors, DN: CD4/CD8 Double-Negative, DP: CD4/CD8 Double-Positive.

## **4.2. Part 2: Role of the transcription factor Duxbl in T-cell development**

### **4.2.1. The transcription factor Duxbl mediates elimination of pre-T cells that fail $\beta$ -selection**

Fabian Klein\*, Mladen Mitrovic, Julien Roux, Corinne Engdahl, Lilly von Muenchow, Lucia Alberti-Servera, Hans Jörg Fehling, Pawel Pelczar, Antonius Rolink, Panagiotis Tsapogas

\*Corresponding author

In press – Journal of Experimental Medicine

---

# The transcription factor Duxbl mediates elimination of pre-T cells that fail $\beta$ -selection

Fabian Klein<sup>1,\*</sup>, Mladen Mitrovic<sup>2</sup>, Julien Roux<sup>3,4</sup>, Corinne Engdahl<sup>1</sup>, Lilly von Muenchow<sup>1</sup>, Lucia Alberti-Servera<sup>1</sup>, Hans Jörg Fehling<sup>5</sup>, Pawel Pelczar<sup>6</sup>, Antonius Rolink<sup>1,†,§</sup> and Panagiotis Tsapogas<sup>1,\*§</sup>

<sup>1</sup>Developmental and Molecular Immunology, Department of Biomedicine, University of Basel, Basel, Switzerland

<sup>2</sup>Immune Regulation, Department of Biomedicine, University of Basel, Basel, Switzerland

<sup>3</sup>Bioinformatics Core Facility, Department of Biomedicine, University of Basel, Basel, Switzerland

<sup>4</sup>Swiss Institute of Bioinformatics, Lausanne, Switzerland

<sup>5</sup>Institute of Immunology, University Hospital, Ulm, Germany

<sup>6</sup>Center for Transgenic Models, University of Basel, Basel, Switzerland

\*Correspondence: Fabian Klein                      f.klein@unibas.ch  
Panagiotis Tsapogas                      panagiotis.tsapogas@unibas.ch

§Equal contribution

†Deceased

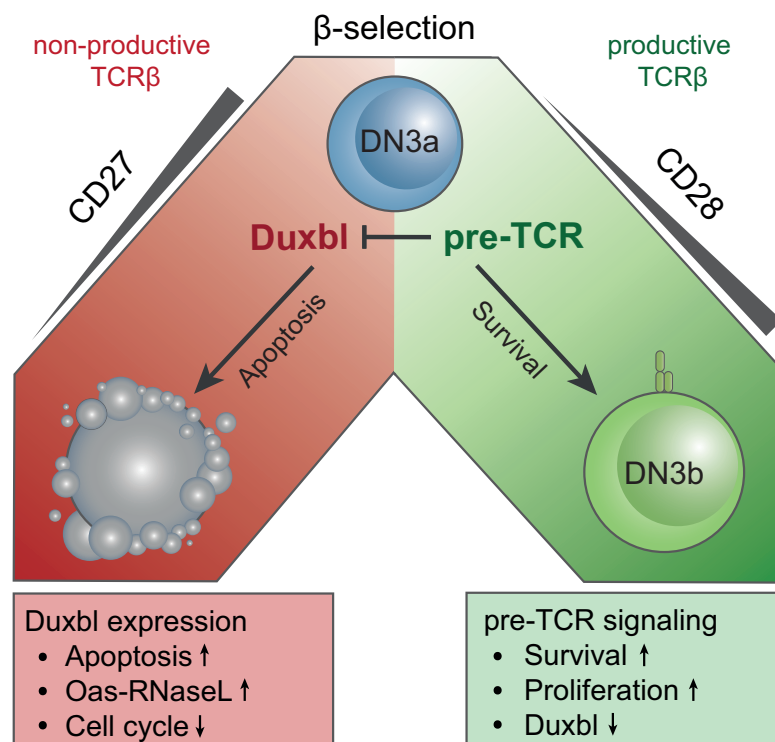
Running title: Duxbl eliminates pre-T cells during  $\beta$ -selection

Non-standard abbreviations: CPM = counts per million, DII = Delta-like, DN = double negative, DP = double positive, FDR = false discovery rate, PCA = principal component analysis, pT $\alpha$  = pre-T cell receptor  $\alpha$

Summary: During  $\beta$ -selection T cells without productive TCR $\beta$  rearrangements are eliminated. Klein et al show that the transcription factor Duxbl regulates this process by inducing apoptosis through activation of the Oas/RNaseL pathway. Successful TCR $\beta$  rearrangement rescues cells by pre-TCR-mediated Duxbl suppression.

## Abstract

T-cell development is critically dependent upon successful rearrangement of antigen-receptor chains. At the  $\beta$ -selection checkpoint only cells with a functional rearrangement continue in development. However, how non-selected T cells proceed in their dead-end fate is not clear. We identified low CD27 expression to mark pre-T cells that have failed to rearrange their  $\beta$ -chain. Expression profiling and single-cell transcriptome clustering identified a developmental trajectory through  $\beta$ -selection and revealed specific expression of the transcription factor Duxbl at a stage of high recombination activity prior to  $\beta$ -selection. Conditional transgenic expression of Duxbl resulted in a developmental block at the DN3-to-DN4 transition due to reduced proliferation and enhanced apoptosis, whereas RNA silencing led to a decrease in apoptosis. Transcriptome analysis linked Duxbl to elevated expression of the apoptosis-inducing Oas/RNaseL-pathway. RNaseL deficiency or sustained Bcl2 expression led to a partial rescue of cells in Duxbl transgenic mice. These findings identify Duxbl as a regulator of  $\beta$ -selection by inducing apoptosis in cells with a non-functional rearrangement.



## 1. Introduction

T-cell development occurs in the thymus and is initiated by a bone marrow derived multipotent progenitor, named thymus settling progenitor (Zlotoff and Bhandoola, 2011). The identity of the exact cell type that migrates to the thymus is still under debate, since several possible candidates have been described (Kondo et al., 1997; Krueger and von Boehmer, 2007; Rodewald et al., 1994; Saran et al., 2010; Serwold et al., 2009). There is consensus that this progenitor retains the ability to give rise to several lineages including B cells, natural killer cells, dendritic cells as well as other myeloid lineages (Balciunaite et al., 2005b; Bell and Bhandoola, 2008; Ceredig et al., 2007; Luis et al., 2016; Wada et al., 2008). Final commitment to the T-cell pathway is achieved upon Notch engagement (Balciunaite et al., 2005a; Radtke et al., 1999; Sambandam et al., 2005).

Thymic T-cell development is a stepwise process that involves several successive stages, which are phenotypically distinguished by the expression of various cell surface markers. The most immature populations are characterized by the absence of CD4 and CD8 and are therefore named double negative cells (DN) (Ceredig and Rolink, 2002). The DN population can be further subdivided based on the expression pattern of CD25, CD44, and CD117 (Godfrey et al., 1993; Godfrey et al., 1992; Massa et al., 2006). High level expression of CD44, CD117 and the absence of CD25 mark DN1 cells, which retain the potential to give rise to different lineages. At the next stage, DN2, progenitors are additionally characterized by expression of CD25. Upon progression to the DN3 stage, which displays lower CD44 and CD117 expression, final commitment to the T-cell lineage takes place (Yui and Rothenberg, 2014). Downregulation of CD25 marks the onset of the DN4 stage that is negative for all three surface markers (Godfrey et al., 1994). After the DN4 stage CD4 as well as CD8 become upregulated and therefore cells are named double positive (DP). Finally, CD4 or CD8 single positive cells expressing a functional T-cell receptor (TCR) will undergo positive and negative selection, thereby completing their maturation in the thymus (Germain, 2002).

T-cell development can also be subdivided into developmentally distinct stages by the use of the rearrangement status of the  $\beta$ - and the  $\alpha$ -chain of the TCR.  $\beta$ -chain rearrangement starts at the DN2 and is completed at the DN3 stage (Capone et al., 1998) whereas rearrangement of the  $\alpha$ -chain takes place at the DP stage (Livak et al., 1999). An essential checkpoint for this process, called  $\beta$ -selection, selects cells with a productive rearrangement of their  $\beta$ -chain to continue in their development, whereas cells with a non-functional rearrangement will undergo apoptosis (Dudley et al., 1994). Pairing of productively rearranged  $\beta$ -chains with the pre-T cell receptor  $\alpha$  ( $pT\alpha$ ) chain and the CD3 molecules results in the expression of the pre-T cell receptor (pre-TCR) (Saint-Ruf et al., 1994), which induces survival

and a massive proliferative expansion of these cells (Kreslavsky et al., 2012) by autonomous signaling (Irving et al., 1998; Jacobs et al., 1996; Saint-Ruf et al., 1994). The requirement of pre-TCR signaling during this checkpoint is manifested in the arrest of T-cell development in mice with defects in the pT $\alpha$  chain (Fehling et al., 1995), the CD3 signaling components (Malissen et al., 1995) or the genes responsible for the recombination of the  $\beta$ -chain (Shinkai et al., 1992). Additionally, Notch1 signaling and engagement of the chemokine receptor Cxcr4 by its ligand Cxcl12 were shown to be essential for a successful passage through this selection point, since they are crucial for the survival as well as for the proliferation of the cells (Ciofani et al., 2004; Ciofani and Zuniga-Pflucker, 2005; Maillard et al., 2006; Trampont et al., 2010; Tussiwand et al., 2011). The upregulation of several co-stimulatory surface molecules, such as CD27, CD28, and CD71 (Brekelmans et al., 1994; Gravestien et al., 1996; Williams et al., 2005) can also be used to subdivide the DN3 population into cells expressing an intracellular  $\beta$ -chain (DN3b) and cells that do not yet do so (DN3a) (Taghon et al., 2006). The fact that VDJ-recombination can result in a non-productive rearrangement, together with the inability of some  $\beta$ -chains to build a functional pre-TCR, lead to the elimination of the vast majority of cells during  $\beta$ -selection. The exact mechanism and regulation of this process remain still unresolved.

In this study we identify CD27 downregulation at the DN3 stage to be a marker for cells that have failed rearrangement of the  $\beta$ -chain and will therefore undergo apoptosis. Gene expression analysis revealed high expression of the transcription factor Duxbl within this population. We show that conditional transgenic over-expression of Duxbl resulted in a block in T-cell development at the DN3-to-DN4 transition due to reduced proliferation and increased apoptosis, whereas *in vitro* Duxbl knock-down decreased apoptosis, instead. Our results identify Duxbl as an important regulator of the elimination of cells with a non-functional rearrangement at the  $\beta$ -selection checkpoint.

## 2. Materials and Methods

### 2.1. Mice

C57BL/6 wild-type controls, pTα<sup>-/-</sup> (Fehling et al., 1995), Nur77<sup>GFP</sup> (Moran et al., 2011), pTα<sup>Cre</sup> (Luche et al., 2013), Bcl2tg (Domen et al., 1998), Rag2<sup>-/-</sup> (Shinkai et al., 1992), Duxbl<sup>ind</sup>, and RNaseL<sup>-/-</sup> mice were bred and maintained in our animal facility unit under specific pathogen-free conditions. All mice used were 5-7 weeks old and were of the C57BL/6 strain or were bred to it for more than 10 generations (Bcl2tg). As controls littermates were used in every experiment. All animal experiments were carried out within institutional guidelines (authorization numbers 1886 and 1888 from cantonal veterinarian office, Canton Basel-Stadt).

Duxbl<sup>ind</sup> and RNaseL<sup>-/-</sup> mice were generated at the Center for Transgenic Models in Basel. Duxbl<sup>ind</sup> mice were produced by pronuclear DNA microinjection of C57BL/6 zygotes essentially as described in (Palmiter et al., 1982). RNaseL<sup>-/-</sup> mice were generated using Cas9/CRISPR technology. All Cas9 reagents were purchased from IDT. Briefly, RNPs consisting of Cas9 protein (40 ng/ul), tracrRNA (20 ng/ul) and crRNAs (10 ng/ul each) targeting exon 1 of the *RnaseL* gene were microinjected into C57BL/6 zygotes essentially as described in (Jacobi et al., 2017). Embryos surviving the DNA and Cas9 RNP microinjections were transferred into pseudopregnant females generated by mating with genetically vasectomized males (Haueter et al., 2010) and the offspring were allowed to develop to term.

Figure S4A illustrates the construct used to generate the Duxbl<sup>ind</sup> mice by random integration. Figure S4E describes the generation of RNaseL<sup>-/-</sup> mice. The following 20-mers sequences were used to produce the crRNAs that guided Cas9 for the induction of double strand breaks in exon 1 of the *RnaseL* gene (5' to 3'): AATGCCTGTGAAGACACCTG and GACAAAAGGCGATTGAAGCA.

### 2.2. Flow cytometry and cell sorting

For analysis, cells were flushed from femurs of the two hind legs of mice or single-cell suspensions of spleen, thymus, and lymph node (inguinal and axillary) cells were made. Stainings were performed in PBS containing 0.5% BSA and 5mM EDTA. For intra-cellular beta-chain staining, cells were fixed and permeabilized after cell-surface staining using a Fix/Perm buffer set (eBioscience), and subsequently stained with Bv421-conjugated anti-TCRβ (H57). The following antibodies were used for flow cytometry (from BD Biosciences, eBioscience, BioLegend, RnD Systems, or produced in house): anti-CD3 (145-2C11), anti-B220 (RA3-6B2), anti-CD4 (GK1.5), anti-CD8 (53-6.7), anti-CD25 (PC61), anti-CD44 (IM7), anti-CD117 (2B8), anti-CD27 (LG.3A10), anti-CD28 (37.51), anti-TCRβ (H57-597), anti-TCRγ (GL3), anti-CD69 (H1.2F3), anti-MHCI (Y3), anti-CD62L (MEL-14), anti-S1PR1 (713412). For flow cytometry a

BD LSRFortessa (BD Biosciences) was used and data were analyzed using FlowJo Software (Treestar). MACS enrichment was performed using an autoMACS separator (Miltenyi) after cells were stained with anti-CD4/CD8-bio and anti-biotin microbeads (Miltenyi). For cell sorting, a FACSAria IIu (BD Biosciences) was used (>98% purity).

### 2.3. Cell cycle analysis

Cells were sorted with an Aria II FACS sorter (BD). Sorted cells were resuspended in 1mL 70% ethanol and stored at 4°C over-night. Cells were then harvested at 2000rpm for 5min at 4°C and subsequently resuspended in 250µL RNaseA (0.5mg/mL). After 15min of incubation at 37°C, 250µL Pepsin (0.5mg/mL) was added and incubated for 15min at 37°C. Finally, nuclei were stained by adding 500µL ethidium bromide solution and incubation for 10min at room temperature before analysis by flow cytometry.

### 2.4. Retroviral Production

For Duxbl knock-down MSCV-LMP empty vector plus four different MSCV-LMP vectors containing Duxbl directed shRNAs were generated using the following oligo templates: sh2-1, TGCTGTTGACAGTGAGCGAACTCTTCGTGTGTGGTTTGAATAGTGAAGCCACAGATGTA TTCAAACCACACACGAAGAGTGTGCCTACTGCCTCGGA; sh2-2, TGCTGTTGACAGTGAGCGCAGAATCCCAATCCTGATCTAGTAGTGAAGCCACAGATGTA CTAGATCAGGATTGGGATTCTTTGCCTACTGCCTCGGA; sh3-1, TGCTGTTGACAGTGAGCGCTTGCATGCTGTTCTGAAGAAATAGTGAAGCCACAGATGTA TTTCTTCAGAACAGCATGCAAATGCCTACTGCCTCGGA; sh3-2, TGCTGTTGACAGTGAGCGAAGTTTGCATGCTGTTCTGAAGTAGTGAAGCCACAGATGTA CTTCAGAACAGCATGCAAATCTGCCTACTGCCTCGGA.

A total of  $5 \times 10^6$  Plat-E cells were plated one day prior to transfection in 10cm dishes (Falcon) with 10mL DMEM (Sigma) supplemented with 10% fetal bovine serum, 100 U/mL penicillin (BioConcept), 100 mg/mL streptomycin (BioConcept), and 1mM sodium pyruvate (Sigma). The next day 20µg plasmid and 80µg polyethylenimine were mixed in 1ml DMEM without supplements, incubated for 15 minutes at room temperature, and subsequently added dropwise to the Plat-E cells. 24 hours after transfection supernatant was replaced with fresh medium. Viral supernatants were collected 48 hours and 72 hours post transfection and either used directly for transductions or stored at -80°C.

### 2.5. Cell culture

For culturing of sorted DN3 cells 96-well Maxisorp Nunc-Immuno plates (Thermo Fisher) were used. Wells were precoated overnight or longer with 10 µg/mL anti-human IgG-Fc (clone Huf-5.4, generated in house) in PBS (50µL per well) at 4°C. Thereafter, wells were

washed twice with IMDM supplemented with 5% fetal bovine serum,  $5 \times 10^{-5}$  M  $\beta$ -mercaptoethanol, 1 mM glutamine, 0.03% w/v Primatone, 100 U/mL penicillin, and 100 mg/mL streptomycin and then coated with Delta-like (DII) 4-Fc at  $3 \mu\text{g/mL}$  in IMDM ( $50 \mu\text{L}$  per well) overnight at  $4^\circ\text{C}$ . Before addition of the cells wells were washed again twice with IMDM. Sorted cells were adjusted to a concentration of  $2 \times 10^5$  cells/mL with IMDM supplemented additionally with 10 nM Cxcl12 and cultured for 3 or 5 days ( $200 \mu\text{L}$  per well).

For the establishment of in vitro T-cell differentiation fetal liver cells were cultured on OP9-DII1 stromal cells. In short,  $3 \times 10^4$  OP9-DII1 cells were seeded in 24-wells the day before addition of fetal liver cells with  $500 \mu\text{L}$  IMDM supplemented with 10% fetal bovine serum,  $5 \times 10^{-5}$  M  $\beta$ -mercaptoethanol, 1 mM glutamine, 0.03% w/v Primatone, 100 U/mL penicillin, and 100 mg/mL streptomycin. The next day cells were irradiated with 2000 rad. Fetal liver cells were taken from E14.5 C57BL/6 embryos and mononuclear cells were separated by centrifugation on a Ficoll-Paque PLUS (GE Healthcare) gradient. A total of  $5 \times 10^4$  cells per 24-well were added to the irradiated OP9-DII1 and cultured in 1 mL of the previously described medium plus 10% IL-7 supernatant. After 5 days cells were harvested and  $10^6$  cells were transduced with 1.5 mL of viral supernatants of either MSCV-LMP empty vector or the corresponding *Duxbl* shRNAs using 3 hours of spinoculation with  $10 \mu\text{g/mL}$  polybrene. Subsequently,  $5 \times 10^4$  transduced cells were put back into culture onto freshly prepared irradiated OP9-DII1 in the presence of 10% IL-7 for another 5 days. Finally, a total of  $10^5$  cells were passed again onto freshly prepared OP9-DII1 and cultured for 4 more days in the absence of IL-7. Then cells were harvested and stained with the corresponding surface markers as described in 2.2., as well as with AnnexinV (BD Biosciences) and 7AAD (Biolegend) in AnnexinV Binding Buffer (BD Biosciences) following the manufacturer's protocol.

## 2.6. Quantitative PCR

Total RNA was extracted using RNAqueous – Micro Kit (Invitrogen) followed by cDNA synthesis using GoScript Reverse Transcriptase (Promega) according to the manufacturer's protocol. Quantitative PCR was performed using SYBR green PCR Master Mix (Applied Biosystems) and samples were run on an Applied Biosystems StepOnePlus qPCR machine. The following primers were used for PCR amplification (5' to 3'):  *$\beta$ -actin*, TGGAACTCCTGTGGCATCCATGAAAC and TAAAACGCAGCTCAGTAACAG; *Duxbl*, AAGCAGAGTTTGCATGCTGTT and TTGTGAAGTGCCTTCTGCTC; *Rnasel*, TTGATCAGAGCATCCGATGGATGGGAGAG and TTCTCCAGGAGAAAACAGGCAATGAATGAGGT; *Oas1a*, ATTACCTCCTTCCCGACACC and AAGGAACACCACCAGGTCAG; *Oas1b*, TCTGCTTTATGGGGCTTCGG and TCGACTCCATACTCCAGG; *Oas2*, GGCCTGGTACAGCCTTGGAA and AAAGCCTTGTCCTGCCACA; *Oas3*, AAGCCGACACCCAACGTGTA and

---

TTTCGGGGCTCAGTGAAGCA; *Oas1*, GCATCGGCCGACGAAGCTGA and CCGTGGCGAGGCCTTCATCC.

### 2.7. Bulk and single-cell RNA-sequencing

For bulk RNA-seq, total RNA was isolated from 100,000-200,000 cells with an Ambion RNAqueous Micro Kit (Invitrogen). RNA quality was assessed with a Fragment Analyzer (Advanced Analytical). Fifty nanograms of RNA were used for library preparation (Illumina Truseq stranded kit) and sequencing was performed on an Illumina NexSeq 500 machine at the Genomics Facility Basel of the ETH Zurich. Single-end 51-mers reads were obtained and their quality was assessed with the FastQC tool (version 0.11.3). Reads were mapped to the mouse mm10 genome assembly with STAR (version 2.5.2a) (Dobin et al., 2013) with default parameters, except reporting only one hit in the final alignment for multimappers (outSAMmultNmax=1) and filtering reads without evidence in the spliced junction table (outFilterType="BySJout"). All subsequent gene expression data analysis was performed using the R software (version 3.4).

The qCount function of the Bioconductor package QuasR (version 1.18) (Gaidatzis et al., 2015) was used to count the number of reads (5' ends) overlapping with the exons of the Ensembl 84 annotation, assuming an exon union model. Read and alignment quality was evaluated using the qQCReport function of QuasR.

Differentially expressed genes were identified with the Generalized Linear Model (GLM) framework in the edgeR package (version 3.20.9) (Robinson et al., 2010). For the DN3a CD27<sup>high</sup>/DN3a CD27<sup>low</sup>/DN3b dataset, a "replicate" covariate was incorporated into the model to control for systematic differences across flow cytometry sorting runs. Genes with a false discovery rate lower than 5% were considered differentially expressed. Gene set enrichment analysis was performed with the function camera (Wu and Smyth, 2012) from the edgeR package (using the default parameter value of 0.01 for the correlations of genes within gene sets) using gene sets from the hallmark collection (Liberzon et al., 2015) of the Molecular Signature Database (MSigDB v6.0) (Subramanian et al., 2005). We considered only sets containing more than 10 genes and gene sets with a false discovery rate lower than 5% were considered significant. For the heatmap combining the two RNA-seq datasets, data were corrected for batch effects for visualization purposes, using the function removeBatchEffect from the Bioconductor limma package (version 3.34.9).

For single-cell RNA-seq, DN2, DN3, and DN4 cells were sorted from six mice and counted. An estimate of 5,000 cells from the DN2 and DN4 populations were loaded on one well each and 10,000 cells from the DN3 population on two wells of a 10× Genomics Chromium Single Cell Controller. Single-cell capture and cDNA and library preparation were performed with a Single Cell 3' v2 Reagent Kit (10× Genomics) according to manufacturer's instructions.

Sequencing was performed on an Illumina NexSeq 500 machine at the Genomics Facility Basel of the ETH Zurich. Paired-end reads were obtained and their quality was assessed with the FastQC tool (version 0.11.3). The length of the first read was 26-mers, composed of individual cells barcodes (16nt) and molecular barcodes (unique molecular identifiers; 10nt). The length of the second read, composed of the transcript sequence, was 58-mers. The samples in the different wells were identified using sample barcodes of 8nt. Sequencing files were processed with the Cell Ranger software (version 2.1.0, provided by 10× Genomics and available at <https://support.10xgenomics.com/single-cell-gene-expression/software/downloads/latest>) to perform sample and cell demultiplexing, read alignment to the mouse mm10 genome assembly with STAR, and to generate read count table (using the reference transcriptome “refdata-cellranger-mm10-1.2.0” based on Ensembl release 84, provided by 10× Genomics and available at <https://support.10xgenomics.com/single-cell-gene-expression/software/downloads/latest>). Default settings and parameters were used, except for the version of STAR updated to 2.5.3a, and the STAR parameters *outSAMmultNmax* set to 1 and *alignIntronMax* set to 10000. Samples were merged with the “cellranger aggregate” procedure without downsampling.

Further analysis was performed using the *scran* (1.6.9) (Lun et al., 2016) and *scater* (1.6.3) (McCarthy et al., 2017) Bioconductor packages on the UMI counts matrix, following mostly the steps illustrated in the *simpleSingleCell* Bioconductor (release 3.6) workflow.

Cells with log library sizes (or log total number of features detected) more than two median absolute deviations (MADs) below the median log library size (or log total number of features detected) were filtered out. Cells with more than 10% of UMI counts attributed to the mitochondrial genes were removed. Cells with less than 20% of UMI counts attributed to the ribosomal proteins genes were removed. Cells with more than 1% of UMI counts attributed to the Hemoglobin genes were removed. Low-abundance genes with average  $\log_2$ CPM values lower than 0.005 were filtered out.

Expression values of 11,448 genes for 18,128 cells were obtained after filtering. The raw UMI counts were normalized with the size factors estimated from pools of cells to avoid dominance of zeros in the matrix (Lun et al., 2016). A mean-dependent trend was fitted to the variances of the log expression values of endogenous genes to distinguish between genuine biological variability and technical noise, under the assumption that most genes are not differentially expressed across cells, and their variance is mainly technical (*trendVar* function of the *scran* package with loess trend and span of 0.4 to better fit the sparse data). The fitted technical noise was subtracted and the residual “biological” component of the genes variance was used to denoise the PCA with the *denoisePCA* function of the *scran* package.

Clustering of cells into putative subpopulations was done on normalized log-counts values using hierarchical clustering on the Euclidean distances between cells (with Ward’s

criterion to minimize the total variance within each cluster). The clusters of cells were identified by applying a dynamic tree cut, which resulted in seven putative subpopulations. Marker genes specific for each cluster were identified with the *findMarkers* function of the *scrn* package, which fits a linear model to the expression values for each gene using the *limma* framework.

In all analyses, reads assigned to the *Duxbl1* (ENSMUSG00000048502), *Duxbl2* (ENSMUSG00000072675), and *Duxbl3* (ENSMUSG00000072672) genes, 100% identical at the cDNA level, were all assigned to *Duxbl1*.

#### 2.8. Data availability

The RNA-sequencing data generated are available at the Gene Expression Omnibus database under accession number GSE118059.

#### 2.9. Online supplementary materials

Fig. S1 illustrates the gating strategy used to define the different double negative stages of T-cell development in WT and  $pT\alpha^{-/-}$  mice. Fig. S2 compares the transcriptomic sequencing data of DN3a CD27<sup>low</sup>, DN3a CD27<sup>high</sup> and DN3b cells showing a heatmap of spearman correlation and a principal component analysis. Fig. S3 shows the single-cell RNA sequencing-based clustering of DN2, DN3, and DN4 cells. Fig. S4 illustrates the generation of conditional *Duxbl* transgenic and RNaseL<sup>-/-</sup> mice. Fig. S5 shows cell cycle analysis, intracellular  $\beta$ -chain expression, apoptosis, and peripheral T cell numbers in *Duxbl<sup>ind</sup>xpT $\alpha$ <sup>Cre</sup>* mice.

### 3. Results

#### 3.1. CD27 downregulation marks cells failing $\beta$ -chain rearrangement

In mice with a defective pT $\alpha$  chain developing thymocytes are arrested at the DN3 stage and undergo apoptosis due to their inability to form the pre-TCR (Fehling et al., 1995). Comparison of the DN compartments of WT versus pT $\alpha$ <sup>-/-</sup> mice by tSNE (t-distributed stochastic neighbor embedding) confirmed the absence of DN3-4 and DN4 cells in pT $\alpha$ <sup>-/-</sup> mice, but also a clear phenotypical change of the DN3 compartment, which showed lower CD27, CD44, CD117 and higher CD25 expression (Fig. 1A-B, S1). While in pT $\alpha$ <sup>-/-</sup> mice most cells undergo apoptosis due to the complete absence of pre-TCR signaling, in WT mice only a fraction of the DN3 population are eliminated. We therefore sought to phenotypically identify this fraction in the WT DN3 population. CD27 downregulation is also observed in WT mice, whereas high CD27 and CD28 expression marks DN3b cells, which have successfully rearranged their  $\beta$ -chain (Fig. 1C). In pT $\alpha$ <sup>-/-</sup> and Rag2<sup>-/-</sup> mice this CD27<sup>low</sup> population is significantly increased, whereas the DN3b population is barely detectable or completely absent (Fig. 1C+D). Comparison of WT DN3a CD27<sup>low</sup> with CD27<sup>high</sup> cells displays similar differences with regards to lower CD44, CD117 and increased CD25 expression, as observed in the WT versus pT $\alpha$ <sup>-/-</sup> comparison (Fig. 1E).

Previously, high expression of CD27 was linked to intracellular  $\beta$ -chain expression at the DN3 stage (Taghon et al., 2006). In order to assess whether CD27 downregulation is associated with failure of the  $\beta$ -selection checkpoint, intracellular  $\beta$ -chain expression as well as the cell cycle status of the cells was examined. The DN3a CD27<sup>low</sup> population exhibited decreased intracellular  $\beta$ -chain expression as well as almost complete absence of cycling cells (Fig 1F). In addition, analysis of Nur77 reporter mice, reporting activation of TCR or pre-TCR signaling, revealed a signal exclusive to the DN3a CD27<sup>high</sup> and not in the CD27<sup>low</sup> population, whereas the vast majority of DN3b cells were positive (Fig. 1G+H). Co-staining for intracellular  $\beta$ -chain expression further revealed that Nur77 expression marks DN3a cells which started to express a  $\beta$ -chain (Figure 1I). Cultivation of *ex vivo* isolated DN3 cells in wells coated with Dll (Delta-like) 4 and supplemented with Cxcl12 results in a progression of cells with a functional rearrangement to the DP stage, which is accompanied by a proliferative burst (Tussiwand et al., 2011). This progression is vastly reduced in the DN3a CD27<sup>low</sup> compared to the CD27<sup>high</sup> population (Figure 1J). Injection of anti-CD3 $\epsilon$  antibody in pT $\alpha$ <sup>-/-</sup> mice, which provides a signal that compensates for the absent pre-TCR signaling (Fehling et al., 1997), resulted in an almost complete disappearance of the CD27<sup>low</sup> population and in an upregulation of CD28 in the CD27<sup>high</sup> cells, showing their induced progression to the DN4 stage (Fig. 1K+L).

Thus, CD27 downregulation is associated with an unsuccessful  $\beta$ -chain rearrangement and/or pre-TCR formation. On the other hand, high CD27 expression is associated with pre-TCR signaling and successful passage through the  $\beta$ -selection checkpoint.

### 3.2. Specific expression of the transcription factor *Duxbl* during $\beta$ -selection

RNA-sequencing of DN3a CD27<sup>high</sup>, DN3a CD27<sup>low</sup>, and DN3b cells was performed to further investigate the mechanism of  $\beta$ -selection. All three populations were clearly separated from each other on the first axes of a principal component analysis (PCA). However, there was a closer relationship between DN3a CD27<sup>high</sup> and CD27<sup>low</sup> samples, whereas the DN3b samples were more distant (Fig. S2).

Gene set enrichment analysis for MsigDB hallmark signatures comparing DN3a CD27<sup>low</sup> and DN3b cells revealed a higher expression of genes involved in apoptosis-related pathways in DN3a CD27<sup>low</sup> cells, with the significant enrichment of the tumor necrosis factor alpha (TNFA) signaling, interferon alpha and gamma responses, p53, and apoptosis pathways. On the other hand, hallmark signatures that were significantly decreased in the CD27<sup>low</sup> population were related to cell cycle and DNA replication, such as the Myc and E2F targets, mTORC1 signaling, mitotic spindle, and genes involved at the G2 to M checkpoint in the cell-cycle (Fig. 2A). This enrichment of genes involved in cell cycle and proliferation is visible in the top 50 genes downregulated in the DN3a CD27<sup>low</sup> compared to DN3b population (Fig. 2B). Therefore, global gene expression analysis is in agreement with the previous findings of cell cycle arrest and the developmental blockade of cells that will undergo apoptosis in the DN3a CD27<sup>low</sup> population, whereas DN3b cells, after receiving pre-TCR signaling, undergo proliferative expansion. The DN3a CD27<sup>high</sup> population seems to be located in between these two populations as indicated by the gene expression levels shown in Figure 2B and the hierarchical clustering shown in Figure S2A.

The homeobox transcription factor *Duxbl* (double homeobox B-like gene) was found to be the DNA binding protein with the highest fold change between the DN3a CD27<sup>low</sup> and DN3b populations (Fig. 2B-D). This factor was of specific interest since its deregulated expression was shown to result in an impaired DN thymocyte development in an *in vitro* setting (Kawazu et al., 2007). While *Duxbl* was expressed in the DN3a CD27<sup>high</sup> population almost 2-fold less compared to DN3a CD27<sup>low</sup> population, it was expressed at very low levels in DN3b cells (Fig. 2E). Quantitative PCR analysis confirmed these data and additionally highlighted that *Duxbl* is very specifically upregulated at the DN3a stage during T-cell development and immediately downregulated at the DN3b stage after cells have passed  $\beta$ -selection (Fig. 2F-G). This prompted us to test whether pre-TCR signaling is involved in the downregulation of *Duxbl* expression. To this end, we quantified *Duxbl* expression in Nur77<sup>-</sup> as well as Nur77<sup>+</sup> DN3a CD27<sup>high</sup> cells in Nur77<sup>GFP</sup> mice. Our analysis revealed diminished *Duxbl* expression in Nur77<sup>+</sup>

cells (Fig. 2H). Furthermore, *Duxbl* expression was also decreased in DN3 cells from  $pT\alpha^{-/-}$  mice that were injected with anti-CD3 $\epsilon$  antibodies compared to the PBS injected controls (Fig. 2I).

The prominent expression of *Duxbl* at the stage where  $\beta$ -selection occurs, as well as its induced downregulation by pre-TCR signaling, suggest a potential role of this transcription factor in the selection process.

### 3.3. *Single-cell transcriptome clustering of DN cells elucidates Duxbl expression prior to $\beta$ -selection*

To further characterize the  $\beta$ -selection checkpoint, single-cell RNA-sequencing of WT DN2, DN3, and DN4 cells was performed. In total, after quality filtering, we obtained 3,952 DN2, 8,675 DN3, and 5,501 DN4 cells, with an average of 1,988 genes per cell detected. A PCA clearly separated the individual cells of the DN2 population from the other populations on the second principal component (Fig. 3A). While most of the DN3 cells separated from the DN4 population on the first principal component, some merged into the DN4 population. Clustering analysis resulted in 7 clusters, with two clusters composed of DN2 cells, two clusters composed of DN3 cells, two clusters composed of both DN3 and DN4 cells, and one cluster composed of DN4 cells (Fig. 3B-C, Fig. S3A).

Progression from the DN2 to the DN4 stage is accompanied by specific developmental gene expression changes. We used well-defined expression patterns of surface markers, genes involved in recombination, as well as transcriptional regulators of T-cell development in order to establish a developmental trajectory of the obtained clusters (Yui and Rothenberg, 2014). As genes specific for the DN2 stage *Cd117*, *Cd44*, *Hoxa9*, *Lmo2*, *Mef2c*, *Gfi1b*, *Lyl1*, *Spi1*, *Bcl11a*, *Mycn*, and *Hhex* were used. *Il2ra*, *Il7r*, *Erg*, *Notch1*, *Hes1*, and *Runx1* were used as genes expressed in both DN2 and DN3 cells. DN3 cells in particular were defined by high expression of *CD3 $\gamma$* , *CD3 $\delta$* , *CD3 $\epsilon$* , *Rag1*, *Rag2*, *Ptcr*, *Tcf12*, *Ets*, *Ahr*, *Notch3*, and *SpiB*. From the DN3 stage onwards *Tcf12*, *Ets1*, *Bcl11b*, *Ets2*, *Lef1*, *Thy1*, and *Themis* are highly expressed, whereas *Cd4*, *Cd8*, *Rorc*, and *Id3* are increased once the cells have reached DN4 stage. The heatmap shown in Figure S3B illustrates the expression patterns of these marker genes throughout the developmental trajectory. Although these markers are mainly studied at the protein expression level, their expression at the transcriptome level was overall in very good agreement with the expectation. As expected, clusters containing DN2 cells display high expression of the marker genes sets that are early expressed during development. On the other hand, DN3 specific genes split the four clusters containing DN3 cells into two, since they are highly expressed in the clusters exclusively consisting of DN3 cells (clusters 3 and 4), whereas the clusters that map with DN4 cells (5 and 6) show reduced expression of these genes. The fact that many of these DN3-specific genes relate to recombination and pre-TCR

signaling, suggests a separation of DN3 cells into pre- (clusters 3 and 4) and post  $\beta$ -selection (clusters 5 and 6). Expression of DN4 specific genes in clusters 5 and 6 further supports this hypothesis. This is confirmed by isolating from the data the top genes that are the best at discriminating the seven different clusters: recombination- and pre-TCR signaling-related genes are highly expressed in clusters 3 and 4, while their expression is lower in clusters 5 and 6 (Fig. 3D, genes in green). Furthermore, clusters 5 and 6 showed increased expression of genes associated with cell cycle and proliferation (in blue), which are only induced after passage of the  $\beta$ -selection checkpoint, and upregulation of genes involved in the negative regulation of apoptotic processes (in red).

Confirming our previous results, *Duxbl* expression was almost exclusively detected in the clusters consisting of DN3 cells, with maximal expression in cluster 4 (Fig 3E-F), whose cells have expression profile that is the farthest from cells that have passed  $\beta$ -selection (clusters 5 and 6; Fig. 3B, S3A). Thus, cluster 4 most likely represents cells that are undergoing recombination, including the cells that have failed productive rearrangement and are going to die. The highly specific expression of *Duxbl* within this cluster further suggests a potential role for this transcription factor during the  $\beta$ -selection process.

### 3.4. Conditional *Duxbl* transgenic mice display perturbed T-cell development

In order to further investigate the role of *Duxbl* during T-cell development and specifically during  $\beta$ -selection, we generated conditional transgenic mice that over-express *Duxbl* and eGFP after removal of a mCherry stop-cassette by cre-mediated recombination (hereafter *Duxbl*<sup>ind</sup>) (Fig. S4A). To achieve specific expression at the DN3a stage during T-cell development, these mice were crossed to mice expressing the cre recombinase under the control of the pT $\alpha$  promoter (hereafter *Duxbl*<sup>ind</sup>xpT $\alpha$ <sup>Cre</sup>) (Luche et al., 2013). The loss of mCherry and gain of eGFP expression pattern in these mice confirmed specificity of the system (Fig. S4B-D).

Thymic cellularity of *Duxbl*<sup>ind</sup>xpT $\alpha$ <sup>Cre</sup> mice was reduced 10-fold compared to WT and *Duxbl*<sup>ind</sup> control mice. By contrast, the cellularity of the spleen and the bone marrow was not significantly changed (Fig. 4A). Staining with CD4 and CD8 revealed an increase in DN percentage with simultaneous decrease in DP (Fig. 4B). As a result, DN numbers were not increased, whereas DP cell numbers were reduced ~45-fold. Mature CD4 and CD8 T-cell compartments were reduced, ~5-fold and ~3-fold respectively (Fig. 4C). The  $\gamma\delta$ -T-cell compartment was not significantly altered, indicating that *Duxbl* specifically acts during  $\alpha\beta$ -T-cell development.

The separation of the DN stages using CD25, CD44, and CD117 expression revealed a reduction in DN1, DN2, DN3, as well as DN4 fractions, whereas the DN3-4 stage, comprising cells with intermediate levels of CD25, was increased in *Duxbl*<sup>ind</sup>xpT $\alpha$ <sup>Cre</sup> mice (Fig. 4B, D). This

clearly indicates a block in the development of T cells at the transition from the DN3 to the DN4 stage. Cells accumulating at the DN3-4 stage were much smaller in size compared to the ones in WT or *Duxbl<sup>ind</sup>* mice (Fig. 4E). Cell cycle analysis of DN3, DN3-4, and DN4 cells from all mouse strains revealed a decreased percentage of cycling cells in *Duxbl<sup>ind</sup>xpTα<sup>Cre</sup>* mice (Fig. 4F, S5A). On the other hand, the subsequent selection of cells with successful rearrangement of the  $\beta$ -chain seemed not to be affected by *Duxbl*, since the majority of cells stained positive for intracellular  $\beta$ -chain at the DN3-4 stage in all genotypes (Fig. 4G + S5B). Ultimately, the disturbed T-cell development resulted in reduced peripheral CD4 and CD8 T-cell compartments in *Duxbl<sup>ind</sup>xpTα<sup>Cre</sup>* mice (Fig. S5C). On the contrary,  $\gamma\delta$ -T cells were increased in the periphery (Fig. S5C).

To test the abnormalities in the progression to the DP stage in more detail we sorted WT and *Duxbl<sup>ind</sup>xpTα<sup>Cre</sup>* DN3 cells and cultivated them for up to five days in wells coated with Dll4 and medium supplemented with Cxcl12. As shown in Figure 4H and I, WT cells expanded ~2-fold after 3 days and ~3.5-fold after 5 days and expressed CD4 and CD8 on their surface. This progression was almost completely blocked in cells derived from *Duxbl<sup>ind</sup>xpTα<sup>Cre</sup>* mice, demonstrated by the reduction in cell numbers over time and the absence of CD4 and CD8 expression after five days, thus recapitulating the situation observed *in vivo*. For analysis of apoptosis, AnnexinV and 7AAD staining was performed after 3 days of culture (Fig. S5D). A strong decrease in the number of living cells in accordance with an increase in the number of early and late apoptotic cells in cultures containing DN3 cells from *Duxbl<sup>ind</sup>xpTα<sup>Cre</sup>* mice was observed (Fig. 4J).

Taken together, conditional over-expression of *Duxbl* specifically affects the  $\beta$ -selection checkpoint by blocking the developmental progression of cells that should normally continue to their next stage, as shown by the tremendous reduction in DP cells. Induction of apoptosis and cell cycle arrest seem to cause the observed block, indicating that *Duxbl* is involved in the elimination of cells that fail  $\beta$ -selection.

### 3.5. Silencing of *Duxbl* results in decreased apoptosis at the DN3 stage

We designed four different shRNA vectors for retroviral knock-down of *Duxbl* expression via RNA interference. Additionally, transduced cells were marked by GFP expression. Efficiency of the different shRNAs was tested on a cell line that over-expressed *Duxbl* due to transposon-mediated integration of a construct containing the *Duxbl* cDNA under control of a constitutive active promoter. Transduction of this cell line with the different shRNAs and subsequent sorting of the GFP<sup>+</sup> fraction revealed reduced mRNA expression of *Duxbl* as determined by qPCR analysis (Figure 5A). The shRNA with the highest knock-down efficiency (sh3-2) was selected for further experiments.

For the establishment of an *in vitro* simulation of T-cell development, fetal liver cells were cultured on OP9-D11 stromal cells. After several days of culture, the majority of cells adopted a DN2 phenotype and only after removal of IL-7 transition through  $\beta$ -selection was initiated, which resulted in the generation of DP cells (data not shown). Since pre-TCR-signaling results in CD25 downregulation, we specifically assessed the potential effect of Duxbl knock-down on CD44<sup>+</sup>CD25<sup>high</sup> cells, the majority of which represent cells prior to  $\beta$ -selection and in which Duxbl is expressed. Knock-down of Duxbl in this system diminished apoptosis at the DN3 stage specifically in the GFP<sup>+</sup> fraction, whereas untransduced GFP<sup>-</sup> cells showed no significant change compared to the empty vector (EV) control (Figure 5B-C).

Thus, in accordance with apoptosis induction after Duxbl over-expression (Figure 4), silencing Duxbl expression results in reduced apoptosis in DN3 cells, further supporting its role in mediating the elimination of DN3 cells that failed  $\beta$ -selection.

### 3.6. Activation of apoptosis in *Duxbl<sup>ind</sup>xpT $\alpha$ <sup>Cre</sup>* mice

To reveal the mechanism involved in the Duxbl-mediated apoptosis induction in T-cell development we investigated gene expression changes in *Duxbl<sup>ind</sup>xpT $\alpha$ <sup>Cre</sup>* DN3-4 cells by RNA-sequencing of these cells in parallel with their WT counterparts. Comparison of these two populations with the previous RNA-seq data revealed a close similarity between WT DN3-4 cells and DN3b cells (Fig. 6A), which is expected since at the level of surface protein expression they only differ slightly in their CD25 expression level. Interestingly, after batch-effect correction, DN3-4 cells derived from *Duxbl<sup>ind</sup>xpT $\alpha$ <sup>Cre</sup>* mice exhibited a gene expression profile most similar to WT DN3a CD27<sup>low</sup> cells, even though they have a successfully rearranged  $\beta$ -chain. This further suggests that continuous Duxbl expression prevents developmental progression and instead induces a transcriptomic phenotype resembling the cells that fail  $\beta$ -selection.

Amongst the most differentially expressed genes between WT DN3-4 cells and DN3-4 cells derived from *Duxbl<sup>ind</sup>xpT $\alpha$ <sup>Cre</sup>* mice, the Oas/RNaseL pathway was clearly over-expressed in transgenic samples (Fig. 6B). This system is important in interferon responses and was shown to be mainly involved in anti-viral immunity by inducing apoptosis in infected cells (Silverman, 2007). RNaseL deficiency also results in an increased resistance of thymocytes to apoptosis, suggesting further involvement of this pathway in thymic development (Zhou et al., 1997). Quantitative-PCR analysis of the expression of different Oas genes, as well as of the *Rnase1* gene, during T-cell development revealed that some, such as *Rnase1* and *Oas1b*, are specifically upregulated at the DN3a stage (Fig. 6C). Even more striking was the silencing of all Oas/RNaseL genes in DN3b cells after  $\beta$ -selection passage (Fig. 6C). This specific expression together with the upregulation in *Duxbl<sup>ind</sup>xpT $\alpha$ <sup>Cre</sup>* DN3-4 cells indicates that this

pathway is involved in the  $\beta$ -selection checkpoint, potentially acting downstream of Duxbl, and thus mediating the T-cell developmental block observed in the Duxbl<sup>ind</sup>xpT $\alpha$ <sup>Cre</sup> mice.

In order to test whether RNaseL is involved in the Duxbl-mediated T-cell developmental block, we generated RNaseL defective mice (Fig. S4) and crossed them to the Duxbl<sup>ind</sup>xpT $\alpha$ <sup>Cre</sup> line. Thymic cellularities of Duxbl<sup>ind</sup>xpT $\alpha$ <sup>Cre</sup>xRNaseL<sup>-/-</sup> mice were significantly increased compared to their Duxbl<sup>ind</sup>xpT $\alpha$ <sup>Cre</sup> counterparts, due to higher numbers of DN, DP, CD4 and CD8 T cells, as well as  $\gamma\delta$ -T cells (Fig. 7A-C). The DP stage was particularly affected, since this population was also increased in percentage, confirming that the T-cell developmental block was at least partly suppressed (Fig. 7B, D). The observed upregulation of the Oas/RNaseL system by transgenic Duxbl expression is therefore in part responsible for the disturbed developmental progression of DN3 cells in Duxbl<sup>ind</sup>xpT $\alpha$ <sup>Cre</sup> mice. Of note, since Duxbl<sup>ind</sup>xpT $\alpha$ <sup>Cre</sup>xRNaseL<sup>-/-</sup> mice retain an altered T-cell development compared to WT mice (Fig. 7B), other mechanisms must be additionally involved.

We further investigated the connection of Duxbl to apoptosis by crossing the Duxbl<sup>ind</sup>xpT $\alpha$ <sup>Cre</sup> to Bcl2tg mice, in order to examine whether an additional survival signal would attenuate the block in T-cell development of these mice, as observed in the case of interleukin-7 receptor deficient mice (Akashi et al., 1997). Indeed, the thymic cellularity of Duxbl<sup>ind</sup>xpT $\alpha$ <sup>Cre</sup>xBcl2tg DN, CD4 and CD8 and  $\gamma\delta$ -T cells, but especially of the DP (~3.5-fold change), were all significantly increased compared to Duxbl<sup>ind</sup>xpT $\alpha$ <sup>Cre</sup> mice. The number of DP cells did not reach WT levels and phenotypically the block showing an increased DN and decreased DP compartment was still apparent (Fig. 8A-F), indicating that the development is not completely rescued by additional expression of Bcl2 alone. However, the partial rescue of DP cells in Duxbl<sup>ind</sup>xpT $\alpha$ <sup>Cre</sup>xBcl2tg mice provides further evidence for a role of Duxbl in mediating the elimination of non-selected DN3 cells by inducing apoptosis.

## 4. Discussion

Thymic selection of  $\alpha\beta$ -T cells requires a series of events in which TCR engagement follows defined rules. The majority of cells will undergo apoptosis during  $\beta$ -selection and the underlying mechanisms of this process have not been completely resolved. In the present study CD27 downregulation within the DN3 population was identified as a marker for cells that have failed to rearrange their  $\beta$ -chain and therefore are eliminated. Transcriptome analysis both at population and single-cell level revealed high expression of the transcription factor *Duxbl* exclusively in a cluster of cells that have not yet passed  $\beta$ -selection and display high rearrangement activity. Conditional transgenic expression of *Duxbl* led to a disrupted DN3-to-DN4 transition due to suppressed proliferation and induction of apoptosis, with the developmentally arrested cells highly resembling WT DN3a CD27<sup>low</sup> *Duxbl*<sup>high</sup> cells. Silencing of its expression, on the other hand, resulted in decreased apoptosis. We identified up-regulation of the apoptosis-inducing Oas/RNaseL pathway as a potential mechanism by which *Duxbl* facilitates the elimination of non-selected cells at the  $\beta$ -selection checkpoint.

CD27 expression was previously described to separate intracellular  $\beta$ -chain positive from negative cells, since it gets slightly upregulated in DN3b cells (Taghon et al., 2006). However, the observation of CD27 downregulation in DN3a cells extends the current resolution of the developmental staging during T-cell development, as it marks cells that failed successful rearrangement and that will therefore undergo apoptosis (Fig. 1-2). The DN3a CD27<sup>high</sup> population, on the other hand, seems to be one stage before the rescue-versus-apoptosis decision as indicated by its gene expression profile, which clusters in between CD27<sup>low</sup> and DN3b cells (Fig. 2). This suggests that DN3a CD27<sup>high</sup> cells are still in the process of  $\beta$ -selection, and are not yet assigned to a specific fate.

The expression of *Duxbl* in DN3a cells, which mostly occurs in the CD27<sup>low</sup> population, indicates a role during  $\beta$ -selection (Fig. 2C-D). An association, whose molecular mechanisms was not defined, was suggested by *in vitro* studies in which expression of *Duxbl* affected the development of the DN stages (Kawazu et al., 2007). Our findings provide *in vivo* proof for this role of *Duxbl* and further identify this transcription factor as initiator of developmental arrest and apoptosis in DN3a cells that fail  $\beta$ -selection. It is currently unknown what signals initiate *Duxbl* expression at the DN3a stage and two scenarios can be envisaged. In the first case, *Duxbl* could be induced specifically in cells with a non-functional rearrangement. In the second case, it could be induced in all cells that enter the DN3a stage, thus acting as a timer for successful rearrangement. *Duxbl* expression would increase over time in cells failing  $\beta$ -chain rearrangement leading to apoptosis induction. On the contrary, cells with successful

rearrangement would receive a pre-TCR signal that silences *Duxbl* expression and leads to their rescue and developmental progression (Fig 2F-G).

Our studies also showed a profound heterogeneity within the DN3 population. Indeed, single-cell RNA sequencing of DN2, DN3, and DN4 cells unveiled four different clusters in DN3 thymocytes, of which two were shared with DN4 cells (Fig. 3A-C, Fig. S3A). These findings showed partitioning of the DN3 population into cells that have not yet undergone  $\beta$ -selection, (clusters 3 and 4) and cells that already passed this checkpoint (clusters 5 and 6). Consequently, the latter cells are closer to the gene expression profile of DN4 cells. Interestingly, *Duxbl* expression was mainly detected in cluster 4, which is transcriptionally farthest from the DN4 clusters (Fig. 3E-F). Considering the high expression of genes involved in  $\beta$ -chain recombination and the pre-TCR in this cluster, it probably consists of cells continuing the process of rearrangement, including some that have failed rearrangement.

While reduced *Duxbl* expression leads to a decrease in apoptosis at the DN3 stage, the detrimental effect of its expression in cells undergoing  $\beta$ -selection is exhibited in mice conditionally over-expressing *Duxbl*. The increased DN and decreased DP stages in the thymus of these mice showed arrest of T-cell development after the DN3 stage (Fig. 3). However, the block is not absolute, since mature CD4 and CD8 T cells can still be found in the thymus as well as in the periphery. DN3-4 cells of *Duxbl<sup>ind</sup>xpT $\alpha$ <sup>Cre</sup>* mice stain positive for a functionally rearranged  $\beta$ -chain (Fig. 3F). Thus, these cells receive a survival and proliferation signal from the pre-TCR and at the same time express *Duxbl*, which is inhibiting their cell cycle and induces apoptosis (Fig. 3G; Fig. 4A-C). In a WT situation *Duxbl* expression is silenced after pre-TCR activation, but in our system *Duxbl* expression remains also in cells that already received signals via the pre-TCR, which seems to prevent their further differentiation. We therefore envisage that *Duxbl* downregulation upon pre-TCR signaling is an absolute requirement for further differentiation of the cells. In the few cells that have reached the DP stage in *Duxbl<sup>ind</sup>xpT $\alpha$ <sup>Cre</sup>* mice pre-TCR signaling must have overcome the negative signals of the continuous *Duxbl* expression. However, as indicated by the *ex vivo* differentiation this seems to be rarely the case (Fig. 4A-C). Another interesting finding was the impact of *Duxbl* specifically on  $\alpha/\beta$  T-cell development, since there was no detrimental effect on the development of  $\gamma\delta$ -T cells in *Duxbl<sup>ind</sup>xpT $\alpha$ <sup>Cre</sup>* mice. In contrast,  $\gamma\delta$ -T cells were even increased, similar to what was described for *pT $\alpha$ <sup>-/-</sup>* mice (Fehling et al., 1995).

The link of *Duxbl* to apoptosis and in particular to the activation of the Oas/RNaseL pathway was further strengthened by the crossing of the *Duxbl<sup>ind</sup>xpT $\alpha$ <sup>Cre</sup>* to *Bcl2<sup>tg</sup>* and *RNaseL<sup>-/-</sup>* mice, respectively. Both approaches resulted in a significant increase in thymic cellularity (Fig. 7, 8). Remarkably, the DP stage in particular was rescued in these mice, as manifested by a ~3.5-fold increase in *Duxbl<sup>ind</sup>xpT $\alpha$ <sup>Cre</sup>xBcl2<sup>tg</sup>* and ~3.2 in *Duxbl<sup>ind</sup>xpT $\alpha$ <sup>Cre</sup>RNaseL<sup>-/-</sup>* mice. However, neither of the two resulted in completely normalized T-cell development. In the case

of Bcl2 expression this can be explained by the fact that only the apoptotic effects of Duxbl are antagonized, whereas the antiproliferative effects that we observed are not affected. In fact, Bcl2 over-expression itself has a negative effect on the proliferation of cells (O'Reilly et al., 1996), thus potentially compromising the full assessment of its anti-apoptotic effect. Similarly, activation of the Oas/RNaseL system seems to be just part of the mechanism by which Duxbl is preventing developmental progression. Therefore, we can conclude that apoptosis and the Oas/RNaseL system are connected to the Duxbl-mediated effects in T-cell development, and that additional pathways are potentially involved.

Knock-down experiments confirmed the link of Duxbl to apoptosis induction. As implied by the increase of apoptosis in Duxbl transgenic DN3 cells (Figure 4), silencing resulted in a reduced number of apoptotic cells at the DN3 stage (Fig 5B, C). This further indicates that Duxbl mediates the elimination of cells that have failed  $\beta$ -selection and therefore its decreased expression rescues these cells from cell death. Since our experimental setting only leads to a reduction in Duxbl levels and is not resulting in its complete absence it can be envisaged that the remaining Duxbl is still able to efficiently eliminate a fraction of the cells, thus resulting in only a partial rescue.

The Duxbl gene is part of a triplicated region in the mouse genome, which spans more than 300kb and contains three almost identical Duxbl copies, thus making the generation of a conditional knock-out mouse particularly challenging. Each of the three identical Duxbl copies contains two homeodomains that are responsible for sequence-specific DNA binding. The amino acid sequences of these homeodomains exhibit the highest similarity to those of human DUX4 (Wu et al., 2010). The physiological role of DUX4 in humans has not been identified so far. However, mis-expression of DUX4 in skeletal muscle cells is associated with facioscapulohumeral dystrophy, triggered by DUX4-induced apoptosis. A recent study also identified the RNaseL pathway to be involved in DUX4 mediated toxicity. Silencing of RNaseL resulted in increased survival following DUX4 transgene induction in a rhabdomyosarcoma cell line (Shadle et al., 2017). Thus, human DUX4 has characteristics resembling the herein described function of mouse Duxbl with regards to apoptosis and the link to the Oas/RNaseL pathway. In accordance with that, high expression of DUX4 was detected in the thymus, suggesting its actual function in this tissue (Das and Chadwick, 2016). Therefore, it is presumable that, as with Duxbl in mice, DUX4 might be involved in human T-cell development.

Collectively, the findings described in the present study demonstrate that failed  $\beta$ -chain rearrangement coincides with low expression of CD27 in DN3 T cell progenitors. Detailed analysis of this CD27<sup>low</sup> population revealed the homeobox transcription factor Duxbl as a key regulator of  $\beta$ -selection by inducing apoptosis in cells that have failed to rearrange their  $\beta$ -chain.

### Author Contributions

FK, MM, CE, LvM, PP, and PT performed experiments; FK, JR and LA-S analyzed data; HJF and PP provided mice and materials; FK wrote the manuscript; FK, PT, and AR designed the study.

### Acknowledgements

We thank Drs. Rhodri Ceredig, Jan Andersson, and Gennaro De Libero for helpful comments and critical reading of the manuscript. We also thank Dr. Gleb Turchinovich for valuable advice on retroviral production and Katrin Hafen for help with Nur77 reporter mice.

A.R. was holder of the chair in immunology endowed by L. Hoffmann – La Roche Ltd, Basel. This study was supported by the Swiss National Science Foundation (310030B\_160330/1) and by the People Program (Marie Curie Actions) of the European Union's Seventh Framework Program FP7/2007-2013 under Research Executive Agency grant agreement number 315902.

Calculations were performed at sciCORE (<http://scicore.unibas.ch/>) scientific computing center at University of Basel.

The authors declare no competing financial interests.

This paper is dedicated to the memory of our group leader, mentor, colleague, and friend Antonius Rolink.

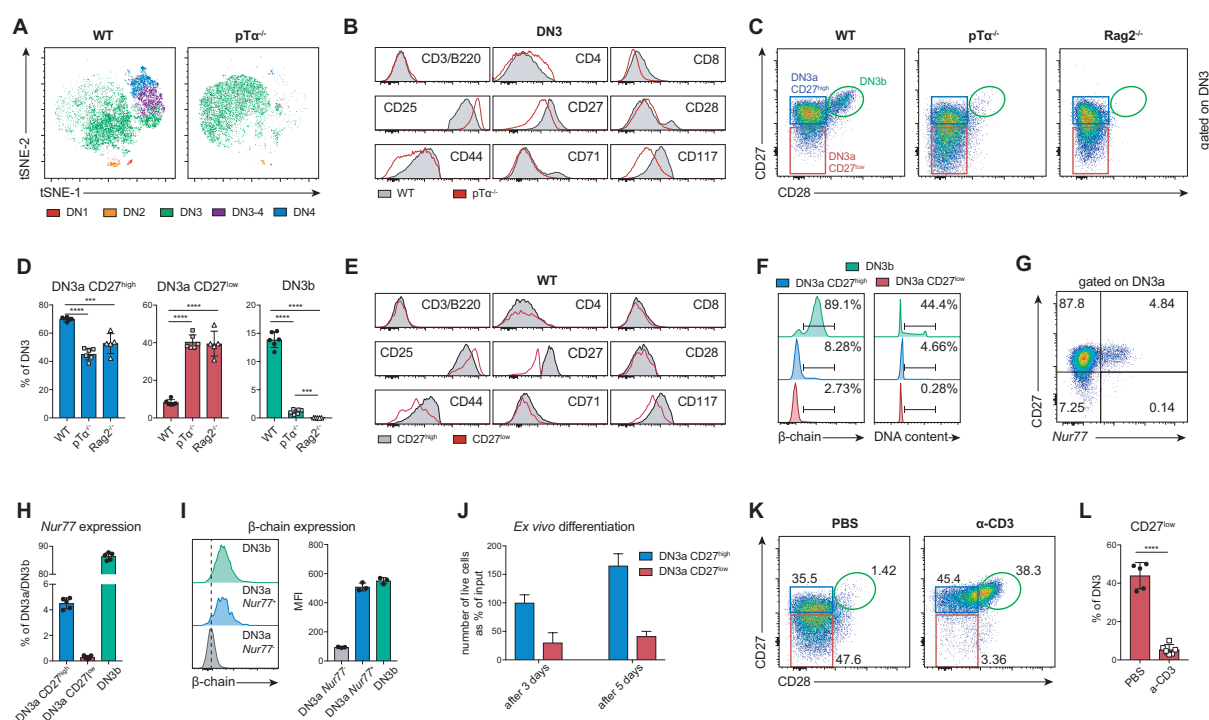


**Figure 1 | CD27 downregulation marks cells failing  $\beta$ -selection**

**A)** tSNE (t-distributed stochastic neighbor embedding) based comparison of  $pT\alpha^{-/-}$  and WT DN cells using the surface markers CD3/B220, CD4, CD8, CD25, CD27, CD28, CD44, CD71, and CD117. DN stages were identified by FACS as shown in Figure S1. **B)** Histograms of markers used in (A) of WT and  $pT\alpha^{-/-}$  DN3 cells. (A, B) Two independent experiments were performed, with representative data from one experiment shown. **C)** Representative FACS plots for the separation of DN3 cells in  $pT\alpha^{-/-}$ ,  $Rag2^{-/-}$ , and WT mice using CD27 and CD28 expression. Three independent experiments were performed, with representative data from one experiment shown. **D)** Frequencies of DN3a CD27<sup>high</sup> (left panel), DN3a CD27<sup>low</sup> (middle panel), and DN3b (right panel) cells as percentage of DN3 in WT (n=6),  $pT\alpha^{-/-}$  (n=6), and  $Rag2^{-/-}$  (n=5) mice. Data were collected from three independent experiments. **E)** Histograms of markers used in (A) of WT DN3a CD27<sup>high</sup> and DN3a CD27<sup>low</sup> cells. Three independent experiments were performed, with representative data from one experiment shown. **F)** Representative histograms showing intracellular  $\beta$ -chain expression (left panel) or DNA content (right panel) of WT DN3a CD27<sup>low</sup>, DN3a CD27<sup>high</sup>, and DN3b cells. Three independent experiments were performed, with representative data from one experiment shown. **G)** Representative FACS plot of Nur77 expression in CD27<sup>high</sup> and CD27<sup>low</sup> DN3a cells in Nur77<sup>GFP</sup> mice. Three independent experiments were performed, with representative data from one experiment shown. **H)** Frequencies of Nur77<sup>+</sup> cells within the DN3a CD27<sup>high</sup> or CD27<sup>low</sup> and DN3b population. Data were collected from three independent experiments. **I)** Representative histograms showing intracellular  $\beta$ -chain expression in Nur77<sup>-</sup> or Nur77<sup>+</sup> DN3a and DN3b cells.

---

Two independent experiments were performed, with representative data from one experiment shown. **J)** Numbers of sorted WT DN3a CD27<sup>high</sup> and DN3a CD27<sup>low</sup> cells as percentage of input after three and five days of culture in wells coated with Dll4 and supplemented with Cxcl12. Two independent experiments were performed, with representative data from one experiment shown. **K)** Representative FACS plots of CD27 and CD28 expression in pTα<sup>-/-</sup> DN3 cells one day after intraperitoneal injection of 100μg anti-CD3ε antibodies or PBS. Three independent experiments were performed, with representative data from one experiment shown. **L)** Frequency of DN3a CD27<sup>low</sup> cells as percentage of DN3 in pTα<sup>-/-</sup> mice one day after intraperitoneal injection of 100μg anti-CD3ε antibodies (n=6) or PBS (n=5). Data were collected from three independent experiments. Gate numbers in FACS plots and histograms indicate frequencies of parent gate. Statistical analysis was done with two-tailed unpaired Student's *t* test. \*: p<0.05, \*\*: p<0.01, \*\*\*: p<0.001, \*\*\*\*: p<0.0001. Error bars indicate standard deviation.

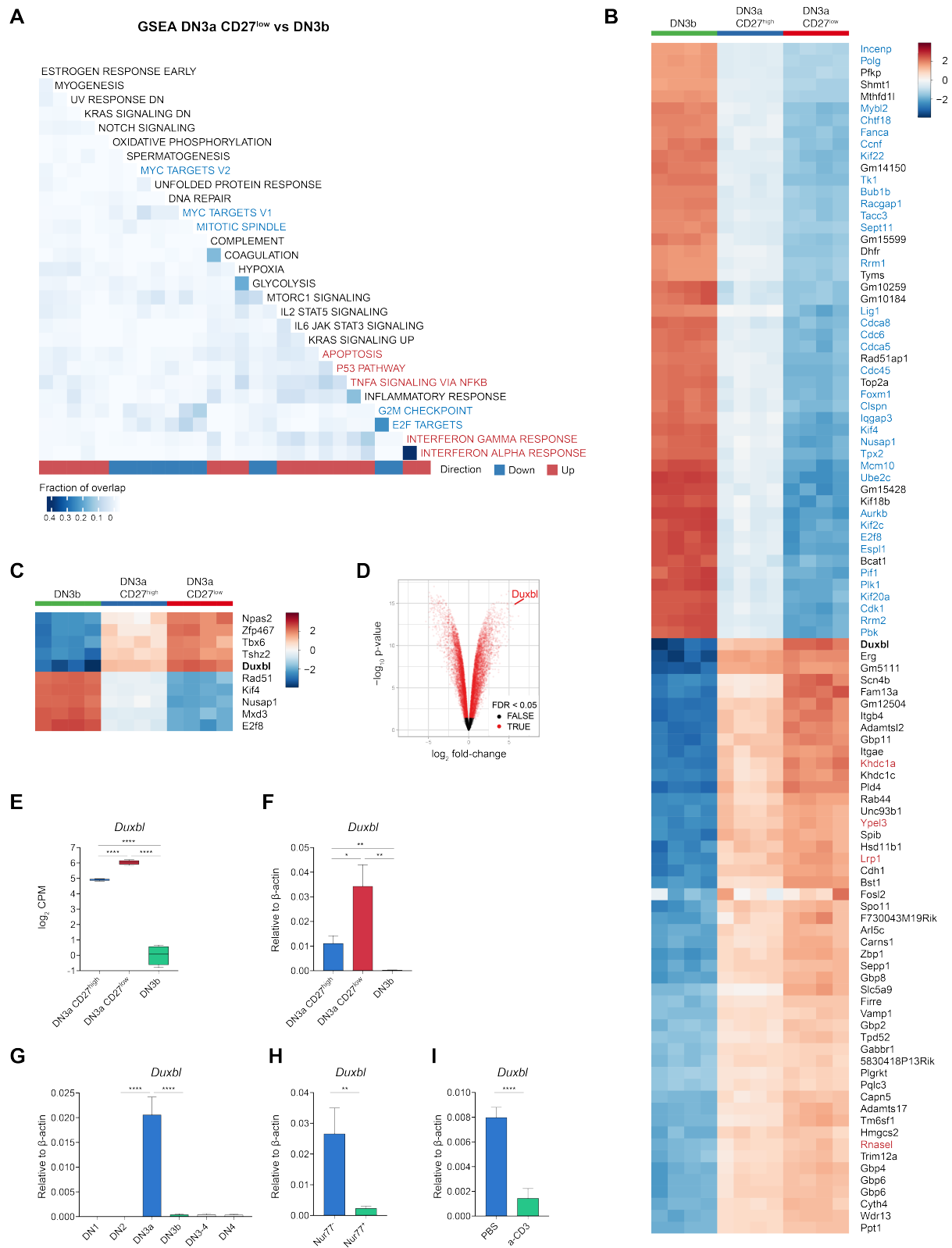


**Figure 2 | Transcriptome comparison reveals specific upregulation of the transcription factor *Duxbl* in DN3a CD27<sup>low</sup> cells**

**A-C)** Bulk RNA sequencing of DN3a CD27<sup>high</sup>, DN3a CD27<sup>low</sup>, and DN3b cells, performed as described in Materials and Methods. **A)** Heatmap illustrating the results of the gene set

enrichment analysis (GSEA) of DN3a CD27<sup>low</sup> versus DN3b cells using gene sets from the hallmark collection of the Molecular Signature Database. Only sets containing more than ten genes and with a false discovery rate (FDR) lower than 5% are illustrated. The fraction of genes overlapping across gene sets is indicated by the color intensity on the heatmap. Downregulated hallmark signatures related to cell cycle/division and DNA replication are highlighted with blue font, and upregulated ones related to apoptosis pathways in red font. **B)** Heatmap displaying the centered gene expression levels of the top 50 significantly over-expressed genes and top 50 significantly under-expressed genes in DN3a CD27<sup>low</sup> compared to DN3b cells. Genes are clustered using hierarchical clustering but the dendrogram is not displayed. Duxbl is marked in bold font. The color gradient illustrates the normalized log<sub>2</sub> counts per million (CPM) values centered across all samples for each gene. **C)** Heatmap displaying the centered gene expression levels of the top ten transcription factors (i.e., annotated to Gene Ontology category GO:0003677) with the highest absolute fold change among differentially expressed genes (FDR<0.05) between DN3a CD27<sup>low</sup> and DN3b cells. Duxbl is marked in bold font. The color gradient illustrates the normalized log<sub>2</sub>CPM values centered across all samples for each gene. **D)** Volcano plot of differentially expressed genes between DN3a CD27<sup>low</sup> and DN3b cells. Genes with an FDR < 0.05 are marked in red, genes with an FDR > 0.05 in black. **E, F)** Normalized log<sub>2</sub>CPM obtained from the bulk RNA sequencing (E) and relative expression obtained by quantitative PCR (F) of Duxbl in DN3a CD27<sup>high</sup>, DN3a CD27<sup>low</sup>, and DN3b cells. **G)** Relative expression of Duxbl in DN1, DN2, DN3a, DN3b, DN3-4, and DN4 cells. **H)** Relative expression of Duxbl in Nur77<sup>-</sup> and Nur77<sup>+</sup> DN3a CD27<sup>high</sup> cells isolated from Nur77<sup>GFP</sup> mice. **I)** Relative expression of Duxbl in DN3 cells isolated from pTα<sup>-/-</sup> mice one day after intraperitoneal injection of 100μg anti-CD3ε antibodies (n=7) or PBS (n=5). As housekeeping gene β-actin was used. Data were collected from four (G, H) or three (F, I) independent experiments. DN stages were identified by FACS as shown in Figure S1. Statistical analysis was done with two-tailed unpaired Student's *t* test. \*: p<0.05, \*\*: p<0.01, \*\*\*: p<0.001, \*\*\*\*: p<0.0001. Error bars indicate standard deviation.

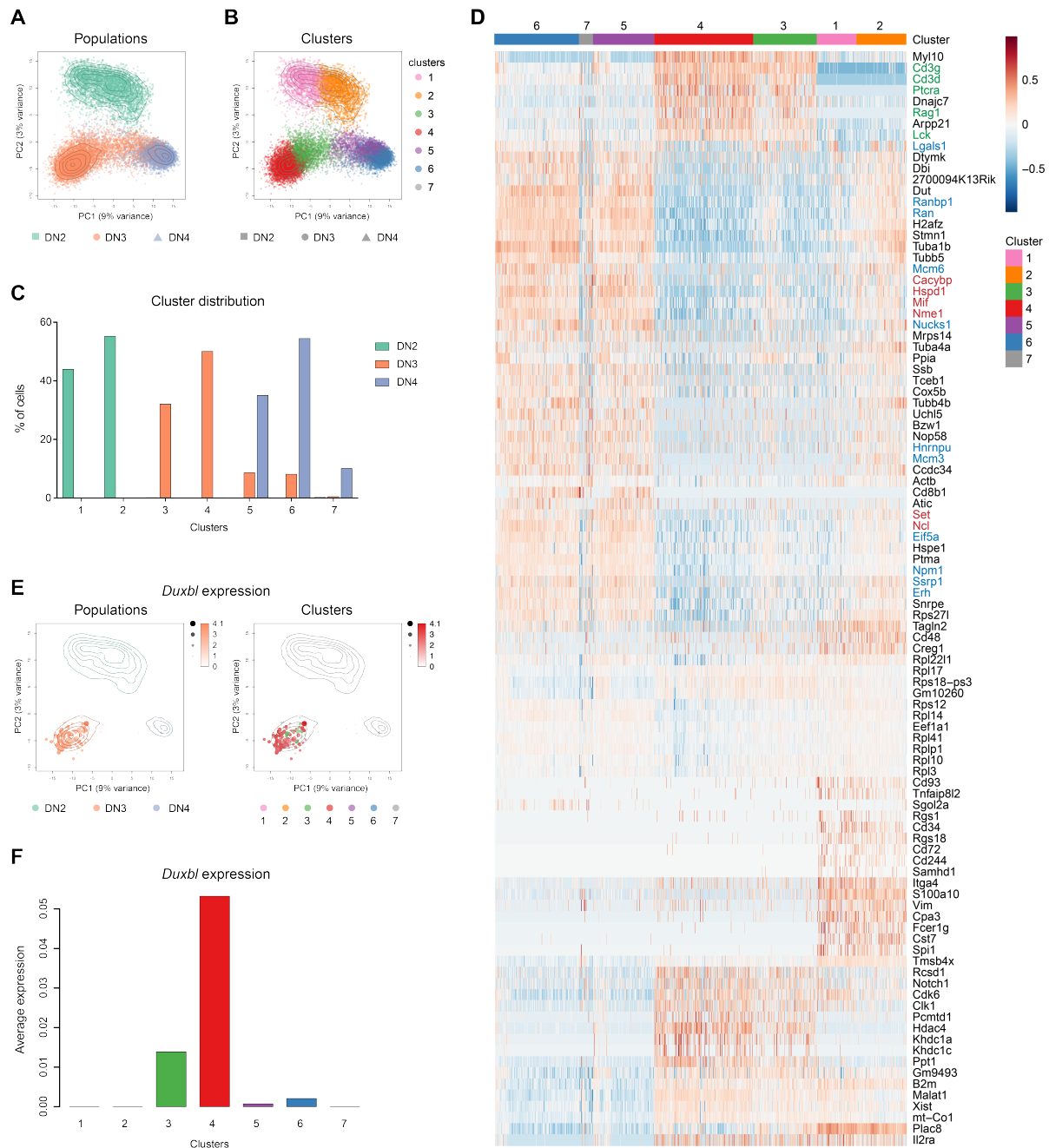


**Figure 3 | Single-cell RNA sequencing elucidates a developmental trajectory through  $\beta$ -selection**

Single-cell RNA sequencing of DN2, DN3, and DN4 cells, performed as described in the Materials and Methods. **A, B**) PCA based on the 500 most variable genes across all cells. The colors represent cells from the different populations (A) or the different clusters (B). Contour lines indicate the density of the DN2, DN3, and DN4 cells in the PCA space. **C**) Relative frequency of DN2, DN3, and DN4 cells within the different clusters. **D**) Heatmap displaying the centered and scaled expression across the 18,128 cells of the top cluster-specific genes (resulting from the union of the top 23 differentially expressed genes from each pairwise

comparison between clusters). The color gradient illustrates the normalized log-counts values centered and scaled across all samples for each gene. Colors at the top indicate the membership of cells to the different clusters. Font colors indicate genes involved in recombination and pre-TCR (green), cell cycle/division and DNA replication (blue), and negative regulation of apoptosis (red). **E**) Expression of *Duxbl* shown in the PCA space. Size and color intensity of the dots indicate relative expression level of *Duxbl* in each cell and the colors correspond to the respective population (left panel) or cluster (right panel). **F**) Bar plot showing the average normalized log-counts of *Duxbl* across all cells from each cluster.

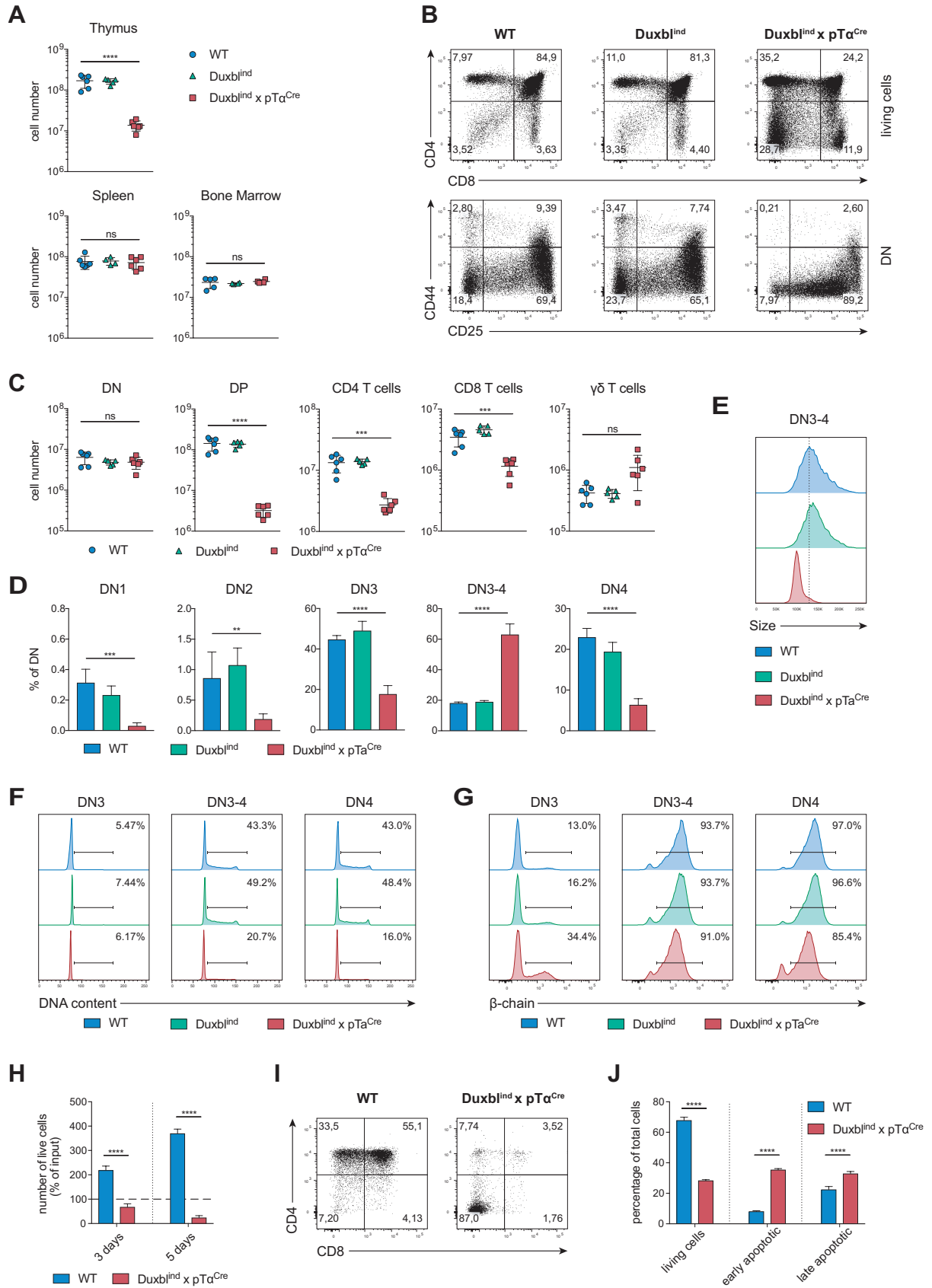


**Figure 4 | Blocked T-cell development in *Duxbl<sup>ind</sup>xpTα<sup>Cre</sup>* mice**

**A)** Total numbers of live, nucleated cells in the thymus, spleen, and bone marrow of WT (n=6), *Duxbl<sup>ind</sup>* (n=5), and *Duxbl<sup>ind</sup>xpTα<sup>Cre</sup>* (n=6) mice. Data were collected from three independent experiments. **B)** Representative FACS plots of CD4 and CD8 expression in total live cells (upper panel) and CD44 and CD25 expression in DN cells (lower panel) of WT, *Duxbl<sup>ind</sup>*, and *Duxbl<sup>ind</sup>xpTα<sup>Cre</sup>* mice. DN cells were gated as CD4, CD8, CD3 and B220 negative. Three independent experiments were performed, with representative data from one experiment shown. **C)** Numbers of DN, DP, CD4 T cells, CD8 T cells, and  $\gamma\delta$ -T cells in WT (n=6), *Duxbl<sup>ind</sup>* (n=5), and *Duxbl<sup>ind</sup>xpTα<sup>Cre</sup>* (n=6) mice. **D)** Frequencies of DN1, DN2, DN3, DN3-4, and DN4 cells as percentage of DN cells in WT (n=6), *Duxbl<sup>ind</sup>* (n=5), and *Duxbl<sup>ind</sup>xpTα<sup>Cre</sup>* (n=6) mice. (C, D) Data were collected from three independent experiments. **E)** Representative histogram showing the size (FSC-A) of DN3-4 cells in WT, *Duxbl<sup>ind</sup>*, and *Duxbl<sup>ind</sup>xpTα<sup>Cre</sup>* mice. Three independent experiments were performed, with representative data from one experiment shown. **F, G)** Histograms showing the DNA content (F) and intracellular  $\beta$ -chain expression (G) of DN3, DN3-4, and DN4 cells in WT, *Duxbl<sup>ind</sup>*, and *Duxbl<sup>ind</sup>xpTα<sup>Cre</sup>* mice. Four independent experiments were performed, with representative data from one experiment shown. **H)** Numbers of sorted DN3 cells from WT and *Duxbl<sup>ind</sup>xpTα<sup>Cre</sup>* mice as percentage of input after three and five days of culture in wells coated with Dll 4 and supplemented with Cxcl12. **I)** Representative FACS plots of sorted DN3 cells from WT and *Duxbl<sup>ind</sup>xpTα<sup>Cre</sup>* mice showing CD4 and CD8 expression after five days of culture. **J)** Frequencies of living, early apoptotic, and late apoptotic cells after three days of culture of sorted DN3 cells from WT and *Duxbl<sup>ind</sup>xpTα<sup>Cre</sup>* mice. Living cells were defined as AnnexinV<sup>-</sup> 7AAD<sup>-</sup>, early apoptotic cells as AnnexinV<sup>+</sup> 7AAD<sup>-</sup>, and late apoptotic cells as AnnexinV<sup>+</sup> 7AAD<sup>+</sup>. (H-J) Three independent experiments were performed, with representative data from one experiment shown. Gate numbers in FACS plots and histograms indicate frequencies of parent gate. DN stages were identified by FACS as shown in Figure S1. Statistical analysis was done with two-tailed unpaired Student's *t* test. \*: p<0.05, \*\*: p<0.01, \*\*\*: p<0.001, \*\*\*\*: p<0.0001. Error bars indicate standard deviation.

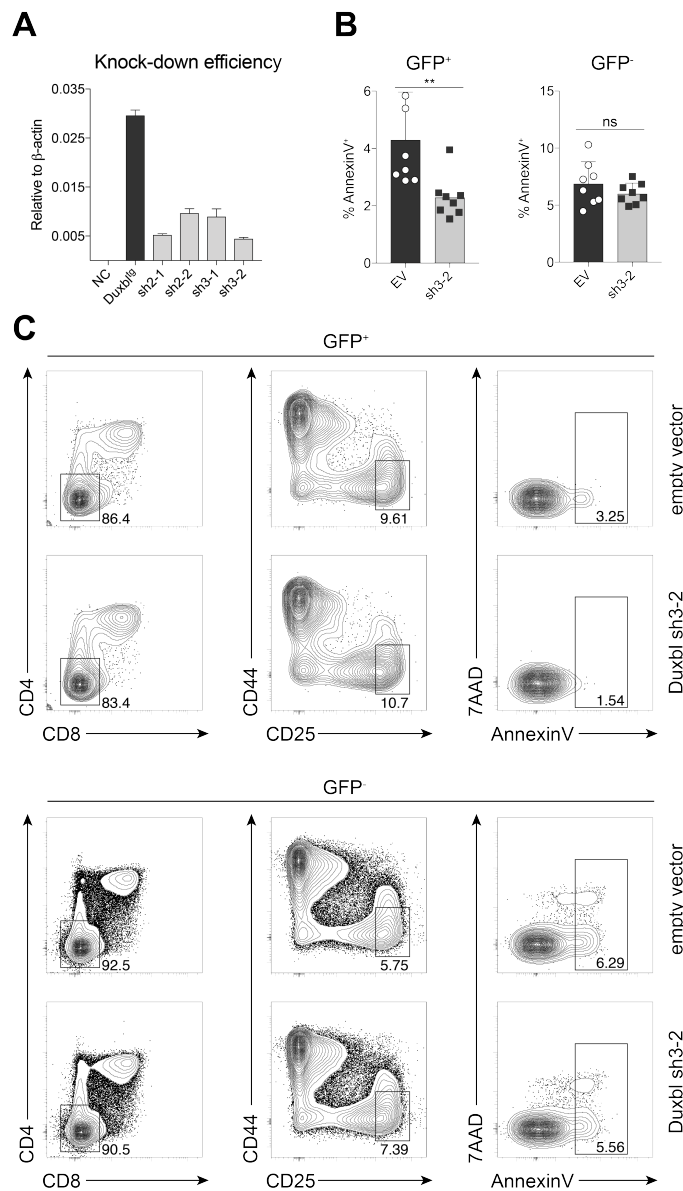


### Figure 5 | Decreased apoptosis in DN3 cells after Duxbl knock-down

**A)** Knockdown efficiency of four different shRNAs illustrated by relative expression of Duxbl in the 40E1 cell line over-expressing Duxbl with or without additional transduction of the described shRNAs. As housekeeping gene  $\beta$ -actin was used. Two independent experiments were performed, with representative data from one experiment shown. **B)** Frequencies of AnnexinV<sup>+</sup> cells within GFP<sup>+</sup> (left panel) or GFP<sup>-</sup> (right panel) cells transduced with an empty vector control or shRNA 3-2 four days after removal of IL-7 from the fetal liver OP9-D111 cultures. Data were collected from three independent experiments. **C)** Representative FACS plots showing CD4 and CD8 expression (left panel), CD44 and CD25 expression within DN (middle panel), and AnnexinV and 7AAD

levels within DN3 cells (right panel) four days after removal of IL-7 from the fetal liver OP9-D111 cultures. Plots were gated either on GFP<sup>+</sup> or GFP<sup>-</sup> cells. Three independent experiments were performed, with representative data from one experiment shown. Gate numbers in FACS plots indicate frequencies of parent gate. Statistical analysis was done with two-tailed unpaired Student's *t* test. \*:  $p < 0.05$ , \*\*:  $p < 0.01$ , \*\*\*:  $p < 0.001$ , \*\*\*\*:  $p < 0.0001$ . Error bars indicate standard deviation.

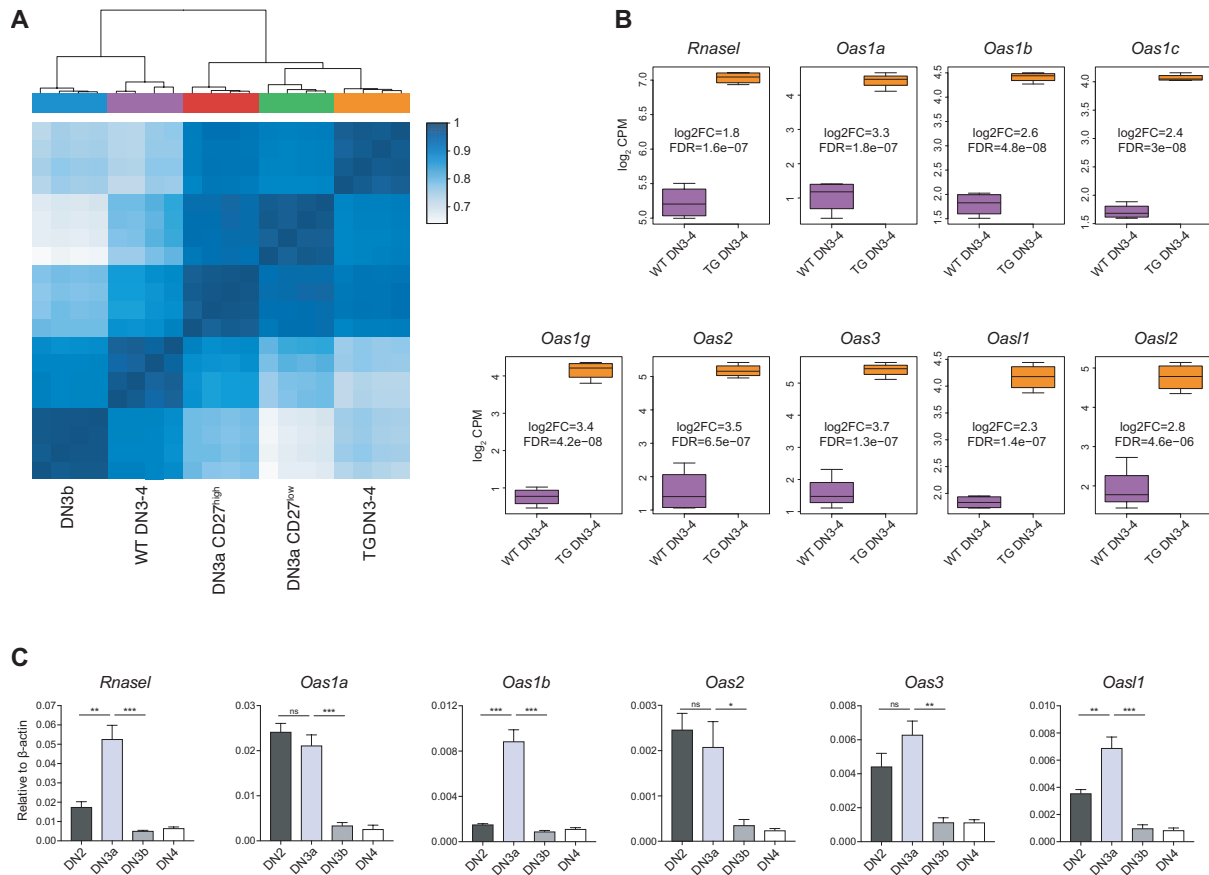


**Figure 6 | Gene expression analysis identifies upregulation of the Oas/RNaseL system in Duxbl transgenic DN3-4 cells**

**A, B)** Bulk RNA sequencing of WT and Duxbl<sup>ind</sup>xpTα<sup>Cre</sup> DN3-4 cells, performed as described in the Materials and Methods. **A)** Heatmap and hierarchical clustering based on the matrix of Spearman correlation across the samples of WT and TG (derived from Duxbl<sup>ind</sup>xpTα<sup>Cre</sup> mice) DN3-4 cells together with WT DN3a CD27<sup>high</sup>, DN3a CD27<sup>low</sup>, and DN3b cells (using the 25% most variable genes). Data were corrected for batch effects across datasets. **B)** Boxplots showing the normalized log<sub>2</sub> CPM of *Rnase1*, *Oas1a*, *Oas1b*, *Oas1c*, *Oas1g*, *Oas2*, *Oas3*, *Oas11*, and *Oas12* in WT and TG (derived from Duxbl<sup>ind</sup>xpTα<sup>Cre</sup> mice) DN3-4 cells. Log<sub>2</sub> FC and FDR are indicated for each gene. **C)** Relative expression of *Rnase1*, *Oas1a*, *Oas1b*, *Oas2*, *Oas3*, and *Oas11* in WT DN2, DN3a, DN3b, and DN4 cells. As housekeeping gene β-actin was used. Data were collected from four independent experiments. Statistical analysis was done with two-tailed unpaired Student's *t* test. \*: p<0.05, \*\*: p<0.01, \*\*\*: p<0.001, \*\*\*\*: p<0.0001. Error bars indicate standard deviation (B) or standard error of the mean (C).



unpaired Student's *t* test. \*:  $p < 0.05$ , \*\*:  $p < 0.01$ , \*\*\*:  $p < 0.001$ , \*\*\*\*:  $p < 0.0001$ . Error bars indicate standard deviation.

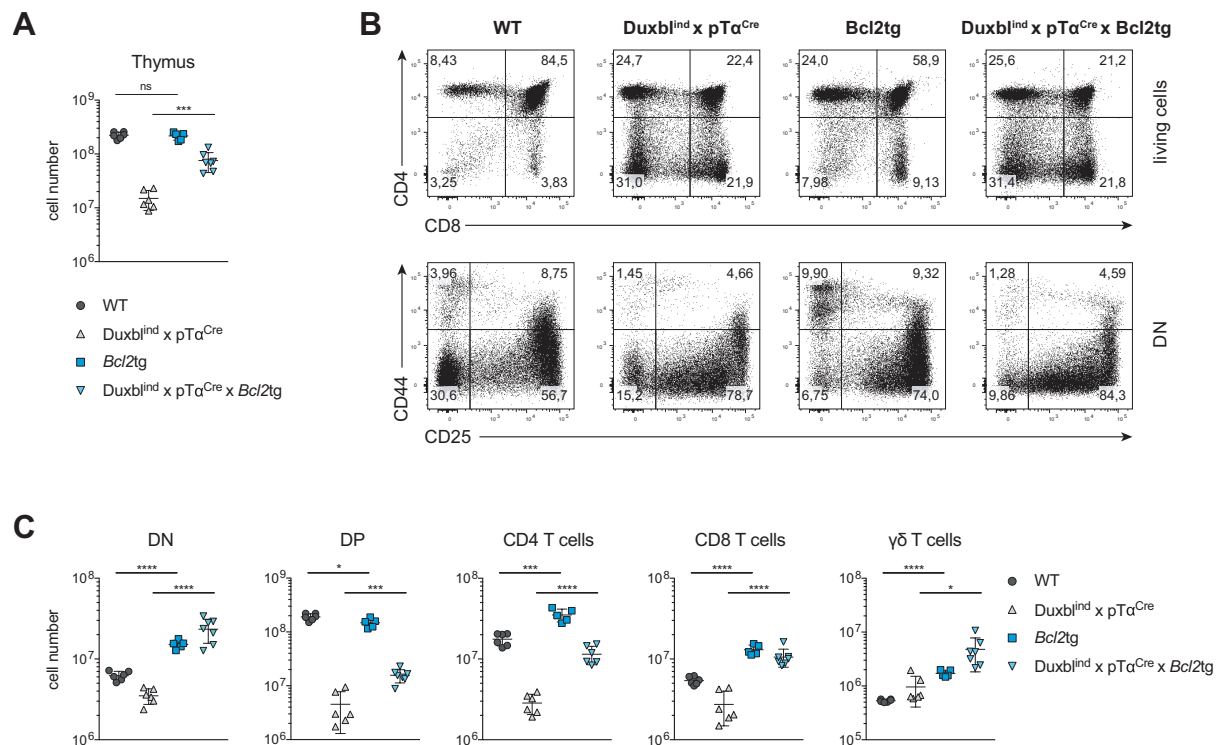


**Figure 8 | Transgenic Bcl2 expression restores T-cell populations in *Duxbl<sup>ind</sup>xpTα<sup>Cre</sup>* mice**

**A)** Total number of live, nucleated cells in the thymus of WT (n=6), *Duxbl<sup>ind</sup>xpTα<sup>Cre</sup>* (n=6), *Bcl2tg* (n=5), and *Duxbl<sup>ind</sup>xpTα<sup>Cre</sup>xBcl2tg* (n=7) mice. Data were collected from four independent experiments. **B)** Representative FACS plots of CD4 and CD8 expression in total live cells (upper panel) and CD44 and CD25 expression in DN cells (lower panel) of WT, *Duxbl<sup>ind</sup>xpTα<sup>Cre</sup>*, *Bcl2tg*, and *Duxbl<sup>ind</sup>xpTα<sup>Cre</sup>xBcl2tg* mice. DN cells were gated as CD4, CD8, CD3 and B220 negative. Four independent experiments were performed, with representative data from one experiment shown. **C)** Numbers of DN, DP, CD4 T cells, CD8 T cells, and  $\gamma\delta$ -T cells in WT (n=6), *Duxbl<sup>ind</sup>xpTα<sup>Cre</sup>* (n=6), *Bcl2tg* (n=5), and *Duxbl<sup>ind</sup>xpTα<sup>Cre</sup>xBcl2tg* (n=7) mice. Data were collected from four independent experiments. Gate numbers in FACS plots indicate frequencies of parent gate. DN stages were identified by FACS as shown in Figure S1. Statistical analysis was done with two-tailed unpaired Student's *t* test. \*:  $p < 0.05$ , \*\*:  $p < 0.01$ , \*\*\*:  $p < 0.001$ , \*\*\*\*:  $p < 0.0001$ . Error bars indicate standard deviation.

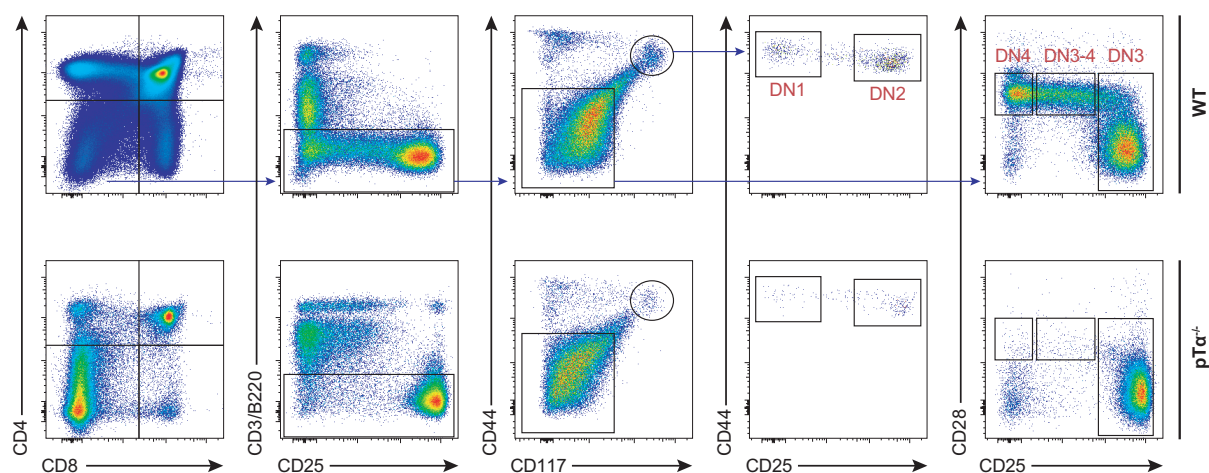


**Figure S1 | Gating strategy for identification of DN stages**

Representative FACS plots showing the gating strategy to identify DN stages in WT (upper panel and  $pT\alpha^{-/-}$  (lower panel) mice. The different populations were all defined as  $CD4^{-}CD8^{-}CD3^{-}B220^{-}$  and additionally as follows: DN1:  $CD25^{-}CD44^{high}CD117^{high}$ ; DN2:  $CD25^{high}CD44^{high}CD117^{high}$ ; DN3:  $CD25^{high}CD44^{low}CD117^{low}$ ; DN3-4:  $CD25^{int}CD44^{low}CD117^{low}CD28^{+}$ ; DN4:  $CD25^{-}CD44^{-}CD117^{-}CD28^{+}$ . Two independent experiments were performed, with representative data from one experiment shown.

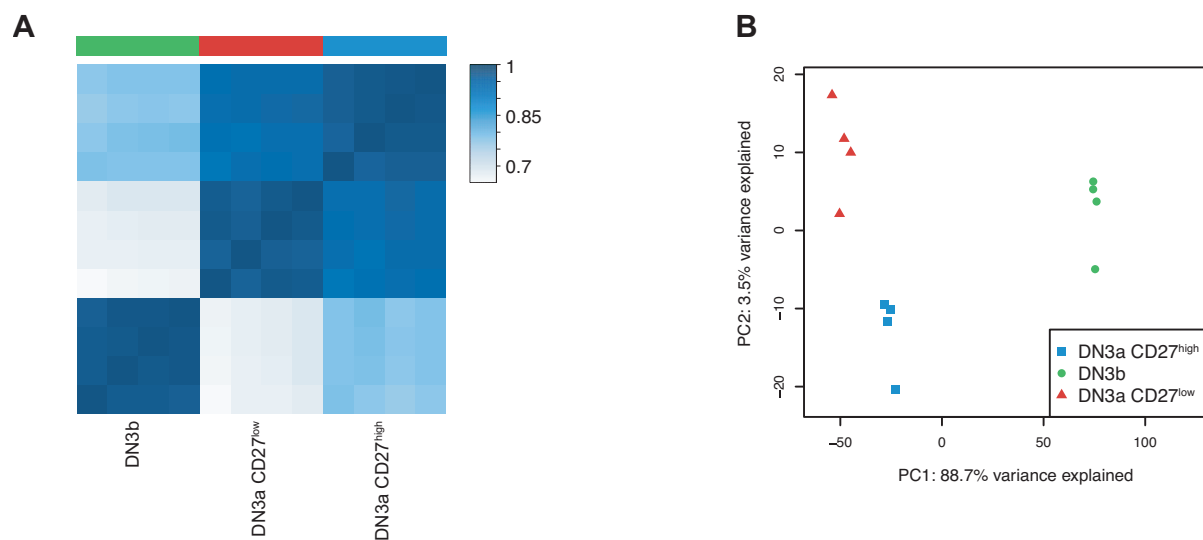


**Figure S2 | Gene expression analysis of WT DN3a CD27<sup>high</sup>, DN3a CD27<sup>low</sup> and DN3b cells**

Bulk RNA-sequencing on DN3a CD27<sup>high</sup>, DN3a CD27<sup>low</sup>, and DN3b cells, performed as described in the Materials and Methods. **A**) Heatmap of Spearman correlation coefficients across samples (using the 25% most variable genes). **B**) Projection of the samples on the 2 first axes of a principal component analysis (based on 25% most variable genes).



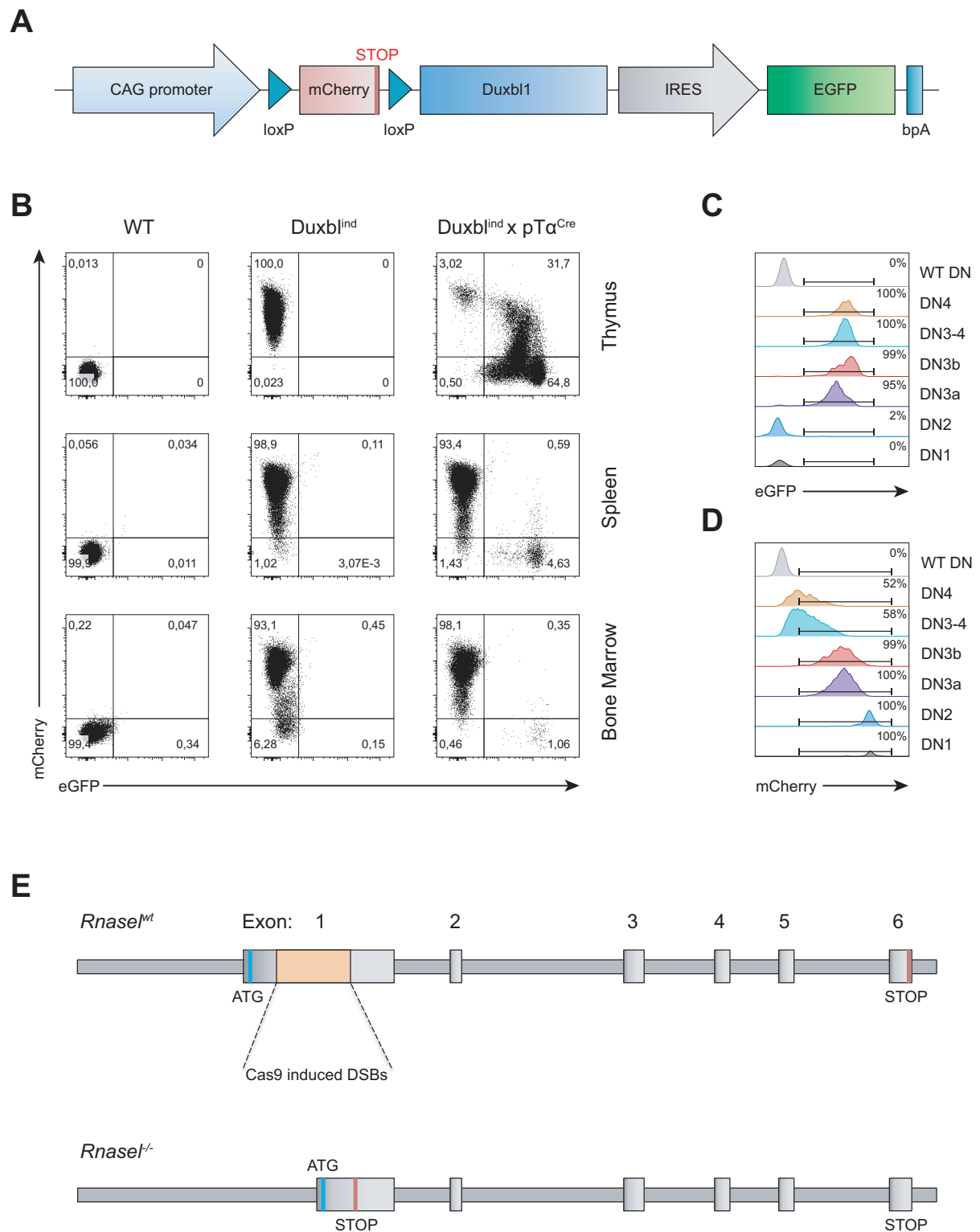


### Figure S4 | Generation of conditional Duxbl transgenic mice

**A)** Schematic figure of the construct used for the generation of conditional Duxbl transgenic mice. CAG promoter driving the expression is followed by an mCherry stop-cassette that is flanked by lox-P sites, followed by Duxbl1 cDNA coupled via an internal-ribosomal-entry-site (IRES) to the enhanced green fluorescent protein (eGFP) gene, ending with the bovine growth

---

hormone polyadenylation site (bpA). **B)** Representative FACS plots of mCherry and eGFP expression in the thymus (upper panel), spleen (middle panel), and bone marrow (lower panel) of WT, *Duxbl<sup>ind</sup>*, and *Duxbl<sup>ind</sup>xpTα<sup>Cre</sup>* mice. **C, D)** Representative histograms showing the frequencies of eGFP (C) and mCherry (D) positive cells of DN1, DN2, DN3a, DN3b, DN3-4, DN4 cells in the thymus of *Duxbl<sup>ind</sup>xpTα<sup>Cre</sup>* mice, and WT DN cells. (B-D) Three independent experiments were performed, with representative data from one experiment shown. **E)** Schematic figure of the genome editing performed for the generation of *RNaseL<sup>-/-</sup>* mice. Two double-strand breaks (DSBs) were introduced in exon 1 of the *Rnase1* gene using the CRISPR/Cas9 system. This resulted in a 328 base-pair deletion, thereby inducing a frame shift and a premature stop-codon (STOP). For analysis mice were bred to homozygosity. Gate numbers in FACS plots and histograms indicate frequencies of parent gate. DN stages were identified by FACS as shown in Figure S1.

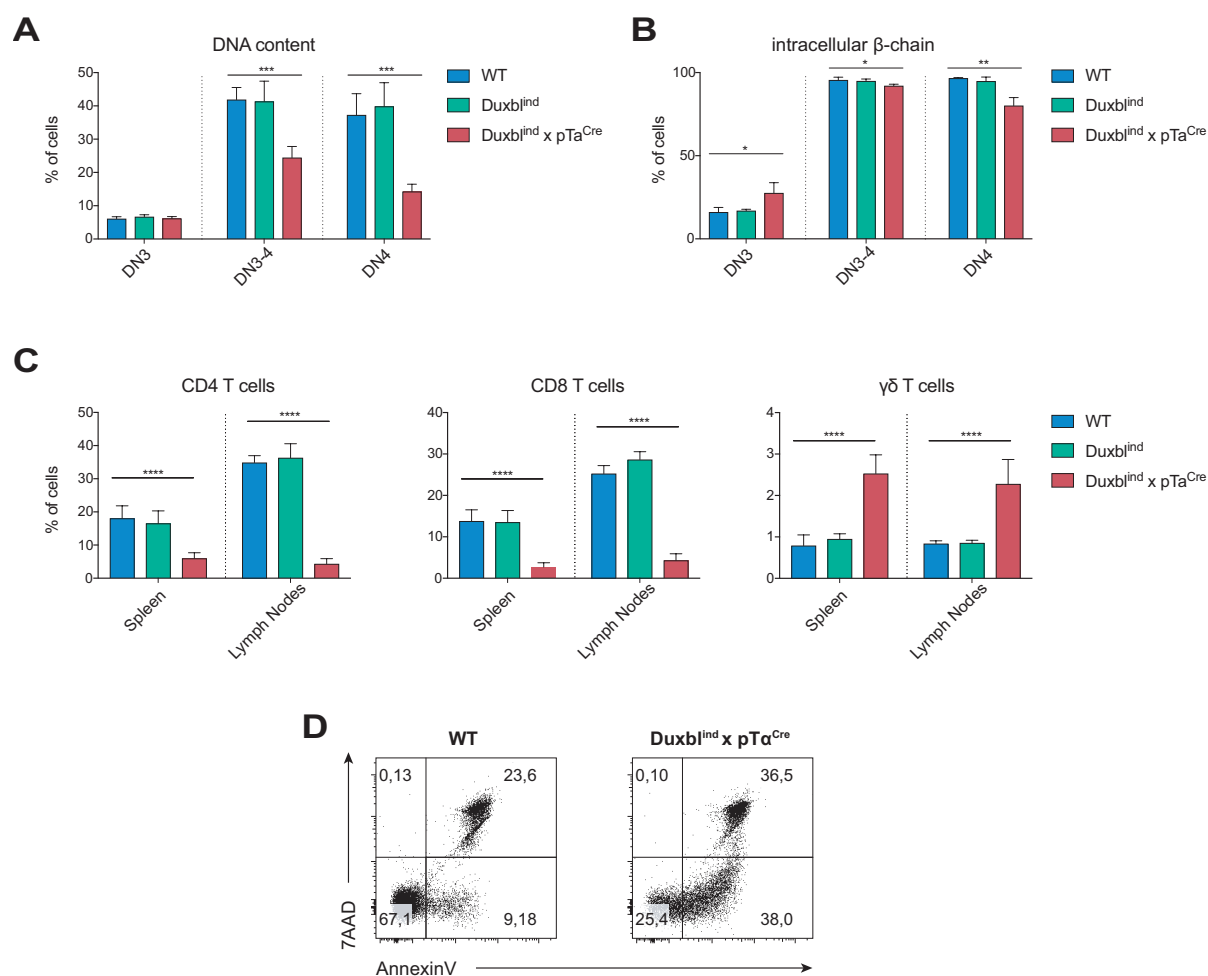


### Figure S5 | Analysis of Duxbl<sup>ind</sup>xpTα<sup>Cre</sup> mice

**A)** Frequency of cells in cycle in DN3, DN3-4, and DN4 cells of WT and Duxbl<sup>ind</sup>xpTα<sup>Cre</sup> mice based on the content of DNA in each cell detected by FACS. **B)** Frequency of cells positive for intracellular β-chain expression in DN3, DN3-4, and DN4 cells of WT and Duxbl<sup>ind</sup>xpTα<sup>Cre</sup> mice. **C)** Frequencies of CD4 T cells (left panel), CD8 T cells (middle panel), and γδ-T cells (right panel) in the spleen and lymph nodes of WT (spleen: n=6, lymph nodes: n=4), Duxbl<sup>ind</sup> (spleen: n=5, lymph nodes: n=4), and Duxbl<sup>ind</sup>xpTα<sup>Cre</sup> (spleen: n=6, lymph nodes: n=4) mice. (A-C) Data were collected from four (A, B) or three (C) independent experiments. **D)** Representative FACS plots of sorted DN3 cells from WT and Duxbl<sup>ind</sup>xpTα<sup>Cre</sup> mice after three days of culture showing living, early apoptotic, and late apoptotic cells based on AnnexinV and 7AAD expression of sorted DN3 cells from WT and Duxbl<sup>ind</sup>xpTα<sup>Cre</sup> mice. Living cells were defined as AnnexinV<sup>-</sup> 7AAD<sup>-</sup>, early apoptotic cells as AnnexinV<sup>+</sup> 7AAD<sup>-</sup>, and late apoptotic cells as AnnexinV<sup>+</sup> 7AAD<sup>+</sup>. Three independent experiments were performed, with representative data from one experiment shown. Gate numbers in FACS plots indicate frequencies of parent gate. DN stages were identified by FACS as shown in Figure S1. Statistical analysis was done with

two-tailed unpaired Student's *t* test. \*:  $p < 0.05$ , \*\*:  $p < 0.01$ , \*\*\*:  $p < 0.001$ , \*\*\*\*:  $p < 0.0001$ . Error bars indicate standard deviation.

---

## References

- Akashi, K., M. Kondo, U. von Freeden-Jeffry, R. Murray, and I.L. Weissman. 1997. Bcl-2 rescues T lymphopoiesis in interleukin-7 receptor-deficient mice. *Cell* 89:1033-1041.
- Balciunaite, G., R. Ceredig, H.J. Fehling, J.C. Zuniga-Pflucker, and A.G. Rolink. 2005a. The role of Notch and IL-7 signaling in early thymocyte proliferation and differentiation. *Eur J Immunol* 35:1292-1300.
- Balciunaite, G., R. Ceredig, and A.G. Rolink. 2005b. The earliest subpopulation of mouse thymocytes contains potent T, significant macrophage, and natural killer cell but no B-lymphocyte potential. *Blood* 105:1930-1936.
- Bell, J.J., and A. Bhandoola. 2008. The earliest thymic progenitors for T cells possess myeloid lineage potential. *Nature* 452:764-767.
- Brekelmans, P., P. van Soest, J. Voerman, P.P. Platenburg, P.J. Leenen, and W. van Ewijk. 1994. Transferrin receptor expression as a marker of immature cycling thymocytes in the mouse. *Cell Immunol* 159:331-339.
- Capone, M., R.D. Hockett, Jr., and A. Zlotnik. 1998. Kinetics of T cell receptor beta, gamma, and delta rearrangements during adult thymic development: T cell receptor rearrangements are present in CD44(+)CD25(+) Pro-T thymocytes. *Proc Natl Acad Sci U S A* 95:12522-12527.
- Ceredig, R., N. Bosco, and A.G. Rolink. 2007. The B lineage potential of thymus settling progenitors is critically dependent on mouse age. *Eur J Immunol* 37:830-837.
- Ceredig, R., and T. Rolink. 2002. A positive look at double-negative thymocytes. *Nat Rev Immunol* 2:888-897.
- Ciofani, M., T.M. Schmitt, A. Ciofani, A.M. Michie, N. Cuburu, A. Aublin, J.L. Maryanski, and J.C. Zuniga-Pflucker. 2004. Obligatory role for cooperative signaling by pre-TCR and Notch during thymocyte differentiation. *J Immunol* 172:5230-5239.
- Ciofani, M., and J.C. Zuniga-Pflucker. 2005. Notch promotes survival of pre-T cells at the beta-selection checkpoint by regulating cellular metabolism. *Nat Immunol* 6:881-888.
- Das, S., and B.P. Chadwick. 2016. Influence of Repressive Histone and DNA Methylation upon D4Z4 Transcription in Non-Myogenic Cells. *PLoS One* 11:e0160022.
- Dobin, A., C.A. Davis, F. Schlesinger, J. Drenkow, C. Zaleski, S. Jha, P. Batut, M. Chaisson, and T.R. Gingeras. 2013. STAR: ultrafast universal RNA-seq aligner. *Bioinformatics* 29:15-21.
- Domen, J., K.L. Gandy, and I.L. Weissman. 1998. Systemic overexpression of BCL-2 in the hematopoietic system protects transgenic mice from the consequences of lethal irradiation. *Blood* 91:2272-2282.
- Dudley, E.C., H.T. Petrie, L.M. Shah, M.J. Owen, and A.C. Hayday. 1994. T cell receptor beta chain gene rearrangement and selection during thymocyte development in adult mice. *Immunity* 1:83-93.
- Fehling, H.J., B.M. Iritani, A. Krotkova, K.A. Forbush, C. Laplace, R.M. Perlmutter, and H. von Boehmer. 1997. Restoration of thymopoiesis in pT alpha<sup>-/-</sup> mice by anti-CD3epsilon antibody treatment or with transgenes encoding activated Lck or tailless pT alpha. *Immunity* 6:703-714.
- Fehling, H.J., A. Krotkova, C. Saint-Ruf, and H. von Boehmer. 1995. Crucial role of the pre-T-cell receptor alpha gene in development of alpha beta but not gamma delta T cells. *Nature* 375:795-798.
- Gaidatzis, D., A. Lerch, F. Hahne, and M.B. Stadler. 2015. QuasR: quantification and annotation of short reads in R. *Bioinformatics* 31:1130-1132.
- Germain, R.N. 2002. T-cell development and the CD4-CD8 lineage decision. *Nat Rev Immunol* 2:309-322.
- Godfrey, D.I., J. Kennedy, P. Mombaerts, S. Tonegawa, and A. Zlotnik. 1994. Onset of TCR-beta gene rearrangement and role of TCR-beta expression during CD3-CD4-CD8-thymocyte differentiation. *J Immunol* 152:4783-4792.

- Godfrey, D.I., J. Kennedy, T. Suda, and A. Zlotnik. 1993. A developmental pathway involving four phenotypically and functionally distinct subsets of CD3-CD4-CD8- triple-negative adult mouse thymocytes defined by CD44 and CD25 expression. *J Immunol* 150:4244-4252.
- Godfrey, D.I., A. Zlotnik, and T. Suda. 1992. Phenotypic and functional characterization of c-kit expression during intrathymic T cell development. *J Immunol* 149:2281-2285.
- Gravestain, L.A., W. van Ewijk, F. Ossendorp, and J. Borst. 1996. CD27 cooperates with the pre-T cell receptor in the regulation of murine T cell development. *J Exp Med* 184:675-685.
- Haueter, S., M. Kawasumi, I. Asner, U. Brykczynska, P. Cinelli, S. Moisyadi, K. Burki, A.H. Peters, and P. Pelczar. 2010. Genetic vasectomy-overexpression of Prm1-EGFP fusion protein in elongating spermatids causes dominant male sterility in mice. *Genesis* 48:151-160.
- Irving, B.A., F.W. Alt, and N. Killeen. 1998. Thymocyte development in the absence of pre-T cell receptor extracellular immunoglobulin domains. *Science* 280:905-908.
- Jacobi, A.M., G.R. Rettig, R. Turk, M.A. Collingwood, S.A. Zeiner, R.M. Quadros, D.W. Harms, P.J. Bonthuis, C. Gregg, M. Ohtsuka, C.B. Gurumurthy, and M.A. Behlke. 2017. Simplified CRISPR tools for efficient genome editing and streamlined protocols for their delivery into mammalian cells and mouse zygotes. *Methods* 121-122:16-28.
- Jacobs, H., J. Iacomini, M. van de Ven, S. Tonegawa, and A. Berns. 1996. Domains of the TCR beta-chain required for early thymocyte development. *J Exp Med* 184:1833-1843.
- Kawazu, M., G. Yamamoto, M. Yoshimi, K. Yamamoto, T. Asai, M. Ichikawa, S. Seo, M. Nakagawa, S. Chiba, M. Kurokawa, and S. Ogawa. 2007. Expression profiling of immature thymocytes revealed a novel homeobox gene that regulates double-negative thymocyte development. *J Immunol* 179:5335-5345.
- Kondo, M., I.L. Weissman, and K. Akashi. 1997. Identification of clonogenic common lymphoid progenitors in mouse bone marrow. *Cell* 91:661-672.
- Kreslavsky, T., M. Gleimer, M. Miyazaki, Y. Choi, E. Gagnon, C. Murre, P. Sicinski, and H. von Boehmer. 2012. beta-Selection-induced proliferation is required for alphabeta T cell differentiation. *Immunity* 37:840-853.
- Krueger, A., and H. von Boehmer. 2007. Identification of a T lineage-committed progenitor in adult blood. *Immunity* 26:105-116.
- Liberzon, A., C. Birger, H. Thorvaldsdottir, M. Ghandi, J.P. Mesirov, and P. Tamayo. 2015. The Molecular Signatures Database (MSigDB) hallmark gene set collection. *Cell Syst* 1:417-425.
- Livak, F., M. Tourigny, D.G. Schatz, and H.T. Petrie. 1999. Characterization of TCR gene rearrangements during adult murine T cell development. *J Immunol* 162:2575-2580.
- Luche, H., T. Nageswara Rao, S. Kumar, A. Tasdogan, F. Beckel, C. Blum, V.C. Martins, H.R. Rodewald, and H.J. Fehling. 2013. In vivo fate mapping identifies pre-TCRalpha expression as an intra- and extrathymic, but not prethymic, marker of T lymphopoiesis. *J Exp Med* 210:699-714.
- Luis, T.C., S. Luc, T. Mizukami, H. Boukarabila, S. Thongjuea, P.S. Woll, E. Azzoni, A. Giustacchini, M. Lutteropp, T. Bouriez-Jones, H. Vaidya, A.J. Mead, D. Atkinson, C. Boiers, J. Carrelha, I.C. Macaulay, R. Patient, F. Geissmann, C. Nerlov, R. Sandberg, M. de Bruijn, C.C. Blackburn, I. Godin, and S.E.W. Jacobsen. 2016. Initial seeding of the embryonic thymus by immune-restricted lympho-myeloid progenitors. *Nat Immunol* 17:1424-1435.
- Lun, A.T., D.J. McCarthy, and J.C. Marioni. 2016. A step-by-step workflow for low-level analysis of single-cell RNA-seq data with Bioconductor. *F1000Res* 5:2122.
- Maillard, I., L. Tu, A. Sambandam, Y. Yashiro-Ohtani, J. Millholland, K. Keeshan, O. Shestova, L. Xu, A. Bhandoola, and W.S. Pear. 2006. The requirement for Notch signaling at the beta-selection checkpoint in vivo is absolute and independent of the pre-T cell receptor. *J Exp Med* 203:2239-2245.

- Malissen, M., A. Gillet, L. Ardouin, G. Bouvier, J. Trucy, P. Ferrier, E. Vivier, and B. Malissen. 1995. Altered T cell development in mice with a targeted mutation of the CD3-epsilon gene. *EMBO J* 14:4641-4653.
- Massa, S., G. Balciunaite, R. Ceredig, and A.G. Rolink. 2006. Critical role for c-kit (CD117) in T cell lineage commitment and early thymocyte development in vitro. *Eur J Immunol* 36:526-532.
- McCarthy, D.J., K.R. Campbell, A.T. Lun, and Q.F. Wills. 2017. Scater: pre-processing, quality control, normalization and visualization of single-cell RNA-seq data in R. *Bioinformatics* 33:1179-1186.
- Moran, A.E., K.L. Holzapfel, Y. Xing, N.R. Cunningham, J.S. Maltzman, J. Punt, and K.A. Hogquist. 2011. T cell receptor signal strength in Treg and iNKT cell development demonstrated by a novel fluorescent reporter mouse. *J Exp Med* 208:1279-1289.
- O'Reilly, L.A., D.C. Huang, and A. Strasser. 1996. The cell death inhibitor Bcl-2 and its homologues influence control of cell cycle entry. *EMBO J* 15:6979-6990.
- Palmiter, R.D., H.Y. Chen, and R.L. Brinster. 1982. Differential regulation of metallothionein-thymidine kinase fusion genes in transgenic mice and their offspring. *Cell* 29:701-710.
- Radtke, F., A. Wilson, G. Stark, M. Bauer, J. van Meerwijk, H.R. MacDonald, and M. Aguet. 1999. Deficient T cell fate specification in mice with an induced inactivation of Notch1. *Immunity* 10:547-558.
- Robinson, M.D., D.J. McCarthy, and G.K. Smyth. 2010. edgeR: a Bioconductor package for differential expression analysis of digital gene expression data. *Bioinformatics* 26:139-140.
- Rodewald, H.R., K. Kretzschmar, S. Takeda, C. Hohl, and M. Dessing. 1994. Identification of pro-thymocytes in murine fetal blood: T lineage commitment can precede thymus colonization. *EMBO J* 13:4229-4240.
- Saint-Ruf, C., K. Ungewiss, M. Groettrup, L. Bruno, H.J. Fehling, and H. von Boehmer. 1994. Analysis and expression of a cloned pre-T cell receptor gene. *Science* 266:1208-1212.
- Sambandam, A., I. Maillard, V.P. Zediak, L. Xu, R.M. Gerstein, J.C. Aster, W.S. Pear, and A. Bhandoola. 2005. Notch signaling controls the generation and differentiation of early T lineage progenitors. *Nat Immunol* 6:663-670.
- Saran, N., M. Lyszkiewicz, J. Pommerencke, K. Witzlau, R. Vakilzadeh, M. Ballmaier, H. von Boehmer, and A. Krueger. 2010. Multiple extrathymic precursors contribute to T-cell development with different kinetics. *Blood* 115:1137-1144.
- Serwold, T., L.I. Ehrlich, and I.L. Weissman. 2009. Reductive isolation from bone marrow and blood implicates common lymphoid progenitors as the major source of thymopoiesis. *Blood* 113:807-815.
- Shadle, S.C., J.W. Zhong, A.E. Campbell, M.L. Conerly, S. Jagannathan, C.J. Wong, T.D. Morello, S.M. van der Maarel, and S.J. Tapscott. 2017. DUX4-induced dsRNA and MYC mRNA stabilization activate apoptotic pathways in human cell models of facioscapulohumeral dystrophy. *PLoS Genet* 13:e1006658.
- Shinkai, Y., G. Rathbun, K.P. Lam, E.M. Oltz, V. Stewart, M. Mendelsohn, J. Charron, M. Datta, F. Young, A.M. Stall, and et al. 1992. RAG-2-deficient mice lack mature lymphocytes owing to inability to initiate V(D)J rearrangement. *Cell* 68:855-867.
- Silverman, R.H. 2007. A scientific journey through the 2-5A/RNase L system. *Cytokine Growth Factor Rev* 18:381-388.
- Subramanian, A., P. Tamayo, V.K. Mootha, S. Mukherjee, B.L. Ebert, M.A. Gillette, A. Paulovich, S.L. Pomeroy, T.R. Golub, E.S. Lander, and J.P. Mesirov. 2005. Gene set enrichment analysis: A knowledge-based approach for interpreting genome-wide expression profiles. *Proc Natl Acad Sci U S A* 102:15545-15550.
- Taghon, T., M.A. Yui, R. Pant, R.A. Diamond, and E.V. Rothenberg. 2006. Developmental and molecular characterization of emerging beta- and gammadelta-selected pre-T cells in the adult mouse thymus. *Immunity* 24:53-64.
- Tramont, P.C., A.C. Tosello-Tramont, Y. Shen, A.K. Duley, A.E. Sutherland, T.P. Bender, D.R. Littman, and K.S. Ravichandran. 2010. CXCR4 acts as a costimulator during thymic beta-selection. *Nat Immunol* 11:162-170.

- 
- Tussiwand, R., C. Engdahl, N. Gehre, N. Bosco, R. Ceredig, and A.G. Rolink. 2011. The preTCR-dependent DN3 to DP transition requires Notch signaling, is improved by CXCL12 signaling and is inhibited by IL-7 signaling. *Eur J Immunol* 41:3371-3380.
- Wada, H., K. Masuda, R. Satoh, K. Kakugawa, T. Ikawa, Y. Katsura, and H. Kawamoto. 2008. Adult T-cell progenitors retain myeloid potential. *Nature* 452:768-772.
- Williams, J.A., K.S. Hathcock, D. Klug, Y. Harada, B. Choudhury, J.P. Allison, R. Abe, and R.J. Hodes. 2005. Regulated costimulation in the thymus is critical for T cell development: dysregulated CD28 costimulation can bypass the pre-TCR checkpoint. *J Immunol* 175:4199-4207.
- Wu, D., and G.K. Smyth. 2012. Camera: a competitive gene set test accounting for inter-gene correlation. *Nucleic Acids Res* 40:e133.
- Wu, S.L., M.S. Tsai, S.H. Wong, H.M. Hsieh-Li, T.S. Tsai, W.T. Chang, S.L. Huang, C.C. Chiu, and S.H. Wang. 2010. Characterization of genomic structures and expression profiles of three tandem repeats of a mouse double homeobox gene: *Duxbl*. *Dev Dyn* 239:927-940.
- Yui, M.A., and E.V. Rothenberg. 2014. Developmental gene networks: a triathlon on the course to T cell identity. *Nat Rev Immunol* 14:529-545.
- Zhou, A., J. Paranjape, T.L. Brown, H. Nie, S. Naik, B. Dong, A. Chang, B. Trapp, R. Fairchild, C. Colmenares, and R.H. Silverman. 1997. Interferon action and apoptosis are defective in mice devoid of 2',5'-oligoadenylate-dependent RNase L. *EMBO J* 16:6355-6363.
- Zlotoff, D.A., and A. Bhandoola. 2011. Hematopoietic progenitor migration to the adult thymus. *Ann N Y Acad Sci* 1217:122-138.

## 5. Discussion

During life blood cells have to be continuously produced in the bone marrow. The developmental process starts with the hematopoietic stem cells at the apex, which gradually differentiate into the different cell types of the hematopoietic system. Multiple extrinsic and intrinsic molecular mechanisms guide this progress by regulating transcriptional networks and thereby establishing gene expression profiles that direct the cells through intermediate progenitor stages up to their final maturation. For the generation of the adaptive immunity, in addition, random recombination of the gene segments encoding antigen receptors has to be initiated and controlled ensuring the production of the incredible diversity of the antigen receptor specificities resulting in the protection against any pathogen. Any alteration in these strictly controlled processes can result in severe disturbances of the body's immune system, which can cause the development of immunodeficiency, autoimmunity, and leukemia. Therefore, investigation of the molecular mechanisms and regulations that guide the differentiation and selection processes is important for the understanding and potential treatment of immune pathology.

### 5.1. The roles of Flt3-ligand and IL-7 in lymphopoiesis

With the use of different transgenic and knockout mouse models we explored the role of the cytokines Flt3-ligand and IL-7 in lymphocyte development. The crucial function of IL-7 for the generation of B and T cells has been previously demonstrated by the dramatic effect of the absence either of the cytokine or its receptor (Peschon et al., 1994; von Freeden-Jeffry et al., 1995). Upon Bcl2 over-expression, T-cell but not B-cell development was rescued, indicating that IL-7 acts in an instructive manner on B-cell progenitors (Akashi et al., 1997; Kondo et al., 1997a; Maraskovsky et al., 1997; Maraskovsky et al., 1998). This hypothesis was further strengthened by the observation of reduced Ebf1 expression in CLPs of IL-7 deficient mice, suggesting that IL-7 initiates the B-cell fate by induction of Ebf1 and subsequently of Pax5 expression (Dias et al., 2005). However, more recently results opposing that hypothesis were reported. Thus, Bcl2 over-expression in conditional Stat5<sup>-/-</sup> mice was shown to be sufficient to rescue the development of CD19<sup>+</sup> cells (Malin et al., 2010). Moreover, it was shown that Stat5 signaling is responsible for the induction of the anti-apoptotic factor Mcl1, suggesting a role of IL-7 as survival factor. In accordance with that, the Ebf1 reduction within the CLP compartment in *Il7*<sup>-/-</sup> mice (Tsapogas et al., 2011) could also be explained by the specific loss of Ebf1<sup>+</sup> cells within the Ly6D<sup>+</sup> CLP compartment, caused by missing survival signals rather than an active induction of Ebf1 by IL-7.

Even though the role of IL-7 in survival of CD19<sup>+</sup> cells has been elegantly shown by over-expressing Bcl2 in Stat5<sup>-/-</sup> mice (Malin et al., 2010), these studies could not address the potential role of IL-7 in instructing B cell commitment, which is initiated at the molecular level prior to CD19 expression, at the Ly6D<sup>+</sup> CLP/EPLM stage (Jensen et al., 2018; Mansson et al., 2008). Indeed, in the conditional Rag1<sup>Cre</sup>xStat5<sup>-/-</sup> mice used by Malin et al no reduction was observed in the number of CLP, as it is the case with IL-7<sup>-/-</sup> mice (Dias et al., 2005; Tsapogas et al., 2011), suggesting that efficient deletion of Stat5 occurred only after commitment to the B-cell lineage and CD19 expression. Therefore, we further investigated the role of IL-7 in the Ly6D<sup>+</sup> CLP and EPLM compartments. Breeding of IL-7<sup>-/-</sup> to Flt3-ligand transgenic mice (hereafter FLtg and FLtgxIL-7<sup>-/-</sup> mice) resulted in a complete rescue of the Ly6D<sup>+</sup> CLP/EPLM compartment as well as of the early B-cell populations (section 4.1.1.; Figure 2). The main effect of Flt3-ligand is induction of proliferation of Flt3<sup>+</sup>CD19<sup>-</sup> cells, as seen by increased cycling and the expansion of the CLP/EPLM progenitors in FLtg mice (section 4.1.1.; Figure 1+6). Furthermore, it expands also upstream precursors within the LSK compartment, thereby further increasing the input into the CLP/EPLM compartment (Tsapogas et al., 2014). Transgenic expression of IL-7 on the other hand does not lead to an expansion of Ly6D<sup>+</sup> CLP/EPLM cells or any significant change in their cycling profile, therefore excluding a proliferative role at that stage in development (section 4.1.1.; Figure 5). Due to the use of ligand and not receptor knockout mice we were further able to assess the B-cell potential of these cells *in vitro*. In agreement with the recovery of early B-cell populations in FLtgxIL-7<sup>-/-</sup> mice, the B-cell potential of Ly6D<sup>+</sup> uncommitted progenitors was fully restored (section 4.1.11; Figure 3A). Interestingly, the same rescue of potential was also observed after crossing of the IL-7<sup>-/-</sup> mice to the Bcl2 transgenic strain, confirming that the major role of IL-7 prior to commitment is survival (section 4.1.1.; Figure 4). Thus, the dramatic increase of Ly6D<sup>+</sup> CLP and EPLM due to high levels of Flt3-ligand surpasses the need of IL-7 as survival factor at this stage, resulting in enough cells committing to the B-cell lineage for efficient populating of the early B-cell progenitor pool. This clearly indicates a rather permissive role of IL-7 in B-cell differentiation, acting as a survival factor on uncommitted progenitor cells. However, Flt3-ligand cannot replace the proliferative function of IL-7 on pre-B cells, explaining the still apparent reduction of the IgM<sup>+</sup> compartments in these mice (section 4.1.1.; Figure 2C+D).

The observation that high levels of Flt3-ligand can replace the need of IL-7 for the generation of B-cells might also be the explanation for the discrepancy on the IL-7 dependency of fetal and adult B-cell development. It can be postulated that fetal Ly6D<sup>+</sup> CLP/EPLM progenitors are exposed to higher levels of Flt3-ligand and/or are more sensitive to its downstream signaling than their adult counterparts, thus eliminating the need for IL-7. This hypothesis is supported by the strong dependency of fetal B lymphopoiesis on Flt3-ligand (Jensen et al., 2008).

Even though these results clearly demonstrate the importance of Flt3-ligand for the generation of B cells, there is no evidence for an instructive role, but rather for a permissive proliferative function on the uncommitted progenitor cells. This is evident by the reduced levels of Ebf1 and Pax5 in FLtg Ly6D<sup>+</sup> EPLM progenitors compared to their WT counterparts, which is most likely due to reduced numbers of Ebf1<sup>+</sup>Ly6D<sup>+</sup>CD19<sup>-</sup> progenitor cells (section 4.1.1.; Figure 3B-D). Since Flt3 and Pax5 are not expressed on the same cells, one possible explanation is that enhanced Flt3 signaling keeps the uncommitted CD19<sup>-</sup> cells in a more “undifferentiated” state (Holmes et al., 2006), or it might be that another not yet known factor that is responsible for Ebf1 and Pax5 induction is limited in FLtg mice. Moreover, as recently shown by Rodrigues et al, Ly6D<sup>+</sup>IL-7R<sup>+</sup>Flt3<sup>+</sup>CD19<sup>-</sup> progenitors can also differentiate to pDCs (Rodrigues et al., 2018). Thus, high Flt3-ligand could lead to more cells differentiating towards this pathway, resulting in a reduced fraction of the progenitors committing to the B-cell pathway. Indeed, pDCs are one of the most increased populations in FLtg mice (Tsapogas et al., 2014).

Remarkably, even though high levels of Flt3-ligand can rescue the initiation of B-cell commitment in IL-7<sup>-/-</sup> mice, over-expression of Flt3-ligand results in reduced numbers of pre-B and immature B cells under physiological IL-7 levels (Tsapogas et al., 2014). As Flt3 is not expressed by pre-B cells this effect can only be indirect. Since IL-7R<sup>+</sup> progenitor populations and pDCs are heavily increased in these mice, we hypothesized that IL-7 availability might become limited for pre-B cells, which would dampen sufficient proliferation at that stage. Binding of IL-7 to its receptor was previously suggested as a mechanism that is regulating the abundance of the cytokine (Mazzucchelli and Durum, 2007). Previous experiments have shown that injection of IL-7/anti-IL-7 complexes into FLtg mice indeed restored the numbers of pre-B cells (Tsapogas et al., 2014). In order to further test this theory and to investigate the synergistic role of Flt3-ligand and IL-7 in lymphopoiesis, we crossed FLtg with mice over-expressing IL-7 (hereafter IL-7tg and FLtgxIL-7tg). Analysis of bone marrow B-cell development in FLtgxIL-7tg mice revealed a similar decrease in numbers of the pre-B and immature B cells stage compared to IL-7tg mice (section 4.1.2.; Figure 2B+C). Thus, reduced IL-7 availability can be excluded as the reason for the reduced pre-B cells in FLtg mice. It is still feasible that a not yet known, but required factor gets limited upon Flt3-ligand over-expression. Alternatively, a factor that has a detrimental effect on pre-B cells might be elevated in FLtg mice. Potential candidates that could cause such an effect are type I interferons, which inhibit the IL-7 dependent growth of B-cell progenitors as well as of DN thymocytes (Lin et al., 1998; Su et al., 1997; Wang et al., 1995). Elevated levels of type I interferons in FLtg mice could be a result of the massive expansion of cells like pDCs, which are the main source of type I interferons in the context of viral infections, or bone marrow resident macrophages. Similar to B-cell progenitors, early DN stages in the thymus are reduced upon Flt3-ligand over-

expression (section 4.1.2.; Suppl. Figure 2). A secondary effect, such as elevated interferon levels, could be envisaged for this observation as well. Since already DN1 cells are also affected by high Flt3-ligand levels, the homing capacity of the thymus seeding progenitor might be changed due to high levels of Flt3-ligand, resulting in a reduced number of seeding cells, even though all the potential thymus seeding progenitor (TSP) populations are dramatically increased in the bone marrow of these mice. Alternatively, the TSP or ETP lineage potential might be altered due to high levels of Flt3-ligand, leading to the divergence from T-cell generation to the production of, for instance, myeloid cells.

Further analyses of FLtgxIL-7tg mice revealed a synergistic effect of the two cytokines in lymphopoiesis. This is evident in the tremendous expansion of progenitor and mature lymphocyte populations, resulting in a huge enlargement of secondary lymphoid organs like the spleen and lymph nodes (section 4.1.2.; Figure 1-5). High levels of Flt3-ligand expand the early progenitor population such as MPPs, CLPs, and EPLMs. Additional IL-7 expression does not affect the proliferation of CLPs and EPLMs, but it acts as a survival factor on these cells. However, IL-7 instead promotes the proliferation of committed CD19<sup>+</sup> progenitors. Together the elevated levels of both cytokines result in a not only additive effect on the expansion of the cells, but rather in a synergistic one in comparison to the single transgenic counterparts. This is most profoundly manifested in the secondary lymphoid organs which can enlarge their size to incorporate more cells, contrary to the bone marrow where space is restricted. Strikingly, the spleen and also the lymph nodes of FLtgxIL-7tg mice contained not only mature, but also significant numbers of all B-cell progenitor stages (section 4.1.2.; Figure 3). Since Flt3-ligand expands also MPPs, we wondered whether these cells are present in the secondary lymphoid organs of the double transgenic mice as well. Indeed, we were able to detect substantial numbers of MPPs in the spleen and also within lymph nodes (section 4.1.2.; Figure 5). This effect cannot be attributed to high levels of IL-7, since MPPs are negative for its receptor. One potential explanation for the accumulation of all these progenitor populations in the periphery is that they are pushed into migration due to space and resource restrictions in the bone marrow. Indeed, an increase of all precursor B-cell stages as well as uncommitted progenitors such as CLPs, EPLMs, and even MPPs could be detected in the blood of FLtgxIL-7tg mice (section 4.1.2.; Figure 6). Interestingly, true HSCs, defined as CD48<sup>-</sup>CD150<sup>+</sup> LSK, could not be detected in the lymph nodes and only in small numbers in the spleen, and were even decreased in the bone marrow (section 4.1.2.; Figure 5). This reduction was already previously described for FLtg mice and is therefore a consequence of increased availability of Flt3-ligand (Tsapogas et al., 2014). Again, this reduction might be caused by an indirect effect, since HSCs themselves are surface negative for Flt3. However, it has to be considered that low amounts of the receptor might be expressed below the FACS detection limit, since in some of

them Flt3 mRNA could be detected (Mooney et al., 2017). Moreover, an effect on SLAM marker expression by high Flt3-ligand levels cannot be excluded.

The functionality of the precursors found in lymph nodes of FLtgxIL-7tg mice was assessed by transplantation experiments, revealing multilineage reconstitution after the primary and even after a secondary transplantation (section 4.1.2.; Figure 7+8). Thus, lymph nodes of double transgenic mice can support the accumulation of functional multipotent progenitors and potentially even HSCs, since reconstitution of multiple lineages after a secondary transplantation is indicative of self-renewal capacity. Furthermore, the functionality of the precursors indicates that the lymph node is a site of active ongoing hematopoiesis, but further investigations are needed to fully resolve this notion. As a result of the described data, it becomes evident that hematopoiesis can take place also in secondary lymphoid organs under extreme circumstances as it is the case in FLtgxIL-7tg mice. These animals exhibit the phenotype of a lympho- and myelo-proliferative disease. Therefore, these findings have also a clinical significance. In patients with leukemia or a lympho-proliferative disease, apart from the bone marrow, peripheral lymphoid organs should also be considered as a site where therapy-resistant leukemic cells could reside after treatment.

Collectively, the presented data on the role of Flt3-ligand and IL-7 demonstrate their collaborative promotion of B-cell development. Flt3-ligand instructs the cells at the MPP stage into the direction of the lymphoid and myeloid lineages and further supports their proliferation as well as the expansion of downstream uncommitted lymphoid progenitors such as CLPs and EPLMs. IL-7 on the other hand is mainly responsible for survival of the CLP and EPLM populations, whereas it becomes essential as a survival and proliferation factor for early CD19<sup>+</sup> B-cell progenitors. Thus, Flt3-ligand as well as IL-7 possess permissive functions for the effective development of lymphocytes and are crucial for the establishment of a functional adaptive immune system.

## 5.2. Regulation of $\beta$ -selection by Duxbl

The second part of the thesis was focused on the molecular mechanisms that guide the development of T-cell progenitors, and in particular their passage through  $\beta$ -selection. The major aim of T-cell development is the successful production of a TCR. Prerequisite for success is the passage of several important checkpoints that ensure the developmental progression only of cells with functional rearrangements of their antigen-receptor chains. During  $\beta$ -selection almost half of the cells fail to productively rearrange their  $\beta$ -chain and therefore have to undergo apoptosis in order to prevent the accumulation of non-functional cells (Mallick et al., 1993). However, until now only little is known about the exact molecular mechanisms that regulate the efficient elimination of these cells.

High CD27 expression within the DN3 population was previously linked to successful passage through  $\beta$ -selection, as the majority of these cells stained positive for the  $\beta$ -chain intracellularly (Taghon et al., 2006). In the present study we were able to show that in addition to that, the downregulation of CD27 is associated with the failure of productive recombination (section 4.2.1.; Figure 1). Thus, these CD27<sup>-</sup> cells are blocked in their development and will undergo apoptosis. Using this addition to the currently established set of markers for the description of T-cell development, the DN3 stage could be further subdivided into CD27<sup>+</sup>CD28<sup>+</sup> DN3b cells, that have successfully passed  $\beta$ -selection, CD27<sup>-</sup>CD28<sup>-</sup> DN3a cells, which are prone to undergo apoptosis due to unproductive rearrangements, and CD27<sup>+</sup>CD28<sup>-</sup> DN3a cells, whose fate seems to be not yet decided and are still in the process of recombination. These findings enabled us to investigate the transcriptional changes and events that occur during  $\beta$ -selection in much more detail than ever before.

Transcriptomic analysis of the different DN3 subsets revealed an up-regulation of apoptosis related pathways in CD27<sup>-</sup> DN3a cells (section 4.2.1.; Figure 2). This confirmed our initial conclusions that this population mainly contains cells, which will be eliminated because of unsuccessful  $\beta$ -chain rearrangements. In particular, p53 pathway associated genes were increased, which matches with previous reports that argued for a main function of this pathway during apoptosis induction at the  $\beta$ -selection checkpoint (Anderson et al., 2007; Bogue et al., 1996; Costello et al., 2000; Haks et al., 1999; Mombaerts et al., 1995; Rashkovan et al., 2014; Saba et al., 2011; Stadanlick et al., 2011). By focusing on the differential gene expression of transcriptional regulators, our attention was drawn to the specific expression of the transcription factor Duxbl in DN3a cells and in the CD27<sup>low</sup> population in particular (section 4.2.1.; Figure 2B-G). A single-cell RNA-seq analysis of the DN2, DN3, and DN4 stages further confirmed the heterogeneity observed in the DN3 population, by subdividing them into cells prior to and post  $\beta$ -selection (section 4.2.1.; Figure 3A-C). Similarly, in this dataset Duxbl expression was restricted to cells that have not yet passed  $\beta$ -selection and that are transcriptionally farthest from cells of the DN4 stage (section 4.2.1.; Figure 3E+F). Considering additionally the high expression at this stage of genes associated with the recombination process and pre-TCR formation, these data confirm that Duxbl expressing cells are most likely either in the process of rearrangement or have failed to do so. Together with a previous *in vitro* report that described Duxbl as a regulator of DN thymocyte development (Kawazu et al., 2007), this precise expression pattern indicated a potential role of Duxbl in the process of  $\beta$ -selection. Indeed, conditional transgenic expression of Duxbl resulted in a blocked DN3-to-DP transition due to reduced cell-cycle induction and increased apoptosis (section 4.2.1.; Figure 4). Therefore, we propose Duxbl to be a key regulator of  $\beta$ -selection that mediates developmental arrest and the elimination of DN3 cells that failed successful  $\beta$ -chain recombination. Since the mechanism that initiates Duxbl expression is currently unknown, two

potential scenarios of how Duxbl mediates effective and specific elimination are conceivable. In the first scenario, Duxbl expression is specifically induced in cells that failed to productively rearrange their  $\beta$ -chain on both alleles. Alternatively, Duxbl expression could be induced in all cells that initiate  $\beta$ -chain recombination, coming into effect in a time dependent manner. For instance, in cells that fail successful rearrangements, Duxbl expression would increase over time ultimately resulting in cell death. On the contrary, in cells with a productive  $\beta$ -chain that subsequently is able to pair with pT $\alpha$  to form the pre-TCR, Duxbl expression would be turned off, allowing these cells to proceed to further differentiation. The latter hypothesis is supported by the fact that Duxbl expression is terminated upon triggering of the pre-TCR (section 4.2.1.; Figure 2H+I).

The fact that T-cell development is not completely blocked in conditional Duxbl transgenic mice might arise from the obscurity that cells which managed to rearrange a productive  $\beta$ -chain receive two conflicting signals in these mice. On one side, since they express a  $\beta$ -chain, they get proliferation and survival signals from the pre-TCR, whereas at the same time contradictory Duxbl expression inhibits their cycling and induces apoptosis. Thus, in Duxbl transgenic mice, in order for DN3 progenitors to reach the next developmental stages, the pro-survival signals must overcome the detrimental effects of Duxbl expression. This could explain the accumulation of cells between the DN3 and DN4 stage of Duxbl transgenic mice. Nevertheless, the majority of cells are eliminated by Duxbl as clearly indicated by the almost complete block observed during *ex vivo* differentiation of DN3 cells isolated from Duxbl transgenic mice (section 4.2.1.; Figure 4H-J).

Interestingly, high Duxbl expression exclusively affects  $\alpha/\beta$  T-cell development.  $\gamma/\delta$  T-cell numbers are even slightly increased (section 4.2.1.; Figure 4C), even though the pT $\alpha^{\text{Cre}}$  induces Duxbl expression also in the  $\gamma/\delta$  T-cell lineage (Luche et al., 2013). In order to investigate the effects of transgenic Duxbl expression on other hematopoietic cell types two additional Cre lines were used. Targeted expression in B cells was achieved using the mb1<sup>Cre</sup> line. Strikingly, transgenic Duxbl expression blocked the development of B cells at the pre-BCR checkpoint (unpublished observation). Since no endogenous Duxbl expression can be detected during B-cell development this must be a result of the artificial over-expression of Duxbl in these cells. However, the concordance with its effect on T-cell development, as it blocks both at the pre-BCR and pre-TCR checkpoint, suggests that the reason for its impact on the development of B cells results from the high similarities between these processes. Expression of Duxbl in all hematopoietic lineages was induced by the use of the vav<sup>Cre</sup> line. In accordance with the pT $\alpha^{\text{Cre}}$  and the mb1<sup>Cre</sup> intercrosses, T- and B-cell development showed the corresponding block as described above. Of particular interest was also the potential effect of transgenic Duxbl expression on pDCs, as they are the only hematopoietic cells apart from DN3 thymocytes that display endogenous Duxbl expression. pDCs numbers were not affected

by over-expression of *Duxbl* (unpublished observation). However, a potential role for the functionality of pDCs cannot be excluded from these experiments and further investigations are needed to unravel the reason for *Duxbl* expression in these cells. In accordance with the unchanged phenotype of pDCs, all other populations we analyzed, such as conventional DCs, NK cells, granulocytes, and macrophages/monocytes were not affected by transgenic *Duxbl* expression (unpublished observation). Thus, no general detrimental effect of *Duxbl* could be detected, indicating a specific context-dependent action of *Duxbl* on  $\alpha/\beta$  DN3 thymocytes, with the exception of pre-B cells, that display a similar phenotype at the corresponding developmental stage in development.

The connection of *Duxbl* expression to apoptosis induction was further strengthened by the profound up-regulation of the *Oas/RNaseL* pathway upon *Duxbl* over-expression (section 4.2.1.; Figure 6). Previously, deficiency of *RNaseL* was shown to result in resistance of thymocytes to apoptosis and thereby to increased total thymocyte numbers (Castelli et al., 1998; Zhou et al., 1997). We approached this potential link by the generation and breeding of *RNaseL*<sup>-/-</sup> to *Duxbl* transgenic mice. In these double-mutant mice thymocyte numbers were significantly increased at all developmental stages, clearly indicating that *Duxbl* acts via the *Oas/RNaseL* pathway in pre-T cells (section 4.2.1.; Figure 7). However, the still present block of development indicates that other mechanisms and pathways must be additionally involved. The same holds true for the rescue in thymocyte numbers after crossing of the *Duxbl* transgenic to the *Bcl2* transgenic mouse line (section 4.2.1.; Figure 8). While it nicely demonstrated that the observed block after transgenic expression of *Duxbl* is connected to apoptosis, the incomplete rescue argues that further mechanisms must be involved. For instance, *Bcl2* expression is only antagonizing the pro-apoptotic effects of *Duxbl*, whereas its observed anti-proliferative action is not rescued. This might be of particular importance, since *Bcl2* itself exhibits a negative effect on the proliferation of cells (O'Reilly et al., 1996).

A full characterization of how *Duxbl* mediates the elimination of pre-T cells that fail  $\beta$ -selection requires loss-of-function analysis of *Duxbl* during T-cell development. However, the triplication of the *Duxbl* gene on mouse chromosome 14 prevented the successful generation of a conditional *Duxbl* deficient mouse until now (Wu et al., 2010). We overcame these difficulties by collapsing the triplicated locus to one remaining copy by the use of CRISPR/Cas9 mediated integration of loxP-sites into an intron of all three *Duxbl* copies (Figure 9). Subsequent provision of *Cre* resulted in a stepwise recombination of the introduced loxP-sites, first reducing the number to two remaining *Duxbl* copies, and finally to only one remaining copy. Only using this time-consuming approach, we can now specifically target the remaining *Duxbl* copy for the generation of a conditional or even full knock-out mouse strain. Since this process takes several years, we additionally attempted a loss-of-function approach using short-hairpin RNA-mediated knock-down of *Duxbl* expression in fetal liver derived pro-T

cultures on OP9- $\Delta$ 1 stromal cells. A decreased amount of apoptotic cells at the DN3 stage in Duxbl knock-down cultures, confirmed the pro-apoptotic function of Duxbl during  $\beta$ -selection (section 4.2.1.; Figure 5).

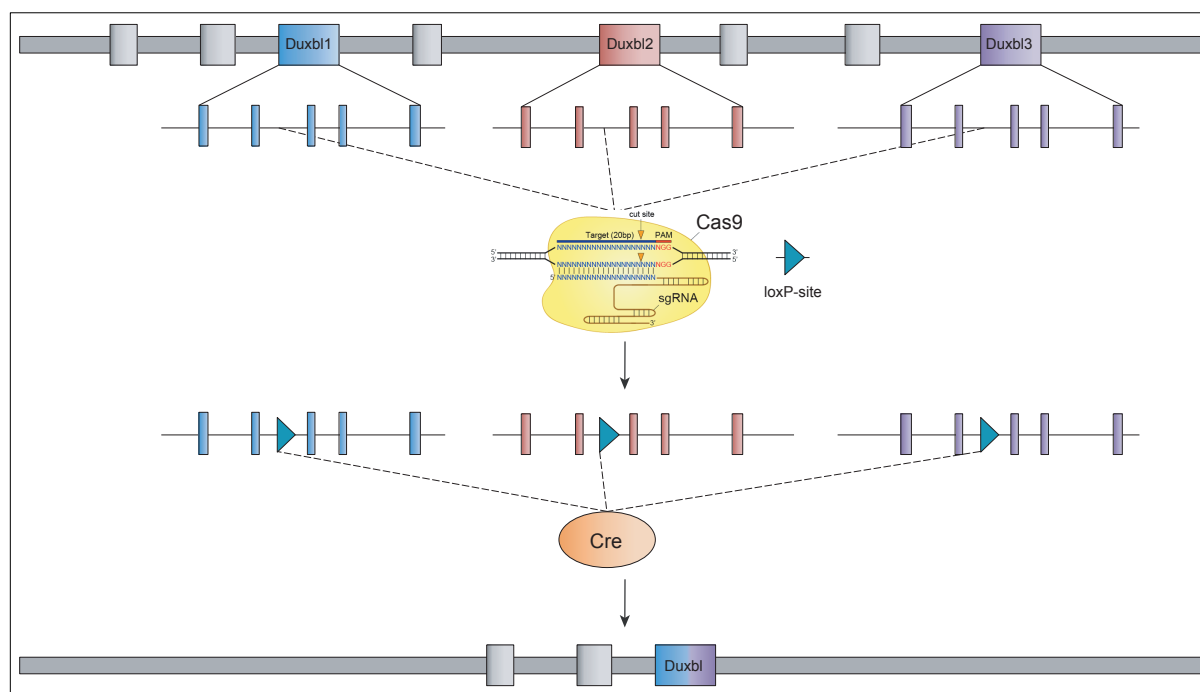


**Figure 9 | Generation of Duxbl deficient mice.** Schematic representation of the performed collapse of the Duxbl locus. First loxP-sites were introduced into an intron of each Duxbl copy, with the use of the CRISPR/Cas9-system. Addition of the Cre recombinase resulted in the deletion of the genomic region between the first and last loxP-sites. Thus, only one Duxbl copy remains.

Another unresolved issue is the identification of potential downstream target genes of Duxbl. The Oas/RNaseL pathway was shown to be part of the mechanism Duxbl is using to induce apoptosis, but whether these genes are directly targeted remains unknown. To address this issue, we generated a mouse strain in which Duxbl is tagged by a short additional peptide at the C-terminus. Specific biotinylation of this tag allows for efficient chromatin immunoprecipitation followed by sequencing, which results in sequencing peaks for regions in the chromatin where Duxbl is bound. Using these data, potential target genes, which are bound by Duxbl in their promoter or enhancer regions, can be further investigated with regards to a potential role during  $\beta$ -selection downstream of Duxbl.

The two homeodomains within the *Duxbl* gene that are responsible for sequence-specific DNA binding share the highest amino acid sequence similarity to those of human *DUX4* (Wu et al., 2010). Interestingly, mis-expression of DUX4 in skeletal muscle cells triggers the induction of apoptosis, which results in a disease called facioscapulohumeral dystrophy. The mechanism behind this was shown to involve the RNaseL pathway, since RNaseL knock-down experiments resulted in an increased survival after DUX4 induction (Shadle et al., 2017).

Thus, human DUX4 function resembles the one we observe in Duxbl transgenic pre-T cells. However, the physiological role of DUX4 in human T-cell development has not been described so far, but the thymus was one of the organs with highest DUX4 expression in humans (Das and Chadwick, 2016). Therefore, it can be envisaged that, similar to Duxbl in mice, DUX4 is involved in the regulation of human T-cell development. Further studies including human T-cell differentiation assays are necessary in order to investigate this possibility in detail.

In conclusion, we were able to identify a novel molecular mechanism that regulates  $\beta$ -selection. We discovered that CD27 downregulation can be used as a marker for cells that have failed to productively rearrange their TCR $\beta$  locus. This enabled us to demonstrate the key role of the transcription factor Duxbl during the  $\beta$ -selection checkpoint. Transgenic mouse models as well as *in vitro* silencing revealed that Duxbl functions as a key mediator of  $\beta$ -selection by inducing apoptosis in cells with a non-functional rearrangement.

## 6. Abbreviations

ALP .....	all lymphoid progenitor
BCR .....	B-cell receptor
BLP .....	B-cell biased lymphoid progenitor
cDC .....	conventional dendritic cell
CLP .....	common lymphoid progenitor
CMP .....	common myeloid progenitor
cTEC .....	cortical thymic epithelial cell
DC .....	dendritic cell
DN .....	double negative
DP .....	double positive
EPLM .....	early progenitor with lymphoid and myeloid potential
ETP .....	early thymic progenitor
FACS .....	fluorescence-activated cell sorting
Flt3 .....	Fms-like tyrosine kinase 3
FoB .....	follicular B cell
GM-CSF .....	granulocyte-macrophage colony-stimulating factor
GMP .....	granulocytic-monocytic progenitor
HSC .....	hematopoietic stem cell
IL-7 .....	interleukin-7
IL-7R .....	interleukin-7 receptor
ILC .....	innate lymphoid cell
Jak .....	Janus kinase
LMPP .....	lymphoid-primed multipotent progenitor
LTi cell .....	lymphoid tissue inducer cell
M-CSF .....	macrophage colony-stimulating factor
MEP .....	megakaryocytic-erythroid progenitor
MHC .....	major histocompatibility complex
MPP .....	multipotent progenitor
mTEC .....	medullary thymic epithelial cell
MZB .....	marginal zone B cell
NK cell .....	natural killer cell
pDC .....	plasmacytoid dendritic cell

---

pT $\alpha$	pre-T cell receptor $\alpha$
S1PR <sub>1</sub>	sphingosine-1 phosphate receptor 1
SCF	stem cell factor
SCID	severe combined immunodeficiency
SP	single positive
Stat	signal transducer and activator of transcription
TCR	T-cell receptor
TNF	tumor necrosis factor
TSLPR	thymic stromal lymphopoietin receptor
TSP	thymus seeding progenitor
vWF	von Willebrand factor

## 7. Acknowledgements

The accomplishment of all this work wouldn't have been possible without the help and support of many other people during the past four years. My heartfelt thank you goes to everyone who was part of that fantastic community.

First and foremost, these lines are directed to my supervisor and mentor Ton. It was a great honor to be part of his lab and to get inspired by his enthusiasm and his nearly infinite knowledge about the development of the immune system. The fantastic projects I was allowed to work on are owed to his experience and brilliant ideas. So much the worse it was when he left us far too early in his life. I hope he would be happy and pleased with the way we proceeded with the projects and with me as his last PhD student. Therefore, this work is dedicated to his memory.

Due to this big loss in the middle of my thesis, personally as well as scientifically, it was absolutely crucial for the continuation of my projects that someone with the knowledge and experience and who was willing to spend the time and energy took over the supervision of my studies. To my great luck Panos did so without the need that I had to ask him. Thank you for all the help and support in the form of discussions, advises, teaching, preparation and designing of experiments, correcting the manuscripts, genotyping mice, and so much more I do not have the space here to write. It was a great time and fun to work with you together on these projects and it would have not been feasible to finish my PhD studies in that way without you.

Furthermore, I want to thank Gennaro, who kindly agreed to take over the responsibilities as my official PhD supervisor without even knowing what he might saddle himself with. I hope you never had to regret this decision and I want to thank you as well as Daniela and Patrick as part of my PhD committee to be always reachable for questions and discussions, not only in the committee meetings, but also whenever I needed your help.

The next big thank you goes to all the former and current lab members of the "Team Ton" and the growing "Team Tussiwand". You are the people who made working in the lab so much fun. This section is therefore dedicated to Lilly, Llucia, Stefan, Mike, Corinne, Giusy, Hannie, Jan, as well as Patrick, Anna, Valentina, Gogi, Mladen, Jannes, Marzia, and Roxane. Thank you all for your continuous help, support, input, discussions, cookies, cakes, jokes, ... this list is endless.

Besides those people from my own lab, I also want to thank all the other contributors to the success of my thesis. Those are amongst others: Kathrin, Gleb, Pawel, Heide, Julien,

Rhodri, Shuang, Saulius, and Thomas. Thank you very much. Your help und input was essential and is highly appreciated.

Auch von meiner Familie zu Hause konnte ich stets jegliche Unterstützung erfahren, die ich benötigt habe um auch schwierige Zeiten mit Erfolg hinter mir zu lassen. Danke Mutti, Vater, und meine Brüder Achim und Andi. Ihr seid immer für mich da, das bedeutet mir sehr viel.

Zusätzlich zu einer großartigen Zeit im Labor hatte ich auch das Glück Lilly dort kennen zu lernen. Mein größter Dank gilt dir für all die Hilfe und die Unterstützung während der letzten Jahre. Die besten Tipps und Tricks im Labor habe ich von dir gelernt und die Zeit mir dir als Laborpartnerin war einfach unschlagbar. Danke auch dafür, dass du all meine Launen erträgst, die manchmal doch sehr stark von den Resultaten der Experimente abhängen und mir immer mit Rat in schwierigen Situationen zur Seite stehst. Ohne dich wäre das alles tausendmal schwieriger gewesen.

## 8. References

- Adachi, S., H. Yoshida, K. Honda, K. Maki, K. Saijo, K. Ikuta, T. Saito, and S.I. Nishikawa. 1998. Essential role of IL-7 receptor alpha in the formation of Peyer's patch anlage. *Int Immunol* 10:1-6.
- Adolfsson, J., O.J. Borge, D. Bryder, K. Theilgaard-Monch, I. Astrand-Grundstrom, E. Sitnicka, Y. Sasaki, and S.E. Jacobsen. 2001. Upregulation of Flt3 expression within the bone marrow Lin(-)Sca1(+)c-kit(+) stem cell compartment is accompanied by loss of self-renewal capacity. *Immunity* 15:659-669.
- Adolfsson, J., R. Mansson, N. Buza-Vidas, A. Hultquist, K. Liuba, C.T. Jensen, D. Bryder, L. Yang, O.J. Borge, L.A. Thoren, K. Anderson, E. Sitnicka, Y. Sasaki, M. Sigvardsson, and S.E. Jacobsen. 2005. Identification of Flt3+ lympho-myeloid stem cells lacking erythro-megakaryocytic potential a revised road map for adult blood lineage commitment. *Cell* 121:295-306.
- Aifantis, I., O. Azogui, J. Feinberg, C. Saint-Ruf, J. Buer, and H. von Boehmer. 1998. On the role of the pre-T cell receptor in alphabeta versus gammadelta T lineage commitment. *Immunity* 9:649-655.
- Aifantis, I., C. Borowski, F. Gounari, H.D. Lacorazza, J. Nikolich-Zugich, and H. von Boehmer. 2002. A critical role for the cytoplasmic tail of pTalpha in T lymphocyte development. *Nat Immunol* 3:483-488.
- Aifantis, I., F. Gounari, L. Scorrano, C. Borowski, and H. von Boehmer. 2001. Constitutive pre-TCR signaling promotes differentiation through Ca<sup>2+</sup> mobilization and activation of NF-kappaB and NFAT. *Nat Immunol* 2:403-409.
- Akashi, K., M. Kondo, U. von Freeden-Jeffry, R. Murray, and I.L. Weissman. 1997. Bcl-2 rescues T lymphopoiesis in interleukin-7 receptor-deficient mice. *Cell* 89:1033-1041.
- Akashi, K., D. Traver, T. Miyamoto, and I.L. Weissman. 2000. A clonogenic common myeloid progenitor that gives rise to all myeloid lineages. *Nature* 404:193-197.
- Akerblad, P., M. Rosberg, T. Leanderson, and M. Sigvardsson. 1999. The B29 (immunoglobulin beta-chain) gene is a genetic target for early B-cell factor. *Mol Cell Biol* 19:392-401.
- Akerblad, P., and M. Sigvardsson. 1999. Early B cell factor is an activator of the B lymphoid kinase promoter in early B cell development. *J Immunol* 163:5453-5461.
- Alberti-Servera, L., L. von Muenchow, P. Tzapogas, G. Capoferri, K. Eschbach, C. Beisel, R. Ceredig, R. Ivanek, and A. Rolink. 2017. Single-cell RNA sequencing reveals developmental heterogeneity among early lymphoid progenitors. *EMBO J* 36:3619-3633.
- Allende, M.L., G. Tuymetova, B.G. Lee, E. Bonifacino, Y.P. Wu, and R.L. Proia. 2010. S1P1 receptor directs the release of immature B cells from bone marrow into blood. *J Exp Med* 207:1113-1124.
- Allman, D., R.C. Lindsley, W. DeMuth, K. Rudd, S.A. Shinton, and R.R. Hardy. 2001. Resolution of three nonproliferative immature splenic B cell subsets reveals multiple selection points during peripheral B cell maturation. *J Immunol* 167:6834-6840.
- Amin, R.H., and M.S. Schlissel. 2008. Foxo1 directly regulates the transcription of recombination-activating genes during B cell development. *Nat Immunol* 9:613-622.
- Anderson, M.K., A.H. Weiss, G. Hernandez-Hoyos, C.J. Dionne, and E.V. Rothenberg. 2002. Constitutive expression of PU.1 in fetal hematopoietic progenitors blocks T cell development at the pro-T cell stage. *Immunity* 16:285-296.
- Anderson, S.J., J.P. Lauritsen, M.G. Hartman, A.M. Foushee, J.M. Lefebvre, S.A. Shinton, B. Gerhardt, R.R. Hardy, T. Oravec, and D.L. Wiest. 2007. Ablation of ribosomal protein L22 selectively impairs alphabeta T cell development by activation of a p53-dependent checkpoint. *Immunity* 26:759-772.

- Ashkenazi, A., and V.M. Dixit. 1998. Death receptors: signaling and modulation. *Science* 281:1305-1308.
- Baerenwaldt, A., N. von Burg, M. Kreuzaler, S. Sitte, E. Horvath, A. Peter, D. Voehringer, A.G. Rolink, and D. Finke. 2016. Flt3 Ligand Regulates the Development of Innate Lymphoid Cells in Fetal and Adult Mice. *J Immunol* 196:2561-2571.
- Bain, G., E.C. Maandag, D.J. Izon, D. Amsen, A.M. Kruisbeek, B.C. Weintraub, I. Krop, M.S. Schlissel, A.J. Feeney, M. van Roon, and et al. 1994. E2A proteins are required for proper B cell development and initiation of immunoglobulin gene rearrangements. *Cell* 79:885-892.
- Balciunaite, G., R. Ceredig, H.J. Fehling, J.C. Zuniga-Pflucker, and A.G. Rolink. 2005a. The role of Notch and IL-7 signaling in early thymocyte proliferation and differentiation. *Eur J Immunol* 35:1292-1300.
- Balciunaite, G., R. Ceredig, S. Massa, and A.G. Rolink. 2005b. A B220+ CD117+ CD19-hematopoietic progenitor with potent lymphoid and myeloid developmental potential. *Eur J Immunol* 35:2019-2030.
- Balciunaite, G., R. Ceredig, and A.G. Rolink. 2005c. The earliest subpopulation of mouse thymocytes contains potent T, significant macrophage, and natural killer cell but no B-lymphocyte potential. *Blood* 105:1930-1936.
- Banerjee, A., D. Northrup, H. Boukarabila, S.E. Jacobsen, and D. Allman. 2013. Transcriptional repression of Gata3 is essential for early B cell commitment. *Immunity* 38:930-942.
- Banu, N., B. Deng, S.D. Lyman, and H. Avraham. 1999. Modulation of haematopoietic progenitor development by FLT-3 ligand. *Cytokine* 11:679-688.
- Becker, A.J., C.E. Mc, and J.E. Till. 1963. Cytological demonstration of the clonal nature of spleen colonies derived from transplanted mouse marrow cells. *Nature* 197:452-454.
- Bell, J.J., and A. Bhandoola. 2008. The earliest thymic progenitors for T cells possess myeloid lineage potential. *Nature* 452:764-767.
- Boehm, T. 2008. Thymus development and function. *Curr Opin Immunol* 20:178-184.
- Bogue, M.A., C. Zhu, E. Aguilar-Cordova, L.A. Donehower, and D.B. Roth. 1996. p53 is required for both radiation-induced differentiation and rescue of V(D)J rearrangement in scid mouse thymocytes. *Genes Dev* 10:553-565.
- Boller, S., and R. Grosschedl. 2014. The regulatory network of B-cell differentiation: a focused view of early B-cell factor 1 function. *Immunol Rev* 261:102-115.
- Boller, S., S. Ramamoorthy, D. Akbas, R. Nechanitzky, L. Burger, R. Murr, D. Schubeler, and R. Grosschedl. 2016. Pioneering Activity of the C-Terminal Domain of EBF1 Shapes the Chromatin Landscape for B Cell Programming. *Immunity* 44:527-541.
- Borge, O.J., J. Adolfsson, A. Martensson, I.L. Martensson, and S.E. Jacobsen. 1999. Lymphoid-restricted development from multipotent candidate murine stem cells: distinct and complimentary functions of the c-kit and flt3-ligands. *Blood* 94:3781-3790.
- Boudil, A., I.R. Matei, H.Y. Shih, G. Bogdanoski, J.S. Yuan, S.G. Chang, B. Montpelier, P.E. Kowalski, V. Voisin, S. Bashir, G.D. Bader, M.S. Krangel, and C.J. Gidos. 2015. IL-7 coordinates proliferation, differentiation and Tcra recombination during thymocyte beta-selection. *Nat Immunol* 16:397-405.
- Boyer, S.W., A.V. Schroeder, S. Smith-Berdan, and E.C. Forsberg. 2011. All hematopoietic cells develop from hematopoietic stem cells through Flk2/Flt3-positive progenitor cells. *Cell Stem Cell* 9:64-73.
- Boyman, O., C. Ramsey, D.M. Kim, J. Sprent, and C.D. Surh. 2008. IL-7/anti-IL-7 mAb complexes restore T cell development and induce homeostatic T Cell expansion without lymphopenia. *J Immunol* 180:7265-7275.
- Brasel, K., T. De Smedt, J.L. Smith, and C.R. Maliszewski. 2000. Generation of murine dendritic cells from flt3-ligand-supplemented bone marrow cultures. *Blood* 96:3029-3039.
- Brawand, P., D.R. Fitzpatrick, B.W. Greenfield, K. Brasel, C.R. Maliszewski, and T. De Smedt. 2002. Murine plasmacytoid pre-dendritic cells generated from Flt3 ligand-supplemented bone marrow cultures are immature APCs. *J Immunol* 169:6711-6719.

- Brekelmans, P., P. van Soest, J. Voerman, P.P. Platenburg, P.J. Leenen, and W. van Ewijk. 1994. Transferrin receptor expression as a marker of immature cycling thymocytes in the mouse. *Cell Immunol* 159:331-339.
- Brown, G., P. Tsapogas, and R. Ceredig. 2018. The changing face of hematopoiesis: a spectrum of options is available to stem cells. *Immunol Cell Biol*
- Broxmeyer, H.E., L. Lu, S. Cooper, L. Ruggieri, Z.H. Li, and S.D. Lyman. 1995. Flt3 ligand stimulates/costimulates the growth of myeloid stem/progenitor cells. *Exp Hematol* 23:1121-1129.
- Buckley, R.H. 2004. Molecular defects in human severe combined immunodeficiency and approaches to immune reconstitution. *Annu Rev Immunol* 22:625-655.
- Busch, K., K. Klapproth, M. Barile, M. Flossdorf, T. Holland-Letz, S.M. Schlenner, M. Reth, T. Hofer, and H.R. Rodewald. 2015. Fundamental properties of unperturbed haematopoiesis from stem cells in vivo. *Nature* 518:542-546.
- Buza-Vidas, N., P. Woll, A. Hultquist, S. Duarte, M. Lutteropp, T. Bouriez-Jones, H. Ferry, S. Luc, and S.E. Jacobsen. 2011. FLT3 expression initiates in fully multipotent mouse hematopoietic progenitor cells. *Blood* 118:1544-1548.
- Cabezas-Wallscheid, N., F. Buettner, P. Sommerkamp, D. Klimmeck, L. Ladel, F.B. Thalheimer, D. Pastor-Flores, L.P. Roma, S. Renders, P. Zeisberger, A. Przybylla, K. Schonberger, R. Scognamiglio, S. Altamura, C.M. Florian, M. Fawaz, D. Vonficht, M. Tesio, P. Collier, D. Pavlinic, H. Geiger, T. Schroeder, V. Benes, T.P. Dick, M.A. Rieger, O. Stegle, and A. Trumpp. 2017. Vitamin A-Retinoic Acid Signaling Regulates Hematopoietic Stem Cell Dormancy. *Cell* 169:807-823 e819.
- Capone, M., R.D. Hockett, Jr., and A. Zlotnik. 1998. Kinetics of T cell receptor beta, gamma, and delta rearrangements during adult thymic development: T cell receptor rearrangements are present in CD44(+)CD25(+) Pro-T thymocytes. *Proc Natl Acad Sci U S A* 95:12522-12527.
- Carotta, S., A. Dakic, A. D'Amico, S.H. Pang, K.T. Greig, S.L. Nutt, and L. Wu. 2010. The transcription factor PU.1 controls dendritic cell development and Flt3 cytokine receptor expression in a dose-dependent manner. *Immunity* 32:628-641.
- Carsetti, R., G. Kohler, and M.C. Lamers. 1995. Transitional B cells are the target of negative selection in the B cell compartment. *J Exp Med* 181:2129-2140.
- Carvalho, T.L., T. Mota-Santos, A. Cumano, J. Demengeot, and P. Vieira. 2001. Arrested B lymphopoiesis and persistence of activated B cells in adult interleukin 7(-/-) mice. *J Exp Med* 194:1141-1150.
- Casellas, R., T.A. Shih, M. Kleinewietfeld, J. Rakonjac, D. Nemazee, K. Rajewsky, and M.C. Nussenzweig. 2001. Contribution of receptor editing to the antibody repertoire. *Science* 291:1541-1544.
- Casola, S., K.L. Otipoby, M. Alimzhanov, S. Humme, N. Uyttersprot, J.L. Kutok, M.C. Carroll, and K. Rajewsky. 2004. B cell receptor signal strength determines B cell fate. *Nat Immunol* 5:317-327.
- Castelli, J.C., B.A. Hassel, A. Maran, J. Paranjape, J.A. Hewitt, X.L. Li, Y.T. Hsu, R.H. Silverman, and R.J. Youle. 1998. The role of 2'-5' oligoadenylate-activated ribonuclease L in apoptosis. *Cell Death Differ* 5:313-320.
- Ceradini, D.J., A.R. Kulkarni, M.J. Callaghan, O.M. Tepper, N. Bastidas, M.E. Kleinman, J.M. Capla, R.D. Galiano, J.P. Levine, and G.C. Gurtner. 2004. Progenitor cell trafficking is regulated by hypoxic gradients through HIF-1 induction of SDF-1. *Nat Med* 10:858-864.
- Ceredig, R., N. Bosco, P.N. Maye, J. Andersson, and A. Rolink. 2003. In interleukin-7-transgenic mice, increasing B lymphopoiesis increases follicular but not marginal zone B cell numbers. *Eur J Immunol* 33:2567-2576.
- Ceredig, R., N. Bosco, and A.G. Rolink. 2007. The B lineage potential of thymus settling progenitors is critically dependent on mouse age. *Eur J Immunol* 37:830-837.
- Ceredig, R., and A.G. Rolink. 2012. The key role of IL-7 in lymphopoiesis. *Semin Immunol* 24:159-164.
- Ceredig, R., A.G. Rolink, and G. Brown. 2009. Models of haematopoiesis: seeing the wood for the trees. *Nat Rev Immunol* 9:293-300.

- Ceredig, R., and T. Rolink. 2002. A positive look at double-negative thymocytes. *Nat Rev Immunol* 2:888-897.
- Chappaz, S., and D. Finke. 2010. The IL-7 signaling pathway regulates lymph node development independent of peripheral lymphocytes. *J Immunol* 184:3562-3569.
- Cheshier, S.H., S.J. Morrison, X. Liao, and I.L. Weissman. 1999. In vivo proliferation and cell cycle kinetics of long-term self-renewing hematopoietic stem cells. *Proc Natl Acad Sci U S A* 96:3120-3125.
- Chetoui, N., M. Boisvert, S. Gendron, and F. Aoudjit. 2010. Interleukin-7 promotes the survival of human CD4+ effector/memory T cells by up-regulating Bcl-2 proteins and activating the JAK/STAT signalling pathway. *Immunology* 130:418-426.
- Christensen, J.L., and I.L. Weissman. 2001. Flk-2 is a marker in hematopoietic stem cell differentiation: a simple method to isolate long-term stem cells. *Proc Natl Acad Sci U S A* 98:14541-14546.
- Ciofani, M., T.M. Schmitt, A. Ciofani, A.M. Michie, N. Cuburu, A. Aublin, J.L. Maryanski, and J.C. Zuniga-Pflucker. 2004. Obligatory role for cooperative signaling by pre-TCR and Notch during thymocyte differentiation. *J Immunol* 172:5230-5239.
- Ciofani, M., and J.C. Zuniga-Pflucker. 2005. Notch promotes survival of pre-T cells at the beta-selection checkpoint by regulating cellular metabolism. *Nat Immunol* 6:881-888.
- Clark, M.R., M. Mandal, K. Ochiai, and H. Singh. 2014. Orchestrating B cell lymphopoiesis through interplay of IL-7 receptor and pre-B cell receptor signalling. *Nat Rev Immunol* 14:69-80.
- Cobaleda, C., A. Schebesta, A. Delogu, and M. Busslinger. 2007. Pax5: the guardian of B cell identity and function. *Nat Immunol* 8:463-470.
- Cooper, A.B., C.M. Sawai, E. Sicinska, S.E. Powers, P. Sicinski, M.R. Clark, and I. Aifantis. 2006. A unique function for cyclin D3 in early B cell development. *Nat Immunol* 7:489-497.
- Copley, M.R., P.A. Beer, and C.J. Eaves. 2012. Hematopoietic stem cell heterogeneity takes center stage. *Cell Stem Cell* 10:690-697.
- Costello, P.S., S.C. Cleverley, R. Galandrini, S.W. Henning, and D.A. Cantrell. 2000. The GTPase rho controls a p53-dependent survival checkpoint during thymopoiesis. *J Exp Med* 192:77-85.
- Das, S., and B.P. Chadwick. 2016. Influence of Repressive Histone and DNA Methylation upon D4Z4 Transcription in Non-Myogenic Cells. *PLoS One* 11:e0160022.
- Daussy, C., F. Faure, K. Mayol, S. Viel, G. Gasteiger, E. Charrier, J. Bienvenu, T. Henry, E. Debien, U.A. Hasan, J. Marvel, K. Yoh, S. Takahashi, I. Prinz, S. de Bernard, L. Buffat, and T. Walzer. 2014. T-bet and Eomes instruct the development of two distinct natural killer cell lineages in the liver and in the bone marrow. *J Exp Med* 211:563-577.
- De Obaldia, M.E., J.J. Bell, X. Wang, C. Harly, Y. Yashiro-Ohtani, J.H. DeLong, D.A. Zlotoff, D.A. Sultana, W.S. Pear, and A. Bhandoola. 2013. T cell development requires constraint of the myeloid regulator C/EBP-alpha by the Notch target and transcriptional repressor Hes1. *Nat Immunol* 14:1277-1284.
- Decker, D.J., N.E. Boyle, J.A. Koziol, and N.R. Klinman. 1991. The expression of the Ig H chain repertoire in developing bone marrow B lineage cells. *J Immunol* 146:350-361.
- DeKoter, R.P., H.J. Lee, and H. Singh. 2002. PU.1 regulates expression of the interleukin-7 receptor in lymphoid progenitors. *Immunity* 16:297-309.
- DeKoter, R.P., and H. Singh. 2000. Regulation of B lymphocyte and macrophage development by graded expression of PU.1. *Science* 288:1439-1441.
- DeKoter, R.P., J.C. Walsh, and H. Singh. 1998. PU.1 regulates both cytokine-dependent proliferation and differentiation of granulocyte/macrophage progenitors. *EMBO J* 17:4456-4468.
- Dengler, H.S., G.V. Baracho, S.A. Omori, S. Bruckner, K.C. Arden, D.H. Castrillon, R.A. DePinho, and R.C. Rickert. 2008. Distinct functions for the transcription factor Foxo1 at various stages of B cell differentiation. *Nat Immunol* 9:1388-1398.

- Desiderio, S.V., G.D. Yancopoulos, M. Paskind, E. Thomas, M.A. Boss, N. Landau, F.W. Alt, and D. Baltimore. 1984. Insertion of N regions into heavy-chain genes is correlated with expression of terminal deoxytransferase in B cells. *Nature* 311:752-755.
- Dias, S., R. Mansson, S. Gurbuxani, M. Sigvardsson, and B.L. Kee. 2008. E2A proteins promote development of lymphoid-primed multipotent progenitors. *Immunity* 29:217-227.
- Dias, S., H. Silva, Jr., A. Cumano, and P. Vieira. 2005. Interleukin-7 is necessary to maintain the B cell potential in common lymphoid progenitors. *J Exp Med* 201:971-979.
- Dobin, A., C.A. Davis, F. Schlesinger, J. Drenkow, C. Zaleski, S. Jha, P. Batut, M. Chaisson, and T.R. Gingeras. 2013. STAR: ultrafast universal RNA-seq aligner. *Bioinformatics* 29:15-21.
- Domen, J., K.L. Gandy, and I.L. Weissman. 1998. Systemic overexpression of BCL-2 in the hematopoietic system protects transgenic mice from the consequences of lethal irradiation. *Blood* 91:2272-2282.
- Dose, M., I. Khan, Z. Guo, D. Kovalovsky, A. Krueger, H. von Boehmer, K. Khazaie, and F. Gounari. 2006. c-Myc mediates pre-TCR-induced proliferation but not developmental progression. *Blood* 108:2669-2677.
- Douglas, N.C., H. Jacobs, A.L. Bothwell, and A.C. Hayday. 2001. Defining the specific physiological requirements for c-Myc in T cell development. *Nat Immunol* 2:307-315.
- Dudley, E.C., H.T. Petrie, L.M. Shah, M.J. Owen, and A.C. Hayday. 1994. T cell receptor beta chain gene rearrangement and selection during thymocyte development in adult mice. *Immunity* 1:83-93.
- Dykstra, B., D. Kent, M. Bowie, L. McCaffrey, M. Hamilton, K. Lyons, S.J. Lee, R. Brinkman, and C. Eaves. 2007. Long-term propagation of distinct hematopoietic differentiation programs in vivo. *Cell Stem Cell* 1:218-229.
- Ehlich, A., V. Martin, W. Muller, and K. Rajewsky. 1994. Analysis of the B-cell progenitor compartment at the level of single cells. *Curr Biol* 4:573-583.
- Elhanati, Y., Z. Sethna, Q. Marcou, C.G. Callan, Jr., T. Mora, and A.M. Walczak. 2015. Inferring processes underlying B-cell repertoire diversity. *Philos Trans R Soc Lond B Biol Sci* 370:
- Feeney, A.J. 1992. Comparison of junctional diversity in the neonatal and adult immunoglobulin repertoires. *Int Rev Immunol* 8:113-122.
- Fehling, H.J., B.M. Iritani, A. Krotkova, K.A. Forbush, C. Laplace, R.M. Perlmutter, and H. von Boehmer. 1997. Restoration of thymopoiesis in pT alpha<sup>-/-</sup> mice by anti-CD3epsilon antibody treatment or with transgenes encoding activated Lck or tailless pT alpha. *Immunity* 6:703-714.
- Fehling, H.J., A. Krotkova, C. Saint-Ruf, and H. von Boehmer. 1995. Crucial role of the pre-T-cell receptor alpha gene in development of alpha beta but not gamma delta T cells. *Nature* 375:795-798.
- Fisher, A.G., C. Burdet, C. Bunce, M. Merckenschlager, and R. Ceredig. 1995. Lymphoproliferative disorders in IL-7 transgenic mice: expansion of immature B cells which retain macrophage potential. *Int Immunol* 7:415-423.
- Fleming, H.E., and C.J. Paige. 2001. Pre-B cell receptor signaling mediates selective response to IL-7 at the pro-B to pre-B cell transition via an ERK/MAP kinase-dependent pathway. *Immunity* 15:521-531.
- Foudi, A., K. Hochedlinger, D. Van Buren, J.W. Schindler, R. Jaenisch, V. Carey, and H. Hock. 2009. Analysis of histone 2B-GFP retention reveals slowly cycling hematopoietic stem cells. *Nat Biotechnol* 27:84-90.
- Foxwell, B.M., C. Beadling, D. Guschin, I. Kerr, and D. Cantrell. 1995. Interleukin-7 can induce the activation of Jak 1, Jak 3 and STAT 5 proteins in murine T cells. *Eur J Immunol* 25:3041-3046.
- Fujiwara, Y., C.P. Browne, K. Cunniff, S.C. Goff, and S.H. Orkin. 1996. Arrested development of embryonic red cell precursors in mouse embryos lacking transcription factor GATA-1. *Proc Natl Acad Sci U S A* 93:12355-12358.

- Gaidatzis, D., A. Lerch, F. Hahne, and M.B. Stadler. 2015. QuasR: quantification and annotation of short reads in R. *Bioinformatics* 31:1130-1132.
- Garcia-Ojeda, M.E., R.G. Klein Wolterink, F. Lemaitre, O. Richard-Le Goff, M. Hasan, R.W. Hendriks, A. Cumano, and J.P. Di Santo. 2013. GATA-3 promotes T-cell specification by repressing B-cell potential in pro-T cells in mice. *Blood* 121:1749-1759.
- Gay, D., T. Saunders, S. Camper, and M. Weigert. 1993. Receptor editing: an approach by autoreactive B cells to escape tolerance. *J Exp Med* 177:999-1008.
- Gehre, N., A. Nusser, L. von Muenchow, R. Tussiwand, C. Engdahl, G. Capoferri, N. Bosco, R. Ceredig, and A.G. Rolink. 2015. A stromal cell free culture system generates mouse pro-T cells that can reconstitute T-cell compartments in vivo. *Eur J Immunol* 45:932-942.
- Gekas, C., and T. Graf. 2013. CD41 expression marks myeloid-biased adult hematopoietic stem cells and increases with age. *Blood* 121:4463-4472.
- Georgescu, C., W.J. Longabaugh, D.D. Scripture-Adams, E.S. David-Fung, M.A. Yui, M.A. Zarnegar, H. Bolouri, and E.V. Rothenberg. 2008. A gene regulatory network armature for T lymphocyte specification. *Proc Natl Acad Sci U S A* 105:20100-20105.
- Germain, R.N. 2002. T-cell development and the CD4-CD8 lineage decision. *Nat Rev Immunol* 2:309-322.
- Germar, K., M. Dose, T. Konstantinou, J. Zhang, H. Wang, C. Lobry, K.L. Arnett, S.C. Blacklow, I. Aifantis, J.C. Aster, and F. Gounari. 2011. T-cell factor 1 is a gatekeeper for T-cell specification in response to Notch signaling. *Proc Natl Acad Sci U S A* 108:20060-20065.
- Gibb, D.R., M. El Shikh, D.J. Kang, W.J. Rowe, R. El Sayed, J. Cichy, H. Yagita, J.G. Tew, P.J. Dempsey, H.C. Crawford, and D.H. Conrad. 2010. ADAM10 is essential for Notch2-dependent marginal zone B cell development and CD23 cleavage in vivo. *J Exp Med* 207:623-635.
- Gilliland, D.G., and J.D. Griffin. 2002. The roles of FLT3 in hematopoiesis and leukemia. *Blood* 100:1532-1542.
- Glanville, J., W. Zhai, J. Berka, D. Telman, G. Huerta, G.R. Mehta, I. Ni, L. Mei, P.D. Sundar, G.M. Day, D. Cox, A. Rajpal, and J. Pons. 2009. Precise determination of the diversity of a combinatorial antibody library gives insight into the human immunoglobulin repertoire. *Proc Natl Acad Sci U S A* 106:20216-20221.
- Godfrey, D.I., J. Kennedy, P. Mombaerts, S. Tonegawa, and A. Zlotnik. 1994. Onset of TCR-beta gene rearrangement and role of TCR-beta expression during CD3-CD4-CD8-thymocyte differentiation. *J Immunol* 152:4783-4792.
- Godfrey, D.I., J. Kennedy, T. Suda, and A. Zlotnik. 1993. A developmental pathway involving four phenotypically and functionally distinct subsets of CD3-CD4-CD8- triple-negative adult mouse thymocytes defined by CD44 and CD25 expression. *J Immunol* 150:4244-4252.
- Godfrey, D.I., A. Zlotnik, and T. Suda. 1992. Phenotypic and functional characterization of c-kit expression during intrathymic T cell development. *J Immunol* 149:2281-2285.
- Goodell, M.A., K. Brose, G. Paradis, A.S. Conner, and R.C. Mulligan. 1996. Isolation and functional properties of murine hematopoietic stem cells that are replicating in vivo. *J Exp Med* 183:1797-1806.
- Goodman, J.W., and G.S. Hodgson. 1962. Evidence for stem cells in the peripheral blood of mice. *Blood* 19:702-714.
- Gossens, K., S. Naus, S.Y. Corbel, S. Lin, F.M. Rossi, J. Kast, and H.J. Ziltener. 2009. Thymic progenitor homing and lymphocyte homeostasis are linked via S1P-controlled expression of thymic P-selectin/CCL25. *J Exp Med* 206:761-778.
- Gravestain, L.A., W. van Ewijk, F. Ossendorp, and J. Borst. 1996. CD27 cooperates with the pre-T cell receptor in the regulation of murine T cell development. *J Exp Med* 184:675-685.
- Grawunder, U., T.M. Leu, D.G. Schatz, A. Werner, A.G. Rolink, F. Melchers, and T.H. Winkler. 1995. Down-regulation of RAG1 and RAG2 gene expression in preB cells after functional immunoglobulin heavy chain rearrangement. *Immunity* 3:601-608.

- Gronke, K., M. Kofoed-Nielsen, and A. Diefenbach. 2016. Innate lymphoid cells, precursors and plasticity. *Immunol Lett* 179:9-18.
- Gross, J.A., S.R. Dillon, S. Mudri, J. Johnston, A. Littau, R. Roque, M. Rixon, O. Schou, K.P. Foley, H. Haugen, S. McMillen, K. Waggle, R.W. Schreckhise, K. Shoemaker, T. Vu, M. Moore, A. Grossman, and C.H. Clegg. 2001. TACI-Ig neutralizes molecules critical for B cell development and autoimmune disease. impaired B cell maturation in mice lacking BlyS. *Immunity* 15:289-302.
- Grover, A., E. Mancini, S. Moore, A.J. Mead, D. Atkinson, K.D. Rasmussen, D. O'Carroll, S.E. Jacobsen, and C. Nerlov. 2014. Erythropoietin guides multipotent hematopoietic progenitor cells toward an erythroid fate. *J Exp Med* 211:181-188.
- Gyory, I., S. Boller, R. Nechanitzky, E. Mandel, S. Pott, E. Liu, and R. Grosschedl. 2012. Transcription factor Ebf1 regulates differentiation stage-specific signaling, proliferation, and survival of B cells. *Genes Dev* 26:668-682.
- Hagman, J., A. Travis, and R. Grosschedl. 1991. A novel lineage-specific nuclear factor regulates mb-1 gene transcription at the early stages of B cell differentiation. *EMBO J* 10:3409-3417.
- Haks, M.C., P. Krimpenfort, J.H. van den Brakel, and A.M. Kruisbeek. 1999. Pre-TCR signaling and inactivation of p53 induces crucial cell survival pathways in pre-T cells. *Immunity* 11:91-101.
- Hammad, H., M. Vanderkerken, P. Pouliot, K. Deswarte, W. Toussaint, K. Vergote, L. Vandersarren, S. Janssens, I. Ramou, S.N. Savvides, J.J. Haigh, R. Hendriks, M. Kopf, K. Craessaerts, B. de Strooper, J.F. Kearney, D.H. Conrad, and B.N. Lambrecht. 2017. Transitional B cells commit to marginal zone B cell fate by Taok3-mediated surface expression of ADAM10. *Nat Immunol* 18:313-320.
- Hardy, R.R., and K. Hayakawa. 2001. B cell development pathways. *Annu Rev Immunol* 19:595-621.
- Hathcock, K.S., L. Farrington, I. Ivanova, F. Livak, R. Selimyan, R. Sen, J. Williams, X. Tai, and R.J. Hodes. 2011. The requirement for pre-TCR during thymic differentiation enforces a developmental pause that is essential for V-DJbeta rearrangement. *PLoS One* 6:e20639.
- Haueter, S., M. Kawasumi, I. Asner, U. Brykczynska, P. Cinelli, S. Moisyadi, K. Burki, A.H. Peters, and P. Pelczar. 2010. Genetic vasectomy-overexpression of Prm1-EGFP fusion protein in elongating spermatids causes dominant male sterility in mice. *Genesis* 48:151-160.
- Hayakawa, K., R.R. Hardy, D.R. Parks, and L.A. Herzenberg. 1983. The "Ly-1 B" cell subpopulation in normal immunodeficient, and autoimmune mice. *J Exp Med* 157:202-218.
- Heizmann, B., P. Kastner, and S. Chan. 2013. Ikaros is absolutely required for pre-B cell differentiation by attenuating IL-7 signals. *J Exp Med* 210:2823-2832.
- Hennighausen, L., and G.W. Robinson. 2008. Interpretation of cytokine signaling through the transcription factors STAT5A and STAT5B. *Genes Dev* 22:711-721.
- Hirokawa, S., H. Sato, I. Kato, and A. Kudo. 2003. EBF-regulating Pax5 transcription is enhanced by STAT5 in the early stage of B cells. *Eur J Immunol* 33:1824-1829.
- Ho, T.T., M.R. Warr, E.R. Adelman, O.M. Lansinger, J. Flach, E.V. Verovskaya, M.E. Figueroa, and E. Passegue. 2017. Autophagy maintains the metabolism and function of young and old stem cells. *Nature* 543:205-210.
- Holmes, M.L., S. Carotta, L.M. Corcoran, and S.L. Nutt. 2006. Repression of Flt3 by Pax5 is crucial for B-cell lineage commitment. *Genes Dev* 20:933-938.
- Hoppe, P.S., M. Schwarzfischer, D. Loeffler, K.D. Kokkaliaris, O. Hilsenbeck, N. Moritz, M. Ende, A. Filipczyk, A. Gambardella, N. Ahmed, M. Etzrodt, D.L. Coutu, M.A. Rieger, C. Marr, M.K. Strasser, B. Schaubberger, I. Burtscher, O. Ermakova, A. Burger, H. Lickert, C. Nerlov, F.J. Theis, and T. Schroeder. 2016. Early myeloid lineage choice is not initiated by random PU.1 to GATA1 protein ratios. *Nature* 535:299-302.
- Horcher, M., A. Souabni, and M. Busslinger. 2001. Pax5/BSAP maintains the identity of B cells in late B lymphopoiesis. *Immunity* 14:779-790.

- Hosoya, T., T. Kuroha, T. Moriguchi, D. Cummings, I. Maillard, K.C. Lim, and J.D. Engel. 2009. GATA-3 is required for early T lineage progenitor development. *J Exp Med* 206:2987-3000.
- Hosoya, T., I. Maillard, and J.D. Engel. 2010. From the cradle to the grave: activities of GATA-3 throughout T-cell development and differentiation. *Immunol Rev* 238:110-125.
- Hoyler, T., C.S. Klose, A. Souabni, A. Turqueti-Neves, D. Pfeifer, E.L. Rawlins, D. Voehringer, M. Busslinger, and A. Diefenbach. 2012. The transcription factor GATA-3 controls cell fate and maintenance of type 2 innate lymphoid cells. *Immunity* 37:634-648.
- Huang, J., S.K. Durum, and K. Muegge. 2001. Cutting edge: histone acetylation and recombination at the TCR gamma locus follows IL-7 induction. *J Immunol* 167:6073-6077.
- Ikawa, T., S. Hirose, K. Masuda, K. Kakugawa, R. Satoh, A. Shibano-Satoh, R. Kominami, Y. Katsura, and H. Kawamoto. 2010. An essential developmental checkpoint for production of the T cell lineage. *Science* 329:93-96.
- Ikawa, T., H. Kawamoto, A.W. Goldrath, and C. Murre. 2006. E proteins and Notch signaling cooperate to promote T cell lineage specification and commitment. *J Exp Med* 203:1329-1342.
- Inlay, M.A., D. Bhattacharya, D. Sahoo, T. Serwold, J. Seita, H. Karsunky, S.K. Plevritis, D.L. Dill, and I.L. Weissman. 2009. Ly6d marks the earliest stage of B-cell specification and identifies the branchpoint between B-cell and T-cell development. *Genes Dev* 23:2376-2381.
- Irving, B.A., F.W. Alt, and N. Killeen. 1998. Thymocyte development in the absence of pre-T cell receptor extracellular immunoglobulin domains. *Science* 280:905-908.
- Jacobi, A.M., G.R. Rettig, R. Turk, M.A. Collingwood, S.A. Zeiner, R.M. Quadros, D.W. Harms, P.J. Bonthuis, C. Gregg, M. Ohtsuka, C.B. Gurumurthy, and M.A. Behlke. 2017. Simplified CRISPR tools for efficient genome editing and streamlined protocols for their delivery into mammalian cells and mouse zygotes. *Methods* 121-122:16-28.
- Jacobs, H., J. Iacomini, M. van de Ven, S. Tonegawa, and A. Berns. 1996. Domains of the TCR beta-chain required for early thymocyte development. *J Exp Med* 184:1833-1843.
- Jacobs, S.R., R.D. Michalek, and J.C. Rathmell. 2010. IL-7 is essential for homeostatic control of T cell metabolism in vivo. *J Immunol* 184:3461-3469.
- Jacobsen, S.E., C. Okkenhaug, J. Myklebust, O.P. Veiby, and S.D. Lyman. 1995. The FLT3 ligand potently and directly stimulates the growth and expansion of primitive murine bone marrow progenitor cells in vitro: synergistic interactions with interleukin (IL) 11, IL-12, and other hematopoietic growth factors. *J Exp Med* 181:1357-1363.
- Janas, M.L., G. Varano, K. Gudmundsson, M. Noda, T. Nagasawa, and M. Turner. 2010. Thymic development beyond beta-selection requires phosphatidylinositol 3-kinase activation by CXCR4. *J Exp Med* 207:247-261.
- Jensen, C.T., J. Ahsberg, M.N.E. Sommarin, T. Strid, R. Somasundaram, K. Okuyama, J. Ungerback, J. Kupari, M.S. Airaksinen, S. Lang, D. Bryder, S. Soneji, G. Karlsson, and M. Sigvardsson. 2018. Dissection of progenitor compartments resolves developmental trajectories in B-lymphopoiesis. *J Exp Med* 215:1947-1963.
- Jensen, C.T., S. Kharazi, C. Boiers, M. Cheng, A. Lubking, E. Sitnicka, and S.E. Jacobsen. 2008. FLT3 ligand and not TSLP is the key regulator of IL-7-independent B-1 and B-2 B lymphopoiesis. *Blood* 112:2297-2304.
- Jiang, Q., W.Q. Li, F.B. Aiello, R. Mazzucchelli, B. Asefa, A.R. Khaled, and S.K. Durum. 2005. Cell biology of IL-7, a key lymphotrophin. *Cytokine Growth Factor Rev* 16:513-533.
- Jiang, Q., W.Q. Li, R.R. Hofmeister, H.A. Young, D.R. Hodge, J.R. Keller, A.R. Khaled, and S.K. Durum. 2004. Distinct regions of the interleukin-7 receptor regulate different Bcl2 family members. *Mol Cell Biol* 24:6501-6513.
- Johanson, T.M., A.T.L. Lun, H.D. Coughlan, T. Tan, G.K. Smyth, S.L. Nutt, and R.S. Allan. 2018. Transcription-factor-mediated supervision of global genome architecture maintains B cell identity. *Nat Immunol* 19:1257-1264.
- Johnson, G.R., and M.A. Moore. 1975. Role of stem cell migration in initiation of mouse foetal liver haemopoiesis. *Nature* 258:726-728.

- Johnson, J.L., G. Georgakilas, J. Petrovic, M. Kurachi, S. Cai, C. Harly, W.S. Pear, A. Bhandoola, E.J. Wherry, and G. Vahedi. 2018. Lineage-Determining Transcription Factor TCF-1 Initiates the Epigenetic Identity of T Cells. *Immunity* 48:243-257 e210.
- Kadish, J.L., and R.S. Basch. 1976. Hematopoietic thymocyte precursors. I. Assay and kinetics of the appearance of progeny. *J Exp Med* 143:1082-1099.
- Kantor, A.B., C.E. Merrill, L.A. Herzenberg, and J.L. Hillson. 1997. An unbiased analysis of V(H)-D-J(H) sequences from B-1a, B-1b, and conventional B cells. *J Immunol* 158:1175-1186.
- Karasuyama, H., A. Kudo, and F. Melchers. 1990. The proteins encoded by the VpreB and lambda 5 pre-B cell-specific genes can associate with each other and with mu heavy chain. *J Exp Med* 172:969-972.
- Karsunky, H., M.A. Inlay, T. Serwold, D. Bhattacharya, and I.L. Weissman. 2008. Flk2+ common lymphoid progenitors possess equivalent differentiation potential for the B and T lineages. *Blood* 111:5562-5570.
- Karsunky, H., M. Merad, A. Cozzio, I.L. Weissman, and M.G. Manz. 2003. Flt3 ligand regulates dendritic cell development from Flt3+ lymphoid and myeloid-committed progenitors to Flt3+ dendritic cells in vivo. *J Exp Med* 198:305-313.
- Kasai, H., T. Kuwabara, Y. Matsui, K. Nakajima, and M. Kondo. 2018. Identification of an Essential Cytoplasmic Region of Interleukin-7 Receptor alpha Subunit in B-Cell Development. *Int J Mol Sci* 19:
- Kawazu, M., G. Yamamoto, M. Yoshimi, K. Yamamoto, T. Asai, M. Ichikawa, S. Seo, M. Nakagawa, S. Chiba, M. Kurokawa, and S. Ogawa. 2007. Expression profiling of immature thymocytes revealed a novel homeobox gene that regulates double-negative thymocyte development. *J Immunol* 179:5335-5345.
- Kenins, L., J.W. Gill, G.A. Hollander, and A. Wodnar-Filipowicz. 2010. Flt3 ligand-receptor interaction is important for maintenance of early thymic progenitor numbers in steady-state thymopoiesis. *Eur J Immunol* 40:81-90.
- Khaled, A.R., W.Q. Li, J. Huang, T.J. Fry, A.S. Khaled, C.L. Mackall, K. Muegge, H.A. Young, and S.K. Durum. 2002. Bax deficiency partially corrects interleukin-7 receptor alpha deficiency. *Immunity* 17:561-573.
- Khan, W.N., F.W. Alt, R.M. Gerstein, B.A. Malynn, I. Larsson, G. Rathbun, L. Davidson, S. Muller, A.B. Kantor, L.A. Herzenberg, and et al. 1995. Defective B cell development and function in Btk-deficient mice. *Immunity* 3:283-299.
- Kiel, M.J., O.H. Yilmaz, T. Iwashita, O.H. Yilmaz, C. Terhorst, and S.J. Morrison. 2005. SLAM family receptors distinguish hematopoietic stem and progenitor cells and reveal endothelial niches for stem cells. *Cell* 121:1109-1121.
- Kikuchi, K., A.Y. Lai, C.L. Hsu, and M. Kondo. 2005. IL-7 receptor signaling is necessary for stage transition in adult B cell development through up-regulation of EBF. *J Exp Med* 201:1197-1203.
- Kitamura, D., A. Kudo, S. Schaal, W. Muller, F. Melchers, and K. Rajewsky. 1992. A critical role of lambda 5 protein in B cell development. *Cell* 69:823-831.
- Klein, L., M. Hinterberger, G. Wirnsberger, and B. Kyewski. 2009. Antigen presentation in the thymus for positive selection and central tolerance induction. *Nat Rev Immunol* 9:833-844.
- Koch, U., and F. Radtke. 2011. Mechanisms of T cell development and transformation. *Annu Rev Cell Dev Biol* 27:539-562.
- Kondo, M., K. Akashi, J. Domen, K. Sugamura, and I.L. Weissman. 1997a. Bcl-2 rescues T lymphopoiesis, but not B or NK cell development, in common gamma chain-deficient mice. *Immunity* 7:155-162.
- Kondo, M., I.L. Weissman, and K. Akashi. 1997b. Identification of clonogenic common lymphoid progenitors in mouse bone marrow. *Cell* 91:661-672.
- Kreslavsky, T., M. Gleimer, M. Miyazaki, Y. Choi, E. Gagnon, C. Murre, P. Sicinski, and H. von Boehmer. 2012. beta-Selection-induced proliferation is required for alphabeta T cell differentiation. *Immunity* 37:840-853.

- Krueger, A., and H. von Boehmer. 2007. Identification of a T lineage-committed progenitor in adult blood. *Immunity* 26:105-116.
- Krueger, A., S. Willenzon, M. Lyszkiewicz, E. Kremmer, and R. Forster. 2010. CC chemokine receptor 7 and 9 double-deficient hematopoietic progenitors are severely impaired in seeding the adult thymus. *Blood* 115:1906-1912.
- Kudo, A., and F. Melchers. 1987. A second gene, VpreB in the lambda 5 locus of the mouse, which appears to be selectively expressed in pre-B lymphocytes. *EMBO J* 6:2267-2272.
- Kulesa, H., J. Frampton, and T. Graf. 1995. GATA-1 reprograms avian myelomonocytic cell lines into eosinophils, thromboblats, and erythroblasts. *Genes Dev* 9:1250-1262.
- Lai, A.Y., and M. Kondo. 2007. Identification of a bone marrow precursor of the earliest thymocytes in adult mouse. *Proc Natl Acad Sci U S A* 104:6311-6316.
- Lali, F.V., J. Crawley, D.A. McCulloch, and B.M. Foxwell. 2004. A late, prolonged activation of the phosphatidylinositol 3-kinase pathway is required for T cell proliferation. *J Immunol* 172:3527-3534.
- Lam, K.P., and K. Rajewsky. 1999. B cell antigen receptor specificity and surface density together determine B-1 versus B-2 cell development. *J Exp Med* 190:471-477.
- Laouar, Y., T. Welte, X.Y. Fu, and R.A. Flavell. 2003. STAT3 is required for Flt3L-dependent dendritic cell differentiation. *Immunity* 19:903-912.
- Laurenti, E., and B. Gottgens. 2018. From haematopoietic stem cells to complex differentiation landscapes. *Nature* 553:418-426.
- Lazorchak, A.S., M.S. Schlissel, and Y. Zhuang. 2006. E2A and IRF-4/Pip promote chromatin modification and transcription of the immunoglobulin kappa locus in pre-B cells. *Mol Cell Biol* 26:810-821.
- Li, L., M. Leid, and E.V. Rothenberg. 2010a. An early T cell lineage commitment checkpoint dependent on the transcription factor Bcl11b. *Science* 329:89-93.
- Li, L., J.A. Zhang, M. Dose, H.Y. Kueh, R. Mosadeghi, F. Gounari, and E.V. Rothenberg. 2013. A far downstream enhancer for murine Bcl11b controls its T-cell specific expression. *Blood* 122:902-911.
- Li, P., S. Burke, J. Wang, X. Chen, M. Ortiz, S.C. Lee, D. Lu, L. Campos, D. Goulding, B.L. Ng, G. Dougan, B. Huntly, B. Gottgens, N.A. Jenkins, N.G. Copeland, F. Colucci, and P. Liu. 2010b. Reprogramming of T cells to natural killer-like cells upon Bcl11b deletion. *Science* 329:85-89.
- Li, R., P. Cauchy, S. Ramamoorthy, S. Boller, L. Chavez, and R. Grosschedl. 2018. Dynamic EBF1 occupancy directs sequential epigenetic and transcriptional events in B-cell programming. *Genes Dev* 32:96-111.
- Li, W.Q., T. Guszczynski, J.A. Hixon, and S.K. Durum. 2010c. Interleukin-7 regulates Bim proapoptotic activity in peripheral T-cell survival. *Mol Cell Biol* 30:590-600.
- Liberzon, A., C. Birger, H. Thorvaldsdottir, M. Ghandi, J.P. Mesirov, and P. Tamayo. 2015. The Molecular Signatures Database (MSigDB) hallmark gene set collection. *Cell Syst* 1:417-425.
- Lin, H., and R. Grosschedl. 1995. Failure of B-cell differentiation in mice lacking the transcription factor EBF. *Nature* 376:263-267.
- Lin, Q., C. Dong, and M.D. Cooper. 1998. Impairment of T and B cell development by treatment with a type I interferon. *J Exp Med* 187:79-87.
- Lin, W.C., and S. Desiderio. 1994. Cell cycle regulation of V(D)J recombination-activating protein RAG-2. *Proc Natl Acad Sci U S A* 91:2733-2737.
- Lin, Y.C., S. Jhunjunwala, C. Benner, S. Heinz, E. Welinder, R. Mansson, M. Sigvardsson, J. Hagman, C.A. Espinoza, J. Dutkowski, T. Ideker, C.K. Glass, and C. Murre. 2010. A global network of transcription factors, involving E2A, EBF1 and Foxo1, that orchestrates B cell fate. *Nat Immunol* 11:635-643.
- Lindner, S.E., M. Lohmuller, B. Kotkamp, F. Schuler, Z. Knust, A. Villunger, and S. Herzog. 2017. The miR-15 family reinforces the transition from proliferation to differentiation in pre-B cells. *EMBO Rep* 18:1604-1617.

- Liu, K., G.D. Victora, T.A. Schwickert, P. Guermonprez, M.M. Meredith, K. Yao, F.F. Chu, G.J. Randolph, A.Y. Rudensky, and M. Nussenzweig. 2009. In vivo analysis of dendritic cell development and homeostasis. *Science* 324:392-397.
- Liu, Q., A.J. Oliveira-Dos-Santos, S. Mariathasan, D. Bouchard, J. Jones, R. Sarao, I. Kozieradzki, P.S. Ohashi, J.M. Penninger, and D.J. Dumont. 1998. The inositol polyphosphate 5-phosphatase *SHIP* is a crucial negative regulator of B cell antigen receptor signaling. *J Exp Med* 188:1333-1342.
- Livak, F., M. Tourigny, D.G. Schatz, and H.T. Petrie. 1999. Characterization of TCR gene rearrangements during adult murine T cell development. *J Immunol* 162:2575-2580.
- Loder, F., B. Mutschler, R.J. Ray, C.J. Paige, P. Sideras, R. Torres, M.C. Lamers, and R. Carsetti. 1999. B cell development in the spleen takes place in discrete steps and is determined by the quality of B cell receptor-derived signals. *J Exp Med* 190:75-89.
- Lopez-Rodriguez, C., J. Aramburu, and R. Berga-Bolanos. 2015. Transcription factors and target genes of pre-TCR signaling. *Cell Mol Life Sci* 72:2305-2321.
- Love, P.E., and A. Bhandoola. 2011. Signal integration and crosstalk during thymocyte migration and emigration. *Nat Rev Immunol* 11:469-477.
- Lu, R., K.L. Medina, D.W. Lancki, and H. Singh. 2003. IRF-4,8 orchestrate the pre-B-to-B transition in lymphocyte development. *Genes Dev* 17:1703-1708.
- Luc, S., T.C. Luis, H. Boukarabila, I.C. Macaulay, N. Buza-Vidas, T. Bouriez-Jones, M. Lutteropp, P.S. Woll, S.J. Loughran, A.J. Mead, A. Hultquist, J. Brown, T. Mizukami, S. Matsuoka, H. Ferry, K. Anderson, S. Duarte, D. Atkinson, S. Soneji, A. Domanski, A. Farley, A. Sanjuan-Pla, C. Carella, R. Patient, M. de Bruijn, T. Enver, C. Nerlov, C. Blackburn, I. Godin, and S.E. Jacobsen. 2012. The earliest thymic T cell progenitors sustain B cell and myeloid lineage potential. *Nat Immunol* 13:412-419.
- Luche, H., T. Nageswara Rao, S. Kumar, A. Tasdogan, F. Beckel, C. Blum, V.C. Martins, H.R. Rodewald, and H.J. Fehling. 2013. In vivo fate mapping identifies pre-TCR $\alpha$  expression as an intra- and extrathymic, but not prethymic, marker of T lymphopoiesis. *J Exp Med* 210:699-714.
- Luis, T.C., S. Luc, T. Mizukami, H. Boukarabila, S. Thongjuea, P.S. Woll, E. Azzoni, A. Giustacchini, M. Lutteropp, T. Bouriez-Jones, H. Vaidya, A.J. Mead, D. Atkinson, C. Boiers, J. Carrelha, I.C. Macaulay, R. Patient, F. Geissmann, C. Nerlov, R. Sandberg, M. de Bruijn, C.C. Blackburn, I. Godin, and S.E.W. Jacobsen. 2016. Initial seeding of the embryonic thymus by immune-restricted lympho-myeloid progenitors. *Nat Immunol* 17:1424-1435.
- Lun, A.T., D.J. McCarthy, and J.C. Marioni. 2016. A step-by-step workflow for low-level analysis of single-cell RNA-seq data with Bioconductor. *F1000Res* 5:2122.
- Ma, S., A. Turetsky, L. Trinh, and R. Lu. 2006. IFN regulatory factor 4 and 8 promote Ig light chain kappa locus activation in pre-B cell development. *J Immunol* 177:7898-7904.
- Mackarechtschian, K., J.D. Hardin, K.A. Moore, S. Boast, S.P. Goff, and I.R. Lemischka. 1995. Targeted disruption of the *flk2/flt3* gene leads to deficiencies in primitive hematopoietic progenitors. *Immunity* 3:147-161.
- Maillard, I., L. Tu, A. Sambandam, Y. Yashiro-Ohtani, J. Millholland, K. Keeshan, O. Shestova, L. Xu, A. Bhandoola, and W.S. Pear. 2006. The requirement for Notch signaling at the beta-selection checkpoint in vivo is absolute and independent of the pre-T cell receptor. *J Exp Med* 203:2239-2245.
- Malin, S., S. McManus, C. Cobaleda, M. Novatchkova, A. Delogu, P. Bouillet, A. Strasser, and M. Busslinger. 2010. Role of STAT5 in controlling cell survival and immunoglobulin gene recombination during pro-B cell development. *Nat Immunol* 11:171-179.
- Malissen, M., A. Gillet, L. Ardouin, G. Bouvier, J. Trucy, P. Ferrier, E. Vivier, and B. Malissen. 1995. Altered T cell development in mice with a targeted mutation of the CD3-epsilon gene. *EMBO J* 14:4641-4653.
- Mallick, C.A., E.C. Dudley, J.L. Viney, M.J. Owen, and A.C. Hayday. 1993. Rearrangement and diversity of T cell receptor beta chain genes in thymocytes: a critical role for the beta chain in development. *Cell* 73:513-519.

- Mandal, M., C. Borowski, T. Palomero, A.A. Ferrando, P. Oberdoerffer, F. Meng, A. Ruiz-Vela, M. Ciofani, J.C. Zuniga-Pflucker, I. Screpanti, A.T. Look, S.J. Korsmeyer, K. Rajewsky, H. von Boehmer, and I. Aifantis. 2005. The BCL2A1 gene as a pre-T cell receptor-induced regulator of thymocyte survival. *J Exp Med* 201:603-614.
- Mandal, M., K.M. Crusio, F. Meng, S. Liu, M. Kinsella, M.R. Clark, O. Takeuchi, and I. Aifantis. 2008. Regulation of lymphocyte progenitor survival by the proapoptotic activities of Bim and Bid. *Proc Natl Acad Sci U S A* 105:20840-20845.
- Mandal, M., S.E. Powers, M. Maienschein-Cline, E.T. Bartom, K.M. Hamel, B.L. Kee, A.R. Dinner, and M.R. Clark. 2011. Epigenetic repression of the Igk locus by STAT5-mediated recruitment of the histone methyltransferase Ezh2. *Nat Immunol* 12:1212-1220.
- Mandal, M., S.E. Powers, K. Ochiai, K. Georgopoulos, B.L. Kee, H. Singh, and M.R. Clark. 2009. Ras orchestrates exit from the cell cycle and light-chain recombination during early B cell development. *Nat Immunol* 10:1110-1117.
- Mansson, R., A. Hultquist, S. Luc, L. Yang, K. Anderson, S. Kharazi, S. Al-Hashmi, K. Liuba, L. Thoren, J. Adolfsson, N. Buza-Vidas, H. Qian, S. Soneji, T. Enver, M. Sigvardsson, and S.E. Jacobsen. 2007. Molecular evidence for hierarchical transcriptional lineage priming in fetal and adult stem cells and multipotent progenitors. *Immunity* 26:407-419.
- Mansson, R., S. Zandi, K. Anderson, I.L. Martensson, S.E. Jacobsen, D. Bryder, and M. Sigvardsson. 2008. B-lineage commitment prior to surface expression of B220 and CD19 on hematopoietic progenitor cells. *Blood* 112:1048-1055.
- Maraskovsky, E., L.A. O'Reilly, M. Teepe, L.M. Corcoran, J.J. Peschon, and A. Strasser. 1997. Bcl-2 can rescue T lymphocyte development in interleukin-7 receptor-deficient mice but not in mutant rag-1<sup>-/-</sup> mice. *Cell* 89:1011-1019.
- Maraskovsky, E., J.J. Peschon, H. McKenna, M. Teepe, and A. Strasser. 1998. Overexpression of Bcl-2 does not rescue impaired B lymphopoiesis in IL-7 receptor-deficient mice but can enhance survival of mature B cells. *Int Immunol* 10:1367-1375.
- Marchetto, S., E. Fournier, N. Beslu, T. Aurran-Schleinitz, P. Dubreuil, J.P. Borg, D. Birnbaum, and O. Rosnet. 1999. SHC and SHIP phosphorylation and interaction in response to activation of the FLT3 receptor. *Leukemia* 13:1374-1382.
- Massa, S., G. Balciunaite, R. Ceredig, and A.G. Rolink. 2006. Critical role for c-kit (CD117) in T cell lineage commitment and early thymocyte development in vitro. *Eur J Immunol* 36:526-532.
- Masuda, K., K. Kakugawa, T. Nakayama, N. Minato, Y. Katsura, and H. Kawamoto. 2007. T cell lineage determination precedes the initiation of TCR beta gene rearrangement. *J Immunol* 179:3699-3706.
- Matloubian, M., C.G. Lo, G. Cinamon, M.J. Lesneski, Y. Xu, V. Brinkmann, M.L. Allende, R.L. Proia, and J.G. Cyster. 2004. Lymphocyte egress from thymus and peripheral lymphoid organs is dependent on S1P receptor 1. *Nature* 427:355-360.
- Matthews, W., C.T. Jordan, G.W. Wiegand, D. Pardoll, and I.R. Lemischka. 1991. A receptor tyrosine kinase specific to hematopoietic stem and progenitor cell-enriched populations. *Cell* 65:1143-1152.
- Mazzucchelli, R., and S.K. Durum. 2007. Interleukin-7 receptor expression: intelligent design. *Nat Rev Immunol* 7:144-154.
- McCarthy, D.J., K.R. Campbell, A.T. Lun, and Q.F. Wills. 2017. Scater: pre-processing, quality control, normalization and visualization of single-cell RNA-seq data in R. *Bioinformatics* 33:1179-1186.
- McCulloch, E.A., and J.E. Till. 1960. The radiation sensitivity of normal mouse bone marrow cells, determined by quantitative marrow transplantation into irradiated mice. *Radiat Res* 13:115-125.
- McKenna, H.J., K.L. Stocking, R.E. Miller, K. Brasel, T. De Smedt, E. Maraskovsky, C.R. Maliszewski, D.H. Lynch, J. Smith, B. Pulendran, E.R. Roux, M. Teepe, S.D. Lyman, and J.J. Peschon. 2000. Mice lacking flt3 ligand have deficient hematopoiesis affecting hematopoietic progenitor cells, dendritic cells, and natural killer cells. *Blood* 95:3489-3497.

- Mead, A.J., W.H. Neo, N. Barkas, S. Matsuoka, A. Giustacchini, R. Facchini, S. Thongjuea, L. Jamieson, C.A.G. Booth, N. Fordham, C. Di Genua, D. Atkinson, O. Chowdhury, E. Repapi, N. Gray, S. Kharazi, S.A. Clark, T. Bouriez, P. Woll, T. Suda, C. Nerlov, and S.E.W. Jacobsen. 2017. Niche-mediated depletion of the normal hematopoietic stem cell reservoir by Flt3-ITD-induced myeloproliferation. *J Exp Med* 214:2005-2021.
- Medvinsky, A., and E. Dzierzak. 1996. Definitive hematopoiesis is autonomously initiated by the AGM region. *Cell* 86:897-906.
- Merrell, K.T., R.J. Benschop, S.B. Gauld, K. Aviszus, D. Decote-Ricardo, L.J. Wysocki, and J.C. Cambier. 2006. Identification of anergic B cells within a wild-type repertoire. *Immunity* 25:953-962.
- Mertsching, E., C. Burdet, and R. Ceredig. 1995. IL-7 transgenic mice: analysis of the role of IL-7 in the differentiation of thymocytes in vivo and in vitro. *Int Immunol* 7:401-414.
- Mertsching, E., U. Grawunder, V. Meyer, T. Rolink, and R. Ceredig. 1996. Phenotypic and functional analysis of B lymphopoiesis in interleukin-7-transgenic mice: expansion of pro/pre-B cell number and persistence of B lymphocyte development in lymph nodes and spleen. *Eur J Immunol* 26:28-33.
- Metcalfe, D. 2008. Hematopoietic cytokines. *Blood* 111:485-491.
- Metcalfe, D., and A.W. Burgess. 1982. Clonal analysis of progenitor cell commitment of granulocyte or macrophage production. *J Cell Physiol* 111:275-283.
- Mikkola, I., B. Heavey, M. Horcher, and M. Busslinger. 2002. Reversion of B cell commitment upon loss of Pax5 expression. *Science* 297:110-113.
- Mingueneau, M., T. Kreslavsky, D. Gray, T. Heng, R. Cruse, J. Ericson, S. Bendall, M.H. Spitzer, G.P. Nolan, K. Kobayashi, H. von Boehmer, D. Mathis, C. Benoist, C. Immunological Genome, A.J. Best, J. Knell, A. Goldrath, V. Joic, D. Koller, T. Shay, A. Regev, N. Cohen, P. Brennan, M. Brenner, F. Kim, T. Nageswara Rao, A. Wagers, T. Heng, J. Ericson, K. Rothamel, A. Ortiz-Lopez, D. Mathis, C. Benoist, N.A. Bezman, J.C. Sun, G. Min-Oo, C.C. Kim, L.L. Lanier, J. Miller, B. Brown, M. Merad, E.L. Gautier, C. Jakubzick, G.J. Randolph, P. Monach, D.A. Blair, M.L. Dustin, S.A. Shinton, R.R. Hardy, D. Laidlaw, J. Collins, R. Gazit, D.J. Rossi, N. Malhotra, K. Sylvia, J. Kang, T. Kreslavsky, A. Fletcher, K. Elpek, A. Bellemare-Pelletier, D. Malhotra, and S. Turley. 2013. The transcriptional landscape of alphabeta T cell differentiation. *Nat Immunol* 14:619-632.
- Misslitz, A., O. Pabst, G. Hintzen, L. Ohl, E. Kremmer, H.T. Petrie, and R. Forster. 2004. Thymic T cell development and progenitor localization depend on CCR7. *J Exp Med* 200:481-491.
- Mombaerts, P., J. Iacomini, R.S. Johnson, K. Herrup, S. Tonegawa, and V.E. Papaioannou. 1992. RAG-1-deficient mice have no mature B and T lymphocytes. *Cell* 68:869-877.
- Mombaerts, P., C. Terhorst, T. Jacks, S. Tonegawa, and J. Sancho. 1995. Characterization of immature thymocyte lines derived from T-cell receptor or recombination activating gene 1 and p53 double mutant mice. *Proc Natl Acad Sci U S A* 92:7420-7424.
- Montecino-Rodriguez, E., H. Leathers, and K. Dorshkind. 2006. Identification of a B-1 B cell-specified progenitor. *Nat Immunol* 7:293-301.
- Mooney, C.J., A. Cunningham, P. Tsapogas, K.M. Toellner, and G. Brown. 2017. Selective Expression of Flt3 within the Mouse Hematopoietic Stem Cell Compartment. *Int J Mol Sci* 18:
- Moran, A.E., K.L. Holzapfel, Y. Xing, N.R. Cunningham, J.S. Maltzman, J. Punt, and K.A. Hogquist. 2011. T cell receptor signal strength in Treg and iNKT cell development demonstrated by a novel fluorescent reporter mouse. *J Exp Med* 208:1279-1289.
- Morita, Y., H. Ema, and H. Nakauchi. 2010. Heterogeneity and hierarchy within the most primitive hematopoietic stem cell compartment. *J Exp Med* 207:1173-1182.
- Morrison, S.J., and I.L. Weissman. 1994. The long-term repopulating subset of hematopoietic stem cells is deterministic and isolatable by phenotype. *Immunity* 1:661-673.
- Mossadegh-Keller, N., S. Sarrazin, P.K. Kandalla, L. Espinosa, E.R. Stanley, S.L. Nutt, J. Moore, and M.H. Sieweke. 2013. M-CSF instructs myeloid lineage fate in single haematopoietic stem cells. *Nature* 497:239-243.

- Mostoslavsky, R., F.W. Alt, and K. Rajewsky. 2004. The lingering enigma of the allelic exclusion mechanism. *Cell* 118:539-544.
- Mostoslavsky, R., N. Singh, A. Kirillov, R. Pelanda, H. Cedar, A. Chess, and Y. Bergman. 1998. Kappa chain monoallelic demethylation and the establishment of allelic exclusion. *Genes Dev* 12:1801-1811.
- Muller-Sieburg, C.E., R.H. Cho, L. Karlsson, J.F. Huang, and H.B. Sieburg. 2004. Myeloid-biased hematopoietic stem cells have extensive self-renewal capacity but generate diminished lymphoid progeny with impaired IL-7 responsiveness. *Blood* 103:4111-4118.
- Munitic, I., J.A. Williams, Y. Yang, B. Dong, P.J. Lucas, N. El Kassar, R.E. Gress, and J.D. Ashwell. 2004. Dynamic regulation of IL-7 receptor expression is required for normal thymopoiesis. *Blood* 104:4165-4172.
- Nadel, B., and A.J. Feeney. 1997. Nucleotide deletion and P addition in V(D)J recombination: a determinant role of the coding-end sequence. *Mol Cell Biol* 17:3768-3778.
- Naik, S.H., L. Perie, E. Swart, C. Gerlach, N. van Rooij, R.J. de Boer, and T.N. Schumacher. 2013. Diverse and heritable lineage imprinting of early haematopoietic progenitors. *Nature* 496:229-232.
- Nakao, M., S. Yokota, T. Iwai, H. Kaneko, S. Horiike, K. Kashima, Y. Sonoda, T. Fujimoto, and S. Misawa. 1996. Internal tandem duplication of the *flt3* gene found in acute myeloid leukemia. *Leukemia* 10:1911-1918.
- Namen, A.E., A.E. Schmierer, C.J. March, R.W. Overell, L.S. Park, D.L. Urdal, and D.Y. Mochizuki. 1988. B cell precursor growth-promoting activity. Purification and characterization of a growth factor active on lymphocyte precursors. *J Exp Med* 167:988-1002.
- Namikawa, R., M.O. Muench, J.E. de Vries, and M.G. Roncarolo. 1996. The FLK2/FLT3 ligand synergizes with interleukin-7 in promoting stromal-cell-independent expansion and differentiation of human fetal pro-B cells in vitro. *Blood* 87:1881-1890.
- Nechanitzky, R., D. Akbas, S. Scherer, I. Gyory, T. Hoyler, S. Ramamoorthy, A. Diefenbach, and R. Grosschedl. 2013. Transcription factor EBF1 is essential for the maintenance of B cell identity and prevention of alternative fates in committed cells. *Nat Immunol* 14:867-875.
- Nerlov, C., and T. Graf. 1998. PU.1 induces myeloid lineage commitment in multipotent hematopoietic progenitors. *Genes Dev* 12:2403-2412.
- Neuberger, M.S., H.M. Caskey, S. Pettersson, G.T. Williams, and M.A. Surani. 1989. Isotype exclusion and transgene down-regulation in immunoglobulin-lambda transgenic mice. *Nature* 338:350-352.
- Newton, K., A.W. Harris, and A. Strasser. 2000. FADD/MORT1 regulates the pre-TCR checkpoint and can function as a tumour suppressor. *EMBO J* 19:931-941.
- Ng, S.Y., T. Yoshida, J. Zhang, and K. Georgopoulos. 2009. Genome-wide lineage-specific transcriptional networks underscore Ikaros-dependent lymphoid priming in hematopoietic stem cells. *Immunity* 30:493-507.
- Nichogiannopoulou, A., M. Trevisan, S. Neben, C. Friedrich, and K. Georgopoulos. 1999. Defects in hemopoietic stem cell activity in Ikaros mutant mice. *J Exp Med* 190:1201-1214.
- Noguchi, M., H. Yi, H.M. Rosenblatt, A.H. Filipovich, S. Adelstein, W.S. Modi, O.W. McBride, and W.J. Leonard. 1993. Interleukin-2 receptor gamma chain mutation results in X-linked severe combined immunodeficiency in humans. *Cell* 73:147-157.
- Nutt, S.L., D. Eberhard, M. Horcher, A.G. Rolink, and M. Busslinger. 2001. Pax5 determines the identity of B cells from the beginning to the end of B-lymphopoiesis. *Int Rev Immunol* 20:65-82.
- Nutt, S.L., B. Heavey, A.G. Rolink, and M. Busslinger. 1999. Commitment to the B-lymphoid lineage depends on the transcription factor Pax5. *Nature* 401:556-562.
- Nutt, S.L., and B.L. Kee. 2007. The transcriptional regulation of B cell lineage commitment. *Immunity* 26:715-725.

- Nutt, S.L., A.M. Morrison, P. Dorfler, A. Rolink, and M. Busslinger. 1998. Identification of BSAP (Pax-5) target genes in early B-cell development by loss- and gain-of-function experiments. *EMBO J* 17:2319-2333.
- Nutt, S.L., P. Urbanek, A. Rolink, and M. Busslinger. 1997. Essential functions of Pax5 (BSAP) in pro-B cell development: difference between fetal and adult B lymphopoiesis and reduced V-to-DJ recombination at the IgH locus. *Genes Dev* 11:476-491.
- O'Reilly, L.A., D.C. Huang, and A. Strasser. 1996. The cell death inhibitor Bcl-2 and its homologues influence control of cell cycle entry. *EMBO J* 15:6979-6990.
- Ochiai, K., M. Maienschein-Cline, M. Mandal, J.R. Triggs, E. Bertolino, R. Sciammas, A.R. Dinner, M.R. Clark, and H. Singh. 2012. A self-reinforcing regulatory network triggered by limiting IL-7 activates pre-BCR signaling and differentiation. *Nat Immunol* 13:300-307.
- Ohnishi, K., and F. Melchers. 2003. The nonimmunoglobulin portion of lambda5 mediates cell-autonomous pre-B cell receptor signaling. *Nat Immunol* 4:849-856.
- Okada, S., H. Nakauchi, K. Nagayoshi, S. Nishikawa, Y. Miura, and T. Suda. 1992. In vivo and in vitro stem cell function of c-kit- and Sca-1-positive murine hematopoietic cells. *Blood* 80:3044-3050.
- Onai, N., K. Kurabayashi, M. Hosoi-Amaike, N. Toyama-Sorimachi, K. Matsushima, K. Inaba, and T. Ohteki. 2013. A clonogenic progenitor with prominent plasmacytoid dendritic cell developmental potential. *Immunity* 38:943-957.
- Opferman, J.T., A. Letai, C. Beard, M.D. Sorcinelli, C.C. Ong, and S.J. Korsmeyer. 2003. Development and maintenance of B and T lymphocytes requires antiapoptotic MCL-1. *Nature* 426:671-676.
- Orkin, S.H., and L.I. Zon. 2008. Hematopoiesis: an evolving paradigm for stem cell biology. *Cell* 132:631-644.
- Osawa, M., K. Hanada, H. Hamada, and H. Nakauchi. 1996a. Long-term lymphohematopoietic reconstitution by a single CD34-low/negative hematopoietic stem cell. *Science* 273:242-245.
- Osawa, M., K. Nakamura, N. Nishi, N. Takahashi, Y. Tokumoto, H. Inoue, and H. Nakauchi. 1996b. In vivo self-renewal of c-Kit+ Sca-1+ Lin(low/-) hemopoietic stem cells. *J Immunol* 156:3207-3214.
- Osmond, D.G., A. Rolink, and F. Melchers. 1998. Murine B lymphopoiesis: towards a unified model. *Immunol Today* 19:65-68.
- Page, T.H., F.V. Lali, and B.M. Foxwell. 1995. Interleukin-7 activates p56lck and p59fyn, two tyrosine kinases associated with the p90 interleukin-7 receptor in primary human T cells. *Eur J Immunol* 25:2956-2960.
- Palmer, E. 2003. Negative selection--clearing out the bad apples from the T-cell repertoire. *Nat Rev Immunol* 3:383-391.
- Palmiter, R.D., H.Y. Chen, and R.L. Brinster. 1982. Differential regulation of metallothionein-thymidine kinase fusion genes in transgenic mice and their offspring. *Cell* 29:701-710.
- Panda, S., and J.L. Ding. 2015. Natural antibodies bridge innate and adaptive immunity. *J Immunol* 194:13-20.
- Pandey, A., K. Ozaki, H. Baumann, S.D. Levin, A. Puel, A.G. Farr, S.F. Ziegler, W.J. Leonard, and H.F. Lodish. 2000. Cloning of a receptor subunit required for signaling by thymic stromal lymphopoietin. *Nat Immunol* 1:59-64.
- Pang, S.H.M., C.A. de Graaf, D.J. Hilton, N.D. Huntington, S. Carotta, L. Wu, and S.L. Nutt. 2018. PU.1 Is Required for the Developmental Progression of Multipotent Progenitors to Common Lymphoid Progenitors. *Front Immunol* 9:1264.
- Panigada, M., S. Porcellini, E. Barbier, S. Hoeflinger, P.A. Cazenave, H. Gu, H. Band, H. von Boehmer, and F. Grassi. 2002. Constitutive endocytosis and degradation of the pre-T cell receptor. *J Exp Med* 195:1585-1597.
- Park, J.H., Q. Yu, B. Erman, J.S. Appelbaum, D. Montoya-Durango, H.L. Grimes, and A. Singer. 2004. Suppression of IL7Ralpha transcription by IL-7 and other prosurvival cytokines: a novel mechanism for maximizing IL-7-dependent T cell survival. *Immunity* 21:289-302.

- Park, L.S., U. Martin, K. Garka, B. Gliniak, J.P. Di Santo, W. Muller, D.A. Largaespada, N.G. Copeland, N.A. Jenkins, A.G. Farr, S.F. Ziegler, P.J. Morrissey, R. Paxton, and J.E. Sims. 2000. Cloning of the murine thymic stromal lymphopoietin (TSLP) receptor: Formation of a functional heteromeric complex requires interleukin 7 receptor. *J Exp Med* 192:659-670.
- Parker, M.J., S. Licence, L. Erlandsson, G.R. Galler, L. Chakalova, C.S. Osborne, G. Morgan, P. Fraser, H. Jumaa, T.H. Winkler, J. Skok, and I.L. Martensson. 2005. The pre-B-cell receptor induces silencing of VpreB and lambda5 transcription. *EMBO J* 24:3895-3905.
- Parrish, Y.K., I. Baez, T.A. Milford, A. Benitez, N. Galloway, J.W. Rogerio, E. Sahakian, M. Kagoda, G. Huang, Q.L. Hao, Y. Sevilla, L.W. Barsky, E. Zielinska, M.A. Price, N.R. Wall, S. Dovat, and K.J. Payne. 2009. IL-7 Dependence in human B lymphopoiesis increases during progression of ontogeny from cord blood to bone marrow. *J Immunol* 182:4255-4266.
- Paul, F., Y. Arkin, A. Giladi, D.A. Jaitin, E. Kenigsberg, H. Keren-Shaul, D. Winter, D. Lara-Astiaso, M. Gury, A. Weiner, E. David, N. Cohen, F.K. Lauridsen, S. Haas, A. Schlitzer, A. Mildner, F. Ginhoux, S. Jung, A. Trumpp, B.T. Porse, A. Tanay, and I. Amit. 2015. Transcriptional Heterogeneity and Lineage Commitment in Myeloid Progenitors. *Cell* 163:1663-1677.
- Pei, W., T.B. Feyerabend, J. Rossler, X. Wang, D. Postrach, K. Busch, I. Rode, K. Klapproth, N. Dietlein, C. Quedenau, W. Chen, S. Sauer, S. Wolf, T. Hofer, and H.R. Rodewald. 2017. Polylox barcoding reveals haematopoietic stem cell fates realized in vivo. *Nature* 548:456-460.
- Pellegrini, M., P. Bouillet, M. Robati, G.T. Belz, G.M. Davey, and A. Strasser. 2004. Loss of Bim increases T cell production and function in interleukin 7 receptor-deficient mice. *J Exp Med* 200:1189-1195.
- Perry, S.S., R.S. Welner, T. Kouro, P.W. Kincade, and X.H. Sun. 2006. Primitive lymphoid progenitors in bone marrow with T lineage reconstituting potential. *J Immunol* 177:2880-2887.
- Peschon, J.J., P.J. Morrissey, K.H. Grabstein, F.J. Ramsdell, E. Maraskovsky, B.C. Gliniak, L.S. Park, S.F. Ziegler, D.E. Williams, C.B. Ware, J.D. Meyer, and B.L. Davison. 1994. Early lymphocyte expansion is severely impaired in interleukin 7 receptor-deficient mice. *J Exp Med* 180:1955-1960.
- Pevny, L., M.C. Simon, E. Robertson, W.H. Klein, S.F. Tsai, V. D'Agati, S.H. Orkin, and F. Costantini. 1991. Erythroid differentiation in chimaeric mice blocked by a targeted mutation in the gene for transcription factor GATA-1. *Nature* 349:257-260.
- Pietras, E.M., D. Reynaud, Y.A. Kang, D. Carlin, F.J. Calero-Nieto, A.D. Leavitt, J.M. Stuart, B. Gottgens, and E. Passegue. 2015. Functionally Distinct Subsets of Lineage-Biased Multipotent Progenitors Control Blood Production in Normal and Regenerative Conditions. *Cell Stem Cell* 17:35-46.
- Pillai, S., and A. Cariappa. 2009. The follicular versus marginal zone B lymphocyte cell fate decision. *Nat Rev Immunol* 9:767-777.
- Pillai, S., A. Cariappa, and S.T. Moran. 2005. Marginal zone B cells. *Annu Rev Immunol* 23:161-196.
- Pitchford, S.C., R.C. Furze, C.P. Jones, A.M. Wengner, and S.M. Rankin. 2009. Differential mobilization of subsets of progenitor cells from the bone marrow. *Cell Stem Cell* 4:62-72.
- Pleiman, C.M., S.D. Gimpel, L.S. Park, H. Harada, T. Taniguchi, and S.F. Ziegler. 1991. Organization of the murine and human interleukin-7 receptor genes: two mRNAs generated by differential splicing and presence of a type I-interferon-inducible promoter. *Mol Cell Biol* 11:3052-3059.
- Pongubala, J.M., D.L. Northrup, D.W. Lancki, K.L. Medina, T. Treiber, E. Bertolino, M. Thomas, R. Grosschedl, D. Allman, and H. Singh. 2008. Transcription factor EBF restricts alternative lineage options and promotes B cell fate commitment independently of Pax5. *Nat Immunol* 9:203-215.

- Pronk, C.J., D.J. Rossi, R. Mansson, J.L. Attema, G.L. Norddahl, C.K. Chan, M. Sigvardsson, I.L. Weissman, and D. Bryder. 2007. Elucidation of the phenotypic, functional, and molecular topography of a myeloerythroid progenitor cell hierarchy. *Cell Stem Cell* 1:428-442.
- Puel, A., S.F. Ziegler, R.H. Buckley, and W.J. Leonard. 1998. Defective IL7R expression in T(-)B(+)NK(+) severe combined immunodeficiency. *Nat Genet* 20:394-397.
- Pui, J.C., D. Allman, L. Xu, S. DeRocco, F.G. Karnell, S. Bakkour, J.Y. Lee, T. Kadesch, R.R. Hardy, J.C. Aster, and W.S. Pear. 1999. Notch1 expression in early lymphopoiesis influences B versus T lineage determination. *Immunity* 11:299-308.
- Radtke, F., H.R. MacDonald, and F. Tacchini-Cottier. 2013. Regulation of innate and adaptive immunity by Notch. *Nat Rev Immunol* 13:427-437.
- Radtke, F., A. Wilson, G. Stark, M. Bauer, J. van Meerwijk, H.R. MacDonald, and M. Aguet. 1999. Deficient T cell fate specification in mice with an induced inactivation of Notch1. *Immunity* 10:547-558.
- Ramond, C., C. Berthault, O. Burlen-Defranoux, A.P. de Sousa, D. Guy-Grand, P. Vieira, P. Pereira, and A. Cumano. 2014. Two waves of distinct hematopoietic progenitor cells colonize the fetal thymus. *Nat Immunol* 15:27-35.
- Rashkovan, M., C. Vadnais, J. Ross, M. Gigoux, W.K. Suh, W. Gu, C. Kosan, and T. Moroy. 2014. Miz-1 regulates translation of Trp53 via ribosomal protein L22 in cells undergoing V(D)J recombination. *Proc Natl Acad Sci U S A* 111:E5411-5419.
- Rauch, M., R. Tussiwand, N. Bosco, and A.G. Rolink. 2009. Crucial role for BAFF-BAFF-R signaling in the survival and maintenance of mature B cells. *PLoS One* 4:e5456.
- Reizis, B., and P. Leder. 2002. Direct induction of T lymphocyte-specific gene expression by the mammalian Notch signaling pathway. *Genes Dev* 16:295-300.
- Retter, M.W., and D. Nemazee. 1998. Receptor editing occurs frequently during normal B cell development. *J Exp Med* 188:1231-1238.
- Reynaud, D., I.A. Demarco, K.L. Reddy, H. Schjerven, E. Bertolino, Z. Chen, S.T. Smale, S. Winandy, and H. Singh. 2008. Regulation of B cell fate commitment and immunoglobulin heavy-chain gene rearrangements by Ikaros. *Nat Immunol* 9:927-936.
- Rieger, M.A., P.S. Hoppe, B.M. Smejkal, A.C. Eitelhuber, and T. Schroeder. 2009. Hematopoietic cytokines can instruct lineage choice. *Science* 325:217-218.
- Robinette, M.L., J.K. Bando, W. Song, T.K. Ulland, S. Gilfillan, and M. Colonna. 2017. IL-15 sustains IL-7R-independent ILC2 and ILC3 development. *Nat Commun* 8:14601.
- Robinson, M.D., D.J. McCarthy, and G.K. Smyth. 2010. edgeR: a Bioconductor package for differential expression analysis of digital gene expression data. *Bioinformatics* 26:139-140.
- Rodewald, H.R., K. Kretzschmar, S. Takeda, C. Hohl, and M. Dessing. 1994. Identification of pro-thymocytes in murine fetal blood: T lineage commitment can precede thymus colonization. *EMBO J* 13:4229-4240.
- Rodrigues, P.F., L. Alberti-Servera, A. Eremin, G.E. Grajales-Reyes, R. Ivanek, and R. Tussiwand. 2018. Distinct progenitor lineages contribute to the heterogeneity of plasmacytoid dendritic cells. *Nat Immunol*
- Rodriguez-Fraticelli, A.E., S.L. Wolock, C.S. Weinreb, R. Panero, S.H. Patel, M. Jankovic, J. Sun, R.A. Calogero, A.M. Klein, and F.D. Camargo. 2018. Clonal analysis of lineage fate in native haematopoiesis. *Nature* 553:212-216.
- Roessler, S., I. Gyory, S. Imhof, M. Spivakov, R.R. Williams, M. Busslinger, A.G. Fisher, and R. Grosschedl. 2007. Distinct promoters mediate the regulation of Ebf1 gene expression by interleukin-7 and Pax5. *Mol Cell Biol* 27:579-594.
- Rolink, A., U. Grawunder, D. Haasner, A. Strasser, and F. Melchers. 1993. Immature surface Ig+ B cells can continue to rearrange kappa and lambda L chain gene loci. *J Exp Med* 178:1263-1270.
- Rolink, A., U. Grawunder, T.H. Winkler, H. Karasuyama, and F. Melchers. 1994. IL-2 receptor alpha chain (CD25, TAC) expression defines a crucial stage in pre-B cell development. *Int Immunol* 6:1257-1264.

- Rolink, A.G., J. Andersson, and F. Melchers. 1998. Characterization of immature B cells by a novel monoclonal antibody, by turnover and by mitogen reactivity. *Eur J Immunol* 28:3738-3748.
- Rolink, A.G., J. Andersson, and F. Melchers. 2004. Molecular mechanisms guiding late stages of B-cell development. *Immunol Rev* 197:41-50.
- Rolink, A.G., T. Brocker, H. Bluethmann, M.H. Kosco-Vilbois, J. Andersson, and F. Melchers. 1999a. Mutations affecting either generation or survival of cells influence the pool size of mature B cells. *Immunity* 10:619-628.
- Rolink, A.G., S.L. Nutt, F. Melchers, and M. Busslinger. 1999b. Long-term in vivo reconstitution of T-cell development by Pax5-deficient B-cell progenitors. *Nature* 401:603-606.
- Rolink, A.G., C. Schaniel, L. Bruno, and F. Melchers. 2002. In vitro and in vivo plasticity of Pax5-deficient pre-B I cells. *Immunol Lett* 82:35-40.
- Rolink, A.G., T. Winkler, F. Melchers, and J. Andersson. 2000. Precursor B cell receptor-dependent B cell proliferation and differentiation does not require the bone marrow or fetal liver environment. *J Exp Med* 191:23-32.
- Rosnet, O., S. Marchetto, O. deLapeyriere, and D. Birnbaum. 1991. Murine Flt3, a gene encoding a novel tyrosine kinase receptor of the PDGFR/CSF1R family. *Oncogene* 6:1641-1650.
- Rossi, F.M., S.Y. Corbel, J.S. Merzaban, D.A. Carlow, K. Gossens, J. Duenas, L. So, L. Yi, and H.J. Ziltener. 2005. Recruitment of adult thymic progenitors is regulated by P-selectin and its ligand PSGL-1. *Nat Immunol* 6:626-634.
- Rothenberg, E.V. 2011. T cell lineage commitment: identity and renunciation. *J Immunol* 186:6649-6655.
- Rothenberg, E.V. 2014. Transcriptional control of early T and B cell developmental choices. *Annu Rev Immunol* 32:283-321.
- Saba, I., C. Kosan, L. Vassen, L. Klein-Hitpass, and T. Moroy. 2011. Miz-1 is required to coordinate the expression of TCRbeta and p53 effector genes at the pre-TCR "beta-selection" checkpoint. *J Immunol* 187:2982-2992.
- Saint-Ruf, C., M. Panigada, O. Azogui, P. Debey, H. von Boehmer, and F. Grassi. 2000. Different initiation of pre-TCR and gammadeltaTCR signalling. *Nature* 406:524-527.
- Saint-Ruf, C., K. Ungewiss, M. Groettrup, L. Bruno, H.J. Fehling, and H. von Boehmer. 1994. Analysis and expression of a cloned pre-T cell receptor gene. *Science* 266:1208-1212.
- Saito, T., S. Chiba, M. Ichikawa, A. Kunisato, T. Asai, K. Shimizu, T. Yamaguchi, G. Yamamoto, S. Seo, K. Kumano, E. Nakagami-Yamaguchi, Y. Hamada, S. Aizawa, and H. Hirai. 2003. Notch2 is preferentially expressed in mature B cells and indispensable for marginal zone B lineage development. *Immunity* 18:675-685.
- Sakaguchi, N., and F. Melchers. 1986. Lambda 5, a new light-chain-related locus selectively expressed in pre-B lymphocytes. *Nature* 324:579-582.
- Sambandam, A., I. Maillard, V.P. Zediak, L. Xu, R.M. Gerstein, J.C. Aster, W.S. Pear, and A. Bhandoola. 2005. Notch signaling controls the generation and differentiation of early T lineage progenitors. *Nat Immunol* 6:663-670.
- Sanjuan-Pla, A., I.C. Macaulay, C.T. Jensen, P.S. Woll, T.C. Luis, A. Mead, S. Moore, C. Carella, S. Matsuoka, T. Bouriez Jones, O. Chowdhury, L. Stenson, M. Lutteropp, J.C. Green, R. Facchini, H. Boukarabila, A. Grover, A. Gambardella, S. Thongjuea, J. Carrelha, P. Tarrant, D. Atkinson, S.A. Clark, C. Nerlov, and S.E. Jacobsen. 2013. Platelet-biased stem cells reside at the apex of the haematopoietic stem-cell hierarchy. *Nature* 502:232-236.
- Saran, N., M. Lyszkiewicz, J. Pommerencke, K. Witzlau, R. Vakilzadeh, M. Ballmaier, H. von Boehmer, and A. Krueger. 2010. Multiple extrathymic precursors contribute to T-cell development with different kinetics. *Blood* 115:1137-1144.
- Sato, S., N. Ono, D.A. Steeber, D.S. Pisetsky, and T.F. Tedder. 1996. CD19 regulates B lymphocyte signaling thresholds critical for the development of B-1 lineage cells and autoimmunity. *J Immunol* 157:4371-4378.
- Sawai, C.M., S. Babovic, S. Upadhaya, D. Knapp, Y. Lavin, C.M. Lau, A. Goloborodko, J. Feng, J. Fujisaki, L. Ding, L.A. Mirny, M. Merad, C.J. Eaves, and B. Reizis. 2016.

- Hematopoietic Stem Cells Are the Major Source of Multilineage Hematopoiesis in Adult Animals. *Immunity* 45:597-609.
- Schiemann, B., J.L. Gommerman, K. Vora, T.G. Cachero, S. Shulga-Morskaya, M. Dobles, E. Frew, and M.L. Scott. 2001. An essential role for BAFF in the normal development of B cells through a BCMA-independent pathway. *Science* 293:2111-2114.
- Schwarz, B.A., and A. Bhandoola. 2004. Circulating hematopoietic progenitors with T lineage potential. *Nat Immunol* 5:953-960.
- Schwarz, B.A., A. Sambandam, I. Maillard, B.C. Harman, P.E. Love, and A. Bhandoola. 2007. Selective thymus settling regulated by cytokine and chemokine receptors. *J Immunol* 178:2008-2017.
- Scimone, M.L., I. Aifantis, I. Apostolou, H. von Boehmer, and U.H. von Andrian. 2006. A multistep adhesion cascade for lymphoid progenitor cell homing to the thymus. *Proc Natl Acad Sci U S A* 103:7006-7011.
- Scott, E.W., M.C. Simon, J. Anastasi, and H. Singh. 1994. Requirement of transcription factor PU.1 in the development of multiple hematopoietic lineages. *Science* 265:1573-1577.
- Seet, C.S., R.L. Brumbaugh, and B.L. Kee. 2004. Early B cell factor promotes B lymphopoiesis with reduced interleukin 7 responsiveness in the absence of E2A. *J Exp Med* 199:1689-1700.
- Serwold, T., L.I. Ehrlich, and I.L. Weissman. 2009. Reductive isolation from bone marrow and blood implicates common lymphoid progenitors as the major source of thymopoiesis. *Blood* 113:807-815.
- Shadle, S.C., J.W. Zhong, A.E. Campbell, M.L. Conerly, S. Jagannathan, C.J. Wong, T.D. Morello, S.M. van der Maarel, and S.J. Tapscott. 2017. DUX4-induced dsRNA and MYC mRNA stabilization activate apoptotic pathways in human cell models of facioscapulohumeral dystrophy. *PLoS Genet* 13:e1006658.
- Shimazu, T., R. Iida, Q. Zhang, R.S. Welner, K.L. Medina, J. Alberola-Lla, and P.W. Kincade. 2012. CD86 is expressed on murine hematopoietic stem cells and denotes lymphopoietic potential. *Blood* 119:4889-4897.
- Shinkai, Y., G. Rathbun, K.P. Lam, E.M. Oltz, V. Stewart, M. Mendelsohn, J. Charron, M. Datta, F. Young, A.M. Stall, and et al. 1992. RAG-2-deficient mice lack mature lymphocytes owing to inability to initiate V(D)J rearrangement. *Cell* 68:855-867.
- Shivdasani, R.A., Y. Fujiwara, M.A. McDevitt, and S.H. Orkin. 1997. A lineage-selective knockout establishes the critical role of transcription factor GATA-1 in megakaryocyte growth and platelet development. *EMBO J* 16:3965-3973.
- Shortman, K., and S.H. Naik. 2007. Steady-state and inflammatory dendritic-cell development. *Nat Rev Immunol* 7:19-30.
- Signer, R.A., J.A. Magee, A. Salic, and S.J. Morrison. 2014. Haematopoietic stem cells require a highly regulated protein synthesis rate. *Nature* 509:49-54.
- Silverman, R.H. 2007. A scientific journey through the 2-5A/RNase L system. *Cytokine Growth Factor Rev* 18:381-388.
- Simsek, T., F. Kocabas, J. Zheng, R.J. Deberardinis, A.I. Mahmoud, E.N. Olson, J.W. Schneider, C.C. Zhang, and H.A. Sadek. 2010. The distinct metabolic profile of hematopoietic stem cells reflects their location in a hypoxic niche. *Cell Stem Cell* 7:380-390.
- Sitnicka, E., C. Brakebusch, I.L. Martensson, M. Svensson, W.W. Agace, M. Sigvardsson, N. Buza-Vidas, D. Bryder, C.M. Cilio, H. Ahlenius, E. Maraskovsky, J.J. Peschon, and S.E. Jacobsen. 2003. Complementary signaling through flt3 and interleukin-7 receptor alpha is indispensable for fetal and adult B cell genesis. *J Exp Med* 198:1495-1506.
- Sitnicka, E., D. Bryder, K. Theilgaard-Monch, N. Buza-Vidas, J. Adolfsson, and S.E. Jacobsen. 2002. Key role of flt3 ligand in regulation of the common lymphoid progenitor but not in maintenance of the hematopoietic stem cell pool. *Immunity* 17:463-472.
- Sitnicka, E., N. Buza-Vidas, H. Ahlenius, C.M. Cilio, C. Gekas, J.M. Nygren, R. Mansson, M. Cheng, C.T. Jensen, M. Svensson, K. Leandersson, W.W. Agace, M. Sigvardsson, and S.E. Jacobsen. 2007. Critical role of FLT3 ligand in IL-7 receptor independent T

- lymphopoiesis and regulation of lymphoid-primed multipotent progenitors. *Blood* 110:2955-2964.
- Smith, E.M., R. Gisler, and M. Sigvardsson. 2002. Cloning and characterization of a promoter flanking the early B cell factor (EBF) gene indicates roles for E-proteins and autoregulation in the control of EBF expression. *J Immunol* 169:261-270.
- Souabni, A., C. Cobaleda, M. Schebesta, and M. Busslinger. 2002. Pax5 promotes B lymphopoiesis and blocks T cell development by repressing Notch1. *Immunity* 17:781-793.
- Spangrude, G.J., D.M. Brooks, and D.B. Tumas. 1995. Long-term repopulation of irradiated mice with limiting numbers of purified hematopoietic stem cells: in vivo expansion of stem cell phenotype but not function. *Blood* 85:1006-1016.
- Spangrude, G.J., S. Heimfeld, and I.L. Weissman. 1988. Purification and characterization of mouse hematopoietic stem cells. *Science* 241:58-62.
- Spangrude, G.J., and R. Scollay. 1990. Differentiation of hematopoietic stem cells in irradiated mouse thymic lobes. Kinetics and phenotype of progeny. *J Immunol* 145:3661-3668.
- Stadanlick, J.E., Z. Zhang, S.Y. Lee, M. Hemann, M. Biery, M.O. Carleton, G.P. Zambetti, S.J. Anderson, T. Oravec, and D.L. Wiest. 2011. Developmental arrest of T cells in Rpl22-deficient mice is dependent upon multiple p53 effectors. *J Immunol* 187:664-675.
- Stadhouders, R., M.J. de Bruijn, M.B. Rother, S. Yuvaraj, C. Ribeiro de Almeida, P. Kolovos, M.C. Van Zelm, W. van Ijcken, F. Grosveld, E. Soler, and R.W. Hendriks. 2014. Pre-B cell receptor signaling induces immunoglobulin kappa locus accessibility by functional redistribution of enhancer-mediated chromatin interactions. *PLoS Biol* 12:e1001791.
- Starr, T.K., S.C. Jameson, and K.A. Hogquist. 2003. Positive and negative selection of T cells. *Annu Rev Immunol* 21:139-176.
- Su, D.M., J. Wang, Q. Lin, M.D. Cooper, and T. Watanabe. 1997. Interferons alpha/beta inhibit IL-7-induced proliferation of CD4- CD8- CD3- CD44+ CD25+ thymocytes, but do not inhibit that of CD4- CD8- CD3- CD44- CD25- thymocytes. *Immunology* 90:543-549.
- Subramanian, A., P. Tamayo, V.K. Mootha, S. Mukherjee, B.L. Ebert, M.A. Gillette, A. Paulovich, S.L. Pomeroy, T.R. Golub, E.S. Lander, and J.P. Mesirov. 2005. Gene set enrichment analysis: A knowledge-based approach for interpreting genome-wide expression profiles. *Proc Natl Acad Sci U S A* 102:15545-15550.
- Sultana, D.A., S.L. Zhang, S.P. Todd, and A. Bhandoola. 2012. Expression of functional P-selectin glycoprotein ligand 1 on hematopoietic progenitors is developmentally regulated. *J Immunol* 188:4385-4393.
- Sun, J., A. Ramos, B. Chapman, J.B. Johnnidis, L. Le, Y.J. Ho, A. Klein, O. Hofmann, and F.D. Camargo. 2014. Clonal dynamics of native haematopoiesis. *Nature* 514:322-327.
- Suzuki, K., H. Nakajima, Y. Saito, T. Saito, W.J. Leonard, and I. Iwamoto. 2000. Janus kinase 3 (Jak3) is essential for common cytokine receptor gamma chain (gamma(c))-dependent signaling: comparative analysis of gamma(c), Jak3, and gamma(c) and Jak3 double-deficient mice. *Int Immunol* 12:123-132.
- Swainson, L., S. Kinet, C. Mongellaz, M. Sourisseau, T. Henriques, and N. Taylor. 2007. IL-7-induced proliferation of recent thymic emigrants requires activation of the PI3K pathway. *Blood* 109:1034-1042.
- Taghon, T., M.A. Yui, R. Pant, R.A. Diamond, and E.V. Rothenberg. 2006. Developmental and molecular characterization of emerging beta- and gammadelta-selected pre-T cells in the adult mouse thymus. *Immunity* 24:53-64.
- Taghon, T., M.A. Yui, and E.V. Rothenberg. 2007. Mast cell lineage diversion of T lineage precursors by the essential T cell transcription factor GATA-3. *Nat Immunol* 8:845-855.
- Tagoh, H., R. Ingram, N. Wilson, G. Salvagiotto, A.J. Warren, D. Clarke, M. Busslinger, and C. Bonifer. 2006. The mechanism of repression of the myeloid-specific c-fms gene by Pax5 during B lineage restriction. *EMBO J* 25:1070-1080.
- Takeuchi, A., S. Yamasaki, K. Takase, F. Nakatsu, H. Arase, M. Onodera, and T. Saito. 2001. E2A and HEB activate the pre-TCR alpha promoter during immature T cell development. *J Immunol* 167:2157-2163.

- Tan, J.T., B. Ernst, W.C. Kieper, E. LeRoy, J. Sprent, and C.D. Surh. 2002. Interleukin (IL)-15 and IL-7 jointly regulate homeostatic proliferation of memory phenotype CD8<sup>+</sup> cells but are not required for memory phenotype CD4<sup>+</sup> cells. *J Exp Med* 195:1523-1532.
- ten Boekel, E., F. Melchers, and A. Rolink. 1995. The status of Ig loci rearrangements in single cells from different stages of B cell development. *Int Immunol* 7:1013-1019.
- Tenno, M., S. Kojo, D.F. Lawir, I. Hess, K. Shiroguchi, T. Ebihara, T.A. Endo, S. Muroi, R. Satoh, H. Kawamoto, T. Boehm, and I. Taniuchi. 2018. Cbfbeta2 controls differentiation of and confers homing capacity to prethymic progenitors. *J Exp Med* 215:595-610.
- Thal, M.A., T.L. Carvalho, T. He, H.G. Kim, H. Gao, J. Hagman, and C.A. Klug. 2009. Ebf1-mediated down-regulation of Id2 and Id3 is essential for specification of the B cell lineage. *Proc Natl Acad Sci U S A* 106:552-557.
- Thompson, E.C., B.S. Cobb, P. Sabbattini, S. Meixlsperger, V. Parelho, D. Liberg, B. Taylor, N. Dillon, K. Georgopoulos, H. Jumaa, S.T. Smale, A.G. Fisher, and M. Merkenschlager. 2007. Ikaros DNA-binding proteins as integral components of B cell developmental-stage-specific regulatory circuits. *Immunity* 26:335-344.
- Thompson, J.S., P. Schneider, S.L. Kalled, L. Wang, E.A. Lefevre, T.G. Cachero, F. MacKay, S.A. Bixler, M. Zafari, Z.Y. Liu, S.A. Woodcock, F. Qian, M. Batten, C. Madry, Y. Richard, C.D. Benjamin, J.L. Browning, A. Tsapis, J. Tschopp, and C. Ambrose. 2000. BAFF binds to the tumor necrosis factor receptor-like molecule B cell maturation antigen and is important for maintaining the peripheral B cell population. *J Exp Med* 192:129-135.
- Tian, B., D.E. Nowak, M. Jamaluddin, S. Wang, and A.R. Brasier. 2005. Identification of direct genomic targets downstream of the nuclear factor-kappaB transcription factor mediating tumor necrosis factor signaling. *J Biol Chem* 280:17435-17448.
- Tiegs, S.L., D.M. Russell, and D. Nemazee. 1993. Receptor editing in self-reactive bone marrow B cells. *J Exp Med* 177:1009-1020.
- Till, J.E., and C.E. Mc. 1961. A direct measurement of the radiation sensitivity of normal mouse bone marrow cells. *Radiat Res* 14:213-222.
- Tomita, K., M. Hattori, E. Nakamura, S. Nakanishi, N. Minato, and R. Kageyama. 1999. The bHLH gene Hes1 is essential for expansion of early T cell precursors. *Genes Dev* 13:1203-1210.
- Tornberg, U.C., and D. Holmberg. 1995. B-1a, B-1b and B-2 B cells display unique VHDJH repertoires formed at different stages of ontogeny and under different selection pressures. *EMBO J* 14:1680-1689.
- Tramont, P.C., A.C. Tosello-Tramont, Y. Shen, A.K. Duley, A.E. Sutherland, T.P. Bender, D.R. Littman, and K.S. Ravichandran. 2010. CXCR4 acts as a costimulator during thymic beta-selection. *Nat Immunol* 11:162-170.
- Tsapogas, P., C.J. Mooney, G. Brown, and A. Rolink. 2017. The Cytokine Flt3-Ligand in Normal and Malignant Hematopoiesis. *Int J Mol Sci* 18:
- Tsapogas, P., L.K. Swee, A. Nusser, N. Nuber, M. Kreuzaler, G. Capoferri, H. Rolink, R. Ceredig, and A. Rolink. 2014. In vivo evidence for an instructive role of fms-like tyrosine kinase-3 (FLT3) ligand in hematopoietic development. *Haematologica* 99:638-646.
- Tsapogas, P., S. Zandi, J. Ahsberg, J. Zetterblad, E. Welinder, J.I. Jonsson, R. Mansson, H. Qian, and M. Sigvardsson. 2011. IL-7 mediates Ebf-1-dependent lineage restriction in early lymphoid progenitors. *Blood* 118:1283-1290.
- Turner, A.M., N.L. Lin, S. Issarachai, S.D. Lyman, and V.C. Broudy. 1996. FLT3 receptor expression on the surface of normal and malignant human hematopoietic cells. *Blood* 88:3383-3390.
- Tussiwand, R., N. Bosco, R. Ceredig, and A.G. Rolink. 2009. Tolerance checkpoints in B-cell development: Johnny B good. *Eur J Immunol* 39:2317-2324.
- Tussiwand, R., C. Engdahl, N. Gehre, N. Bosco, R. Ceredig, and A.G. Rolink. 2011. The preTCR-dependent DN3 to DP transition requires Notch signaling, is improved by CXCL12 signaling and is inhibited by IL-7 signaling. *Eur J Immunol* 41:3371-3380.
- Uehara, S., A. Grinberg, J.M. Farber, and P.E. Love. 2002. A role for CCR9 in T lymphocyte development and migration. *J Immunol* 168:2811-2819.

- Ueno, T., F. Saito, D.H. Gray, S. Kuse, K. Hieshima, H. Nakano, T. Kakiuchi, M. Lipp, R.L. Boyd, and Y. Takahama. 2004. CCR7 signals are essential for cortex-medulla migration of developing thymocytes. *J Exp Med* 200:493-505.
- Ungerback, J., J. Ahsberg, T. Strid, R. Somasundaram, and M. Sigvardsson. 2015. Combined heterozygous loss of Ebf1 and Pax5 allows for T-lineage conversion of B cell progenitors. *J Exp Med* 212:1109-1123.
- Urbanek, P., Z.Q. Wang, I. Fetka, E.F. Wagner, and M. Busslinger. 1994. Complete block of early B cell differentiation and altered patterning of the posterior midbrain in mice lacking Pax5/BSAP. *Cell* 79:901-912.
- Vannini, N., M. Girotra, O. Naveiras, G. Nikitin, V. Campos, S. Giger, A. Roch, J. Auwerx, and M.P. Lutolf. 2016. Specification of haematopoietic stem cell fate via modulation of mitochondrial activity. *Nat Commun* 7:13125.
- Vaziri, H., W. Dragowska, R.C. Allsopp, T.E. Thomas, C.B. Harley, and P.M. Lansdorp. 1994. Evidence for a mitotic clock in human hematopoietic stem cells: loss of telomeric DNA with age. *Proc Natl Acad Sci U S A* 91:9857-9860.
- Venkitaraman, A.R., and R.J. Cowling. 1994. Interleukin-7 induces the association of phosphatidylinositol 3-kinase with the alpha chain of the interleukin-7 receptor. *Eur J Immunol* 24:2168-2174.
- Vogt, T.K., A. Link, J. Perrin, D. Finke, and S.A. Luther. 2009. Novel function for interleukin-7 in dendritic cell development. *Blood* 113:3961-3968.
- Voll, R.E., E. Jimi, R.J. Phillips, D.F. Barber, M. Rincon, A.C. Hayday, R.A. Flavell, and S. Ghosh. 2000. NF-kappa B activation by the pre-T cell receptor serves as a selective survival signal in T lymphocyte development. *Immunity* 13:677-689.
- von Freeden-Jeffry, U., P. Vieira, L.A. Lucian, T. McNeil, S.E. Burdach, and R. Murray. 1995. Lymphopenia in interleukin (IL)-7 gene-deleted mice identifies IL-7 as a nonredundant cytokine. *J Exp Med* 181:1519-1526.
- von Muenchow, L., P. Tsapogas, L. Alberti-Servera, G. Capoferri, M. Doelz, H. Rolink, N. Bosco, R. Ceredig, and A.G. Rolink. 2017. Pro-B cells propagated in stromal cell-free cultures reconstitute functional B-cell compartments in immunodeficient mice. *Eur J Immunol* 47:394-405.
- Wada, H., K. Masuda, R. Satoh, K. Kakugawa, T. Ikawa, Y. Katsura, and H. Kawamoto. 2008. Adult T-cell progenitors retain myeloid potential. *Nature* 452:768-772.
- Wallis, V.J., E. Leuchars, S. Chwalinski, and A.J. Davies. 1975. On the sparse seeding of bone marrow and thymus in radiation chimaeras. *Transplantation* 19:2-11.
- Wang, J., Q. Lin, H. Langston, and M.D. Cooper. 1995. Resident bone marrow macrophages produce type 1 interferons that can selectively inhibit interleukin-7-driven growth of B lineage cells. *Immunity* 3:475-484.
- Weber, B.N., A.W. Chi, A. Chavez, Y. Yashiro-Ohtani, Q. Yang, O. Shestova, and A. Bhandoola. 2011. A critical role for TCF-1 in T-lineage specification and differentiation. *Nature* 476:63-68.
- Wendorff, A.A., U. Koch, F.T. Wunderlich, S. Wirth, C. Dubey, J.C. Bruning, H.R. MacDonald, and F. Radtke. 2010. Hes1 is a critical but context-dependent mediator of canonical Notch signaling in lymphocyte development and transformation. *Immunity* 33:671-684.
- Williams, J.A., K.S. Hathcock, D. Klug, Y. Harada, B. Choudhury, J.P. Allison, R. Abe, and R.J. Hodes. 2005. Regulated costimulation in the thymus is critical for T cell development: dysregulated CD28 costimulation can bypass the pre-TCR checkpoint. *J Immunol* 175:4199-4207.
- Wilson, A., E. Laurenti, G. Oser, R.C. van der Wath, W. Blanco-Bose, M. Jaworski, S. Offner, C.F. Dunant, L. Eshkind, E. Bockamp, P. Lio, H.R. Macdonald, and A. Trumpp. 2008. Hematopoietic stem cells reversibly switch from dormancy to self-renewal during homeostasis and repair. *Cell* 135:1118-1129.
- Wong, S.H., J.A. Walker, H.E. Jolin, L.F. Drynan, E. Hams, A. Camelo, J.L. Barlow, D.R. Neill, V. Panova, U. Koch, F. Radtke, C.S. Hardman, Y.Y. Hwang, P.G. Fallon, and A.N. McKenzie. 2012. Transcription factor RORalpha is critical for nuocyte development. *Nat Immunol* 13:229-236.

- Wright, D.E., A.J. Wagers, A.P. Gulati, F.L. Johnson, and I.L. Weissman. 2001. Physiological migration of hematopoietic stem and progenitor cells. *Science* 294:1933-1936.
- Wu, D., and G.K. Smyth. 2012. Camera: a competitive gene set test accounting for inter-gene correlation. *Nucleic Acids Res* 40:e133.
- Wu, S.L., M.S. Tsai, S.H. Wong, H.M. Hsieh-Li, T.S. Tsai, W.T. Chang, S.L. Huang, C.C. Chiu, and S.H. Wang. 2010. Characterization of genomic structures and expression profiles of three tandem repeats of a mouse double homeobox gene: Duxbl. *Dev Dyn* 239:927-940.
- Xu, W., T. Carr, K. Ramirez, S. McGregor, M. Sigvardsson, and B.L. Kee. 2013. E2A transcription factors limit expression of Gata3 to facilitate T lymphocyte lineage commitment. *Blood* 121:1534-1542.
- Yamasaki, S., E. Ishikawa, M. Sakuma, K. Ogata, K. Sakata-Sogawa, M. Hiroshima, D.L. Wiest, M. Tokunaga, and T. Saito. 2006. Mechanistic basis of pre-T cell receptor-mediated autonomous signaling critical for thymocyte development. *Nat Immunol* 7:67-75.
- Yamasaki, S., and T. Saito. 2007. Molecular basis for pre-TCR-mediated autonomous signaling. *Trends Immunol* 28:39-43.
- Yan, M., J.R. Brady, B. Chan, W.P. Lee, B. Hsu, S. Harless, M. Cancro, I.S. Grewal, and V.M. Dixit. 2001. Identification of a novel receptor for B lymphocyte stimulator that is mutated in a mouse strain with severe B cell deficiency. *Curr Biol* 11:1547-1552.
- Yang, J., F. Cornelissen, N. Papazian, R.M. Reijmers, M. Llorian, T. Cupedo, M. Coles, and B. Seddon. 2018. IL-7-dependent maintenance of ILC3s is required for normal entry of lymphocytes into lymph nodes. *J Exp Med* 215:1069-1077.
- Yang, L., D. Bryder, J. Adolfsson, J. Nygren, R. Mansson, M. Sigvardsson, and S.E. Jacobsen. 2005. Identification of Lin(-)Sca1(+)kit(+)CD34(+)Flt3- short-term hematopoietic stem cells capable of rapidly reconstituting and rescuing myeloablated transplant recipients. *Blood* 105:2717-2723.
- Yashiro-Ohtani, Y., Y. He, T. Ohtani, M.E. Jones, O. Shestova, L. Xu, T.C. Fang, M.Y. Chiang, A.M. Intlekofer, S.C. Blacklow, Y. Zhuang, and W.S. Pear. 2009. Pre-TCR signaling inactivates Notch1 transcription by antagonizing E2A. *Genes Dev* 23:1665-1676.
- Yasuda, T., H. Sanjo, G. Pages, Y. Kawano, H. Karasuyama, J. Pouyssegur, M. Ogata, and T. Kurosaki. 2008. Erk kinases link pre-B cell receptor signaling to transcriptional events required for early B cell expansion. *Immunity* 28:499-508.
- Yasutomo, K., K. Maeda, H. Hisaeda, R.A. Good, Y. Kuroda, and K. Himeno. 1997. The Fas-deficient SCID mouse exhibits the development of T cells in the thymus. *J Immunol* 158:4729-4733.
- Ye, S.K., Y. Agata, H.C. Lee, H. Kurooka, T. Kitamura, A. Shimizu, T. Honjo, and K. Ikuta. 2001. The IL-7 receptor controls the accessibility of the TCRgamma locus by Stat5 and histone acetylation. *Immunity* 15:813-823.
- Yoshida, H., K. Honda, R. Shinkura, S. Adachi, S. Nishikawa, K. Maki, K. Ikuta, and S.I. Nishikawa. 1999. IL-7 receptor alpha+ CD3(-) cells in the embryonic intestine induces the organizing center of Peyer's patches. *Int Immunol* 11:643-655.
- Yoshida, T., S.Y. Ng, J.C. Zuniga-Pflucker, and K. Georgopoulos. 2006. Early hematopoietic lineage restrictions directed by Ikaros. *Nat Immunol* 7:382-391.
- Yui, M.A., and E.V. Rothenberg. 2014. Developmental gene networks: a triathlon on the course to T cell identity. *Nat Rev Immunol* 14:529-545.
- Zandi, S., R. Mansson, P. Tsapogas, J. Zetterblad, D. Bryder, and M. Sigvardsson. 2008. EBF1 is essential for B-lineage priming and establishment of a transcription factor network in common lymphoid progenitors. *J Immunol* 181:3364-3372.
- Zarnegar, M.A., and E.V. Rothenberg. 2012. Ikaros represses and activates PU.1 cell-type-specifically through the multifunctional Sfp1 URE and a myeloid specific enhancer. *Oncogene* 31:4647-4654.
- Zhang, S., and H.E. Broxmeyer. 2000. Flt3 ligand induces tyrosine phosphorylation of gab1 and gab2 and their association with shp-2, grb2, and PI3 kinase. *Biochem Biophys Res Commun* 277:195-199.

- Zhang, S., S. Fukuda, Y. Lee, G. Hangoc, S. Cooper, R. Spolski, W.J. Leonard, and H.E. Broxmeyer. 2000. Essential role of signal transducer and activator of transcription (Stat)5a but not Stat5b for Flt3-dependent signaling. *J Exp Med* 192:719-728.
- Zhou, A., J. Paranjape, T.L. Brown, H. Nie, S. Naik, B. Dong, A. Chang, B. Trapp, R. Fairchild, C. Colmenares, and R.H. Silverman. 1997. Interferon action and apoptosis are defective in mice devoid of 2',5'-oligoadenylate-dependent RNase L. *EMBO J* 16:6355-6363.
- Zhuang, Y., P. Soriano, and H. Weintraub. 1994. The helix-loop-helix gene E2A is required for B cell formation. *Cell* 79:875-884.
- Zlotoff, D.A., and A. Bhandoola. 2011. Hematopoietic progenitor migration to the adult thymus. *Ann N Y Acad Sci* 1217:122-138.
- Zlotoff, D.A., A. Sambandam, T.D. Logan, J.J. Bell, B.A. Schwarz, and A. Bhandoola. 2010. CCR7 and CCR9 together recruit hematopoietic progenitors to the adult thymus. *Blood* 115:1897-1905.

## **9. Appendix**

### **9.1. Further publications**

#### **9.1.1. Two distinct pathways in mice generate antinuclear antigen-reactive B cell repertoires**

Martin Faderl<sup>1</sup>, [Fabian Klein](#)<sup>1</sup>, Oliver F. Wirz<sup>1</sup>, Stefan Heiler, Lluçia Alberti-Servera, Corinne Engdahl, Jan Andersson and Antonius Rolink

<sup>1</sup> Equal contribution

January 2018 – Frontiers in Immunology



## OPEN ACCESS

# Two Distinct Pathways in Mice Generate Antinuclear Antigen-Reactive B Cell Repertoires

**Edited by:**

Karsten Kretschmer,  
Technische Universität Dresden,  
Germany

**Reviewed by:**

Siegfried Weiss,  
National Research Centre for  
Biotechnology, Germany  
Claudia Berek,  
Charité Universitätsmedizin Berlin,  
Germany

**\*Correspondence:**

Jan Andersson  
jan.andersson@unibas.ch

**†Present address:**

Martin Faderl,  
Experimental Pathology, University of  
Bern, Bern, Switzerland;  
Oliver F. Wirz,  
Swiss Institute of Allergy and Asthma  
Research, Davos, Switzerland

<sup>†</sup>These authors have contributed  
equally to this work.

**Specialty section:**

This article was submitted to  
Immunological Tolerance  
and Regulation,  
a section of the journal  
Frontiers in Immunology

**Received:** 05 October 2017

**Accepted:** 04 January 2018

**Published:** 22 January 2018

**Citation:**

Faderl M, Klein F, Wirz OF, Heiler S,  
Alberti-Servera L, Engdahl C,  
Andersson J and Rolink A (2018)  
Two Distinct Pathways in Mice  
Generate Antinuclear Antigen-  
Reactive B Cell Repertoires.  
*Front. Immunol.* 9:16.  
doi: 10.3389/fimmu.2018.00016

**Martin Faderl<sup>†\*</sup>, Fabian Klein<sup>†</sup>, Oliver F. Wirz<sup>†\*</sup>, Stefan Heiler, Lucia Alberti-Servera, Corinne Engdahl, Jan Andersson\* and Antonius Rolink**

*Developmental and Molecular Immunology, Department of Biomedicine, University of Basel, Basel, Switzerland*

The escape of anti-self B cells from tolerance mechanisms like clonal deletion, receptor editing, and anergy results in the production of autoantibodies, which is a hallmark of many autoimmune disorders. In this study, we demonstrate that both germline sequences and somatic mutations contribute to autospecificity of B cell clones. For this issue, we investigated the development of antinuclear autoantibodies (ANAs) and their repertoire in two different mouse models. First, in aging mice that were shown to gain several autoimmune features over time including ANAs. Second, in mice undergoing a chronic graft-versus-host disease (GVHD), thereby developing systemic lupus erythematosus-like symptoms. Detailed repertoire analysis revealed that somatic hypermutations (SHM) were present in all Vh and practically all Vi regions of ANAs generated in these two models. The ANA B cell repertoire in aging mice was restricted, dominated by clonally related Vh1-26/Vk4-74 antibodies. In the collection of GVHD-derived ANAs, the repertoire was less restricted, but the usage of the Vh1-26/Vk4-74 combination was still apparent. Germline conversion showed that the SHM in the 4-74 light chain are deterministic for autoreactivity. Detailed analysis revealed that antinuclear reactivity of these antibodies could be induced by a single amino acid substitution in the CDR1 of the Vk4-74. In both aging B6 and young GVHD mice, conversion of the somatic mutations in the Vh and Vi regions of non Vh1-26/Vk4-74 using antibodies showed that B cells with a germline-encoded V gene could also contribute to the ANA-reactive B cell repertoire. These findings indicate that two distinct pathways generate ANA-producing B cells in both model systems. In one pathway, they are generated by Vh1-26/Vk4-74 expressing B cells in the course of immune responses to an antigen that is neither a nuclear antigen nor any other self-antigen. In the other pathway, ANA-producing B cells are derived from progenitors in the bone marrow that express B cell receptors (BCRs), which bind to nuclear antigens and that escape tolerance induction, possibly as a result of crosslinking of their BCRs by multivalent determinants of nuclear antigens.

**Keywords:** antinuclear antibodies, autoantibodies, monoclonal antibodies, mouse model, systemic lupus erythematosus-like disease, somatic hypermutation

## INTRODUCTION

A hallmark of the autoimmune disease systemic lupus erythematosus (SLE) is the presence of antinuclear autoantibodies (ANAs) in the serum (1–6). These antibodies are directed against histones, DNA, histone–DNA complexes, and various ribonuclear complexes (anti-SM, anti-Ro, and anti-La) (3–6) and may be found in immune complexes that play an important role in the pathogenesis of SLE. The disease occurs more frequently in females than males (ratio 10:1) with a peak incidence at 45–65 years. Based on the findings that ANA producing B cells have undergone Ig class switching and carry large numbers of somatic mutations, it is very likely that ANAs arise from B cells participating in T cell dependent antigen responses (3–6).

Studies using mouse models spontaneously developing an SLE-like disease have improved our knowledge of the etiology of this disease (7–9). In particular, these studies have highlighted the complex genetic contribution to the development of the disease as well as the important role of somatic mutations of antibody genes in the formation of autoantibodies (7–13).

The generation of a self-tolerant B cell repertoire is critically dependent upon the processes of clonal deletion, receptor editing, and anergy (14–19). Exactly how B cells escape central tolerance is, however, still not completely understood. Ample evidence has been provided indicating that non-autoreactive B cells can become autoreactive through somatic mutations in their variable heavy (Vh) and light (Vl) chain regions (6, 10, 13, 20). Equally, B cells using germline-encoded Vh and Vl regions escaping central tolerance induction in the bone marrow could also generate autoreactive B cells (21).

Recently we showed that almost all aging (8–12 months old) C57BL/6 (B6) mice develop several features characteristic of autoimmunity. This included germinal center formations in the spleen, kidney depositions of IgM, lymphocyte infiltrates in the salivary glands, as well as the production of high titers of IgG ANAs. Furthermore, this IgG ANA generation was shown to be T cell dependent (22). However, aging B6 mice do not develop real signs of disease. Here, we compare the ANA B cell repertoire of such aging B6 mice with that of (B6 × B6.H-2<sup>bm12</sup>)F<sub>1</sub> mice undergoing a chronic graft-versus-host disease (cGVHD) and thus developing an SLE-like disease and death (23). Results indicate that the ANA B cell repertoire of aging B6 mice is more restricted than that of mice undergoing GVHD and is only partially overlapping. Moreover, we show that the ANA producing B cells in aging mice and in GVHD mice are derived from progenitors expressing B cell receptors (BCRs) either recognizing or not recognizing nuclear antigens. These findings indicate that ANA producing B cells in both aging mice and in GVHD mice are generated by two pathways: by defective tolerance induction in the bone marrow or by hypermutation in the V-regions of B cells responding to a foreign antigen.

## MATERIALS AND METHODS

### Mice and Induction of cGVHD

C57BL/6 and (C57BL/6 × B6(C)-H2-Ab<sup>bm12</sup>/KhEg)F<sub>1</sub> mice were bred under specific pathogen free conditions in our animal unit.

A cGVHD was induced by i.v. injection of  $8 \times 10^7$  spleen plus lymph node cells from B6 mice into 8–10 weeks old B6 × bm12 mice, following established protocols (23).

### Generation of Hybridomas

Spleen cells derived from aging B6 mice (aged 8–12 months) or B6 × bm12 mice undergoing a cGVHD were fused to the Sp2/0-Ag14 fusion partner following standard protocols. In brief,  $2 \times 10^7$  Sp2/0 cells were used for the PEG1500 (Roche Diagnostics)-mediated fusion of all lymphoid cells prepared from an entire spleen. The fused cells were plated into 25 flat-bottom 96-well plates containing 200  $\mu$ l HAT-medium (2%FBS; GIBCO, 2% IL6, in house, 1× HAT supplement, Sigma) per well and incubated at 37°C in 10% CO<sub>2</sub> in air. After 10–12 days, supernatants were tested for IgG production by ELISA and for antinuclear reactivity by immunofluorescence (see below). Cells from IgG ANA positive wells were thereafter sub-cloned at limiting dilution. We routinely obtained fusion frequencies between  $10^{-3}$  and  $5 \times 10^{-3}$ . Thus, for each mouse, we have screened between 5,000 and 20,000 hybrids for IgG ANA production. Since the vast majority of B cell hybrids produce IgM, we tested for the success of sub-cloning by performing simultaneous ELISA for IgM and IgG (see below) in supernatants of growing clones. The IgG containing supernatants were re-tested for ANA reactivity, before being further processed for Ig V-gene analyses (see below).

### Determination of IgG Sub-Class and Anti-Histone/DNA/Sm/SS-B/La Reactivity

Determination of IgG sub-class, L-chain, and detection of anti-DNA antibodies was done by standard ELISA. For determination of anti-histone, anti-Sm or anti-SS-B/La ELISA plates were coated with 2.5  $\mu$ g/ml of the respective antigens in PBS (all purchased from Immunovision). Alkaline phosphatase labeled goat anti-mouse IgG, goat anti-mouse L-chain or goat anti-human IgG (Southern Biotech) was used for detection. The ELISA was performed as previously described (24–26).

### Antinuclear Autoantibody Determination

Kidney cryosections from Rag2<sup>-/-</sup> mice of homozygous matings were incubated with supernatants or purified antibodies as described in Ref. (27). For detection, either FITC labeled goat anti-mouse IgG (Jackson ImmunoResearch) or FITC labeled rabbit anti-human IgG (Jackson ImmunoResearch) were used.

### Vh and Vl Sequencing Analysis

RNA from ANA positive hybridomas was extracted using TRI Reagent (Sigma) followed by cDNA synthesis (GoScript Reverse Transcriptase) according to the manufacturer's protocol and using primers as specified in Table S5 in Supplementary Material. Amplification of the heavy and light chain V-regions was performed using Vent polymerase (New England Biolabs) and, subsequently, the Vh and Vl regions were ligated into the pJet1.2 blunt end cloning vector (Thermo Fisher Scientific). For sequencing, plasmids were sent to Microsynth (Balgach, Switzerland).

Resulting sequences were inspected using DNASTAR and aligned to the germline heavy and light chain sequences of the international ImMunoGeneTics information system® (<http://imgt.org>).

### Reversion of Somatic Mutations Back into Germline Configuration

Double-stranded DNA encoding the variable regions of heavy and light chains obtained from ANA positive hybridomas as well as their germline and mutated versions were ordered as gBlock gene fragments from IDT (Integrated DNA Technologies). These fragments were cloned into heavy and light chain expression vectors driven by the human cytomegalovirus promoter and containing the human IgG<sub>1</sub> constant region for the heavy chain and the human kappa constant region for the light chain (28) (a kind gift from Dr. Hedda Wardemann, Deutsches Krebsforschungszentrum, Heidelberg, Germany). Subsequently, antibodies were produced in HEK 293 cells (ATCC, No. CRL-1573) and purified by affinity

chromatography on Protein A Sepharose® (GE Health Care, Uppsala, Sweden) as described (28, 29).

## RESULTS

### IgG ANA Producing Hybridomas from Aging B6 Mice

Hybridomas were generated independently from spleen cells of seven individual aging B6 mice, which had high titers of serum ANA. The resulting IgG producing hybridomas were then tested for ANA reactivity by immunofluorescence, and positive cultures were sub-cloned. In total, 36 hybridomas producing IgG ANA were generated (Table 1). Of these, 16 were IgG<sub>2a</sub>, 19 were IgG<sub>2b</sub>, and only one was IgG<sub>1</sub>. This heavy chain selection suggests that IgG ANA formation in aging B6 mice is mainly driven by a T<sub>H</sub>1 response (30). All ANAs contained a kappa light chain. Sequence analysis of the corresponding Vh and Vk regions used by these hybridomas revealed a restricted repertoire (V, D, and

**TABLE 1** | Characteristics of ANA-reactive mAbs derived from aging B6 mice.<sup>a,b</sup>

Mouse number	Hybridoma number	IgG isotype	Ig-heavy chain v-region			Ig-light chain v-region	
Aging B6 # 1	5.D3.D10	IgG2b	Vh1-26	D1-1	J4	Vk4-74	Jk4
	5.D3.E12	IgG2b	Vh1-26	D1-1	J4	Vk4-74	Jk4
	7.E8.B11	IgG2b	Vh1-26	D1-1	J4	Vk4-74	Jk4
	7.F9.F1	IgG2b	Vh1-75	D2-4	J2	Vk?	
	8G3.E6	IgG2a	Vh1-26	D1-1	J4	Vk4-74	Jk4
	8.H7.D3	IgG2b	Vh1-26	D1-1	J4	Vk4-74	Jk4
	15.G10.F10	IgG2b	Vh1-26	D1-1	J4	Vk4-74	Jk4
	15.H12.E4	IgG2b	Vh1-26	D1-1	J4	Vk4-74	Jk4
	16.B9.C9	IgG2b	Vh1-26	D1-1	J4	Vk4-74	Jk4
	16.D7.A9	IgG2a	Vh1-26	D1-1	J4	Vk4-74	Jk4
	17.A9.E6	IgG2b	Vh1-26	D1-1	J4	Vk4-74	Jk4
	22.C9.G7	IgG2b	Vh1-26	D1-1	J4	Vk4-74	Jk4
Aging B6 # 2	1.G5.B8	IgG1	Vh1-39	D4-1	J1	Vk4-57	Jk5
	8.G9.G4	IgG2b	Vh1-26	D1-1	J4	Vk6-32	Jk2
Aging B6 # 3	13.4.5.A	IgG2a	Vh1-26	D2-4	J3	Vk4-74	Jk2
	13.18.A	IgG2a	Vh1-26	D2-4	J3	Vk4-74	Jk2
	13.27.B	IgG2a	Vh1-26	D2-4	J3	Vk4-74	Jk2
	13.31A	IgG2a	Vh1-26	D2-4	J3	Vk4-74	Jk2
	13.69.B	IgG2a	Vh1-26	D2-4	J3	Vk4-74	Jk2
Aging B6 # 4	1A2.1	IgG2a	Vh1-26	D2-2	J4	Vk4-74	Jk2
	2F8.1	IgG2b	Vh1-26	D1-1	J4	Vk4-74	Jk2
Aging B6 # 5	12.G3.G7	IgG2a	Vh1-26	D1-1	J4	Vk5-43	Jk2
	15.D10B3	IgG2a	Vh1-26	D1-1	J4	Vk5-43	Jk2
Aging B6 # 6	3.2.2A	IgG2b	Vh1-74	D2-4	J3	Vk6-23	Jk5
	3.10.1A	IgG2b	Vh1-26	D1-1	J2	Vk4-61	Jk1
	5.13.1A	IgG2b	Vh1-26	D1-1	J2	Vk4-74	Jk2
	6.15.1A	IgG2a	Vh8-12	D3-1	J1	Vk4-91	Jk2
	7.7.3A	IgG2b	Vh1-22	D2-2	J1	Vk10-96	Jk2
	20.15.1A	IgG2a	Vh1-50	D4-1	J2	Vk4-74	Jk2
	23.6.1A	IgG2a	Vh1-22	D2-2	J1	Vk10-96	Jk2
	24.18.1A	IgG2b	Vh1-22	D2-2	J1	Vk10-96	Jk2
	25.8.1A	IgG2b	Vh3-6	D3-3	J3	Vk4-74	Jk2
	Aging B6 # 7	3.25A	IgG2b	Vh1-50	D2-4	J2	Vk?
3.36A		IgG2a	Vh1-80	D2-4	J3	Vk4-58	Jk2
3.73A		IgG2a	Vh1-26	D1-1	J4	Vk4-74	Jk2

<sup>a</sup>All the mAbs converted into germline sequences are boxed in orange.

<sup>b</sup>All the mAbs using Vh1-26 have been boxed in yellow and those using Vk4-74 in red.

J annotations are according to the IMGT data base). Thus, 25 (69.4%) hybridomas used the Vh1-26 gene and this usage was found among hybridomas of all seven individual mice. Moreover, a very high frequency of Vk4-74 gene usage was also found. Thus, 23 (63.9%) hybridomas, derived from 5 of 7 individual mice, used this particular Vk light chain gene. Strikingly, 21 of the 23 Vk4-74 expressing hybridomas expressed the Vh1-26 heavy chain. Thus, the IgG ANA B cell repertoire of aging B6 mice is dominated by those expressing a Vh1-26 heavy chain gene in combination with a Vk4-74 light chain gene.

We also tested these ANAs for their capacity to bind to histones, Sm antigens, SS-B/La antigens, and DNA. By ELISA, 26 of the 36 showed strong and 5 showed weak histone binding, whereas binding to the other nuclear antigens was undetectable (Figure 1A).

### In Individual Mice, Hybridomas Using Vh1-26/Vk4-74 Were Clonally Related

The fact that we obtained 11 hybridomas from mouse 1, and 6 hybridomas from mouse 3 using the Vh1-26/Vk4-74 combination with the same D, Jh, and Jk elements already strongly suggested a clonal relationship among the B cells that had fused to generate these hybridomas (Table 1). The finding that the amino acid

sequences of the IgH and IgL CDR3 regions of these hybridomas were practically identical (Tables S1 and S2 in Supplementary Material) also supports this conclusion. Thus, at least in mouse 1 and 3, the ANA production seems to be dominated by a single B cell clone.

### IgG ANA from B6 × bm12 Mice Undergoing a Chronic Graft-versus-Host Reaction

We then asked whether the restricted IgG ANA B cell repertoire in aging B6 mice, which do not show obvious signs of disease, was similarly restricted in B6 × bm12 mice undergoing a chronic graft-versus-host reaction and, thus, developing an SLE-like disease. Hybridomas were independently generated from spleen cells of five mice with the highest ANA titers. These fusions resulted in 34 hybridomas with IgG ANA activity (Table 2). A total of 23 ANAs (68%) reacted to histones but again, none reacted to the other nuclear antigens (Figure 1B). IgG constant region usage analysis revealed a distribution rather similar to that in aged mice with 18 IgG<sub>2a</sub>, 13 IgG<sub>2b</sub>, and only 3 IgG<sub>1</sub>, the latter all from mouse 5. Thus, as in aging B6 mice, in B6 × bm12 mice undergoing a cGVHD, the IgG ANA formation appears to be T<sub>H</sub>1 cell driven. Again, all ANAs contained a kappa light chain.

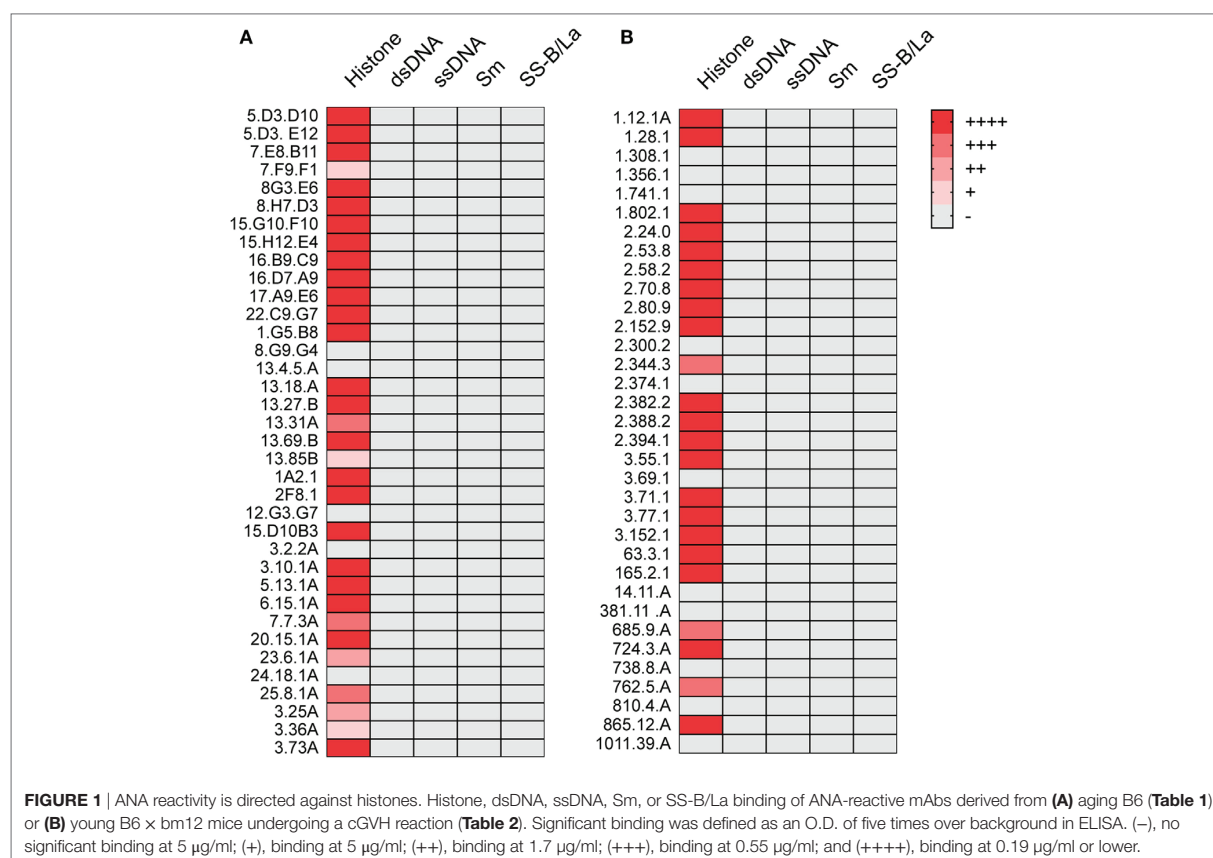


**TABLE 2** | Characteristics of ANA-reactive mAbs derived from graft-versus-host disease (GVHD) mice.<sup>a,b</sup>

Mouse number	Hybridoma number	IgG isotype	Ig-heavy chain v-region			Ig-light chain v-region		
GVHD # 1	1.12.1A	IgG2b	Vh8-8	D2-14	J4	Vk4-74	Jk2	
	1.28.1	IgG2a	Vh1-26	D1-1	J1	Vk4-74	Jk2	
	1.308.1	IgG2a	Vh1-55	D2-4	J3	Vk3-4	Jk1	
	1.356.1	IgG2a	Vh1-55	D2-4	J3	Vk3-4	Jk1	
	1.741.1	IgG2a	Vh1-55	D2-4	J3	Vk3-4	Jk1	
	1.802.1	IgG2b	Vh1-26	D1-1	J1	Vk4-63	Jk5	
GVHD # 2	2.24.0	IgG2a	Vh1-52	D1-1	J1	Vk14-111	Jk5	
	2.53.8	IgG2b	Vh14-2	D2-2	J2	Vk14-111	Jk1	
	2.58.2	IgG2b	Vh14-2	D2-2	J2	Vk14-111	Jk1	
	2.70.8	IgG2a	Vh14-4	D1-1	J3	Vk3-10	Jk1	
	2.80.9	IgG2a	Vh14-4	D1-1	J3	Vk3-12	Jk1	
	2.152.9	IgG2a	Vh1-52	D1-1	J1	Vk3-10	Jk1	
	2.300.2	IgG2b	Vh1-55	D2-1	J2	Vk3-10	Jk5	
	2.344.3	IgG2a	Vh1-52	D1-1	J1	Vk14-111	Jk5	
	2.374.1	IgG2a	Vh1-26	D1-1	J1	Vk3-7	Jk1	
	2.382.2	IgG2a	Vh14-4	D2-1	J3	Vk3-10	Jk1	
	2.388.2	IgG2a	Vh1-31	D2-4	J4	Vk3-10	Jk2	
	2.394.1	IgG2a	Vh14-4	D1-1	J3	Vk3-10	Jk1	
	GVHD # 3	3.55.1	IgG2a	Vh1-26	D1-1	J3	Vk4-74	Jk2
		3.69.1	IgG2b	Vh1-26	D1-1	J3	Vk4-74	Jk2
3.71.1		IgG2a	Vh1-26	D2-5	J1	Vk4-74	Jk2	
3.77.1		IgG2a	Vh1-26	D1-1	J3	Vk4-74	Jk2	
3.152.1		IgG2b	Vh1-26	D1-1	J3	Vk4-74	Jk2	
GVHD # 4	63.3.1	IgG2b	Vh1-55	D2-4	J2	Vk4-74	Jk2	
	165.2.1	IgG2a	Vh8-12	D2-2	J1	Vk15-103	Jk5	
GVHD # 5	14.11.A	IgG2b	Vh1-50	D1-1	J2	Vk1-117	Jk2	
	381.11.A	IgG2b	Vh1-54	D1-1	J3	Vk14-111	Jk2	
	685.9.A	IgG2b	Vh1-59	D2-5	J3	Vk17-127	Jk5	
	724.3.A	IgG1	Vh1-26	D1-1	J3	Vk4-91	Jk4	
	738.8.A	IgG1	Vh1-26	D1-1	J3	Vk3-7	Jk1	
	762.5.A	IgG2a	Vh5-17	D1-2	J4	Vk?		
	810.4.A	IgG1	Vh1-52	D2-12	J2	Vk3-10	Jk1	
	865.12.A	IgG2b	Vh1-72	D3-3	J2	Vk4-74	Jk5	
	1011.39.A	IgG2b	Vh1-53	D1-1	J2	Vk17-127	Jk5	

<sup>a</sup>All the mAbs converted into germline sequences are boxed in orange.

<sup>b</sup>All the mAbs using Vh1-26 are boxed in yellow and those using Vk4-74 in red.

In aging B6 mice, a dominance of Vh1-26 and Vk4-74 usage by the IgG ANA producing hybridomas was observed. In B6 × bm12-derived hybridomas, the same genes were also found to be used, but at a much lower frequency. Thus, ten (29.4%) of these ANAs used Vh1-26 and nine (26.5%) used Vk4-74. Six of the hybridomas using Vk4-74 used the Vh1-26 heavy chain; however, five of these were derived from one mouse (GVHD mouse 3). These findings show that the IgG ANA B cell repertoires of aging B6 mice and B6 × bm12 mice undergoing a cGVHD are partially overlapping. However, the IgG ANA B cell repertoire seems to be more diverse in the B6 × bm12 mice than in the aging B6 mice. Therefore, the mechanisms underlying the generation of these autoreactive B cells might be different in the two model systems.

### Somatic Mutations in the Light Chain Determine the ANA Reactivity of Vh1-26/Vk4-74 Using mAbs

Sequence analysis revealed that most mAbs with ANA reactivity carried somatic mutations in their Vh and Vk regions. These

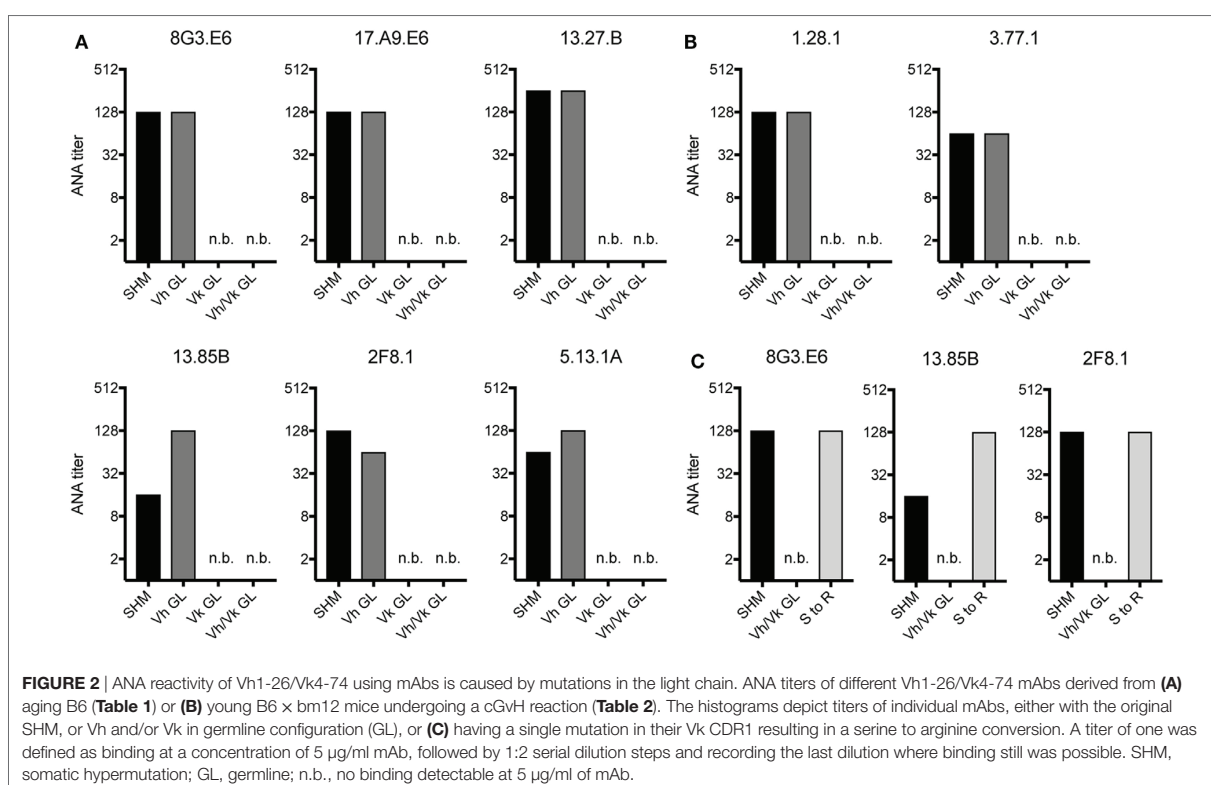
results are summarized in Tables S1–S4 in Supplementary Material.

Since in aging B6 mice the ANA reactivity was dominated by mAbs expressing a Vh1-26/Vk4-74 heavy and light chain combination, we tested if somatic mutations in the Vh and/or the Vk regions of these mAbs were required for their autoreactivity. Therefore, the Vh and Vk regions of six (derived from 4 individual mice) mAbs of aging B6 and two mAbs of GVHD mice using the Vh1-26/Vk4-74 combination were reverted to their germline configuration. After expression and purification, the ANA titers of these reverted mAbs were directly compared to their original, mutated forms. As shown in **Figures 2A,B**, the ANA titers of all mAbs, in which the Vh region had been reverted into germline configuration but the Vk regions were still somatically mutated, behaved like the original ANAs, continuing to recognize the histone antigens. However, all mAbs where the Vh was still somatically mutated but the Vk had been reverted to germline configuration lost ANA reactivity. Also, as expected, all mAbs in which both Vh and Vkappa regions had been reverted to germline configuration lost ANA reactivity. Thus, the ANA reactivity of the Vh1-26/Vk4-74 mAbs is due to somatic mutations in the Vk4-74 gene.

Due to the finding that somatic mutations within the Vk4-74 gene determined the ANA reactivity of Vh1-26/Vk4-74 mAbs and in order to identify a common motif that could account for this autoreactivity, we analyzed the sequence of these Vk4-74 genes in more detail. This analysis revealed that 20 of 23 Vh1-26/Vk4-74 mAbs derived from aging B6 mice had a mutation at position 30 (IMGT numbering) in their CDR1 region of the Vk4-74 gene. The germline-encoded serine in these mAbs was mutated into a positively charged arginine residue. Introduction of such a serine to arginine mutation in non-autoreactive germline versions of three different mAbs resulted in a complete gain of ANA reactivity for all of them (**Figure 2C**). Thus, antinuclear reactivity of these mAbs can be induced by a single base pair substitution changing the serine at position 30 in the CDR1 of the Vk4-74 light chain into an arginine.

### B Cells Expressing a Germline-Encoded Immunoglobulin Vh Gene with a Negatively Charged CDR2 Region Contribute to the ANA-Reactive B Cell Repertoire

We also tested if non-Vh1-26/Vk4-74 using mAbs require somatic mutations in their Vh and/or Vk regions for ANA reactivity. Therefore, the Vh and Vk region of three mAbs of aging B6 mice and six mAbs of the GVHD mice were reverted to their germline configuration. The 1.G5.B8 mAb derived from an aging B6 mouse (No. 2) used a somatically mutated Vh region and a germline-encoded Vk region. Reversion of the Vh region of this mAb into germline sequences resulted in a complete abrogation of its ANA reactivity (**Figure 3A**). In contrast, upon reversion, the other two mAbs (7.7.3A and 6.15.1A, both from mouse 6) kept their ANA reactivity (**Figure 3A**). Thus, B cells expressing a germline-encoded immunoglobulin Vh can also contribute to the ANA-reactive B cell repertoire in aging B6 mice.



From the six GVHD-derived mAbs, one (1.12.1A, mouse 1) lost ANA reactivity upon reversion of the Vk but not the Vh gene into germline configuration (Figure 3B). The fact that this mAb uses the Vk4-74 gene indicates that this Vk gene can also give rise to ANA reactivity when paired with a Vh gene other than Vh1-26. The other five mAbs kept their ANA reactivity upon reversion of their Vh and Vk genes to germline configuration (Figure 3B). Thus, B cells expressing a germline-encoded immunoglobulin can also contribute to the ANA-reactive repertoire in mice undergoing a cGVHD.

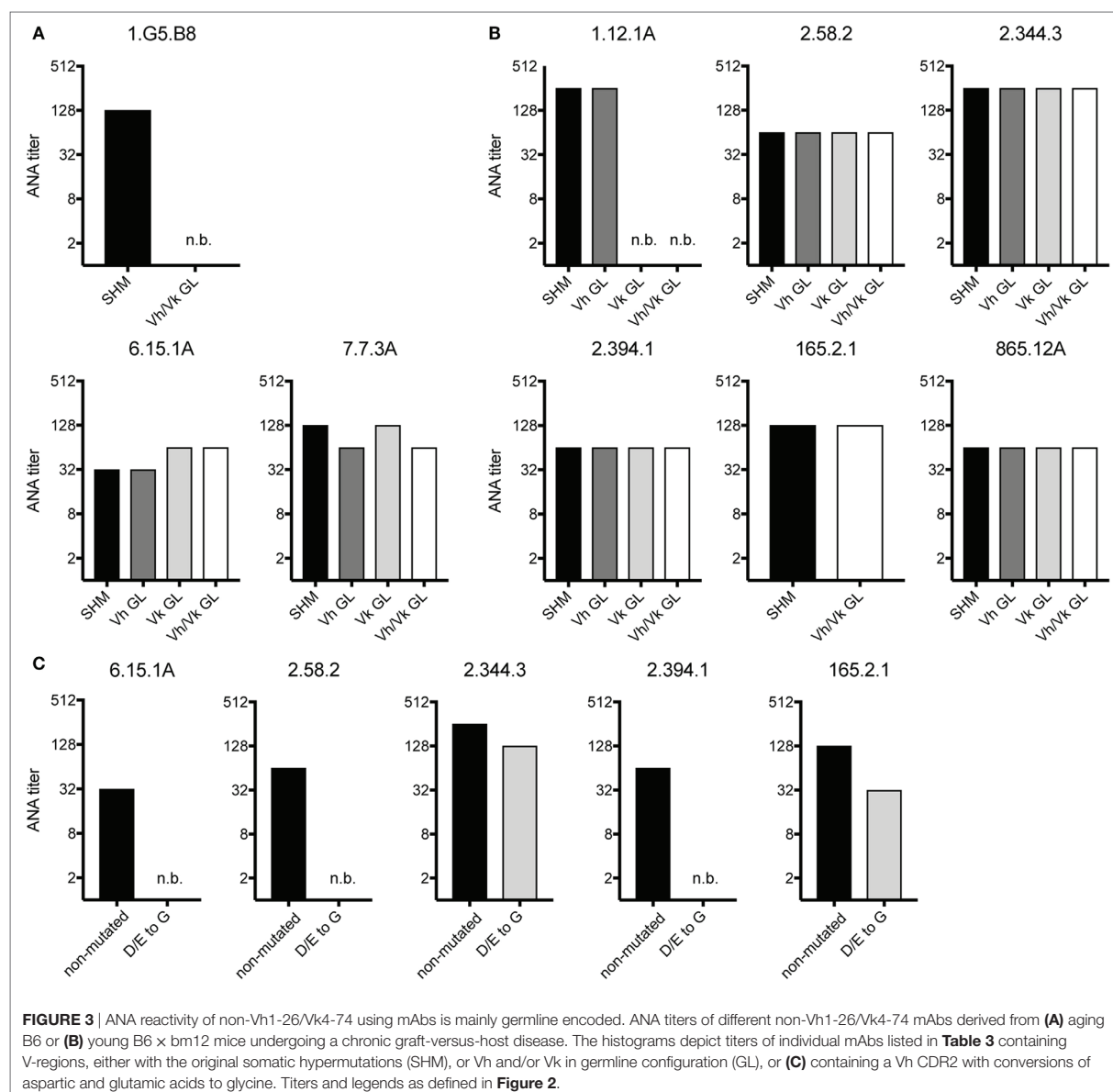
A remarkable observation was that 5 of 7 mAbs (one from aging B6 mice and four from GVHD mice), which kept ANA reactivity upon complete reversion of their Ig genes into germline configuration, had a negatively charged Vh-CDR2 region as defined by having at least two more negatively than positively charged amino acids in this region (see Table 3). This observation prompted us to test if these negatively charged amino acids are involved in ANA reactivity. Therefore, the negatively charged amino acids in the CDR2 regions of these five mAbs were mutated into neutral glycine. As shown in Figure 3C, one mAb derived from an aging B6 mouse (6.15.1A) and two from a GVHD mouse (2.58.2 and 2.394.1), completely lost ANA reactivity upon aspartic acid/glutamic acid conversion into glycine. The ANA titers of the other two GVHD-derived mAbs (2.344.3 and 165.2.1) diminished by a factor of 2 and 3, respectively (Figure 3C). Thus, B cells expressing a germline-encoded immunoglobulin with

a negatively charged Vh-CDR2 region contribute to the ANA-reactive repertoire. At this point, it is noteworthy that 6 of 11 (54.6%) of the non-Vh1-26 using ANA mAbs from aging B6 mice and 14 of 24 (58.3%) from mice undergoing cGVHD indeed carry a negatively charged Vh-CDR2 (Table 3).

## DISCUSSION

### Two Pathways to ANA-Producing B Cells

In the present study, we compared antinuclear autoantibodies (ANAs) from aging B6 mice, which do not show signs of disease, with those derived from mice undergoing a chronic GVH reaction (GVHD mice) and which develop an SLE-like disease (23). In order to study the V-regions of ANAs, we generated B cell hybridomas from mice with high ANA titers in their serum. Almost all monoclonal ANAs bound to a mixture of histones. As expected from previous studies, ANA production was T cell and antigen dependent (1–3, 22), since virtually all V-regions of our monoclonal ANAs contained somatic mutations. To determine whether the ANA-producing B cells were derived from progenitors expressing B cell receptors (BCRs) for nuclear antigens, we reverted the mutated V-regions into the corresponding germline sequences and tested the resulting antibodies for ANA reactivity. Based on such analyses, we found that some ANA-producing B cells in both aging B6 mice and GVHD mice must be derived



from progenitors expressing germline-encoded genes for BCRs specific for nuclear antigens, while several others were derived from progenitors expressing BCRs that showed no ANA reactivity. The vast majority of the latter were derived from progenitors using Vh1-26 in combination with Vk4-74. Antibodies with the germline sequences of these V-regions had no ANA reactivity. It has been shown previously that non-autoreactive B cells can become autoreactive upon acquiring somatic mutations in their Vh and/or V<sub>L</sub> regions (6, 10, 13, 20). In contrast to the findings with Vh1-26/Vk4-74 expressing ANAs, the reversion of other Vh and Vk regions of several monoclonal ANAs to the corresponding germline sequences did not abolish ANA

reactivity. The maintenance of ANA reactivity upon reversion into germline sequences was observed with 2 of 3 monoclonal ANAs from aging B6 mice, and with 5 of 6 monoclonal ANAs from GVHD mice. Thus, two pathways can be envisaged for the generation of ANA specific antibody forming B cells (Figure 4). In pathway one, they are derived from B cells undergoing somatic hypermutations in response to a foreign antigen (Figure 4, red line); in pathway two, they are derived from B cell progenitors expressing ANA-specific receptors that escape tolerance induction in the bone marrow, possibly by exposure to BCR crosslinking by nuclear antigens (Figure 4, blue line). Indeed, we showed previously that anti-dsDNA reactive B cells escaped tolerance

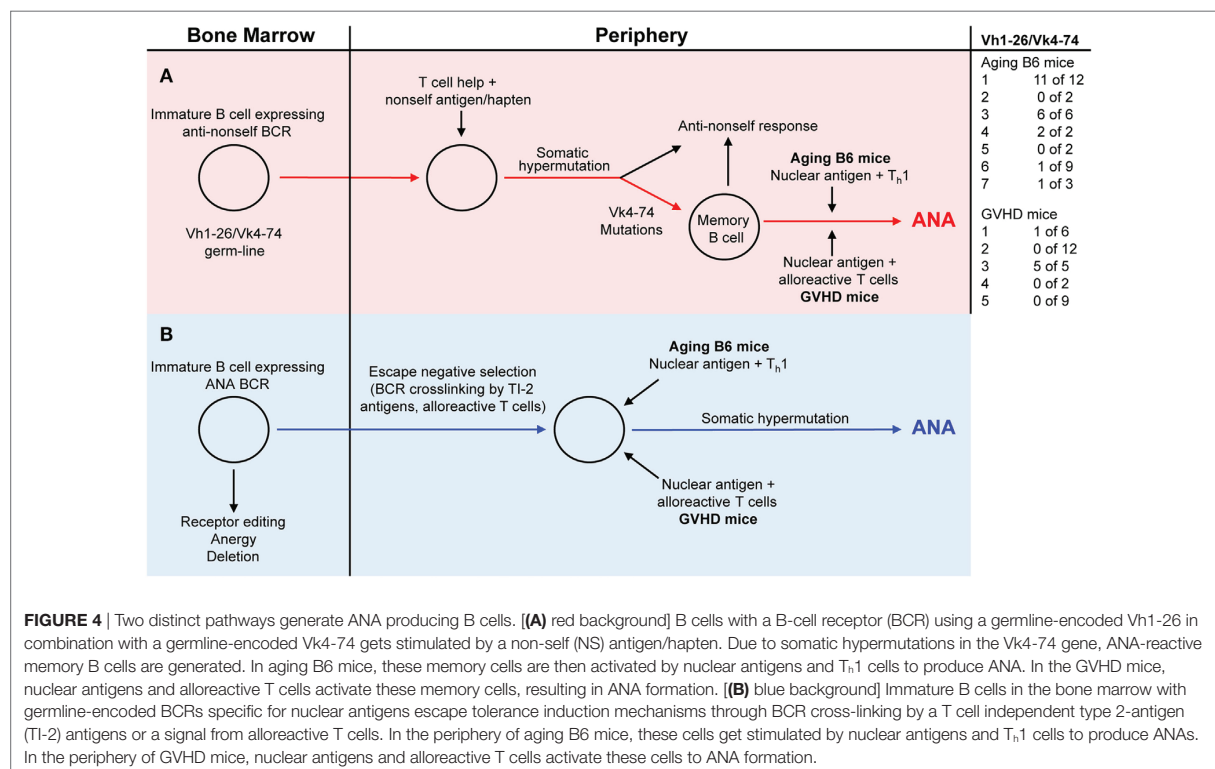
**TABLE 3** | Vh-CDR2 regions of non-Vh1-26 ANA-reactive mAbs of graft-versus-host disease (GVHD) and aging B6 mice.<sup>a,b</sup>

Mouse number	Hybridoma number	Vh-region	Vh-CDR2 region	Mouse number	Hybridoma number	Vh-region	Vh-CDR2 region		
GVHD # 1	1.12.1A	Vh8-8	I W W <b>D D D</b>	Aging B6 # 1	7.F9.F1	Vh1-75	I L P G S G S S		
	1.308.1	Vh1-55	I Y P G S G S T	Aging B6 # 2	1.G5.B8	Vh1-39	V N P N Y G T I		
	1.356.1	Vh1-55	I Y P G S G S T						
	1.741.1	Vh1-55	I Y P G S G S T						
GVHD # 2	2.24.0	Vh1-52	I <b>D P S D G E T</b>	Aging B6 # 6	6.15.1A	Vh8-12	I Y W <b>D D D</b> <b>K</b>		
	2.53.8	Vh14-2	I <b>D P E D G E T</b>			Vh1-22	I N P N N G G T		
	2.58.2	Vh14-2	I <b>D P E D G E S</b>			20.15.1A	Vh1-50	I <b>D P S D T F T</b>	
	2.70.8	Vh14-4	I <b>D P E N G D T</b>			23.6.1A	Vh1-22	I N P N N G <b>D T</b>	
	2.80.9	Vh14-4	I <b>D P E N G D T</b>			24.18.1A	Vh1-22	I N P N N <b>D D T</b>	
	2.152.9	Vh1-52	I <b>D P S D G E T</b>			25.8.1A	Vh3-6	I S C <b>D G S S</b>	
	2.300.2	Vh1-55	I Y P G S V S T	Aging B6 # 7	3.25A	Vh1-50	I <b>D P S D T Y T</b>		
	2.344.3	Vh1-52	I <b>D P S D D E T</b>			Aging B6 # 7	3.36A	Vh1-80	I Y P G <b>D G D T</b>
	2.382.2	Vh14-4	I <b>D P E N G D T</b>						
	2.388.2	Vh1-31	I F P Y N G V S						
	2.394.1	Vh14-4	I <b>D P E N G D T</b>						
GVHD # 4	63.3.1	Vh1-55	I Y P G S G S T						
	165.2.1	Vh8-12	I Y W <b>D D D</b> <b>K</b>						
GVHD # 5	14.11.A	Vh1-50	I <b>D P S D S Y I</b>						
	381.11.A	Vh1-54	I N P G S G G I						
	685.9.A	Vh1-59	I <b>D P S D S S S</b>						
	762.5.A	Vh5-17	I S <b>G</b> G S G I L						
	810.4.A	Vh1-52	I <b>D P S D S E T</b>						
	865.12.A	Vh1-72	I <b>D P S S G G T</b>						
	1011.39.A	Vh1-53	I N P S N <b>D G T</b>						
1011.39.A	Vh1-53	I N P S N <b>D G T</b>							

Bold font highlights negatively and positively charged amino acids.

<sup>a</sup>All mAbs that were converted into germline sequences or in which the negatively charged amino acids in the CDR2 were converted into glycine are marked with orange boxes.

<sup>b</sup>All the negatively charged amino acids in Vh-CDR2 region are marked in yellow and the positively charged amino acids in green.



induction by the crosslinking of their BCRs by a T cell independent type 2-antigen (24).

### Restricted Diversity of ANA Specific B Cells

Inspection of the V-region usage of ANA producing hybridomas shows that many ANAs derived from aging mice (21 of 36) (Table 1; Figure 4) and few from mice undergoing a cGVHD (6 of 34) (Table 2; Figure 4) express Vh1-26 in combination with Vk4-74. Interestingly this Vh/Vk combination is expressed in virtually all ANAs from aging mouse 1 (11 of 12), aging mouse 3 (6 of 6), and from the GVHD mouse 3 (5 of 5). Inspection of the V-regions strongly suggests that these ANAs are generated from single B cell clones with the exception of one clone of the GVHD mouse 3, which differs in the CDR3 compared to the other four. In other mice, ANAs are clearly generated from multiple B cell clones. In aging mouse 6, one ANA expresses the Vh1-26/Vk4-74 combination, one expresses the Vh1-26 with Vk4-61, two express the Vk4-74 with Vh1-50 and Vh3-6, respectively, and five express different Vh/Vk combinations. In GVHD mice, all except one mouse (No. 3) express ANAs derived from multiple B cell clones. Thus, in aging B6 mice, the ANA repertoire tends to be restricted, while in GVHD mice, the ANA repertoire tends to be less restricted. The more important question to be answered is why ANAs are oligoclonal in some mice and polyclonal in others. One reason for this restricted repertoire might be that Vh1-26 and Vk4-74 genes are overrepresented in the B cell repertoire of B6 mice in general. RNA sequence analysis of Vh1 usage by B cells from young and aging B6 mice showed that around 10% of these used Vh1-26 (our unpublished results). Since about 50% of all B cells use a Vh1 family member, Vh1-26 is expressed by 5% of them. We did not attempt to verify this number in the hybrids generated, by, for example, cloning and sequencing the Vh regions of random IgM or IgG antibodies not reacting to nuclear antigens. With respect to Vk4-74 usage, Aoki-Ota et al. (31) analyzed the kappa light chain repertoire in B6 mice. This analysis revealed that B6 B cells rarely use the Vk4-74 gene. We also have determined the Vk usage in developing B6 B cells and found that Vk4-74 was used less than 1% in single Vk-rearrangements of preBII cells and immature B cells of the bone marrow [unpublished observation, (32)]. Thus, the restricted ANA-reactive B cell repertoire does not simply appear to reflect a selective usage of the Vh1-26 and the Vk4-74 genes by the B6 B cells. Instead, and more interestingly, this restricted ANA repertoire may occur through selection by and as yet to be defined T cell dependent antigen.

Many years ago, it was shown that haptens such as NP (4-hydroxy-3-nitrophenyl)acetyl (33, 34), oxazolone (2-phenyl-5-oxazolone) (35, 36), and arsonate (p-azophenyl-arsonate) (37, 38) could elicit an oligoclonal humoral immune response, at least in certain inbred strains of mice. Based on this, one might envisage that a hapten-like structure is responsible for the restricted ANA-reactive B cell repertoire in aging B6 mice. Thus, one could imagine that the frequency of ANA-producing B cells that are derived from hapten-induced memory cells in aging mice (red pathway in Figure 4) is higher than the frequency of B cell progenitors with receptors for nuclear antigens that escape tolerance induction in the bone marrow (blue pathway in Figure 4).

### Activation of ANA-Producing B Cells

In ANA-producing mice, B cells expressing nuclear antigen-specific BCRs must be activated by nuclear antigens and helper T cells. In GVHD mice, the alloreactive T cells act as helper T cells. In their initial report on the “allogeneic effect,” Katz et al. reported a drastic enhancement of IgG responses as a result of a GVH reaction (39). Later, Osborne and Katz showed that a simple non-immunogenic hapten–polypeptide conjugate might elicit a vigorous primary IgG response as a consequence of the allogeneic effect (40). Likewise, Hamilton and Miller reported that otherwise tolerogenic hapten-conjugated syngeneic mouse erythrocytes would elicit a strong primary antibody response as a result of a GVH reaction (41). It is possible that this type of general B cell help by alloreactive T cells contributes to the tendency of the ANA response in cGVHD mice to be more diverse.

In aging mice, the specificity and origin of the T helper cells that are required for ANA production is not known. Based on the IgG class of the ANAs produced in these mice, it is conceivable that the helper cells involved in the ANA response are T<sub>h</sub>1 cells (30).

### Conclusions Regarding the Structure of Anti-Histone Antibodies

Almost 30 years ago, Weigert and coworkers showed that arginine residues in CDR regions play a crucial role for the specificity of anti-dsDNA autoantibodies (10, 11). In the present study, we find an important role of arginine in the Vk-region of certain ANAs. Site-directed mutagenesis revealed that somatic mutations in the Vk4-74 light chains of the Vh1-26/Vk4-74 mAbs determine ANA reactivity, since conversion into their germline sequence completely abolished ANA reactivity. Interestingly, and highly significant, 20 of 23 Vh1-26/Vk4-74-expressing ANAs derived from aging B6 mice had a serine to arginine mutation at position 30 in the CDR1 region of the Vk4-74 gene. In 1 of these 23 mAbs, this change to arginine was the only mutation present in the entire Vk4-74 gene. The finding that one of these (17A9E6) mAb loses ANA-binding activity upon conversion of this arginine into serine strongly indicates the importance of this mutation for ANA reactivity. Furthermore, the introduction of single serine to arginine mutations in the germline configuration of three different mAbs conferred their antinuclear reactivity. This proves that this single mutation can convert an ANA-negative mAb into a positive one and clearly shows how easily Vh1-26/Vk4-74 using mAbs may become autoantibodies. The ANA-reactive B cell repertoire has also been analyzed in B6 mice congenic for a SLE susceptibility locus. Also this analysis revealed a rather frequent usage of Vk4-74 light chains. Thus, Liang et al. (12) found that 9 of 30 ANA producing hybridomas used Vk4-74 light chain (herein called *ai4*). Moreover, it was shown that 3 of these 9 had a serine to arginine mutation at position 30 in the CDR1. In a report by Guo et al. (13), 9 of 33 ANA-producing hybridomas used a Vk4-74 light chain (herein also called *ai4*). At least 5 of these 9 had a serine to arginine mutation at position 30 in the CDR1, like we report herein.

However, since 5 of 6 Vh1-26/Vk4-74 using mAbs derived from the GVHD mice did not have this serine to arginine mutation, other mutations in the Vk4-74 gene can be involved in ANA reactivity.

Yet, another interesting finding reported here is that a high percentage of ANA-reactive mAbs not using the Vh1-26 gene, especially in the repertoire derived from GVHD mice, possess a germline-encoded negatively charged Vh CDR2 region. Thus, 14 of the total 34 monoclonal ANAs (41.2%) derived from the GVHD mice and 6 of 36 (16.7%) derived from the aging B6 mice have such a CDR2 region. Within the total Vh gene repertoire of B6 mice, 11.5% possess such a negatively charged CDR2 (42). Thus, our findings suggest that B cells with such a charged CDR2 might be positively selected into the ANA-reactive B cell repertoire, especially in GVHD mice. The finding that mutations of these negatively charged amino acids into glycine can result in a complete loss of ANA binding supports this hypothesis and, moreover, indicates the potential importance of this region in ANA reactivity. However, additional structural effects of the amino acid change to glycine cannot be excluded, especially since glycine is known to be a helix breaker.

It is noteworthy that despite high ANA serum titers, aging B6 mice do not show the typical lesions that are observed in multiple organs of SLE patients, whereas the GVHD mice do show this. Therefore, one could envisage that the ANA repertoire difference between aging B6 and GVHD mice is playing a role in the pathogenesis of the SLE-like disease observed in GVHD mice.

Overall, the findings described in the present study highlight various new characteristics of ANA-reactive B cell repertoires and argue for similar mechanisms of ANA generation in SLE patients. This might improve our understanding of the pathogenesis of this disease, thereby opening new concepts and therapies for its control.

## ETHICS STATEMENT

The State veterinary authorities of Basel (Kantonales Veterinäramt, Basel-Stadt) had approved all animal experiments under permission numbers 1888 and 2434.

## DATA AVAILABILITY

Sequencing data can be found in GenBank under accession numbers MG733774—MG733908.

## REFERENCES

- Kotzin BL. Systemic lupus erythematosus. *Cell* (1996) 85:303–6. doi:10.1016/S0092-8674(00)81108-3
- Kaul A, Gordon C, Crow MK, Touma Z, Urowitz MB, van Vollenhoven R, et al. Systemic lupus erythematosus. *Nat Rev Dis Primers* (2016) 2:16039. doi:10.1038/nrdp.2016.39
- Elkon K, Casali P. Nature and functions of autoantibodies. *Nat Clin Pract Rheumatol* (2008) 4:491–8. doi:10.1038/ncprheum0895
- Tan EM. Antinuclear antibodies: diagnostic markers for autoimmune diseases and probes for cell biology. *Adv Immunol* (1989) 44:93–151. doi:10.1016/S0065-2776(08)60641-0
- Hahn BH. Antibodies to DNA. *N Engl J Med* (1998) 338:1359–68. doi:10.1056/NEJM199805073381906
- Schroeder K, Herrmann M, Winkler TH. The role of somatic hypermutation in the generation of pathogenic antibodies in SLE. *Autoimmunity* (2013) 46:121–7. doi:10.3109/08916934.2012.748751

## AUTHOR CONTRIBUTIONS

AR conceived the study and designed experiments. All authors performed experiments and analyzed the data. AR, JA, and FK wrote the paper.

## ACKNOWLEDGMENTS

We thank Drs. Rhodri Ceredig, Werner Haas, Fritz Melchers, Michael Parkhouse, and Panagiotis Tsapogas for helpful comments and critical reading of the manuscript. We thank Ricardo Koch, Hannie Rolink, and Mike Rolink for skillful technical assistance. This paper is dedicated to the memory of Antonius (Ton) Rolink, our principal investigator and professor, who unexpectedly died during the preparation of this manuscript.

## FUNDING

AR is holder of the chair in Immunology endowed by E. Hoffmann-La Roche Ltd., Basel to the University of Basel. This study was supported by the Swiss National Science Foundation (310030B\_160330/1). LA-S was supported by the People Program (Marie Curie Actions) of the European Union's Seventh Framework Program FP7/2007-2013 under Research Executive Agency Grant 315902.

## SUPPLEMENTARY MATERIAL

The Supplementary Material for this article can be found online at <http://www.frontiersin.org/articles/10.3389/fimmu.2018.00016/full#supplementary-material>.

**TABLES S1 AND S2** | Nucleotide sequences and their translation into amino acids of Vh- and Vk-regions of all hybridomas described herein, which were derived from aging B6 mice.

**TABLES S3 AND S4** | Nucleotide sequences and their translation into amino acids of Vh- and Vk-regions of all hybridomas described herein, which were derived from young B6 × bm12 mice undergoing a GvH reaction.

**TABLE S5** | Sequences of primers used for cDNA synthesis of total mRNA obtained from ANA-reactive hybridomas. The sequences of primers used for sequencing of Vh- and Vk-regions of the obtained cDNA are also shown.

- Theofilopoulos AN, Dixon FJ. Murine models of systemic lupus erythematosus. *Adv Immunol* (1985) 37:269–390. doi:10.1016/S0065-2776(08)60342-9
- Wakeland EK, Morel L, Mohan C, Yui M. Genetic dissection of lupus nephritis in murine models of SLE. *J Clin Immunol* (1997) 17:272–81. doi:10.1023/A:1027370514198
- Morel L, Mohan C, Yu Y, Croker BP, Tian N, Deng A, et al. Functional dissection of systemic lupus erythematosus using congenic mouse strains. *J Immunol* (1997) 158:6019–28.
- Shlomchik M, Mascelli M, Shan H, Radic MZ, Pisetsky D, Marshak-Rothstein A, et al. Anti-DNA antibodies from autoimmune mice arise by clonal expansion and somatic mutation. *J Exp Med* (1990) 171:265–92. doi:10.1084/jem.171.1.265
- Radic MZ, Weigert M. Genetic and structural evidence for antigen selection of anti-DNA antibodies. *Annu Rev Immunol* (1994) 12:487–520. doi:10.1146/annurev.iy.12.040194.002415
- Liang Z, Chang S, Youn MS, Mohan C. Molecular hallmarks of anti-chromatin antibodies associated with the lupus susceptibility locus, Sle1. *Mol Immunol* (2009) 46:2671–81. doi:10.1016/j.molimm.2008.12.034

13. Guo W, Smith D, Aviszus K, Detanico T, Heiser RA, Wysocki LJ. Somatic hypermutation as a generator of antinuclear antibodies in a murine model of systemic autoimmunity. *J Exp Med* (2010) 207:2225–37. doi:10.1084/jem.20092712
14. Radic MZ, Erikson J, Litwin S, Weigert M. B lymphocytes may escape tolerance by revising their antigen receptors. *J Exp Med* (1993) 177:1165–73. doi:10.1084/jem.177.4.1165
15. Tiegs SL, Russell DM, Nemazee D. Receptor editing in self-reactive bone marrow B cells. *J Exp Med* (1993) 177:1009–20. doi:10.1084/jem.177.4.1009
16. Nemazee D. Receptor editing in lymphocyte development and central tolerance. *Nat Rev Immunol* (2006) 6:728–40. doi:10.1038/nri1939
17. Goodnow CC, Sprent J, Fazekas de St Groth B, Vinuesa CG. Cellular and genetic mechanisms of self tolerance and autoimmunity. *Nature* (2005) 435:590–7. doi:10.1038/nature03724
18. Cambier JC, Gauld SB, Merrell KT, Vilen BJ. B-cell anergy: from transgenic models to naturally occurring anergic B cells? *Nat Rev Immunol* (2007) 7:633–43. doi:10.1038/nri2133
19. Wardemann H, Hammersen J, Nussenzweig MC. Human autoantibody silencing by immunoglobulin light chains. *J Exp Med* (2004) 200:191–9. doi:10.1084/jem.20040818
20. Diamond B, Scharff MD. Somatic mutation of the T15 heavy chain gives rise to an antibody with autoantibody specificity. *Proc Natl Acad Sci U S A* (1984) 81:5841–4. doi:10.1073/pnas.81.18.5841
21. Wardemann H, Yurasov S, Schaefer A, Young JW, Meffre E, Nussenzweig MC. Predominant autoantibody production by early human B cell precursors. *Science* (2003) 301:1374–7. doi:10.1126/science.1086907
22. Nusser A, Nuber N, Wirz OF, Rolink H, Andersson J, Rolink A. The development of autoimmune features in aging mice is closely associated with alterations of the peripheral CD4(+) T-cell compartment. *Eur J Immunol* (2014) 44:2893–902. doi:10.1002/eji.201344408
23. Rolink AG, Pals ST, Gleichmann E. Allosuppressor and allohelper T cells in acute and chronic graft-vs.-host disease. II. F1 recipients carrying mutations at H-2K and/or I-A. *J Exp Med* (1983) 157:755–71. doi:10.1084/jem.157.2.755
24. Andersson J, Melchers F, Rolink A. Stimulation by T cell independent antigens can relieve the arrest of differentiation of immature auto-reactive B cells in the bone marrow. *Scand J Immunol* (1995) 42:21–33. doi:10.1111/1/j.1365-3083.1995.tb03621.x
25. Rolink AG, Radaszkiewicz T, Melchers F. The autoantigen-binding B cell repertoires of normal and of chronically graft-versus-host-diseased mice. *J Exp Med* (1987) 165:1675–87. doi:10.1084/jem.165.6.1675
26. Wellmann U, Werner A, Winkler TH. Altered selection processes of B lymphocytes in autoimmune NZB/W mice, despite intact central tolerance against DNA. *Eur J Immunol* (2001) 31:2800–10. doi:10.1002/1521-4141(200109)31:9<2800::AID-IMMU2800>3.0.CO;2-E
27. Benard A, Ceredig R, Rolink AG. Regulatory T cells control autoimmunity following syngeneic bone marrow transplantation. *Eur J Immunol* (2006) 36:2324–35. doi:10.1002/eji.200636434
28. Tiller T, Meffre E, Yurasov S, Tsuiji M, Nussenzweig MC, Wardemann H. Efficient generation of monoclonal antibodies from single human B cells by single cell RT-PCR and expression vector cloning. *J Immunol Methods* (2008) 329:112–24. doi:10.1016/j.jim.2007.09.017
29. Smith K, Garman L, Wrammert J, Zheng NY, Capra JD, Ahmed R, et al. Rapid generation of fully human monoclonal antibodies specific to a vaccinating antigen. *Nat Protoc* (2009) 4:372–84. doi:10.1038/nprot.2009.3
30. Coffman RL, Savelkoul HF, Leberman DA. Cytokine regulation of immunoglobulin isotype switching and expression. *Semin Immunol* (1989) 1:55–63.
31. Aoki-Ota M, Torkamani A, Ota T, Schork N, Nemazee D. Skewed primary Igkappa repertoire and V-J joining in C57BL/6 mice: implications for recombination accessibility and receptor editing. *J Immunol* (2012) 188:2305–15. doi:10.4049/jimmunol.1103484
32. Yamagami T, ten Boekel E, Schaniel C, Andersson J, Rolink A, Melchers F. Four of five RAG-expressing JcKappa-/- small pre-BII cells have no L chain gene rearrangements: detection by high-efficiency single cell PCR. *Immunity* (1999) 11:309–16. doi:10.1016/S1074-7613(00)80106-5
33. Reth M, Hammerling GJ, Rajewsky K. Analysis of the repertoire of anti-NP antibodies in C57BL/6 mice by cell fusion. I. Characterization of antibody families in the primary and hyperimmune response. *Eur J Immunol* (1978) 8:393–400. doi:10.1002/eji.1830080605
34. Bothwell AL, Paskind M, Reth M, Imanishi-Kari T, Rajewsky K, Baltimore D. Heavy chain variable region contribution to the NPb family of antibodies: somatic mutation evident in a gamma 2a variable region. *Cell* (1981) 24:625–37. doi:10.1016/0092-8674(81)90089-1
35. Kaartinen M, Griffiths GM, Hamlyn PH, Markham AF, Karjalainen K, Pelkonen JL, et al. Anti-oxazolone hybridomas and the structure of the oxazolone idiotype. *J Immunol* (1983) 130:937–45.
36. Kaartinen M, Griffiths GM, Markham AF, Milstein C. mRNA sequences define an unusually restricted IgG response to 2-phenylloxazolone and its early diversification. *Nature* (1983) 304:320–4. doi:10.1038/304320a0
37. Wysocki L, Manser T, Geffer ML. Somatic evolution of variable region structures during an immune response. *Proc Natl Acad Sci U S A* (1986) 83:1847–51. doi:10.1073/pnas.83.6.1847
38. Manser T. Evolution of antibody structure during the immune response. The differentiative potential of a single B lymphocyte. *J Exp Med* (1989) 170:1211–30. doi:10.1084/jem.170.4.1211
39. Katz DH, Paul WE, Benacerraf B. Carrier function in anti-hapten antibody responses. V. Analysis of cellular events in the enhancement of antibody responses by the “allogeneic effect” in DNP-OVA-primed guinea pigs challenged with a heterologous DNP-conjugate. *J Immunol* (1971) 107:1319–28.
40. Osborne DP Jr, Katz DH. The allogeneic effect in inbred mice. IV. Regulatory influences of graft-vs.-host reactions on host T lymphocyte functions. *J Exp Med* (1973) 138:825–38. doi:10.1084/jem.138.4.825
41. Hamilton JA, Miller JF. Induction of a primary antihapten response in vivo by a graft-vs.-host reaction. *J Exp Med* (1973) 138:1009–14. doi:10.1084/jem.138.4.1009
42. Johnston CM, Wood AL, Bolland DJ, Corcoran AE. Complete sequence assembly and characterization of the C57BL/6 mouse Ig heavy chain V region. *J Immunol* (2006) 176:4221–34. doi:10.4049/jimmunol.176.7.4221

**Conflict of Interest Statement:** The authors declare that the research was conducted in the absence of any commercial or financial relationships that could be construed as a potential conflict of interest.

Copyright © 2018 Faderl, Klein, Wirz, Heiler, Alberti-Servera, Engdahl, Andersson and Rolink. This is an open-access article distributed under the terms of the Creative Commons Attribution License (CC BY). The use, distribution or reproduction in other forums is permitted, provided the original author(s) or licensor are credited and that the original publication in this journal is cited, in accordance with accepted academic practice. No use, distribution or reproduction is permitted which does not comply with these terms.

















**Table S5.** Sequences of primers used for cDNA synthesis of total mRNA obtained from ANA-reactive hybridomas. The sequences of primers used for sequencing of Vh- and Vk-regions of the obtained cDNA are also shown

<b>Primer:</b>	<b>Sequence</b>
Ig $\kappa$ C reverse	GATGGTGGGAAGATGGATACAG
5' L-V $\kappa$ 3 Fwd	TGCTGCTGCTCTGGGTTCCAG
5' L-V $\kappa$ 4 Fwd	ATTWTCAGCTTCCTGCTAATC
5' L-V $\kappa$ 5 Fwd	TTTTGCTTTTCTGGATTYCAG
5' L-V $\kappa$ 6 Fwd	TCGTGTTKCTSTGGTTGTCTG
5' L-V $\kappa$ 6,8,9 Fwd	ATGGAATCACAGRCYCWGGT
5' L-V $\kappa$ 14 Fwd	TCTTGTTGCTCTGGTTYCCAG
5' L-V $\kappa$ 19 Fwd	CAGTTCCTGGGGCTCTTGTTGTTC
5' L-V $\kappa$ 20 Fwd	CTCACTAGCTCTTCTCCTC
5' L-V $\lambda$ 1 Fwd	TTGTGACTCAGGAATCTGCA
Ig $\lambda$ C Rev	CTCGGATCCTTCAGAGGAAGGTGGAAACA
V <sub>H</sub> Fwd	GGTSMARCTGCAGSAGTCWGG
$\gamma$ 1 C Rev	CTCGGATCCTTCAGAGGAAGGTGGAAACA
$\gamma$ 3 C Rev	CTTTGACAAGGCATCCCAGT
$\gamma$ 2a C Rev	CCAGGCATCCTAGAGTCACC
$\gamma$ 2b C Rev	CCAGGCATCCCAGAGTCACA
Murine $\beta$ -Actin Fwd	GAAGTCTAGAGCAACATAGCAC
Murine $\beta$ -Actin Rev	GTGGGAATTCGTCAGAAGGACTCCTATGTG
pJET Rev	ATCGATTTTCCATGGCAGCT
T7universal Fwd	TAATACGACTCACTATAGGG

## 9.2. Curriculum vitae

### Fabian Klein

Current working address:  
Mattenstrasse 28  
CH-4058 Basel

klein.fabian@freenet.de  
00491726431256

28<sup>th</sup> of February 1991, Germany

Physical address:  
An der Wiese 30  
D-79650 Schopfheim

Languages

German native speaker  
English fluent

### Education

- 02.2015 – 01.2019 **Doctor of Philosophy (PhD) in Cell Biology**  
Department of Biomedicine, Faculty of Science, University of Basel  
PhD Thesis Extrinsic and intrinsic regulation of differentiation and selection events during lymphocyte development  
Major subject Developmental and Molecular Immunology  
Supervisors Prof. Dr. Antonius Rolink and Prof. Dr. Gennaro De Libero  
Final mark 6.0 summa cum laude
- 09.2013 – 01.2015 **Master of Science in Molecular Biology**  
Department of Biomedicine, Faculty of Science, University of Basel  
Master Thesis Reconstitution of  $\mu$ MT mice with humanized B cells  
Major subject Immunology  
Supervisor Prof. Dr. Antonius Rolink  
Final mark 6.0 (6 excellent to 1 unsatisfactory)
- 09.2010 – 06.2013 **Bachelor of Science in Biology with Major in Molecular Biology**  
Faculty of Science, University of Basel  
Major subjects Structure biology/Biophysics, Biochemistry, Microbiology/Immunology, Neurobiology/Cell biology  
Final mark 5.3 (6 excellent to 1 unsatisfactory)

### Professional Experience

- 02.2015 – 01.2019 **PhD student – Laboratory of Prof. Dr. Antonius Rolink, University of Basel**
- Mechanisms of lymphoid development – transcription factors and cytokines
  - Investigation of pathways generating auto-reactive B-cell repertoires
  - Proteomics in B-cell development – identification of new surface markers
  - Training and supervision of undergraduate students
- 09.2013 – 01.2015 **Master student – Laboratory of Prof. Dr. Antonius Rolink, University of Basel**
- Humanized B-cell reconstitutions in mice for the production of chimeric antibodies
  - Establishment of CRISPR/Cas9 in primary hematopoietic cells and cell lines
- 10.2011 – 01.2015 **Laboratory-assistant (part-time) at 4-Antibody AG / Agenus**  
Lead Optimization Technology Unit, Technology Park Basel, Basel, Switzerland
- Generation of human antibody libraries expressed in mammalian B-lymphocytes
  - High-throughput screening for generation of therapeutic antibody drug candidates
  - Training and supervision of interns
- 06.2011 – 09.2011 **Internship at 4-Antibody AG**  
Lead Optimization Technology/Clone Recovery Unit, Biopark Rosental, Switzerland
- Three months of practical training in a molecular biology and a cell biology lab

## Additional Education

02. – 05.2018 **Analysis of genomic data with R** – University of Basel  
Weekly lecture teaching Biocductor based analysis pipelines including: NGS data processing; differential gene expression analysis; visualization of genomic data
09. – 12.2017 **Introduction to R** – University of Basel  
Weekly lecture teaching basic knowledge of R and how to use it
- 10.2016 **Writing to be Published** – Academic Writing Conventions and Style  
Workshop of the Transferable Skills Program – University of Basel
- 03.2016 **12<sup>th</sup> Spring School on Immunology** in Ettal, Germany  
Advanced training school in specialized immunological topics
- 04.2015 **LTK Module 1** – University of Zurich  
Introductory Course in Laboratory Animal Science (FELASA Category B Course)

## Teaching and Supervision

- Co-supervisor of Master students**
- 09.2016 – 02.2018 Mladen Mitrovic (official supervisor: Prof. A. Rolink)  
“Identification of Notch1 target genes during early T-cell development”
- 09.2016 – 09.2017 Grozdan Cvijetic (official supervisor: Prof. A. Rolink)  
“Generation of a TdT double reporter mouse and the impact of miRNAs on B cell development”
- 03.2014 – 03.2018 **Teaching assistant** – Yearly undergraduate immunology course  
Faculty of Science, University of Basel, Basel, Switzerland
- 10.2011 – 01.2015 **Training and supervision of interns**  
4-Antibody AG / Agenus, Basel, Switzerland

## Oral and Poster Presentations

- 01.2019 **Midwinter Conference** in Seefeld, Austria  
Poster: “The transcription factor Duxbl eliminates pre-T cells that fail  $\beta$ -selection”
- 12.2017/10.2018 **URI Group Meeting** in Strasbourg (2017) and Freiburg (2018)  
Annual meeting of the **Upper Rhine Immunology Group**  
Poster: “Accumulation of multipotent hematopoietic progenitors in peripheral lymphoid organs of mice over-expressing IL7 and Flt3-ligand” (**Poster Prize**; 2018)  
Poster: “Role of the transcription factor Duxbl in T-cell development” (2017)
- 11.2016/2017 **UBICO Retreat** in Engelberg, Switzerland  
Yearly conference of the **UniBasel Immunology Community**  
Presentation: “Role of the transcription factor Duxbl in T-cell development” (2017)  
Poster: “Two pathways generating anti-nuclear reactive B cells” (2017)  
Presentation: “Autoimmunity and Aging” (2016)
- 03.2016 **12<sup>th</sup> Spring School on Immunology** in Ettal, Germany  
Selected participant and chosen for a poster presentation  
Poster: “Role of the transcription factor Duxbl in lymphoid development”
- 02.2016 **28<sup>th</sup> Wolfsberg Meeting** of the Swiss Immunology PhD students, Switzerland  
Poster: “Role of the transcription factor Duxbl in lymphoid development”

## Key skills

- |                    |  |
|--------------------|--|
| Cellular biology   | <ul style="list-style-type: none"> <li>• Multi-color flow cytometry and cell sorting using various devices</li> <li>• Isolation and cultivation of primary immune cells and cell lines</li> <li>• In vitro and in vivo immunological assays – differentiation, apoptosis, proliferation</li> </ul>   |
| Molecular Biology  | <ul style="list-style-type: none"> <li>• Molecular cloning – restriction enzyme based, Gibson assembly, NEBuilder</li> <li>• DNA/RNA extraction and purification for analysis by PCR, qRT-PCR and RNA-seq</li> <li>• Production, expression, and purification of recombinant proteins</li> <li>• Various immunological methods – e.g. ELISA, Western blot</li> </ul> |
| Animal work (mice) | <ul style="list-style-type: none"> <li>• Mouse handling – organ collection, blood sampling, injections</li> <li>• Generation of genetically modified mice using genome editing technologies</li> </ul>   |
| Informatics        | <ul style="list-style-type: none"> <li>• Basic knowledge in R</li> <li>• Proficient in flow cytometry software – FlowJo, FACSDiva, CellQuest, Accuri C6</li> <li>• Profound knowledge of software used in research – e.g. Snppgene, Serial Cloner, EndNote, GraphPad Prism, Adobe Illustrator, Microsoft Office</li> </ul>   |

## Scientific Societies

- Swiss Society for Allergology and Immunology (SGAI)
- German Society for Immunology (DGfI)

## Publications

- [1] **Klein F\***, Mitrovic M, Roux J, Engdahl C, von Muenchow L, Alberti L, Fehling HJ, Pelczar P, Rolink A, Tsapogas P  
The transcription factor Duxbl mediates elimination of pre-T cells that fail  $\beta$ -selection  
*Journal of Experimental Medicine*  
*In press*  
**\*Corresponding author**
- [2] **Klein F**, von Muenchow L, Capoferri G, Heiler S, Alberti L, Rolink H, Engdahl C, Rolink M, Mitrovic M, Cvijetic G, Andersson J, Ceredig R, Tsapogas P, Rolink A  
Accumulation of multi-potent hematopoietic progenitors in peripheral lymphoid organs of mice over-expressing Interleukin-7 and Flt3-ligand  
*Frontiers in Immunology*  
2018 October; 9:2285; doi: 10.3389/fimmu.2018.02258
- [3] Faderl M<sup>1</sup>, **Klein F**<sup>1</sup>, Wirz OF<sup>1</sup>, Heiler S, Alberti L, Engdahl C, Andersson J, Rolink A  
Two distinct pathways in mice generate anti-nuclear antigen reactive B cell repertoires  
*Frontiers in Immunology*  
2018 January; 9:16; doi: 10.3389/fimmu.2018.00016  
<sup>1</sup>Equal contribution
- [4] von Muenchow L, Alberti L, **Klein F**, Finke D, Ceredig R, Rolink A, Tsapogas P  
Permissive roles of cytokines Interleukin-7 and Flt3-ligand in mouse B cell lineage commitment  
*Proceedings of the National Academy of Sciences of the United States of America*  
2016 November; 113(50):E8122-E8130; doi: 10.1073/pnas.1613316113